

Classing it up to get noticed

MHC class 1 antigen display in dendritic cells and neuroblastoma

Lotte Spel

Classing it up to get noticed: MHC class 1 antigen display in dendritic cells and neuroblastoma

PhD thesis, Utrecht University, the Netherlands

Author: Lotte Spel

Cover design: Remi Rough

Lay-out: Lotte Spel

Printing: Gildeprint

ISBN: 978-94-6233-842-5

About the cover. The cover shows a piece of art made by British artist Remi Rough. This piece is called Circumference. Information about Remi Rough can be found at www.remirough.com.

© **Lotte Spel 2018, Utrecht, the Netherlands.** All rights reserved. No parts of this thesis may be reproduced, stored in a retrieval system, or transmitted in any form or by any means without prior permission of the author. The copyright of articles that have been published has been transferred to the respective journals.

Printing of this thesis was kindly financially supported by ChipSoft BV; Infection and Immunity Center Utrecht; Weerstandfonds; Agri Food Health Innovation Center; Servier; Stichting voor Afweerstoornissen.

Classing it up to get noticed: MHC class 1 antigen display in dendritic cells and neuroblastoma

Een opmerkelijke klasse:
MHC-1 antigeen presentatie door dendritische cellen en neuroblastoom

(met een samenvatting in het Nederlands)

Proefschrift

ter verkrijging van de graad van doctor aan de Universiteit Utrecht op gezag van de rector magnificus, prof.dr. G.J. van der Zwaan, ingevolge het besluit van het college voor promoties in het openbaar te verdedigen op

donderdag 8 februari 2018 des middags te 12.45 uur

door

Lotte Spel

geboren op 9 juni 1988 te Oldenzaal

Promotor:

Prof.dr. A.B.J. Prakken

Copromotoren:

Dr. M.L. Boes

Dr. S. Nierkens

This research was financially supported by the Villa Joep foundation and AMMODO

Leescommissie

Prof.dr. J.H.E. Kuball

Prof.dr. E.C. de Jong

Prof.dr. D. van Baarle

Prof.dr. E.J.H.J. Wiertz

Dr. M.M. van Noesel

Paranimfen

Willemijn J.M. Janssen

Lieneke Spel

TABLE OF CONTENTS

Chapter 1	General Introduction	9
Chapter 2	Antitumor immune responses mediated by dendritic cells: How signals derived from dying cancer cells drive antigen cross-presentation. <i>Oncoimmunology 2013</i>	19
Chapter 3	Endocytosed soluble cowpox virus protein CPXV012 inhibits antigen cross-presentation in human monocyte- derived dendritic cells. <i>Immunology & Cell biology 2017</i>	37
Chapter 4	Cognate CD4 T-cell licensing of dendritic cells heralds anti-cytomegalovirus CD8 T-cell immunity after human allogeneic umbilical cord blood transplantation. <i>Journal of Virology 2015</i>	57
Chapter 5	<i>Preliminary Evaluation of a Bunyavirus Vector for Cancer Immunotherapy.</i> <i>Journal of Virology 2015</i>	79
Chapter 6	Natural Killer cells facilitate PRAME-specific T-cell reactivity against neuroblastoma. <i>Oncotarget 2015</i>	87
Chapter 7	A Genome-wide CRISPR-Cas9 screen identifies novel NFκB inhibitors in neuroblastoma.	109
Chapter 8	Reviewing Discussion: Immunogenicity during neuroblastoma development; insights for immunotherapy	133
Chapter 9	Summary	151
&	Closing pages	155
	<i>Nederlandse samenvatting</i>	<i>156</i>
	<i>Dankwoord</i>	<i>158</i>
	<i>Curriculum vitae</i>	<i>160</i>
	<i>List of publications</i>	<i>161</i>

Chapter 1

General Introduction



This thesis describes new insights in mechanisms of MHC class 1 antigen (cross-)presentation in dendritic cells and neuroblastoma tumor cells. MHC-1-mediated peptide presentation is the common denominator regulating not only the initiation of a T cell response but also its efficacy within tissue. On the one hand, MHC-1 (cross-)presentation is required for dendritic cells to effectively activate antigen-specific CD8⁺ T cells. On the other hand, MHC-1 peptide presentation is required on target cells to be effectively recognized and killed by the CD8⁺ T-cells. The work presented in this thesis is aimed to better understand DC and neuroblastoma biology to facilitate optimal anti-tumor CD8⁺ T-cell reactivity for eventual translation into therapeutic use against cancer.

T-cell responses

The human defence against infected or transformed cells relies to large extent on the recognition and killing capacities of cytotoxic CD8⁺ T-cells (also cytotoxic T lymphocytes; CTLs). CTLs differentiate from naive CD8⁺ T-cells upon recognition of their cognate peptide antigen in a stimulatory setting, also providing co-stimulatory and adhesion cues. Each CD8⁺ T-cell carries a unique T-cell receptor (TCR) with which it recognizes peptide/MHC-1 complexes at the surface of infected or transformed cells. Naive T-cells have not yet encountered their cognate peptide antigen, therefore rendering them undifferentiated and unable to actively kill target cells. Stimulation of their specific TCR will induce naive CD8⁺ T-cells to develop into effector CTLs. Additionally, some T-cells will differentiate into long-lived memory T-cells ensuring quick recall defence in case of a second encounter with the same pathogen.

Antigen presentation

The key to CD8⁺ T-cell activation is presentation of the cognate peptide antigen. The molecules involved in antigen presentation belong to the major histocompatibility complex (MHC) genes. It is the MHC class 1 molecule that is equipped for peptide presentation towards CD8⁺ T-cells. In humans, each individual carries 6 alleles encoding for MHC-1 molecules; 2 copies of HLA-A, 2 copies of HLA-B and 2 copies of HLA-C. MHC genes are moreover highly polymorphic. The wide diversity of different HLA alleles ensures MHC-1 peptide presentation towards a wide variety of TCRs. MHC-1 is expressed by all nucleated cells and binds and presents peptides derived from cytosolic proteins. This way, MHC-1 gives a snapshot of what is going on inside the cell on the cellular surface. Infected cells and tumor cells will present unusual peptides that are recognized as foreign by CD8⁺ T-cells.

The antigen presentation machinery (APM) comprises all proteins necessary to present a peptide as complexed with MHC-1 (Fig. 1). Assembly of stable peptide/MHC-1 complexes occurs within the endoplasmic reticulum (ER) with the help of several ER-resident chaperone molecules. MHC-1 incorporates relatively short peptides of 9-14 amino acids. Such peptides are produced in the cytosol through proteolytic activity of the proteasome and subsequently transported from the cytosol into the ER lumen by the transporter associated with antigen processing (TAP). Additional peptide trimming may occur in the ER lumen by endoplasmic reticulum aminopeptidases ERAP1 and ERAP2. Peptides that fit are loaded into the MHC-1 molecule after which the peptide/MHC-1 complex travels towards the plasma membrane (1).

As MHC-1 antigen presentation is critical for T-cell recognition of infected cells, many viruses

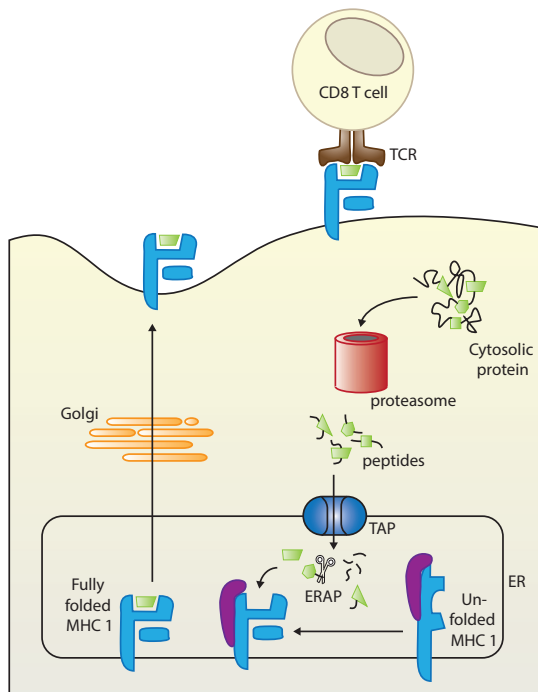


Figure 1. MHC class 1 antigen presentation pathway. Protein that are expressed in the cytoplasm are broken down into smaller peptides by the proteasome. The peptides enter the lumen of the endoplasmic reticulum (ER) through the transporter associated with antigen processing (TAP). The peptides are further trimmed by ER-associated peptidases (ERAP) within the ER. Immature MHC class 1 molecules that reside in the membrane of the ER become fully folded and loaded with peptide through help of chaperone proteins (purple). The mature peptide/MHC class 1-complex travels to the plasma membrane where it can be recognized by the T cell receptors (TCR) of CD8⁺ T cells.

1

have evolved ways to circumvent MHC-1 presentation (2). Viral strategies that hamper antigen presentation include interference with TAP peptide transport, reducing MHC-1 membrane

levels or shielding off the membrane-expressed MHC-1. Moreover, many cancers have acquired mechanisms to avoid anti-tumor T-cell reactivity, including down-regulation of MHC-1, up-regulation of T-cell inhibitory receptors and establishing an immune inhibitory microenvironment (3, 4).

Dendritic cells

Specialized in antigen presentation are the cell subsets collectively called antigen presenting cells (APCs), including B cells, macrophages and dendritic cells. Dendritic cells (DCs) are essential for eliciting CTL responses as they display antigenic peptide/MHC complexes to naive T-cells within the lymph nodes, stimulating T-cell activation and differentiation. Such priming of naive T-cells is crucial for inducing cellular cytotoxicity as well as T-cell memory against a given antigen.

DCs continuously sample the extracellular environment while patrolling tissues of the body. Upon encounter of foreign or otherwise non-self material (such as derived from tumors) in the presence of sufficient inflammatory mediators, DCs take up the material through phagocytosis and travel towards the lymph node. To prime CD8⁺ T-cells, DCs must be able to present the phagocytosed antigen in the context of MHC-1 molecules. As mentioned above, MHC-1 is primarily designed for the presentation of cytosolic peptides. Through a process called cross-presentation, particularly DCs are able to transfer peptides derived from extracellular antigens to the MHC-1 molecule.

Two routes are described by which phagocytosed antigen gains access to the MHC-1 loading machinery; the vacuolar route and the cytosolic route (Fig. 2) (5-10). In the vacuolar route, the antigen is taken up and broken down into peptides inside the endosomal pathway. MHC-1 picks up these antigenic peptides while traveling towards the plasma membrane, or when MHC-1 is recycled from the plasma membrane back into the endosomal pathway. DCs were even described to contain a specific cross-presentation compartment to which both MHC-1 and phagocytosed antigens are targeted (11-14). In the cytosolic route, the antigen inside the phagosome is transported over the endosomal membrane into the cytosol. There, it enters the conventional MHC-1 loading pathway through the proteasome, TAP and the ER lumen. Endosome-to-cytosol transport of antigen has been reported by several groups (15-18). Moreover, increasing evidence indicates that antigen type and surrounding signals shape the DC to use either pathway or both for MHC-1 cross-presentation (19, 20).

As more and more details have been elucidated about the mechanisms of cross-presentation, induction of an antigen-specific CD8⁺ T-cell response could be augmented. For example, targeting of antigens towards certain receptors would allow for particular MHC-1-directed antigen processing and loading. Moreover, combinations of antigen uptake and TRL stimuli may result in higher antigen cross-presentation levels. As our knowledge about antigen presentation in dendritic cells expands, their use in immunotherapies can be improved and fine-tuned.

T-cells against cancer

Cancer immunotherapy is an active field of research with great successes particularly in the last decade, which include tumor-targeting monoclonal antibodies (mAbs), adoptive cell transfers and immune-checkpoint inhibitors (21-23). Tumor-targeting mAbs convey their anti-tumor activity through either 1) altering signaling functions on receptors expressed by tumor cells (i.e. cetuximab; anti-EGFR), 2) neutralizing signals produced by tumor cells (i.e. bevacizumab; anti-VEGF) or 3) recognizing a tumor-associated antigen on the cell surface of tumor cells (i.e. rituximab; anti-CD20). In the latter case, the tumor-bound antibody may activate members of the innate immune system to destroy the tumor cell via antibody-dependent cell-mediated cytotoxicity (24, 25), antibody-dependent cellular phagocytosis (26) and/or complement-dependent cytotoxicity (27).

The recent successes in immune-checkpoint blockade therapy and adoptive cell transfers are focused on activation of adaptive immune cells, in particular T-cells. Immune-checkpoint blockade therapy consists of mAbs directed against T-cell inhibitory receptors, such as CTLA-4, PD-1 or its ligand PDL-1. By blocking inhibitory signals, anti-tumor CTLs are (re)-activated in the host immune system. Although they use a non-specific mechanism of T-cell activation, the clinical efficacy of immune-checkpoint inhibitors has become apparent in recent years (23).

While immune-checkpoint inhibitors strengthen a broadly-activating polyclonal T-cell response, adoptive cell transfers (ACT) pursue tumor-specificity. In ACT, patient-derived lymphocytes are collected, undergo treatment *ex vivo* and are re-administered into the patient. The *ex vivo* treatment may involve expanding and selecting tumor-specific CTLs (28, 29), introducing tumor specificity with a transgenic TCR (30-33) or chimeric antigen receptor (CAR) (34-37) and modifying proliferative, secretory, tumor-infiltrating or cytotoxic potential (38-41). These strategies have resulted in highly effective anti-tumor T-cells in various patients (42).

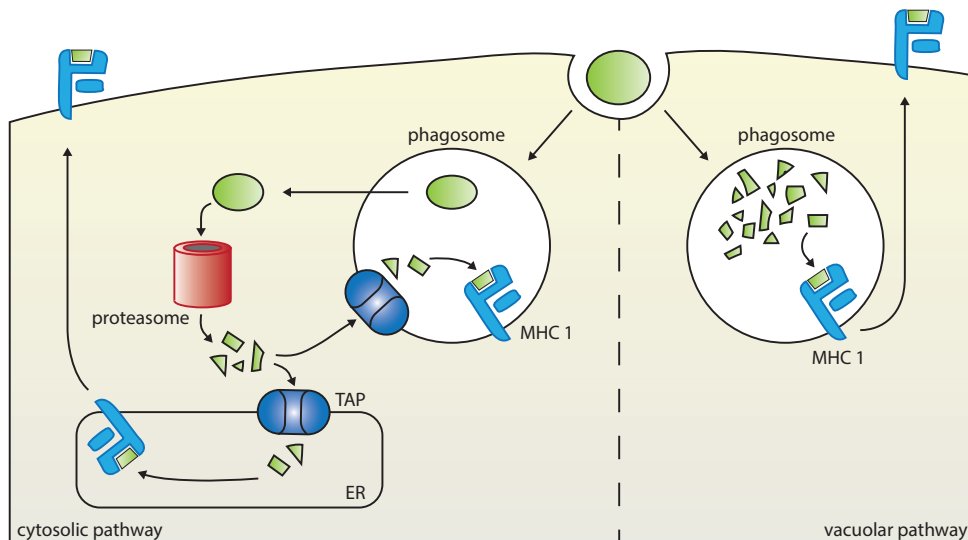


Figure 2. Pathways of antigen cross-presentation in dendritic cells. In the cytosolic pathway (left), antigen (green) is taken up into a phagosome and subsequently transported from the phagosomal lumen into the cytoplasm. There the antigen enters the classical MHC class 1 presentation pathway involving proteasomal degradation, TAP transportation into the ER and loading into ER-resident MHC class 1 molecules. Alternatively, antigenic peptides produced by the proteasome may enter the endosomal pathway through endosomal TAP and are loaded into (recycling) MHC class 1 molecules residing in the endosomal membrane. In the vacuolar pathway (right), antigen is taken up into a phagosome and broken down into peptides by endolysosomal proteases. Antigenic peptides produced inside the phagosome are directly loaded into (recycling) MHC class 1 molecules residing in the endosomal membrane.

T-cell recognition of neuroblastoma tumors

Pediatric neuroblastoma patients face a devastating survival rate of merely 20% when diagnosed with high-risk disease (stage 4). Neuroblastoma is the most common extra-cranial solid tumor in infants and accounts for 15% of all pediatric cancer deaths (43). Neuroblastoma is a tumor of the embryonic neural crest, specifically the peripheral sympathetic nerve precursor cells that give rise to all sympathetic neurons of the body. Neuroblastoma tumors can occur anywhere along the sympathetic chain, but is commonly found in the adrenal gland or the paraspinal ganglia. Instead of differentiating into healthy neurons, numerous errors that may occur during embryonic development of the neural crest cells have ceased their differentiation (44, 45). The cells are led astray and now contribute to the growth of a neuroblastoma tumor.

Immunotherapy for neuroblastoma patients includes an antibody therapy, combined with IL-2, directed against neuroblastoma TAA ganglioside 2 (GD2) that is highly expressed on neuroblastoma membranes. Unfortunately, this immunotherapy appears insufficient as relapses still occurred in the majority of the patients (46, 47). Given that antibody-based immunotherapy relies on innate immune responses, high-risk neuroblastoma patients might benefit more from immunotherapy engaging adaptive immunity focusing on CD8⁺ T-cells. However, strategies to evade T-cell recognition have been observed in neuroblastoma. A lack of MHC-1 expression

has been reported (48-51), making neuroblastoma cells unseen by CTLs. Furthermore, a T-cell antigen that is broadly expressed by neuroblastoma tumors has yet to be found.

The aim of this thesis is to identify key molecules and processes regulating MHC-1 antigen presentation in dendritic cells as well as neuroblastoma tumor cells. Our premise is that under conditions of optimal MHC-1 antigen presentation by both cell types, dendritic cells can instruct antigen-specific T-cells, while neuroblastoma will be their target of destruction. Collectively, this thesis serves as preclinical research towards improved neuroblastoma immunotherapy.

References

1. Blum JS, Wearsch PA, Cresswell P. Pathways of antigen processing. *Annu Rev Immunol.* 2013;31:443-73.
2. Schuren AB, Costa AI, Wiertz EJ. Recent advances in viral evasion of the MHC Class I processing pathway. *Curr Opin Immunol.* 2016;40:43-50.
3. Hanahan D, Weinberg RA. Hallmarks of cancer: the next generation. *Cell.* 2011;144(5):646-74.
4. Vesely MD, Schreiber RD. Cancer immunoediting: antigens, mechanisms, and implications to cancer immunotherapy. *Ann N Y Acad Sci.* 2013;1284:1-5.
5. Grotzke JE, Sengupta D, Lu Q, Cresswell P. The ongoing saga of the mechanism(s) of MHC class I-restricted cross-presentation. *Curr Opin Immunol.* 2017;46:89-96.
6. Segura E, Amigorena S. Cross-Presentation in Mouse and Human Dendritic Cells. *Adv Immunol.* 2015;127:1-31.
7. Joffre OP, Segura E, Savina A, Amigorena S. Cross-presentation by dendritic cells. *Nat Rev Immunol.* 2012;12(8):557-69.
8. Flinsenberg TW, Compeer EB, Boelens JJ, Boes M. Antigen cross-presentation: extending recent laboratory findings to therapeutic intervention. *Clin Exp Immunol.* 2011;165(1):8-18.
9. Kurts C, Robinson BW, Knolle PA. Cross-priming in health and disease. *Nat Rev Immunol.* 2010;10(6):403-14.
10. Blander JM. The comings and goings of MHC class I molecules herald a new dawn in cross-presentation. *Immunol Rev.* 2016;272(1):65-79.
11. van Montfoort N, Camps MG, Khan S, Filipov DV, Weterings JJ, Griffith JM, et al. Antigen storage compartments in mature dendritic cells facilitate prolonged cytotoxic T lymphocyte cross-priming capacity. *Proc Natl Acad Sci U S A.* 2009;106(16):6730-5.
12. Burgdorf S, Scholz C, Kautz A, Tampe R, Kurts C. Spatial and mechanistic separation of cross-presentation and endogenous antigen presentation. *Nat Immunol.* 2008;9(5):558-66.
13. Saveanu L, Carroll O, Weimershaus M, Guermontprez P, Firat E, Lindo V, et al. IRAP identifies an endosomal compartment required for MHC class I cross-presentation. *Science.* 2009;325(5937):213-7.
14. Nair-Gupta P, Baccarini A, Tung N, Seyffer F, Florey O, Huang Y, et al. TLR signals induce phagosomal MHC-I delivery from the endosomal recycling compartment to allow cross-presentation. *Cell.* 2014;158(3):506-21.
15. Rodriguez A, Regnault A, Kleijmeer M, Ricciardi-Castagnoli P, Amigorena S. Selective transport of internalized antigens to the cytosol for MHC class I presentation in dendritic cells. *Nat Cell Biol.* 1999;1(6):362-8.
16. Ackerman AL, Giodini A, Cresswell P. A role for the endoplasmic reticulum protein retrotranslocation machinery during crosspresentation by dendritic cells. *Immunity.* 2006;25(4):607-17.
17. Singh R, Cresswell P. Defective cross-presentation of viral antigens in GILT-free mice. *Science.* 2010;328(5984):1394-8.
18. Zehner M, Marschall AL, Bos E, Schloetel JG, Kreer C, Fehrenschild D, et al. The translocon protein Sec61 mediates antigen transport from endosomes in the cytosol for cross-presentation to CD8(+) T cells. *Immunity.* 2015;42(5):850-63.
19. Alloatti A, Kotsias F, Magalhaes JG, Amigorena S. Dendritic cell maturation and cross-presentation: timing matters! *Immunol Rev.* 2016;272(1):97-108.
20. Wagner CS, Grotzke J, Cresswell P. Intracellular regulation of cross-presentation during dendritic cell maturation. *PLoS One.* 2013;8(10):e76801.
21. Galluzzi L, Vacchelli E, Bravo-San Pedro JM, Buque A, Senovilla L, Baracco EE, et al. Classification of current anticancer immunotherapies. *Oncotarget.* 2014;5(24):12472-508.
22. Yang Y. Cancer immunotherapy: harnessing the immune system to battle cancer. *J Clin Invest.* 2015;125(9):3335-7.
23. Kamta J, Chaar M, Ande A, Altomare DA, Ait-Oudhia S. Advancing Cancer Therapy with Present and Emerging Immuno-Oncology Approaches. *Front Oncol.* 2017;7:64.

24. Weiner LM, Surana R, Wang S. Monoclonal antibodies: versatile platforms for cancer immunotherapy. *Nat Rev Immunol.* 2010;10(5):317-27.
25. Hubert P, Amigorena S. Antibody-dependent cell cytotoxicity in monoclonal antibody-mediated tumor immunotherapy. *Oncoimmunology.* 2012;1(1):103-5.
26. Winiarska M, Glodkowska-Mrowka E, Bil J, Golab J. Molecular mechanisms of the antitumor effects of anti-CD20 antibodies. *Front Biosci (Landmark Ed).* 2011;16:277-306.
27. Zipfel PF. Complement and immune defense: from innate immunity to human diseases. *Immunol Lett.* 2009;126(1-2):1-7.
28. Dudley ME, Wunderlich JR, Shelton TE, Even J, Rosenberg SA. Generation of tumor-infiltrating lymphocyte cultures for use in adoptive transfer therapy for melanoma patients. *J Immunother.* 2003;26(4):332-42.
29. Dudley ME, Gross CA, Langhan MM, Garcia MR, Sherry RM, Yang JC, et al. CD8+ enriched "young" tumor infiltrating lymphocytes can mediate regression of metastatic melanoma. *Clin Cancer Res.* 2010;16(24):6122-31.
30. Rosenberg SA. Cell transfer immunotherapy for metastatic solid cancer--what clinicians need to know. *Nat Rev Clin Oncol.* 2011;8(10):577-85.
31. Ray S, Chhabra A, Chakraborty NG, Hegde U, Dorsky DI, Chodon T, et al. MHC-I-restricted melanoma antigen specific TCR-engineered human CD4+ T cells exhibit multifunctional effector and helper responses, in vitro. *Clin Immunol.* 2010;136(3):338-47.
32. Sadelain M, Riviere I, Brentjens R. Targeting tumours with genetically enhanced T lymphocytes. *Nat Rev Cancer.* 2003;3(1):35-45.
33. Robbins PF, Morgan RA, Feldman SA, Yang JC, Sherry RM, Dudley ME, et al. Tumor regression in patients with metastatic synovial cell sarcoma and melanoma using genetically engineered lymphocytes reactive with NY-ESO-1. *J Clin Oncol.* 2011;29(7):917-24.
34. Dotti G, Gottschalk S, Savoldo B, Brenner MK. Design and development of therapies using chimeric antigen receptor-expressing T cells. *Immunol Rev.* 2014;257(1):107-26.
35. Porter DL, Levine BL, Kalos M, Bagg A, June CH. Chimeric antigen receptor-modified T cells in chronic lymphoid leukemia. *N Engl J Med.* 2011;365(8):725-33.
36. Kochenderfer JN, Rosenberg SA. Treating B-cell cancer with T cells expressing anti-CD19 chimeric antigen receptors. *Nat Rev Clin Oncol.* 2013;10(5):267-76.
37. Long AH, Haso WM, Orentas RJ. Lessons learned from a highly-active CD22-specific chimeric antigen receptor. *Oncoimmunology.* 2013;2(4):e23621.
38. Merhavi-Shoham E, Haga-Friedman A, Cohen CJ. Genetically modulating T-cell function to target cancer. *Semin Cancer Biol.* 2012;22(1):14-22.
39. Liu K, Rosenberg SA. Transduction of an IL-2 gene into human melanoma-reactive lymphocytes results in their continued growth in the absence of exogenous IL-2 and maintenance of specific antitumor activity. *J Immunol.* 2001;167(11):6356-65.
40. Kalbasi A, Shrimali RK, Chinnasamy D, Rosenberg SA. Prevention of interleukin-2 withdrawal-induced apoptosis in lymphocytes retrovirally cotransduced with genes encoding an antitumor T-cell receptor and an antiapoptotic protein. *J Immunother.* 2010;33(7):672-83.
41. Kershaw MH, Teng MW, Smyth MJ, Darcy PK. Supernatural T cells: genetic modification of T cells for cancer therapy. *Nat Rev Immunol.* 2005;5(12):928-40.
42. Yang JC, Rosenberg SA. Adoptive T-Cell Therapy for Cancer. *Adv Immunol.* 2016;130:279-94.
43. Davidoff AM. Neuroblastoma. *Semin Pediatr Surg.* 2012;21(1):2-14.
44. Schulte JH, Eggert A. Neuroblastoma. *Crit Rev Oncog.* 2015;20(3-4):245-70.
45. Cao Y, Jin Y, Yu J, Wang J, Yan J, Zhao Q. Research progress of neuroblastoma related gene variations. *Oncotarget.* 2017;8(11):18444-55.
46. Yu AL, Gilman AL, Ozkaynak MF, London WB, Kreissman SG, Chen HX, et al. Anti-GD2 antibody with GM-CSF, interleukin-2, and isotretinoin for neuroblastoma. *N Engl J Med.* 2010;363(14):1324-34.
47. Maris JM. Recent advances in neuroblastoma. *N Engl J Med.* 2010;362(23):2202-11.
48. Wolf M, Jungbluth AA, Garrido F, Cabrera T, Meyen-Southard S, Spitz R, et al. Expression of MHC

- class I, MHC class II, and cancer germline antigens in neuroblastoma. *Cancer Immunol Immunother.* 2005;54(4):400-6.
49. Bao L, Dunham K, Lucas K. MAGE-A1, MAGE-A3, and NY-ESO-1 can be upregulated on neuroblastoma cells to facilitate cytotoxic T lymphocyte-mediated tumor cell killing. *Cancer Immunol Immunother.* 2011;60(9):1299-307.
50. Gross N, Beck D, Favre S. In vitro modulation and relationship between N-myc and HLA class I RNA steady-state levels in human neuroblastoma cells. *Cancer Res.* 1990;50(23):7532-6.
51. Prigione I, Corrias MV, Airolidi I, Raffaghello L, Morandi F, Bocca P, et al. Immunogenicity of human neuroblastoma. *Ann N Y Acad Sci.* 2004;1028:69-80.

Chapter 2

**Antitumor immune responses mediated by dendritic cells:
How signals derived from dying cancer cells drive antigen
cross-presentation.**

Authors

Lotte Spel, Jaap-Jan Boelens, Stefan Nierkens and Marianne Boes

Published in

OncotImmunology 2013

Abstract

Dendritic cells (DCs) are essential for the induction of adaptive immune responses against tumor cells, by virtue of their capacity to effectively cross-present exogenous antigens. Dying tumor cells are considered as a source of antigens for the development of DC-based vaccines. Tumor cells dying through apoptosis, rather than necrosis, now appear to provide cell-associated antigens that efficiently induce adaptive immune responses. In this review, we describe cell biological processes associated with cross-presentation of apoptotic cell antigens, for increased induction of protective CD8⁺ T-cells.

Introduction

Antigen cross-presentation:

The immune system plays an instrumental role in both development and (treatment-assisted) resolution of malignant tumors (1-3). Within the immune system, dendritic cells (DCs) are pivotal for activation of immune responses. DCs are defined as CD11c⁺ cells, representing a collection of distinct cellular subsets based on additional membrane markers (4) and transcription factors (5). DCs are equipped to present fragments of exogenously acquired antigens as peptide/MHC I complexes to CD8-positive T cells, a process referred to as antigen cross-presentation (6;7). Cross-presentation by DCs is essential for developing CD8⁺ T cell responses against cell-associated antigens such as tumor cells, as was demonstrated by the lack of CD8⁺ T cell responses against cellular-derived antigen upon depletion of CD11c⁺ populations (8).

Cross-presentation is a specialized antigen presentation process, for which DCs are particularly well equipped. Other antigen presenting cells, such as B cells, monocytes and macrophages cannot readily stimulate naïve CD8⁺ T cells after encounter of exogenous antigen (9). Much effort in the last decade was put into understanding underlying mechanisms that facilitate optimal cross-presentation. As a result, distinct DC subsets are now described that possess superior capacity to cross-present antigens, i.e. CD8⁺ and CD103⁺ DCs in mice (6). In 2010, a human counterpart of such a subset was described, defined by the expression of the BDCA3 marker (10). As these studies unfolded, the idea of superiority in cross-presenting DC subsets was challenged, with the postulate that all DCs can cross-present antigens when triggered under the right conditions (11;12). Inflammatory cytokines, Toll-like receptor ligands and CD40 signaling through CD4⁺ T cell help, can mature DCs and efficiently prime them for antigen cross-presentation (13;14).

Encounter of tumor antigens by DCs:

Uptake of soluble or complexed antigens by DCs involves mechanisms including passive pinocytosis, active phagocytosis or translocation via gap junctions (15). Antigen delivery routes greatly influence cross-presentation efficiency within DCs. Hence, antigen cross-presentation can specifically be enhanced through antibody opsonisation and targeting of antigen to DC-expressed cell surface receptors (16-22). Alternatively, DCs can internalize dying tumor cells harbouring tumor antigens. All possible antigens expressed by the dying cell are thereby theoretically made available for cross-presentation, although only a fraction of antigenic peptides end up being presented as peptide/MHC I complexes to CD8⁺ T cells. In the light of tumor vaccination strategies, researchers have now explored the use of ex vivo killed tumor cells as a vaccine in itself or as cargo for DCs as a DC-based vaccine. The types of cell death induced ex vivo to kill tumor cells comes in different flavours, including apoptosis and necrosis. Apoptosis is a form of programmed cell death initiated by multiple signals that altogether trigger a highly regulated intracellular process of destruction (23;24). This cell death process can take up 10-20 hours. During this time, one can observe changes at the plasma membrane, but the process also has organized foci within the cytosol and the nucleus of the dying cell. Of note, necrosis was long considered to be a form of incidental cell death whereby the cell does not follow organized trajectories. Recently this notion has changed with the appearance of evidence showing in vivo necrosis to be subjective to regulation as well (25). Different from such necrotic cells, apoptotic cells maintain their membrane integrity for prolonged duration (26;27) but will eventually also

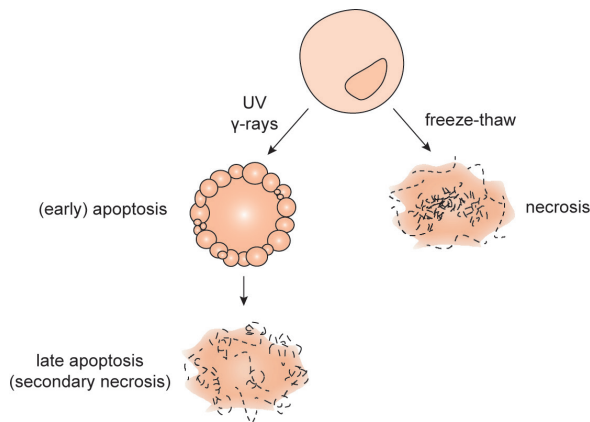


Figure 1. Experimental induction of cell death. Necrosis can be induced by multiple freeze-thaw cycles using liquid nitrogen. In this setting, both the plasma and nuclear membranes are ruptured so that cellular contents leak out and only membrane debris are left. Apoptosis can be induced by radiation with UV light or γ rays. The membrane of apoptotic cells undergo specific alterations, but (at least initially) it remains intact. Eventually, apoptotic cells also lose membrane integrity, a setting that is often referred to as late apoptosis or secondary necrosis.

succumb to membrane rupture, a status called secondary necrosis or late apoptosis (28). From the viewpoint of DCs, (early) apoptotic and necrotic cells are presumably very different entities that will be handled differently by the DC with divergent consequences for the elicitation of immune reactivity.

Approaches to distinguish types of tumor cell death:

For study purposes, apoptosis is often induced *in vitro* by introducing DNA damage via irradiation with ultraviolet light or gamma rays (Figure 1). Apoptotic cells expose phosphatidyl serine on the outer leaflet of the plasma membrane (29) which can specifically be bound by the Annexin (Anx) V protein. Membrane integrity can be visualized by the use of propidium iodide (PI) or 7-aminoactinomycin D (7-AAD) that only stain cells when integrity is lost. Apoptotic cells are thus characterized as AnxV+PI- cells and can be monitored by flow cytometric analyses. Necrosis is commonly induced by multiple freeze-thaw cycles using liquid nitrogen. Freezing the cells will cause damage to the cell membrane leading to inevitable membrane rupture. Some investigators induce necrosis by heating or osmotic shock to the same effect. In theory, apoptosis and necrosis are clearly distinguishable but experimentally, inducing cell death can result in a mixed population of apoptotic and (secondary) necrotic cells. Furthermore, some studies refer to late apoptotic cells as necrotic cells. Such discrepancies can be misleading in crediting biological effects to either apoptotic or necrotic cells.

Taking this into account, in this review we give an overview of studies comparing *in vitro* induced apoptotic and necrotic cells in their efficiency to elicit adaptive immune responses against cellular antigens. Herein, we will refer to apoptotic and necrotic cells as they are shown in figure 1. We will discuss how DCs specifically handle dying cells and the subsequent consequences for immunity. We also highlight which features of dying cells are important for their immunogenicity.

Immune responses against apoptotic versus necrotic cells

In vitro tumor antigen cross-presentation studies:

While for both apoptotic and necrotic cells, adaptive immune responses can be raised against

cell-associated antigens, comparison of the two conditions reveals differences in the efficiency by which they do so. Given its prerequisite for adaptive immunity against cellular antigens (8), cross-presentation is often used as a presage in *in vitro* studies. In such studies, isolated DCs are incubated with either apoptotic or necrotic cells after which cross-presentation is measured by addition of antigen-specific or unfractionated CD8⁺ T cells, followed by measurement of IFN γ release. Alternatively, specific lysis of target cells expressing the antigen by the activated CD8⁺ T cells is measured. For several tumor cell lines it was shown that apoptosis was superior to necrosis in facilitating cross-presentation of tumor-expressed antigen to CD8⁺ T cells by DCs (30;31). These findings were confirmed using primary tumor cells from B cell lymphoma and melanoma patients (32;33). Of note, when TNF was supplemented during tumor cell-DC incubation, T cell activation increased and the superior effect of apoptosis was lost (33). These studies suggested that an inherent stimulatory effect of apoptotic cells accounts for enhanced CD8⁺ T cell activation. When non-tumor cells, however, were used as a source of antigen, apoptotic and necrotic cells induced comparable levels of cross-presentation (34;35). Using a healthy cells system in which antigen was introduced through virus infection and the cells were subsequently induced to undergo cell death, apoptotic cells were again better than necrotic cells (36). Taken together, these data suggest that tumor cells (or virus-infected cells) are more immunogenic under apoptotic conditions than healthy cells.

Immunogenicity of apoptotic cells is further demonstrated using conditions that contain increased numbers of apoptotic cells. Enhanced CD8⁺ T cell activation was observed when DCs received tumor cells with higher apoptotic cell abundance (37). Interestingly, late apoptotic cells were shown to be even more immunogenic than early apoptotic cells (38). The same phenomenon was observed by Buttiglieri et al., although the methods for induction of early and late apoptosis were dissimilar in both studies: immunogenic differences between the dying cells may possibly relate to the specific compounds used to induce cell death instead of the stage of apoptosis observed (39).

In vivo tumor antigen cross-presentation studies:

To test potential efficacy as a tumor cell vaccine, dying tumor cells are injected directly into mice and adaptive immunity against tumor cell antigens is measured. To this end, CD8⁺ T cells are isolated from lymph nodes or spleen and tested for specific lytic capacity against tumor cell targets. In other cases, the mice are re-challenged with live tumor cells and tumor outgrowth is monitored. Such studies consistently reveal apoptotic cell's enhanced capacity for eliciting anti-tumor immune responses (40-44). For example, the differential treatment of established tumors resulted in either apoptotic or necrotic cell death of the tumor mass and respectively resulted in protective and non-protective CD8⁺ T cells responses (41).

A different approach to determine dying cell immunogenicity *in vivo* is through injection of DCs that are pulsed with apoptotic or necrotic cells *ex vivo*. The loaded DCs interact with immune cells *in vivo*, thereby eliciting a particular response. Again, DCs loaded with apoptotic cells performed better than DCs loaded with necrotic cells in protection against tumor development in both therapeutic and vaccination models (31;45;46). Moreover, cytolytic activity of splenic T cells was higher when animals received DCs loaded with apoptotic cells compared to DCs loaded with necrotic cells (45). In contrast, Kotera et al. show that apoptotic and necrotic cells to be equally protective against established tumors or naïve tumor challenge (47).

Besides apoptosis there is a second manner of programmed cell death, which involves breakdown of cellular content by autophagic vesicles. This type of cell death proved favourable, inducing anti-tumor immune responses that were even better than those by apoptotic cells (48). Corroborating this work, in 2004 it was already observed by Schmitt et al. that inoculation of tumor cells undergoing a caspase-independent death was more protective than caspase-dependent cell death against a subsequent tumor cell challenge (49).

While in vitro studies remain ambivalent, in vivo studies robustly show apoptotic cells to be the preferred inducers of CD8⁺ T cells responses against tumors. However, the experimental design of DC vaccination studies do not always clarify how the DCs are handled specifically before injection. For example, in experiments where dying cells are not excluded before injection of DC, MHC-deficient dying cells should be used to prevent direct presentation. Moreover, when using necrotic cells it is often not stated whether only membrane debris or lysates are used. Nevertheless, it is clear that dying cells depend on DCs to facilitate anti-tumor immune responses. This notion has already reached clinical practice, since several groups have used DCs loaded with cell lysates as a therapeutic vaccine in melanoma and pediatric solid tumor patients and showed objective clinical responses in a number of them (50-52). It remains a challenge to improve such vaccines with the application of a more immunogenic form of dead tumor cells, rather than necrotic debris.

Maturation rate of phagosomes determines efficiency of cross-presentation

Dendritic cell subsets:

Since the revelation that DCs represent multiple specialized DC cell subsets, investigators have shown that particularly the murine CD8⁺ DCs cross-present cell-associated antigens in lymphoid tissues and CD103⁺ DCs in non-lymphoid tissues. This capacity was attributed to the ability of CD8⁺ DCs to internalize dying cells (53). Indeed in mice it was shown that injected dying cells were traced back particularly in CD8⁺ DCs of the spleen (54). When the cells were injected intranasally, CD103⁺ DCs but not CD11b⁺ DCs were shown to have taken up the apoptotic cells in the lungs (55). DC subsets in the meantime are now also described in human and include the BDCA3⁺ DCs, considered to be the equivalent of mouse CD8⁺ DCs, and BDCA1⁺ DCs. Isolation of BDCA3⁺ and BDCA1⁺ DCs from peripheral blood allows for in vitro assessment of phagocytosis capacity. Different from mice, both human subsets can take up dying cells but only BDCA3⁺ DCs presented cell-associated antigen to CD8⁺ T cells (56). Comparison of lymphoid tissue-derived BDCA3⁺ and BDCA1⁺ DCs also revealed equal uptake of dying cells and slightly better presentation by the BDCA3⁺ DCs (12).

Receptor engagement:

Differential receptor expression between DCs that cross-presented cell-associated antigen and DCs that do not suggested a possible explanation why dying cells were handled differently between the DC subsets. Clec9A (DNGR1), a member of the C-type lectin receptor family, was identified to be selectively high expressed by CD8⁺, CD103⁺ and BDCA3⁺ DCs (57;58). Further investigation showed that clec9A can sense dying cells through the recognition of F-actin filaments (59), which was favourable for the ability to cross-prime CD8⁺ T cells (20). Interestingly, the uptake of dying cells appeared independent of clec9A expression, which is concordant with the observation that

clec9A-negative DC subsets can take up dying cells as well. Rather, post-internalization events were influenced by clec9A engagement. As such, the activation of clec9A did not result in DC activation, measured by cytokine secretion, but instead, caused clec9A co-localization with early endosomes marked by EEA-1, Rab5a and Rab27a. Likewise, phagocytosed dying cells colocalized with Rab5a+ endosomes 60 minutes after uptake. Subsequently, 240 minutes after uptake the cells were associated with Rab11+ structures, which are considered as recycling endosomes. This localisation with Rab5a+ and Rab11+ vesicles required the expression of clec9A (60).

Receptor engagement can drive cargo-sorting into distinct endosomal compartments, causing cargo to be specifically sorted into either static or dynamic early endosomes that mature into recycling or degrading endosomes, respectively (61). Recycling endosomes differ from degrading endosomes in that they maintain a mild acidic interior whereas degrading endosomes progressively acidify in time. Therefore, proteolytic activity is lower in recycling endosomes compared to degrading endosomes. Several studies provide evidence that low proteolytic activity benefits cross-presentation in both mice and human DCs (62-66). Furthermore, the mannose receptor and DC-SIGN were shown to target their cargo into slow-maturing endosomes (67) and targeting antigens to these receptors can enhance cross-presentation (17;22).

Endosomal pH:

Data from the last decade together suggest that tempering the endosomal acidification can benefit antigen cross-presentation. In this regard it was shown that Rab27a could regulate phagosomal pH by recruiting Nox2 towards the phagosomal membrane (63). Nox2 is part of the NADPH oxidase complex that maintains neutral pH (65). Both the absence of Rab27a or Nox2 was detrimental for cross-presentation (63;66). Slow antigen degradation allows for prolonged storage of the antigen within designated phagosomes. Accordingly, storage compartments were described and were shown to be long-lasting. When peptides were eluted out of MHC I molecules of the DC at 16 hours after antigen uptake, antigen presentation could still be fully recovered indicating the antigen was still intracellularly present to supplement peptides for MHC I presentation (68). Therefore, given the fact that apoptotic cells are recognized by clec9A, their immunogenicity might be the result of being intracellularly navigated into Rab27a+ storing phagosomes, that are characterized by mild acidification and slow proteolysis that thereby facilitates prolonged MHC I cross-presentation of cell-associated antigens (Figure 2).

Apoptotic cells induce prolonged immune responses

The superior cross-priming capacities of apoptotic cells may in part be explained by prolonged antigen storage, although the cell biological bearing for this process are not yet fully understood. Comparison between CD8+ DCs and CD11b+ DCs showed that cross-presentation of apoptotic material was not only higher in CD8+ DCs, but also lasted longer (69). A third DC subset called merocytic (mc)DCs could even exceed the cross-presentation capacity of CD8+ DCs (42). This effect could be blocked by administration of DPI, a compound shown to accelerate endosomal acidification (65;66), suggesting that aberrant antigen processing and storage influenced cross-presentation. Indeed, phagosomal pH remained high in CD8+ and mcDCs but decreased in CD11b+ DCs after uptake. In vivo CD8+ T cells responses after vaccination with loaded DCs were also

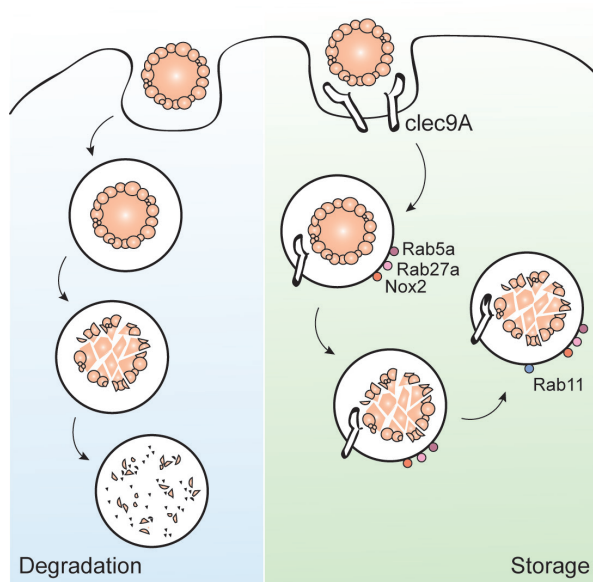


Figure 2. CLEC9A direct apoptotic material toward storage compartments. Apoptotic cells are taken up by dendritic cells (DCs). Upon engagement of C-type lectin domain family 9, member A (CLEC9A) on the DC surface, apoptotic cells are directed to RAB5A⁺RAB27A⁺ endosomes. RAB27A rapidly recruits NOX2 to the endosomal membrane, hence preventing an excessive acidification of the maturing endosome and allow for the establishment of a storage compartment. In the absence of CLEC9A the endosomal cargo is quickly dispatcher to lysosomes and fully degraded. CLEC9A thus facilitates the slow degradation and prolonged storage of apoptotic material, a mechanism that may account for the ability of CLEC9A to enhance the cross-presentation of cell-associated antigens.

stronger and prolonged when CD8⁺ or mDCs were used compared to CD11b⁺ DCs (69). Similar observations were made when directly injecting apoptotic or necrotic tumor cells (40). The specific lysis by CD8⁺ T cells was observed up to 9 days after mice were injected with apoptotic cells. Instead, necrotic cells only induced responses for up to 4 days, with initial responses also being inferior to those induced by apoptotic cells (40). Histological determination of apoptotic or necrotic cell vaccination sites shows rapid recruitment of T cells, B cells, macrophages and DCs by both apoptotic and necrotic cells (44). However, only in case of apoptotic cell vaccination T cells and DCs were still present after 10 days (44). The importance of antigen persistence was also established by the use of MHC I-lacking cells. Such cells were rapidly removed by NK cells, therefore unable to elicit CD8⁺ T cell responses. However, when NK cells were depleted it was shown that the cells persisted and antigen-specific cross-priming of CD8⁺ T cells was observed (70).

From these studies, a dual role for apoptotic cells in antigen persistence can be proposed. First of all, by interfering with phagosomal pH levels apoptotic cells persist longer within the DCs resulting in prolonged cross-presentation of cellular antigens. Secondly, apoptotic cells facilitate persistent immune cell recruitment or alternatively, durable survival of recruited immune cells.

A role for type 1 interferons in antigen persistence

Upon exposure to apoptotic cells, mDCs secreted type 1 interferons whereas CD8⁺ DCs or CD11b⁺ DCs did not (69). Bone marrow-derived Flt3-stimulated DCs also respond to apoptotic cells by producing type 1 interferon (42) while necrotic cells were unable to induce cytokine secretion. In human, so far only plasmacytoid DCs were found to secrete IFN α upon stimulation with apoptotic cells (71;72).

Interestingly, type 1 interferons were shown to be of great importance for immune rejection

of tumors in vivo (73). Blocking the IFN α -receptor (IFNAR) with specific antibodies significantly increased tumor outgrowth. Similarly, IFNAR^{-/-} mice showed enhanced tumor development. The importance of type 1 interferons was also shown in a model where in vivo tumor cell death was induced. Here, cross-presentation of tumor antigens was diminished in IFN α / β knock-out mice that were transferred with antigen-specific CD8⁺ T cells indicating that IFN α / β sensitivity was required on immune cells other than CD8⁺ T cells (74). Indeed, Diamond et al. demonstrated that IFN α / β sensitivity was specifically required on CD8⁺ DCs for induction of anti-tumor CTL responses (73). As such, pre-treatment of CD8⁺ DCs with IFN α increased cross-presentation of cell-associated antigens (75). Apoptotic cells were shown to be persistently present in IFN-treated DCs compared to non-treated DCs, in a DPI-dependent manner which indicates that type 1 interferons may somehow modulate phagosomal pH levels of DCs. In human DCs, delayed endosomal acidification as well as antigen storage in Rab5⁺ and Rab11⁺ compartments was also detected upon exposure to apoptotic cells (76). Additionally, MHC I localized to antigen storage compartments upon IFN α treatment in DCs. Remarkably, besides antigen survival within DCs there is also evidence for survival of the DC itself after IFN α stimulation. CD8⁺ DCs that internalized apoptotic cells particularly upregulated expression of anti-apoptotic genes Bcl2 and Bcl-XI, which resulted in prolonged survival of antigen-bearing DCs (75).

In pDCs, IFN α secretion was associated with LC3-coated phagosomes that internalized DNA-immune complexes (77). In macrophages, apoptotic cells were shown to be taken up into LC3-coated phagosomes (78). Moreover, endosomal ROS production by nox2 specifically recruited LC3 towards the endosomal membrane (79). Given the fact that apoptotic cells were indirectly able to attract nox2 to its phagosomal membrane, it could be speculated that they are also taken up in LC3-coated structures in DCs. Whether LC3 recruitment to the phagosome is necessary for IFN α secretion by the DC however remains elusive.

While it is clear that DCs benefit from IFN α signalling for presentation of cell-associated antigens, the very same DCs do not per se produce type I interferons themselves upon exposure to apoptotic cells. However, neighbouring immune cells have been shown to produce these cytokines when they encounter apoptotic cells. Accordingly, pDCs can help CD11c⁺ DCs to cross-prime tumor cell specific CD8⁺ T cells in an IFN α -dependent manner (80). Also in a vaccination setting using CD8⁺ and merocytic DCs, pre-incubation of the DCs with dying tumor cells in the presence of pDCs increased survival rates, suggesting synergism between pDCs and cDCs in eliciting anti-tumor immune protection (74). Thus, optimal handling of the apoptotic cells may be achieved by DCs in response to IFN α production by surrounding cells, such as pDCs.

Interactions between apoptotic cells and dendritic cells

Recently, a concept of immunological cell death has emerged which proposes that cells can die either a silent or immunological death, depending on the death stimulus they received (81-84). Immunological cell death was supposed to be accompanied by release of so-called danger-associated molecular patterns or DAMPs, including HMGB1, heat shock proteins and ATP. DAMPs consist of secreted or membrane-bound molecules that are immunologically silent when intracellularly expressed by the cells, but have the ability to stimulate immune responses when they are exposed.

An apparent paradox appears when considering that apoptotic cells display superior

immunogenicity compared to necrotic cells, while necrotic cells rather than apoptotic cells release many DAMPs (48;85;86). Indeed, necrotic cells were shown to efficiently mature DCs in vitro (87) whereas apoptotic cells could not. Such observations would suggest that DAMPs do not endorse the immunogenicity of dying cells. However, several studies clearly show a critical role for DAMPs during anti-tumor immune responses.

Supernatants of necrotic cells can act as protective adjuvants for antigen vaccination (88), but when HMGB1 was knocked down in the necrotic cells the adjuvancy of their supernatants was diminished. Accordingly, adding recombinant HMGB1 to cellular antigens induced enhanced anti-tumor immunity and protection against tumor challenge. These results indicate that HMGB1 is a potent stimulator of adaptive immune responses in the presence of antigen, but is not exclusive given the fact that HMGB1 knock-down did not result in 100% rescue phenotype. The importance of HMGB1 was also established by the use of blocking antibodies and siRNA for in vivo cross-presentation of cell-associated antigens and induction of protective anti-tumor immunity (89). In particular, HMGB1 was shown to bind TLR4. Also TLR4^{-/-} mice showed decreased capacity to clear tumor cells.

Heat shock proteins (HSPs) were described as members of the DAMP family as well and published research supports their importance for anti-tumor immunity (90-92). The cross-presentation of soluble and cell-associated antigens was increased when complexed with HSPs (91;93-95). Human recombinant HSP70 did not induce maturation, as measured by surface expression of co-stimulatory molecules or cytokine secretion by DCs (93). Immune signalling therefore is probably not responsible for enhanced cross-presentation by HSPs. Increased uptake of antigen could account for this effect because intracellular peptide concentrations were higher when antigen was delivered in complex with HSP70. Similar results were obtained with the ER-resident protein calreticulin. Calreticulin can translocate to the plasma membrane during apoptosis, a condition in which it could function as a DAMP through facilitating increased target cell uptake by DCs (96). Supplementation of recombinant calreticulin to soluble antigen, however, did not result in enhanced cross-presentation (97) indicating that also calreticulin does not engage in immune signalling within DCs.

Finally, there is evidence for the involvement of the NLRP3 inflammasome in DC-mediated adaptive immune responses against tumors: the exposure of DCs to dying tumor cells activated within DCs the NLRP3 inflammasome which was dependent on expression of purinergic receptors (98). Purinergic receptors can bind ATP that was shown to be secreted by the dying cells. Inflammasome activation leads to caspase 1 activity, thereby facilitating the secretion of bioactive IL1 β . Indeed, caspase 1 and IL1-receptor knock-out mice showed the necessity for IL1 β secretion and sensitivity for cross-priming. Release of ATP by dying cells is therefore of great importance for anti-tumor immune responses. Alternatively, TLR ligands were also observed to stimulate NLRP3-dependent IL1 β production by DCs (99). Perhaps other DAMPs besides ATP may be responsible for inflammasome activation in DCs.

Altogether, for cross-presentation of cell-associated antigens many factors are involved which are either intrinsically expressed by DCs or present in the micro-environment (Table 1). Both an apoptotic cell death modality and DAMP release by necrotic cells are specifically important for induction of tumor-specific adaptive immune responses. At first glance, these observations do not seem to reconcile but this notion might actually be rash. As mentioned previously, apoptotic

Table 1. Factors that contribute to cross-presentation of tumor antigen by dendritic cells.

Intrinsic		Extrinsic	
	Ref.		Ref.
<u>Membrane receptors</u>		<u>Inflammatory cytokines</u>	
Clec9A	20	Type 1 interferons	73-76
Purinergic receptors	98	TNF	33
CD40	14	GM-CSF	13
TLR4	89	<u>DAMPs</u>	
HSP receptor	19	HMGB1	88, 89
Fcy receptor*	18, 21	Heat shock proteins	91, 93-95
DC-SIGN*	22	ATP	98
DEC-205*	16		
<u>Cytosolic proteins</u>			
Rab27a	63		
Rac2	66		
Nox2	66		

cells can also adopt a necrotic state when membrane integrity is eventually lost. The current definitions of apoptotic and necrotic cells suggest static conformations but may be considered as the same entity parted solely by time. As more research on this subject emerges, this apparent paradox will likely be resolved. The regulated changes that are associated with apoptosis are required to make the cells visible for DCs. Apoptotic cells are recognized and internalized, possibly encouraged by DAMPs such as calreticulin and HSPs, leading to degradation of the cellular material. Only when the DC expresses clec9A is the apoptotic cell redirected into storage compartments waiting for what will happen next. During recognition and internalization, the apoptotic cell will continue with the process of dying. One possibility is that apoptotic cells may undergo secondary necrosis within the phagosomes of the DC. Once necrosis within the phagosomal constraints happens, DAMPs will be released locally where they can bind to their receptors and actuate their immunogenic effect. Because clec9A ensures direction towards long-lived recycling compartments, chances are that recycled TLRs will encounter the DAMPs released by the dying cell. Alternatively, DAMPs can be released by surrounding dying cells that are not (yet) internalized. TLR signalling will activate DCs and cause their maturation, to support the subsequent priming of antigen-specific CD8⁺ T cells. In contrast, the direction of apoptotic cells towards degrading lysosomes should propagate full degradation and silent cell death. As such, features of apoptotic cells and DAMP release work together to establish optimal CD8⁺ T cell responses against cell-associated antigens. In particular, the apoptotic cells facilitate efficient uptake, storage and survival of the antigen whereas the DAMPs accomplish DC maturation and activation (Figure 3).

Concluding remarks

As we learn more about the process, it has become even more overt that cross-presentation of cell-associated antigens by DCs is a complex process. Many factors are involved that eventually

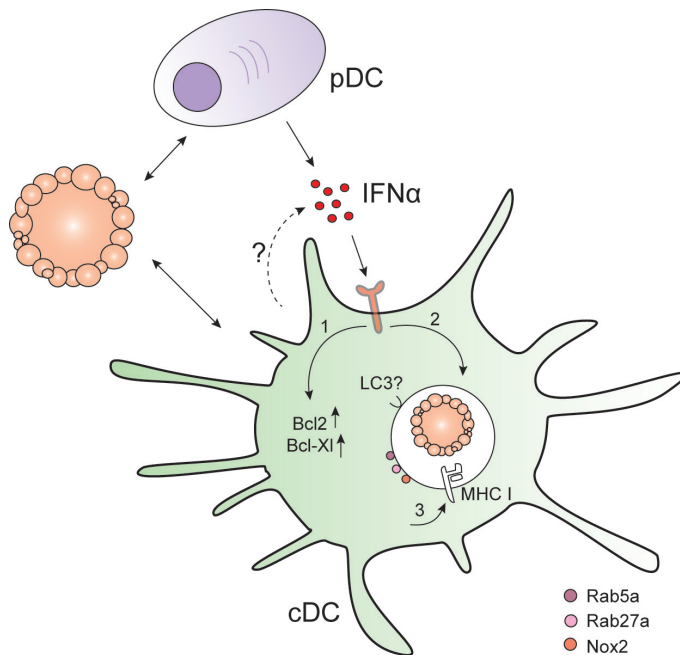


Figure 3. Type I interferon signaling influences antigen persistence within dendritic cells. Plasmacytoid DCs (pDC) and perhaps also conventional DCs (cDC) produce interferon α (IFN α) upon the recognition of apoptotic cells. The exposure of cDCs to IFN α results in 1) the upregulation of pro-survival factors such as BCL-2 and BCL-X_l; 2) the prolonged storage of apoptotic material in intracellular compartments; and 3) the localization of MHC class I molecules to storage compartments.

determine the outcome of a tumor-specific immune response. Important questions include whether some DC subsets have preference for cross-presenting antigens from certain forms of cell death and if there might be a combination of cell death and DAMPs that defines immunogenicity. In addition, much interest goes out to understanding the mechanisms of antigen loading and handling within DCs that lead to optimal cross-presentation and cross-priming of CD8 T cells. Whether DAMPs specifically contribute to antigen processing, we believe is important to understand how adaptive immune responses against tumor cells are raised. Particularly in regard to DC vaccines, which have become increasingly appealing as a treatment of tumor patients. Successes have been made with DC vaccines, but there is clear need for improvement. By elucidating the processes that are critical for the induction of sustained anti-tumor immune responses by DCs, we can continue improving DC vaccines and cancer treatments.

Acknowledgements

We acknowledge the Villa Joep Foundation, Ammodo, KiKa, Vrienden Wilhelmina Kinderziekenhuis en NWO/ZonMW for financial support (to S.N. and J.B.).

Reference List

- (1) Hanahan D, Weinberg RA. Hallmarks of cancer: the next generation. *Cell* 2011 Mar 4;144(5):646-74.
- (2) Rosenberg SA. Progress in the development of immunotherapy for the treatment of patients with cancer. *J Intern Med* 2001 Dec;250(6):462-75.
- (3) Vesely MD, Schreiber RD. Cancer immunoediting: antigens, mechanisms, and implications to cancer immunotherapy. *Ann N Y Acad Sci* 2013 May;1284:1-5.
- (4) Collin M, Bigley V, Haniffa M, Hambleton S. Human dendritic cell deficiency: the missing ID?. *Nat Rev Immunol* 2011 Sep;11(9):575-83.
- (5) Miller JC, Brown BD, Shay T, Gautier EL, Jovic V, Cohain A, et al. Deciphering the transcriptional network of the dendritic cell lineage. *Nat Immunol* 2012 Sep;13(9):888-99.
- (6) Joffre OP, Segura E, Savina A, Amigorena S. Cross-presentation by dendritic cells. *Nat Rev Immunol* 2012 Aug;12(8):557-69.
- (7) Steinman RM, Inaba K, Turley S, Pierre P, Mellman I. Antigen capture, processing, and presentation by dendritic cells: recent cell biological studies. *Hum Immunol* 1999 Jul;60(7):562-7.
- (8) Jung S, Unutmaz D, Wong P, Sano G, De los SK, Sparwasser T, et al. In vivo depletion of CD11c+ dendritic cells abrogates priming of CD8+ T cells by exogenous cell-associated antigens. *Immunity* 2002 Aug;17(2):211-20.
- (9) Banchereau J, Briere F, Caux C, Davoust J, Lebecque S, Liu YJ, et al. Immunobiology of dendritic cells. *Annu Rev Immunol* 2000;18:767-811.
- (10) Villadangos JA, Shortman K. Found in translation: the human equivalent of mouse CD8+ dendritic cells. *J Exp Med* 2010 Jun 7;207(6):1131-4.
- (11) Nierkens S, Tel J, Janssen E, Adema GJ. Antigen cross-presentation by dendritic cell subsets: one general or all sergeants?. *Trends Immunol* 2013 Mar 27.
- (12) Segura E, Durand M, Amigorena S. Similar antigen cross-presentation capacity and phagocytic functions in all freshly isolated human lymphoid organ-resident dendritic cells. *J Exp Med* 2013 May 6;210(5):1035-47.
- (13) Dresch C, Leverrier Y, Marvel J, Shortman K. Development of antigen cross-presentation capacity in dendritic cells. *Trends Immunol* 2012 Aug;33(8):381-8.
- (14) Toes RE, Schoenberger SP, van d, V, Offringa R, Melief CJ. CD40-CD40Ligand interactions and their role in cytotoxic T lymphocyte priming and anti-tumor immunity. *Semin Immunol* 1998 Dec;10(6):443-8.
- (15) Pang B, Neijssen J, Qiao X, Janssen L, Janssen H, Lippuner C, et al. Direct antigen presentation and gap junction mediated cross-presentation during apoptosis. *J Immunol* 2009 Jul 15;183(2):1083-90.
- (16) Bozzacco L, Trumpfheller C, Siegal FP, Mehandru S, Markowitz M, Carrington M, et al. DEC-205 receptor on dendritic cells mediates presentation of HIV gag protein to CD8+ T cells in a spectrum of human MHC I haplotypes. *Proc Natl Acad Sci U S A* 2007 Jan 23;104(4):1289-94.
- (17) Burgdorf S, Lukacs-Kornek V, Kurts C. The mannose receptor mediates uptake of soluble but not of cell-associated antigen for cross-presentation. *J Immunol* 2006 Jun 1;176(11):6770-6.
- (18) Flinsenberg TW, Compeer EB, Koning D, Klein M, Amelung FJ, van BD, et al. Fcgamma receptor antigen targeting potentiates cross-presentation by human blood and lymphoid tissue BDCA-3+ dendritic cells. *Blood* 2012 Dec 20;120(26):5163-72.
- (19) Murshid A, Gong J, Calderwood SK. The role of heat shock proteins in antigen cross presentation. *Front Immunol* 2012;3:63.
- (20) Sancho D, Joffre OP, Keller AM, Rogers NC, Martinez D, Hernanz-Falcon P, et al. Identification of a dendritic cell receptor that couples sensing of necrosis to immunity. *Nature* 2009 Apr 16;458(7240):899-903.
- (21) Schuurhuis DH, Ioan-Facsinay A, Nagelkerken B, van Schip JJ, Sedlik C, Melief CJ, et al. Antigen-antibody immune complexes empower dendritic cells to efficiently prime specific CD8+ CTL responses in vivo. *J Immunol* 2002 Mar 1;168(5):2240-6.
- (22) Tacken PJ, de V, I, Gijzen K, Joosten B, Wu D, Rother RP, et al. Effective induction of naive and recall T-cell responses by targeting antigen to human dendritic cells via a humanized anti-DC-SIGN antibody. *Blood* 2005 Aug 15;106(4):1278-85.
- (23) Kerr JF, Wyllie AH, Currie AR. Apoptosis: a basic biological phenomenon with wide-ranging implications in tissue kinetics. *Br J Cancer* 1972 Aug;26(4):239-57.
- (24) Wyllie AH, Kerr JF, Currie AR. Cell death: the significance of apoptosis. *Int Rev Cytol* 1980;68:251-306.

- (25) Vandenabeele P, Galluzzi L, Vanden BT, Kroemer G. Molecular mechanisms of necroptosis: an ordered cellular explosion. *Nat Rev Mol Cell Biol* 2010 Oct;11(10):700-14.
- (26) Edinger AL, Thompson CB. Death by design: apoptosis, necrosis and autophagy. *Curr Opin Cell Biol* 2004 Dec;16(6):663-9.
- (27) Kanduc D, Mittelman A, Serpico R, Sinigaglia E, Sinha AA, Natale C, et al. Cell death: apoptosis versus necrosis (review). *Int J Oncol* 2002 Jul;21(1):165-70.
- (28) Silva MT. Secondary necrosis: the natural outcome of the complete apoptotic program. *FEBS Lett* 2010 Nov 19;584(22):4491-9.
- (29) Fadok VA, de CA, Daleke DL, Henson PM, Bratton DL. Loss of phospholipid asymmetry and surface exposure of phosphatidylserine is required for phagocytosis of apoptotic cells by macrophages and fibroblasts. *J Biol Chem* 2001 Jan 12;276(2):1071-7.
- (30) Schnurr M, Scholz C, Rothenfusser S, Galambos P, Dauer M, Robe J, et al. Apoptotic pancreatic tumor cells are superior to cell lysates in promoting cross-priming of cytotoxic T cells and activate NK and gammadelta T cells. *Cancer Res* 2002 Apr 15;62(8):2347-52.
- (31) Strome SE, Voss S, Wilcox R, Wakefield TL, Tamada K, Flies D, et al. Strategies for antigen loading of dendritic cells to enhance the antitumor immune response. *Cancer Res* 2002 Mar 15;62(6):1884-9.
- (32) Manches O, Lui G, Molens JP, Sotto JJ, Chaperot L, Plumas J. Whole lymphoma B cells allow efficient cross-presentation of antigens by dendritic cells. *Cytotherapy* 2008;10(6):642-9.
- (33) Pietra G, Mortarini R, Parmiani G, Anichini A. Phases of apoptosis of melanoma cells, but not of normal melanocytes, differently affect maturation of myeloid dendritic cells. *Cancer Res* 2001 Nov 15;61(22):8218-26.
- (34) Ferlazzo G, Semino C, Spaggiari GM, Meta M, Mingari MC, Melioli G. Dendritic cells efficiently cross-prime HLA class I-restricted cytolytic T lymphocytes when pulsed with both apoptotic and necrotic cells but not with soluble cell-derived lysates. *Int Immunol* 2000 Dec;12(12):1741-7.
- (35) Fonteneau JF, Kavanagh DG, Lirvall M, Sanders C, Cover TL, Bhardwaj N, et al. Characterization of the MHC class I cross-presentation pathway for cell-associated antigens by human dendritic cells. *Blood* 2003 Dec 15;102(13):4448-55.
- (36) Albert ML, Sauter B, Bhardwaj N. Dendritic cells acquire antigen from apoptotic cells and induce class I-restricted CTLs. *Nature* 1998 Mar 5;392(6671):86-9.
- (37) Galetto A, Buttiglieri S, Forno S, Moro F, Mussa A, Matera L. Drug- and cell-mediated antitumor cytotoxicities modulate cross-presentation of tumor antigens by myeloid dendritic cells. *Anticancer Drugs* 2003 Nov;14(10):833-43.
- (38) Brusa D, Garetto S, Chiorino G, Scatolini M, Migliore E, Camussi G, et al. Post-apoptotic tumors are more palatable to dendritic cells and enhance their antigen cross-presentation activity. *Vaccine* 2008 Nov 25;26(50):6422-32.
- (39) Buttiglieri S, Galetto A, Forno S, De AM, Matera L. Influence of drug-induced apoptotic death on processing and presentation of tumor antigens by dendritic cells. *Int J Cancer* 2003 Sep 10;106(4):516-20.
- (40) Buckwalter MR, Srivastava PK. Mechanism of dichotomy between CD8+ responses elicited by apoptotic and necrotic cells. *Cancer Immun* 2013;13:2.
- (41) Gamrekelashvili J, Ormandy LA, Heimesaat MM, Kirschning CJ, Manns MP, Korangy F, et al. Primary sterile necrotic cells fail to cross-prime CD8(+) T cells. *Oncoimmunology* 2012 Oct 1;1(7):1017-26.
- (42) Janssen E, Tabeta K, Barnes MJ, Rutschmann S, McBride S, Bahjat KS, et al. Efficient T cell activation via a Toll-Interleukin 1 Receptor-independent pathway. *Immunity* 2006 Jun;24(6):787-99.
- (43) Ronchetti A, Rovere P, Iezzi G, Galati G, Heltai S, Protti MP, et al. Immunogenicity of apoptotic cells in vivo: role of antigen load, antigen-presenting cells, and cytokines. *J Immunol* 1999 Jul 1;163(1):130-6.
- (44) Scheffer SR, Nave H, Korangy F, Schlote K, Pabst R, Jaffee EM, et al. Apoptotic, but not necrotic, tumor cell vaccines induce a potent immune response in vivo. *Int J Cancer* 2003 Jan 10;103(2):205-11.
- (45) Henry F, Boisteau O, Bretaudeau L, Lieubeau B, Meflah K, Gregoire M. Antigen-presenting cells that phagocytose apoptotic tumor-derived cells are potent tumor vaccines. *Cancer Res* 1999 Jul 15;59(14):3329-32.
- (46) Hoffmann TK, Meidenbauer N, Dworacki G, Kanaya H, Whiteside TL. Generation of tumor-specific T-lymphocytes by cross-priming with human dendritic cells ingesting apoptotic tumor cells. *Cancer Res* 2000 Jul 1;60(13):3542-9.
- (47) Kotera Y, Shimizu K, Mule JJ. Comparative analysis of necrotic and apoptotic tumor cells as a source of antigen(s) in dendritic cell-based immunization. *Cancer Res* 2001 Nov 15;61(22):8105-9.

- (48) Uhl M, Kepp O, Jusforgues-Saklani H, Vicencio JM, Kroemer G, Albert ML. Autophagy within the antigen donor cell facilitates efficient antigen cross-priming of virus-specific CD8+ T cells. *Cell Death Differ* 2009 Jul;16(7):991-1005.
- (49) Schmitt E, Parcellier A, Ghiringhelli F, Casares N, Gurbuxani S, Droin N, et al. Increased immunogenicity of colon cancer cells by selective depletion of cytochrome C. *Cancer Res* 2004 Apr 15;64(8):2705-11.
- (50) Geiger JD, Hutchinson RJ, Hohenkirk LF, McKenna EA, Yanik GA, Levine JE, et al. Vaccination of pediatric solid tumor patients with tumor lysate-pulsed dendritic cells can expand specific T cells and mediate tumor regression. *Cancer Res* 2001 Dec 1;61(23):8513-9.
- (51) Palucka AK, Ueno H, Connolly J, Kerneis-Norvell F, Blanck JP, Johnston DA, et al. Dendritic cells loaded with killed allogeneic melanoma cells can induce objective clinical responses and MART-1 specific CD8+ T-cell immunity. *J Immunother* 2006 Sep;29(5):545-57.
- (52) Salcedo M, Bercovici N, Taylor R, Vereecken P, Massicard S, Duriau D, et al. Vaccination of melanoma patients using dendritic cells loaded with an allogeneic tumor cell lysate. *Cancer Immunol Immunother* 2006 Jul;55(7):819-29.
- (53) Schulz O, Reis e Sousa. Cross-presentation of cell-associated antigens by CD8alpha+ dendritic cells is attributable to their ability to internalize dead cells. *Immunology* 2002 Oct;107(2):183-9.
- (54) Iyoda T, Shimoyama S, Liu K, Omatsu Y, Akiyama Y, Maeda Y, et al. The CD8+ dendritic cell subset selectively endocytoses dying cells in culture and in vivo. *J Exp Med* 2002 May 20;195(10):1289-302.
- (55) Desch AN, Randolph GJ, Murphy K, Gautier EL, Kedl RM, Lahoud MH, et al. CD103+ pulmonary dendritic cells preferentially acquire and present apoptotic cell-associated antigen. *J Exp Med* 2011 Aug 29;208(9):1789-97.
- (56) Jongbloed SL, Kassianos AJ, McDonald KJ, Clark GJ, Ju X, Angel CE, et al. Human CD141+ (BDCA-3)+ dendritic cells (DCs) represent a unique myeloid DC subset that cross-presents necrotic cell antigens. *J Exp Med* 2010 Jun 7;207(6):1247-60.
- (57) Huysamen C, Willment JA, Dennehy KM, Brown GD. CLEC9A is a novel activation C-type lectin-like receptor expressed on BDCA3+ dendritic cells and a subset of monocytes. *J Biol Chem* 2008 Jun 13;283(24):16693-701.
- (58) Sancho D, Mourao-Sa D, Joffre OP, Schulz O, Rogers NC, Pennington DJ, et al. Tumor therapy in mice via antigen targeting to a novel, DC-restricted C-type lectin. *J Clin Invest* 2008 Jun;118(6):2098-110.
- (59) Zhang JG, Czabotar PE, Policheni AN, Caminschi I, Wan SS, Kitsoulis S, et al. The dendritic cell receptor Clec9A binds damaged cells via exposed actin filaments. *Immunity* 2012 Apr 20;36(4):646-57.
- (60) Zelenay S, Keller AM, Whitney PG, Schraml BU, Deddouche S, Rogers NC, et al. The dendritic cell receptor DNGR-1 controls endocytic handling of necrotic cell antigens to favor cross-priming of CTLs in virus-infected mice. *J Clin Invest* 2012 May 1;122(5):1615-27.
- (61) Lakadamyali M, Rust MJ, Zhuang X. Ligands for clathrin-mediated endocytosis are differentially sorted into distinct populations of early endosomes. *Cell* 2006 Mar 10;124(5):997-1009.
- (62) Delamarre L, Pack M, Chang H, Mellman I, Trombetta ES. Differential lysosomal proteolysis in antigen-presenting cells determines antigen fate. *Science* 2005 Mar 11;307(5715):1630-4.
- (63) Jancic C, Savina A, Wasmeier C, Tolmachova T, El-Benna J, Dang PM, et al. Rab27a regulates phagosomal pH and NADPH oxidase recruitment to dendritic cell phagosomes. *Nat Cell Biol* 2007 Apr;9(4):367-78.
- (64) Mantegazza AR, Savina A, Vermeulen M, Perez L, Geffner J, Hermine O, et al. NADPH oxidase controls phagosomal pH and antigen cross-presentation in human dendritic cells. *Blood* 2008 Dec 1;112(12):4712-22.
- (65) Savina A, Jancic C, Hugues S, Guermonprez P, Vargas P, Moura IC, et al. NOX2 controls phagosomal pH to regulate antigen processing during crosspresentation by dendritic cells. *Cell* 2006 Jul 14;126(1):205-18.
- (66) Savina A, Peres A, Cebrian I, Carmo N, Moita C, Hacohen N, et al. The small GTPase Rac2 controls phagosomal alkalization and antigen crosspresentation selectively in CD8(+) dendritic cells. *Immunity* 2009 Apr 17;30(4):544-55.
- (67) Burgdorf S, Kautz A, Bohnert V, Knolle PA, Kurts C. Distinct pathways of antigen uptake and intracellular routing in CD4 and CD8 T cell activation. *Science* 2007 Apr 27;316(5824):612-6.
- (68) van MN, Camps MG, Khan S, Filippov DV, Weterings JJ, Griffith JM, et al. Antigen storage compartments in mature dendritic cells facilitate prolonged cytotoxic T lymphocyte cross-priming capacity. *Proc Natl Acad Sci U S A* 2009 Apr 21;106(16):6730-5.
- (69) Reboulet RA, Hennies CM, Garcia Z, Nierkens S, Janssen EM. Prolonged antigen storage endows

- merocytic dendritic cells with enhanced capacity to prime anti-tumor responses in tumor-bearing mice. *J Immunol* 2010 Sep 15;185(6):3337-47.
- (70) Jusforgues-Saklani H, Uhl M, Blachere N, Lemaitre F, Lantz O, Bouso P, et al. Antigen persistence is required for dendritic cell licensing and CD8+ T cell cross-priming. *J Immunol* 2008 Sep 1;181(5):3067-76.
- (71) Heyder P, Bekeredjian-Ding I, Parcina M, Blank N, Ho AD, Herrmann M, et al. Purified apoptotic bodies stimulate plasmacytoid dendritic cells to produce IFN-alpha. *Autoimmunity* 2007 Jun;40(4):331-2.
- (72) Schiller M, Parcina M, Heyder P, Foermer S, Ostrop J, Leo A, et al. Induction of type I IFN is a physiological immune reaction to apoptotic cell-derived membrane microparticles. *J Immunol* 2012 Aug 15;189(4):1747-56.
- (73) Diamond MS, Kinder M, Matsushita H, Mashayekhi M, Dunn GP, Archambault JM, et al. Type I interferon is selectively required by dendritic cells for immune rejection of tumors. *J Exp Med* 2011 Sep 26;208(10):1989-2003.
- (74) Nierkens S, den Brok MH, Garcia Z, Togher S, Wagenaars J, Wassink M, et al. Immune adjuvant efficacy of CpG oligonucleotide in cancer treatment is founded specifically upon TLR9 function in plasmacytoid dendritic cells. *Cancer Res* 2011 Oct 15;71(20):6428-37.
- (75) Lorenzi S, Mattei F, Sistigu A, Bracci L, Spadaro F, Sanchez M, et al. Type I IFNs control antigen retention and survival of CD8alpha(+) dendritic cells after uptake of tumor apoptotic cells leading to cross-priming. *J Immunol* 2011 May 1;186(9):5142-50.
- (76) Spadaro F, Lapenta C, Donati S, Abalsamo L, Barnaba V, Belardelli F, et al. IFN-alpha enhances cross-presentation in human dendritic cells by modulating antigen survival, endocytic routing, and processing. *Blood* 2012 Feb 9;119(6):1407-17.
- (77) Henault J, Martinez J, Riggs JM, Tian J, Mehta P, Clarke L, et al. Noncanonical autophagy is required for type I interferon secretion in response to DNA-immune complexes. *Immunity* 2012 Dec 14;37(6):986-97.
- (78) Martinez J, Almendinger J, Oberst A, Ness R, Dillon CP, Fitzgerald P, et al. Microtubule-associated protein 1 light chain 3 alpha (LC3)-associated phagocytosis is required for the efficient clearance of dead cells. *Proc Natl Acad Sci U S A* 2011 Oct 18;108(42):17396-401.
- (79) Huang J, Brumell JH. NADPH oxidases contribute to autophagy regulation. *Autophagy* 2009 Aug;5(6):887-9.
- (80) Shimizu K, Asakura M, Shinga J, Sato Y, Kitahara S, Hoshino K, et al. Invariant NKT cells induce plasmacytoid dendritic cell (DC) cross-talk with conventional DCs for efficient memory CD8+ T cell induction. *J Immunol* 2013 Jun 1;190(11):5609-19.
- (81) Green DR, Ferguson T, Zitvogel L, Kroemer G. Immunogenic and tolerogenic cell death. *Nat Rev Immunol* 2009 May;9(5):353-63.
- (82) Hoves S, Sutton VR, Haynes NM, Hawkins ED, Fernandez RD, Baschuk N, et al. A critical role for granzymes in antigen cross-presentation through regulating phagocytosis of killed tumor cells. *J Immunol* 2011 Aug 1;187(3):1166-75.
- (83) Kroemer G, Galluzzi L, Kepp O, Zitvogel L. Immunogenic cell death in cancer therapy. *Annu Rev Immunol* 2013;31:51-72.
- (84) Krysko DV, Garg AD, Kaczmarek A, Krysko O, Agostinis P, Vandenabeele P. Immunogenic cell death and DAMPs in cancer therapy. *Nat Rev Cancer* 2012 Dec;12(12):860-75.
- (85) Basu S, Binder RJ, Suto R, Anderson KM, Srivastava PK. Necrotic but not apoptotic cell death releases heat shock proteins, which deliver a partial maturation signal to dendritic cells and activate the NF-kappa B pathway. *Int Immunol* 2000 Nov;12(11):1539-46.
- (86) Scaffidi P, Misteli T, Bianchi ME. Release of chromatin protein HMGB1 by necrotic cells triggers inflammation. *Nature* 2002 Jul 11;418(6894):191-5.
- (87) Sauter B, Albert ML, Francisco L, Larsson M, Somersan S, Bhardwaj N. Consequences of cell death: exposure to necrotic tumor cells, but not primary tissue cells or apoptotic cells, induces the maturation of immunostimulatory dendritic cells. *J Exp Med* 2000 Feb 7;191(3):423-34.
- (88) Rovere-Querini P, Capobianco A, Scaffidi P, Valentini B, Catalanotti F, Giazson M, et al. HMGB1 is an endogenous immune adjuvant released by necrotic cells. *EMBO Rep* 2004 Aug;5(8):825-30.
- (89) Apetoh L, Ghiringhelli F, Tesniere A, Criollo A, Ortiz C, Lidereau R, et al. The interaction between HMGB1 and TLR4 dictates the outcome of anticancer chemotherapy and radiotherapy. *Immunol Rev* 2007 Dec;220:47-59.
- (90) Chen X, Tao Q, Yu H, Zhang L, Cao X. Tumor cell membrane-bound heat shock protein 70 elicits antitumor immunity. *Immunol Lett* 2002 Nov 1;84(2):81-7.

- (91) Dai J, Liu B, Caudill MM, Zheng H, Qiao Y, Podack ER, et al. Cell surface expression of heat shock protein gp96 enhances cross-presentation of cellular antigens and the generation of tumor-specific T cell memory. *Cancer Immun* 2003 Jan 28;3:1.
- (92) Wang MH, Grossmann ME, Young CY. Forced expression of heat-shock protein 70 increases the secretion of Hsp70 and provides protection against tumour growth. *Br J Cancer* 2004 Feb 23;90(4):926-31.
- (93) Bendz H, Ruhland SC, Pandya MJ, Hainzl O, Riegelsberger S, Brauchle C, et al. Human heat shock protein 70 enhances tumor antigen presentation through complex formation and intracellular antigen delivery without innate immune signaling. *J Biol Chem* 2007 Oct 26;282(43):31688-702.
- (94) Kurotaki T, Tamura Y, Ueda G, Oura J, Kutomi G, Hirohashi Y, et al. Efficient cross-presentation by heat shock protein 90-peptide complex-loaded dendritic cells via an endosomal pathway. *J Immunol* 2007 Aug 1;179(3):1803-13.
- (95) Susumu S, Nagata Y, Ito S, Matsuo M, Valmori D, Yui K, et al. Cross-presentation of NY-ESO-1 cytotoxic T lymphocyte epitope fused to human heat shock cognate protein 70 by dendritic cells. *Cancer Sci* 2008 Jan;99(1):107-12.
- (96) Obeid M, Tesniere A, Ghiringhelli F, Fimia GM, Apetoh L, Perfettini JL, et al. Calreticulin exposure dictates the immunogenicity of cancer cell death. *Nat Med* 2007 Jan;13(1):54-61.
- (97) Del CN, Shen L, Belleisle J, Raghavan M. Assessment of roles for calreticulin in the cross-presentation of soluble and bead-associated antigens. *PLoS One* 2012;7(7):e41727.
- (98) Ghiringhelli F, Apetoh L, Tesniere A, Aymeric L, Ma Y, Ortiz C, et al. Activation of the NLRP3 inflammasome in dendritic cells induces IL-1beta-dependent adaptive immunity against tumors. *Nat Med* 2009 Oct;15(10):1170-8.
- (99) He Y, Franchi L, Nunez G. TLR agonists stimulate Nlrp3-dependent IL-1beta production independently of the purinergic P2X7 receptor in dendritic cells and in vivo. *J Immunol* 2013 Jan 1;190(1):334-9.

Chapter 3

Endocytosed soluble cowpox virus protein CPXV012 inhibits antigen cross-presentation in human monocyte-derived dendritic cells.



Authors

Lotte Spel*, Rutger D. Luteijn*, Jan W. Drijfhout, Stefan Nierkens, Marianne Boes^, Emmanuel J.H. Wiertz^

* Equal contribution, ^ Shared supervision

Published in

Immunology & Cell Biology 2017

Abstract

Viruses may interfere with the MHC class I antigen presentation pathway in order to avoid CD8⁺ T cell-mediated immunity. A key target within this pathway is the peptide transporter TAP. This transporter plays a central role in MHC class I-mediated peptide presentation of endogenous antigens. In addition, TAP plays a role in antigen cross-presentation of exogenously derived antigens by dendritic cells (DCs). In this study, a soluble form of the cowpox virus TAP inhibitor CPXV012 is synthesized for exogenous delivery into the antigen cross-presentation route of human monocyte-derived (mo)DCs. We show that soluble CPXV012 localizes to TAP⁺ compartments that carry internalized antigen and is a potent inhibitor of antigen cross-presentation. CPXV012 stimulates the prolonged deposition of antigen fragments in storage compartments of moDCs, as a result of reduced endosomal acidification and reduced antigen proteolysis when soluble CPXV012 is present. Thus, a dual function can be proposed for CPXV012: inhibition of TAP-mediated peptide transport and inhibition of endosomal antigen degradation. We propose this second function for soluble CPXV012 can serve to interfere with antigen cross-presentation in a peptide transport-independent manner.

Introduction

Cytotoxic CD8⁺ T lymphocytes (CTLs) are vital for the defense against cancerous or virus-infected cells. CTLs mount an immune response upon recognition of antigenic peptides presented by MHC class I (MHC I) molecules on the surface of target cells. In most cells, the peptides presented by MHC I are derived from proteasomal degradation of cytosolic proteins. The generated peptides are subsequently transported into the ER by the transporter associated with antigen processing (TAP). TAP and other proteins of the MHC I peptide-loading complex ensure proper loading of peptides into the peptide-binding groove of MHC I molecules. Upon successful peptide loading, MHC I travels from the ER to the cell surface, where it displays its peptide cargo to CD8⁺ T cells. Besides its prominent role in presentation of antigens derived from intracellular proteins, MHC I can also function in presentation of exogenous antigens in certain cell types. This process, called antigen cross-presentation, plays an important role in the activation of naive CD8⁺ T cells by antigen presenting cells (APCs), most notably by dendritic cells (DCs) ¹⁻³. Cross-presentation requires phagocytosis of extracellular antigen and subsequent endosomal processing ⁴. In addition, proteins typically involved in endogenous MHC I antigen presentation may also play a role in cross-presentation, including the proteasome and TAP ⁴⁻⁹.

Upon exogenous antigen uptake by DCs, two main pathways are involved in MHC I antigen cross-presentation (reviewed in ¹⁰⁻¹⁴). A TAP-independent vacuolar pathway requires lysosomal acidification and subsequent antigen degradation by endolysosomal proteases. The generated peptides are directly loaded onto MHC I molecules in endo-lysosomal compartments ¹⁵⁻²¹. A second, TAP-dependent, cross-presentation pathway involves the translocation of phagocytosed cargo into the cytosol. There, the proteins are degraded into peptides by the proteasome. These peptides are translocated by TAP into the ER lumen for access to the endogenous MHC I loading route. Alternatively, peptides may be re-imported into the endo-lysosomal compartment by endosomal TAP ⁶⁻⁸ for access to recycling MHC I molecules ^{9, 22, 23}. Human dendritic cells generally depend on both TAP-dependent and -independent pathways for antigen cross-presentation ^{4, 24-26}. The preferred pathway for cross-presentation may vary depending on the nature and size of the internalized antigen.

Various viruses have developed proteins to tackle critical nodes in the MHC I presentation pathway, including TAP. Through TAP inhibition, viruses interfere with MHC I presentation of viral peptides, thereby avoiding T cell immunity ²⁷⁻³³. To date, viral TAP inhibitors are found in herpesviruses, including herpes simplex virus, varicelloviruses, human cytomegalovirus and Epstein-Barr virus ³⁴, and several cowpox virus (CPXV) strains ^{33, 35, 36}. By blocking TAP, these viral inhibitors deprive MHC I molecules from antigenic peptides and interfere with the subsequent induction of a robust CTL response.

Recently, the mechanism of action of the cowpox virus-derived TAP inhibitor CPXV012 was elucidated ^{36, 37}. CPXV012 is a type II transmembrane protein that localizes to the ER. Here, it directly binds to TAP and blocks peptide transport by steric interference with ATP binding. The ER-luminal domain of CPXV012 is necessary and sufficient for this inhibitory effect ³⁶.

Here, we made use of the luminal active domain of CPXV012 (soluble CPXV012; sCPXV012) outside the physiological context of CPXV infection and tested its effects during exogenous delivery into endosomes of human DCs. We found sCPXV012 to inhibit antigen cross-presentation without affecting antigen uptake or MHC I surface display. Soluble CPXV012 is internalized into

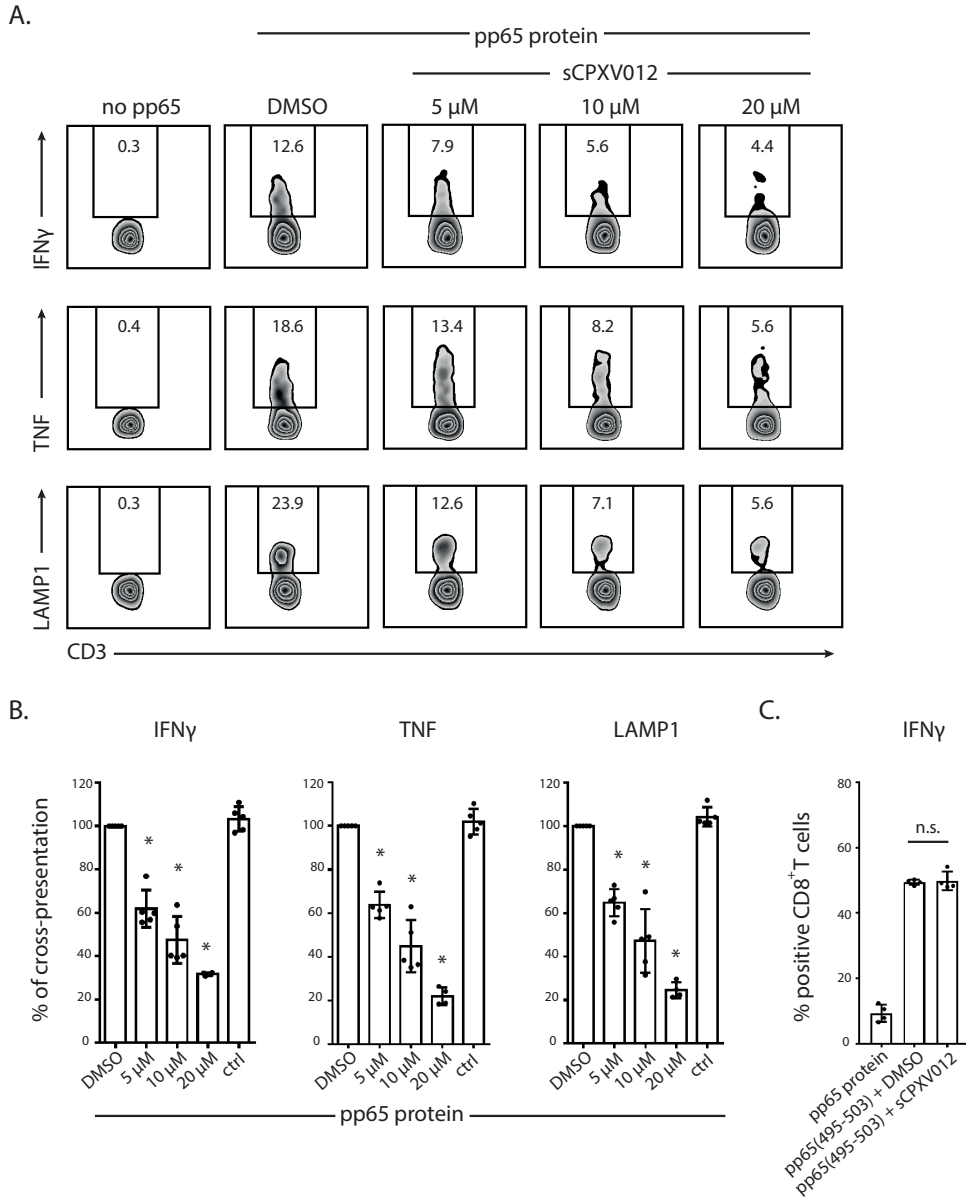


Figure 1. Levels of antigen cross-presentation in CPXV012-treated moDCs (n=5). Human moDCs were cultured, harvested and replated in the absence of presence of soluble CPXV012 or control peptide. After 2 hours, 3 μ g pp65 antigen (A and B) or 10^{-7} M pre-processed pp65(495-503) (C) was added to the culture. The next day, pp65-specific CTLs were added to the moDCs in a 1:1 ratio in the presence of Golgi-stop. After 4,5 hours, activation of the CTLs was evaluated by determining intracellular levels of IFN γ and TNF, and surface LAMP1 expression by antibody staining. Expression levels were measured by flow cytometry. Statistical analysis was performed on (B) treated conditions compared to DMSO control using one-sample t-tests and (C) comparison between treated conditions using Mann-Whitney U test, $p < 0.05$ were considered significant.

TAP⁺LAMP1⁺ compartments that also include internalized antigen. Surprisingly, sCPXV012 blocks endosomal acidification, which results in antigen preservation and thus, reduced production of antigenic peptides for MHC I presentation. We identified the soluble CPXV012 protein, previously characterized as a potent inhibitor of TAP, to inhibit antigen cross-presentation in DCs through a second, TAP-independent mechanism. To our knowledge, this is the first protein-based compound to interfere with endosomal acidification.

Results

Soluble CPXV012 inhibits antigen cross-presentation. The cowpox virus protein CPXV012 interferes with the MHC I antigen presentation pathway by blocking TAP in the ER^{33, 35-37}. The TAP-inhibiting domain of CPXV012 is located in the ER-luminal 35 amino acid residues of CPXV012³⁶. Endogenous expression of the active domain of CPXV012 is sufficient for TAP inhibition and preventing MHC I antigen presentation at the cell surface³⁶. To evaluate the ability of the CPXV012 active domain to interfere with cross-presentation of exogenous antigen by dendritic cells, a synthetic peptide comprising amino acid residues 35-69 of full length CPXV012, sCPXV012, was prepared. The inhibitory capacity of sCPXV012 was tested in a cross-presentation assay using human monocyte-derived dendritic cells (moDCs). In this assay, moDCs are incubated with the viral antigen pp65. This results in endocytosis and processing of pp65, and MHC I-mediated presentation of pp65-derived peptides⁴. We have shown previously that pp65 cross-presentation can occur through both the cytosolic and the vacuolar pathway⁴. MHC I-mediated cross-presentation of pp65-derived peptides was measured using MHC I-restricted pp65-specific CTLs. Activation of the CTLs upon cognate interaction was evaluated by measuring LAMP1 (CD107 α) surface expression and intracellular IFN γ and TNF cytokine production (figure 1). The addition of sCPXV012 reduced antigen cross-presentation in a concentration-dependent manner. At the highest concentration of sCPXV012 (20 μ M), cytokine production and LAMP1 expression by CTLs was reduced by 70-80% (figure 1). At lower concentrations of sCPXV012, cytokine production and LAMP1 expression by CTLs was reduced to 50-60% (using 10 μ M sCPXV012) or 35-40% (using 5 μ M sCPXV012). As negative controls, we included DMSO only or an irrelevant peptide, both showing no effect on antigen cross-presentation by moDCs (figure 1B). sCPXV012 did not change general MHC I surface expression levels (figure S1), suggesting that endogenous peptide presentation is not hampered. Indeed, T cell activation through direct presentation of pre-processed pp65(495-503) peptide remained unchanged in the presence of sCPXV012 (figure 1C). These combined results indicate that exogenous addition of sCPXV012 can inhibit antigen cross-presentation of pp65 by moDCs.

Identification of the minimal region in sCPXV012 required for inhibition of cross-presentation.

To identify the amino acid residues within the active domain of sCPXV012 that are crucial for inhibition of cross-presentation, a series of sCPXV012 peptide variants were synthesized and tested (figure 2).

Stretches of five amino acids were replaced by alanine residues in sCPXV012 (figure 2A). The viability of moDCs was not affected when incubated with sCPXV012 peptide variants (data not shown). The peptides were added to moDCs in the presence of pp65 antigen, and pp65-specific CTL activation was measured (figure 2B). In these experiments, wild type sCPXV012

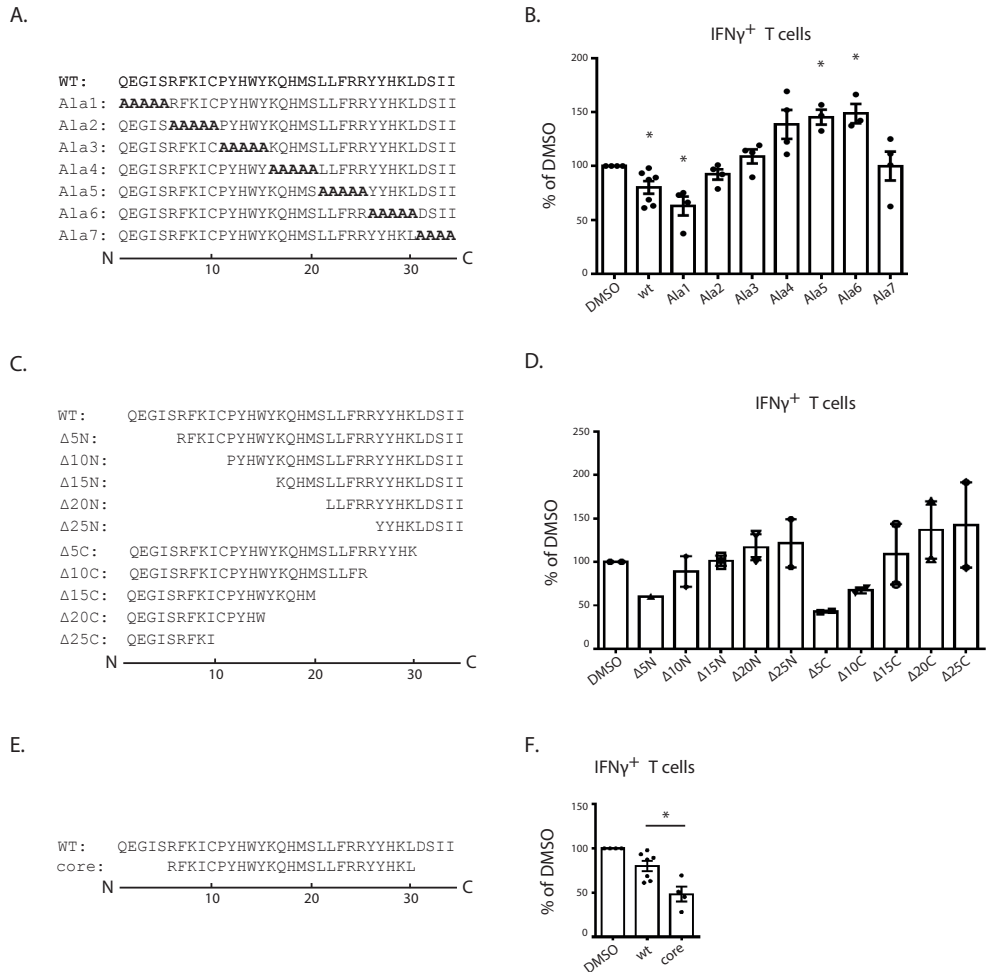


Figure 2. CPXV012 core domain facilitates inhibition of antigen cross-presentation (n=4). A, C and E. Overview of soluble mutant CPXV012 peptides used. In each variant, a stretch of five amino acids is replaced by alanine residues. B, D and F. Antigen cross-presentation by human monocyte-derived dendritic cells in the absence or presence of 5 μ M of the indicated CPXV012 peptide variants. Data are shown as % of DMSO control. Statistical analysis was performed on (B) treated conditions compared to DMSO control using one-sample t-tests and (F) comparison between treated conditions using Mann-Whitney U test, $p < 0.05$ were considered significant.

reduced cross-presentation to 80% of the levels of untreated moDCs. Replacement of the first 5 N-terminal amino acids by alanine residues (Ala1) increased the inhibitory activity of sCPXV012 almost two-fold, to approximately 63% of the levels of untreated moDCs, whereas peptides Ala2-Ala7 showed no inhibition at all. In fact, Ala5 and Ala6 even increased the amount of activated pp65-specific CTLs possibly suggesting an increase of antigen cross-presentation.

In addition to alanine-substituted peptides, we synthesized peptides that were truncated at the N- or C-terminus (figure 2C). Soluble CPXV012 with 5 N-terminal amino acid residues removed (Δ 5N) robustly inhibited antigen cross-presentation (figure 2D). Further N-terminal truncations

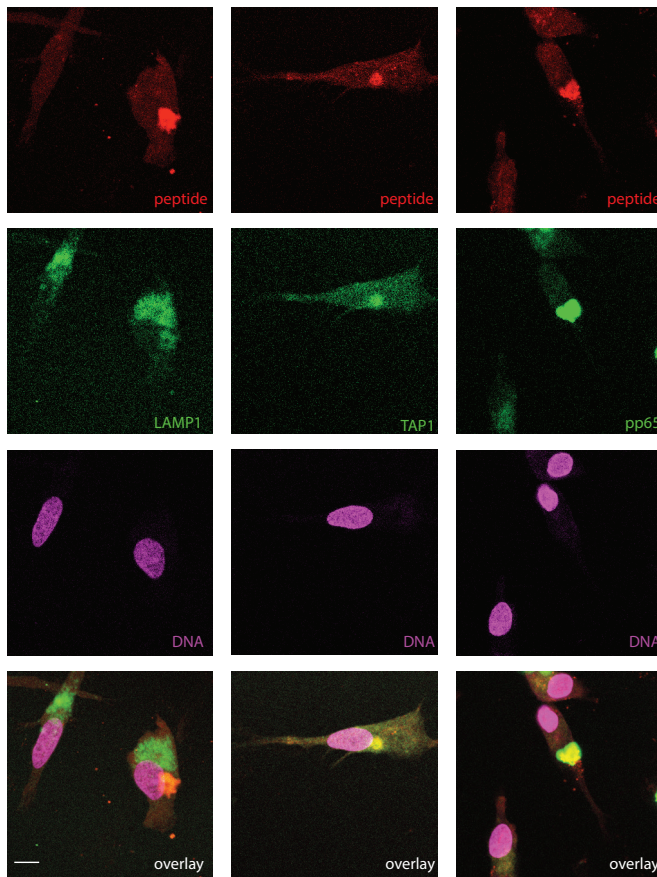


Figure 3. CPXV012 core peptide and pp65 antigen are taken up into TAP⁺LAMP1⁺ compartments (n=3). Confocal images of human moDCs loaded with CPXV012 core peptide for 2 hours, followed by pp65 internalization for four more hours. DCs were stained for either LAMP1, TAP1 or pp65. Overlays are shown in the bottom panel. Each column represents a distinct visual field. Bar size: 7.5 μ m.

3

of sCPXV012 abolished its inhibitory activity. The C-terminally truncated peptides Δ 5C and Δ 10C also inhibited antigen cross-presentation, but removal of 15 or more C-terminal amino acid residues completely abrogated the inhibitory activity of sCPXV012.

Previous mutagenesis studies on endogenously expressed full length CPXV012 indicated that the core 25 amino acid residues in the active domain are crucial for TAP inhibition, whereas residues 1-5 and 31-34 are dispensable³⁶. In line with this study, the results obtained with the peptide variants indicate that a core region, represented by amino acid residues 6-30 of sCPXV012, is essential for its inhibitory function. Therefore, a smaller CPXV012 peptide was tested, comprising these 25 amino acid residues (figure 2E). This core peptide showed superior inhibitory capacity compared to wild type sCPXV012 as well as the other peptide variants tested (figure 2F). Thus, sCPXV012 contains a core domain that allows for highly effective inhibition of antigen cross-presentation when delivered to human moDCs exogenously.

Co-localisation of antigen and sCPXV012 in LAMP1⁺ compartments. Antigens endocytosed by DCs are routed to various compartments of the endolysosomal pathway. Specific antigen storage compartments facilitate efficient loading of MHC I with peptides^{6, 12, 22, 38-40}. In these LAMP1⁺ and

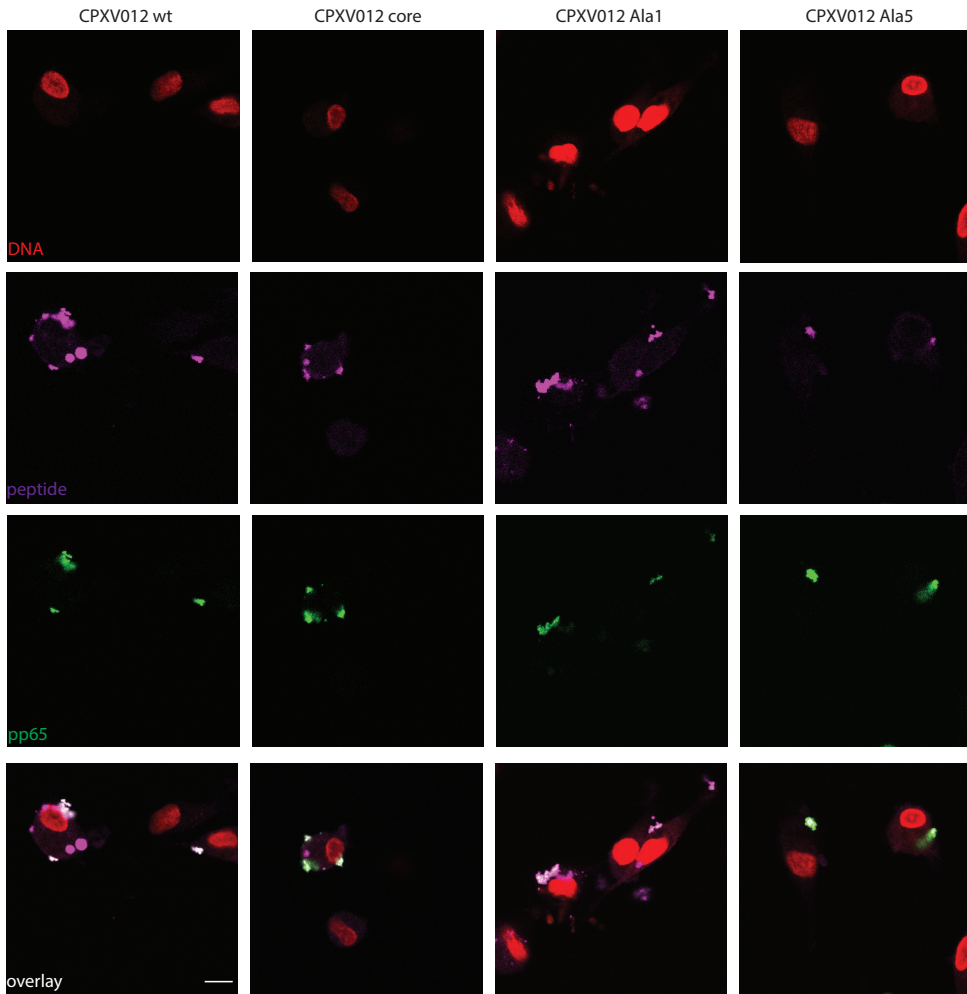


Figure 4. CPXV012 peptide variants localize to endosomal compartments also containing internalized pp65 antigen (n=3). Confocal images of human moDCs loaded with CPXV012 peptide variants (2hrs) and pp65 antigen (4hrs), respectively. Overlays are shown in the bottom panel. Each column represents a distinct visual field. Bar size: 7.5 μ m.

TAP⁺ compartments, antigen is further processed for cross-presentation by MHC I.

To test whether sCPXV012 is directed to LAMP1⁺TAP⁺ compartments after uptake by moDCs, the intracellular location of the sCPXV012 core peptide was visualized in moDCs using confocal microscopy. MoDCs were exposed to sCPXV012 core peptide for 2 hours prior to incubation with pp65 antigen. After 4 hours, cells were stained for sCPXV012 peptide and either LAMP1, TAP1, or pp65 (figure 3). Soluble CPXV012 core peptide was internalized by dendritic cells and partially colocalized with LAMP1 and TAP1. In addition, sCPXV012 core peptide showed strong colocalization with pp65 antigen. These results indicate that both sCPXV012 core peptide and pp65 are endocytosed and colocalize in part to the TAP1⁺ and LAMP1⁺ antigen storage compartment.

Not all sCPXV012 variants efficiently inhibited cross-presentation (see figure 2). This may result from a lack of inhibitory activity, or inefficient trafficking to pp65⁺ antigen storage compartments after uptake of CPXV012 peptide by moDCs. Therefore, colocalization of inhibitory and non-inhibitory CPXV012 variants and pp65 was investigated 4 hours after incubation with moDCs (figure 4).

Similar to the uptake of CPXV012 core peptide (figure 3), Ala1, Ala5 and the wild type CPXV012 peptide were endocytosed and colocalized with pp65. Although Ala5 lost its capacity to inhibit cross-presentation (figure 2B), it still traffics to pp65⁺ intracellular compartments, and its intracellular location is similar to that of the peptides still inhibiting cross-presentation. These results show that the differences in MHC I cross-presentation inhibition by sCPXV012 are not explained by differential uptake of the sCPXV012 peptide variants.

Preservation of pp65 protein in the presence of sCPXV012. Cross-presentation of internalized antigen requires degradation of the antigen for the release of antigenic peptides, suitable for loading onto MHC I molecules. To investigate whether sCPXV012 interferes with the process of antigen break-down we measured the levels of pp65 antigen in dendritic cells.

Dendritic cells were loaded with sCPXV012 for 2 hours after which pp65 antigen was added for another 4 hours. Then, DCs were harvested and stained intracellularly with anti-pp65 antibodies. WT sCPXV012-treated moDCs contained higher levels of pp65 antigen compared to DMSO-treated control cells (Figure 5). Similarly, treatment with Ala1 or core peptide also showed increased presence of pp65 antigen. In contrast, the non-inhibitory peptide Ala5 failed to enhance intracellular pp65 antigen levels.

Thus, inhibition of cross-presentation by sCPXV012 coincides with increased intracellular antigen levels, suggesting a role for sCPXV012 in antigen preservation within endosomes.

Soluble CPXV012 inhibits antigen degradation by blocking endosomal acidification. As sCPXV012 causes retention of intracellular antigen in moDCs, we tested the effects of sCPXV012 on antigen degradation. To this end, sCPXV012 was added to moDCs in combination with DQ-BSA, a protein that releases fluorescence upon degradation within the endosomal pathway. Four hours after uptake, the fluorescence within moDCs was measured (figure 6A). While BSA uptake was similar between the tested conditions (figure 6A, right panel), moDCs incubated with WT sCPXV012 showed less fluorescence compared to DMSO-treated moDCs when using protease-sensitive DQ-BSA (figure 6A, left panel) indicating blocked protein degradation. Accordingly, mutant sCPXV012 peptides with superior inhibitory capacity (Ala1 and core) further inhibited protein degradation. Furthermore, protein degradation levels measured in moDCs treated with the non-inhibitory Ala5 peptide was comparable to the levels of the DMSO control.

Endosomal proteolysis is dependent on the activity of proteases within the endosome and is regulated by the pH. For optimal proteolysis, an acidic environment is required established by proton influx into the endosomes, as mediated by vacuolar ATPase proton pumps⁴¹. Soluble CPXV012 may thus inhibit protein degradation by preventing acidification of endosomes. The endosomal pH was tested by adding sCPXV012 to dendritic cells in combination with pHRododextran, a compound eliciting fluorescence in acidic environments (figure 6B). DMSO-treated control DCs showed the highest fluorescence, indicating normal endosomal acidification. Acidification was prevented by sCPXV012 peptide, as the fluorescence measured in these moDCs

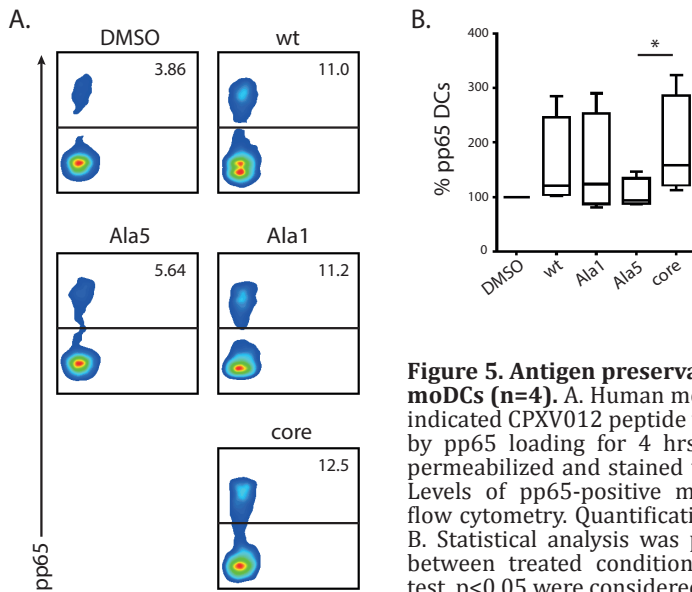


Figure 5. Antigen preservation in CPXV012-treated moDCs (n=4). A. Human moDCs were loaded with the indicated CPXV012 peptide variants for 2 hrs, followed by pp65 loading for 4 hrs. moDCs were harvested, permeabilized and stained with anti-pp65 antibodies. Levels of pp65-positive moDCs were measured by flow cytometry. Quantification of the data is shown in B. Statistical analysis was performed on comparison between treated conditions using Mann-Whitney U test, $p < 0.05$ were considered significant.

was significantly decreased. Similarly, Ala1 and core peptides that inhibited cross-presentation as well as DQ-BSA proteolysis, also blocked endosomal acidification. In contrast, Ala5 peptide, which lacks inhibition of cross-presentation or DQ-BSA proteolysis indeed shows higher pH-dependent fluorescence compared to WT sCPXV012. The inability of antigen cross-presentation in the presence of sCPXV012 strongly correlated with a decrease in antigen processing in the presence of sCPXV012, showing a Spearman rank correlation coefficient of $R = 0.833$ (figure 6C). Altogether, sCPXV012 interferes with the antigen cross-presentation abilities of moDCs through prevention of endosomal acidification. This results in antigen preservation rather than degradation into antigenic peptides.

Discussion

When endogenously expressed, the active domain of CPXV012 is present in the ER lumen where it limits the availability of peptides for loading onto class I complexes, through blockage of the TAP transporter^{33, 35-37}. During CPXV infection, direct antigen presentation by infected cells is therefore blocked while antigen cross-presentation by DCs was not affected⁴². In this study, we take the active domain of CPXV012 outside its physiological context of CPXV infection and show that it is able to inhibit antigen cross-presentation when exogenously delivered to moDCs. Soluble CPXV012 is internalized into LAMP1⁺ endosomal compartments that carry TAP in their membrane. Pp65 antigen is also targeted to these compartments, where it is processed for cross-presentation. Unexpectedly, sCPXV012 interferes with the endosomal processing of antigen by blocking acidification of the endosome, thereby preventing antigen proteolysis. Thus, we show a second function for CPXV012, in interfering with DC antigen cross-presentation in a TAP-independent manner.

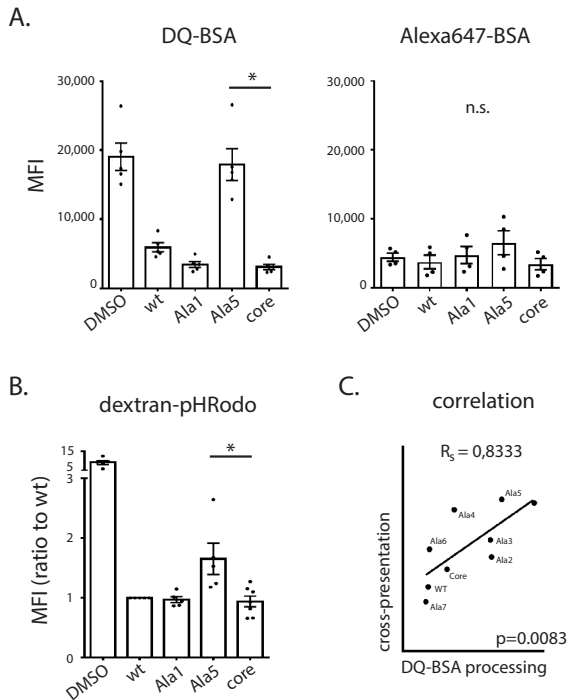


Figure 6. CPXV012 blocks antigen processing in dendritic cells (n=5). Human moDCs were loaded with the indicated CPXV012 peptide variants for 2 hrs, followed by DQ-BSA (A, left panel), Alexa647-BSA (A, right panel) or pHRodo-dextran (B) loading for 4 hrs. DCs were harvested and levels of fluorescence were measured by flow cytometry. C. Cross-presentation data (figure 2B) and DQ-BSA processing data (figure 6A, left panel) of sCPXV012 peptide variants were tested for correlation using Spearman's rank correlation test. Statistical analysis was performed on comparison between treated conditions using Mann-Whitney U test, $p < 0.05$ were considered significant.

3

The TAP-independent vacuolar pathway of cross-presentation includes antigen processing and MHC I loading within endo-lysosomal compartments. Several reports indicate that antigen cross-presentation can depend exclusively on the vacuolar pathway¹⁷⁻¹⁹. Inhibition of endosomal acidification^{17, 19} or endosomal proteases^{17, 18} abrogated cross-presentation through TAP-independent pathways. Our study shows that sCPXV012 inhibits antigen cross-presentation by preventing antigen degradation. Upon entering the endosomal pathway through endocytosis, sCPXV012 can block antigen cross-presentation through interference with pH-dependent antigen degradation, separate from its function as TAP inhibitor.

Our finding that sCPXV012 can target pH-dependent endosomal antigen degradation is relevant, as for both TAP-dependent and TAP-independent pathways of antigen cross-presentation, endosomal proteolysis is considered crucial^{4, 16, 43-45}.

In addition, sCPXV012 may directly affect the TAP-dependent cross-presentation pathway by inhibiting TAP in the endosome. CPXV012 peptide was shown to act on the luminal domain of TAP³⁶ which is accessible from inside the endosome. As CPXV012 peptide localizes to TAP⁺ compartments, it is possible that endosomal TAP is inhibited by CPXV012 peptide. In line with this, the inhibitory capacity of CPXV012 alanine variants correlates well with the ability of full-length endogenously-expressed CPXV012 variants to inhibit peptide transport by TAP³⁶. There, TAP inhibition was observed for full-length variants with an intact core domain exactly corresponding to those variants that showed inhibitory activity against cross-presentation in the study presented here.

Possibly, inhibition of endosomal acidification may even promote the TAP-dependent antigen-

cross presentation route ⁴⁶, but such analysis falls beyond the scope of our manuscript. Our data do however support that sCPXV012 might have a dual role by inhibiting both endosomal acidification and blocking import of antigens by TAP.

Nevertheless, without excluding a possible role for sCPXV012 blocking endosomal TAP, the pronounced inhibition of antigen proteolysis by sCPXV012 observed in the current study smother antigen cross-presentation directly at initiation. Thereby, sCPXV012 is the first protein-based compound to block endosomal acidification. Other acidification inhibitors include lysomotropic agents such as chloroquine, ammonium chloride or siramesine that broadly block acidification of the entire endo-lysosomal pathway within the cell. A protein-based acidification inhibitor offers the possibility of affecting specific compartments using targeted delivery by antibody-receptor engagement or by fusion to ligands. CPXV012 peptide can thus be used to investigate the role of acidification in different endosomal uptake routes, including pathways used by plasma membrane proteins and intracellular pathogens.

Methods

Reagents and antibodies. DQ-BSA (Cat. D12050), pHRodo-dextran (Cat. P10361), Hoechst (Cat. H1399) and TO-PRO3 (T3605) were purchased from Thermo Fisher Scientific. Antibodies used: anti-HLA-A/B/C (Clone W6/32, Biolegend); anti-CD11c (Clone B-Ly6, BD Biosciences); anti-CD3 (Clone UCHT1, Sony Biotechnology); anti-CD8 (Clone RPA-T8, BD Biosciences); anti-LAMP1 (Clone H4A3, BD Biosciences); anti-TNF (Clone MAB11, Sony Biotechnology); anti-IFN γ (Clone 4S.B3, BD Biosciences); anti-MHC-I (W6/32, Sony Biotechnology); anti-pp65 mouse mAb (Advanced Biotechnologies Inc, Eldersburg, MD, USA); anti-TAP1 (clone 148.3, EMD Millipore); anti-mouse FITC-conjugated donkey pAb (Jackson ImmunoResearch); Cy3-conjugated streptavidin (Jackson ImmunoResearch).

CPXV012 peptide synthesis. The sequences of the CPXV012 peptide variants are indicated in Fig. 2. The control peptide is derived from the ER-luminal domain of pseudorabies virus TAP inhibitor UL49.5, and comprises amino acid residues 28-59 of this protein (sequence: STEGPLLLREESRINFWNAACAARGVPVDQP). The ER-luminal domain of UL49.5 is not capable of inhibiting TAP when expressed in cells ⁴⁷ or when added as a peptide (figure 1B). Synthetic peptides were prepared by normal Fmoc chemistry using preloaded Tentagel resins, using PyBop/N-methylmorpholine for in situ activation and 20% piperidine in N-methylpyrrolidinon for Fmoc removal ⁴⁸. Couplings were performed for 75 min. After final Fmoc removal, peptides were cleaved with trifluoroacetic acid/H₂O 19:1 v/v containing additional scavengers when C or W residues were present in the peptide sequence. Peptides were isolated by ether/pentane precipitation and checked for purity using reversed-phase UPLC–mass spectrometry. The integrity was tested using MALDI-TOF mass spectrometry. Cysteines were replaced by the isosteric alpha-amino-n-butyric acid. Lyophilized peptides were dissolved in DMSO. Peptide concentrations were confirmed by the NanoDrop spectrophotometer (Thermo Scientific) using the absorbance of Trp at 280 nm. Peptides were aliquoted in Eppendorf LoBind microcentrifuge tubes (Sigma-Aldrich) and kept at -20 °C for short-term storage.

Human monocyte-derived DC culture. Peripheral blood mononuclear cells (PBMCs) from healthy donors were separated from peripheral blood by ficoll isopaque density gradient centrifugation (GE Healthcare Bio-Sciences AB). CD14⁺ monocytes were isolated by positive selection with CD14 MACS beads (Miltenyi). CD14⁺ cells were cultured at a concentration of 1×10^6 /ml for 5 days at 37°C and 5% CO₂ in X-VIVO15 medium containing 450 U/mL GM-CSF (Immunotools) and 300 U/mL IL-4 (Immunotools). Cytokines were refreshed after 3 days. DCs were collected for experiments on day 5 by incubation in PBS (4°C) for 1 hour. Generally, moDCs cultured from at least 3 different donors were used for experiments.

Cross-presentation assay. A HCMV pp65-specific CD8⁺ T-cell clone was prepared previously ⁴. In brief, T-cells from an HLA-A*0201⁺ donor were stained with HLA-A2/pp65₄₉₅₋₅₀₃ tetramers, and subsequently single-cell sorted in a 96-well plate (Thermo) containing irradiated B-LCL feeder cells (1×10^5 cells/mL, irradiated with 70 Gy) and PBMCs from 3 healthy donors (1×10^6 cells/mL, irradiated with 30 Gy). One µg/mL leucoagglutinin PHA-L (Sigma-Aldrich) and 120 U/mL of recombinant IL-2 (Immunotools) were added. T-cell clones specific to pp65₄₉₅₋₅₀₃ were selected using tetramer staining. Positive clones were restimulated and expanded during several stimulation cycles and frozen in aliquots that were freshly thawed before each use in an assay. DCs were loaded with soluble HCMV pp65 protein (Miltenyi Biotec, purity > 95%, low endotoxin; < 10 EU/mL) and incubated overnight at 37°C and 5% CO₂ for processing. HCMV pp65-specific CD8⁺T cells were cocultured with pp65-loaded DCs for 4 to 6 hours in the presence of Golgistop (1/1500; BD Bioscience). Cells were subsequently stained for surface markers and presence of intracellular IFN γ and TNF, followed by flow cytometry-based analysis.

Flow cytometry. For stainings, cells were first washed twice in PBS containing 2% FCS (Invitrogen) and 0.1% sodium azide (NaN₃ Sigma-Aldrich). Next, antigen nonspecific binding was prevented by prior incubation of cells with 10% mouse serum (Fitzgerald). Cells were incubated with indicated fluorophore-conjugated mouse anti-human antibodies for 20 minutes on ice and washed twice. In case of intracellular stainings, cells were fixed and permeabilized (Fix/Perm kit BD Biosciences) after surface staining and subsequently stained with indicated antibodies for 30 minutes on ice and washed twice. Cells were taken up in PBS (2% FCS/0,1% NaN₃) to be used for measurement using either FACSCanto II or Fortessa with FACS Diva Version 6.13 (BD Bioscience). Analysis was done using FlowJo Version 10 software.

Confocal microscopy. MoDCs were cultured in a LabTek 8 well chamber coated with 8GX alcian blue. After five days, cells were incubated with peptide (5 µM) or DMSO as a vehicle control. After 2h, pp65 (3 µg/ml) was added and cells were incubated for 4 hours. Cells were subsequently washed and fixed for 10 min at RT using PBS supplemented with 4 % formaldehyde. Cells were permeabilized in PBS supplemented with 0.1 % Triton for 10 min at RT, and blocked for 30 min with PBS supplemented with 5% normal goat serum. Next, slides were incubated with primary antibodies. Cells were washed and incubated with secondary antibodies. After washing, slides mounted on a microscope slide using Mowiol 4-88 (Carl Roth, Germany). Samples were imaged using a Leica TCS SP5 confocal microscope equipped with a HCX PL APO CS x 63/1.40-0.60 OIL objective (Leica Microsystems, The Netherlands). Fluorescent signals were detected with PMTs set at the appropriate bandwidth using the 488 nm argon laser for FITC, the 543 helium neon

laser for Cy3, and the 633 nm helium neon laser for TO-PRO3. Images were processed using the Leica SP5 software.

Statistics. For statistical testing between two groups non-parametric Mann-Whitney tests are used. P-value of $p < 0,05$ is considered significant. All calculations were performed using GraphPad Prism 6.

Acknowledgements

We thank the Villa Joep foundation for financial support. We acknowledge helpful discussions with members of the Wiertz laboratory and the Boes laboratory.

Conflict of interest

The authors declare no conflict of interest.

References

1. Joffre OP, Segura E, Savina A, Amigorena S. Cross-presentation by dendritic cells. *Nat Rev Immunol.* 2012; **12**: 557-569.
2. Kurts C, Robinson BW, Knolle PA. Cross-priming in health and disease. *Nat Rev Immunol.* 2010; **10**: 403-414.
3. Shen L, Rock KL. Priming of T cells by exogenous antigen cross-presented on MHC class I molecules. *Curr Opin Immunol.* 2006; **18**: 85-91.
4. Flinsenberg TW, Compeer EB, Koning D, Klein M, Amelung FJ, van Baarle D, *et al.* Fcγ receptor antigen targeting potentiates cross-presentation by human blood and lymphoid tissue BDCA-3+ dendritic cells. *Blood.* 2012; **120**: 5163-5172.
5. Adiko AC, Babdor J, Gutierrez-Martinez E, Guermonprez P, Saveanu L. Intracellular Transport Routes for MHC I and Their Relevance for Antigen Cross-Presentation. *Front Immunol.* 2015; **6**: 335.
6. Ackerman AL, Kyritsis C, Tampe R, Cresswell P. Early phagosomes in dendritic cells form a cellular compartment sufficient for cross presentation of exogenous antigens. *Proc Natl Acad Sci U S A.* 2003; **100**: 12889-12894.
7. Ackerman AL, Giodini A, Cresswell P. A role for the endoplasmic reticulum protein retrotranslocation machinery during crosspresentation by dendritic cells. *Immunity.* 2006; **25**: 607-617.
8. Burgdorf S, Scholz C, Kautz A, Tampe R, Kurts C. Spatial and mechanistic separation of cross-presentation and endogenous antigen presentation. *Nat Immunol.* 2008; **9**: 558-566.
9. Castellino F, Boucher PE, Eichelberg K, Mayhew M, Rothman JE, Houghton AN, *et al.* Receptor-mediated uptake of antigen/heat shock protein complexes results in major histocompatibility complex class I antigen presentation via two distinct processing pathways. *J Exp Med.* 2000; **191**: 1957-1964.
10. Alloatti A, Kotsias F, Magalhaes JG, Amigorena S. Dendritic cell maturation and cross-presentation: timing matters! *Immunol Rev.* 2016; **272**: 97-108.
11. van Endert P. Intracellular recycling and cross-presentation by MHC class I molecules. *Immunol Rev.* 2016; **272**: 80-96.
12. Blander JM. The comings and goings of MHC class I molecules herald a new dawn in cross-presentation. *Immunol Rev.* 2016; **272**: 65-79.
13. Cruz FM, Colbert JD, Merino E, Kriegsman BA, Rock KL. The Biology and Underlying Mechanisms of Cross-Presentation of Exogenous Antigens on MHC-I Molecules. *Annu Rev Immunol.* 2017; **35**: 149-176.
14. Grotzke JE, Sengupta D, Lu Q, Cresswell P. The ongoing saga of the mechanism(s) of MHC class I-restricted cross-presentation. *Curr Opin Immunol.* 2017; **46**: 89-96.
15. Lawand M, Abramova A, Manceau V, Springer S, van Endert P. TAP-Dependent and -Independent Peptide Import into Dendritic Cell Phagosomes. *J Immunol.* 2016; **197**: 3454-3463.
16. Merzougui N, Kratzer R, Saveanu L, van Endert P. A proteasome-dependent, TAP-independent pathway for cross-presentation of phagocytosed antigen. *EMBO Rep.* 2011; **12**: 1257-1264.
17. Kurotaki T, Tamura Y, Ueda G, Oura J, Kutomi G, Hirohashi Y, *et al.* Efficient cross-presentation by heat shock protein 90-peptide complex-loaded dendritic cells via an endosomal pathway. *J Immunol.* 2007; **179**: 1803-1813.
18. Chen L, Jondal M. TLR9 activation increases TAP-independent vesicular MHC class I processing in vivo. *Scand J Immunol.* 2009; **70**: 431-438.
19. Bertholet S, Goldszmid R, Morrot A, Debrabant A, Afrin F, Collazo-Custodio C, *et al.* Leishmania antigens are presented to CD8+ T cells by a transporter associated with antigen processing-independent pathway in vitro and in vivo. *J Immunol.* 2006; **177**: 3525-3533.
20. Norbury CC, Princiotta MF, Bacik I, Brutkiewicz RR, Wood P, Elliott T, *et al.* Multiple antigen-specific processing pathways for activating naive CD8+ T cells in vivo. *J Immunol.* 2001; **166**: 4355-4362.
21. Oura J, Tamura Y, Kamiguchi K, Kutomi G, Sahara H, Torigoe T, *et al.* Extracellular heat shock protein 90 plays a role in translocating chaperoned antigen from endosome to proteasome for generating antigenic peptide to be cross-presented by dendritic cells. *Int Immunol.* 2011; **23**: 223-237.
22. Guermonprez P, Saveanu L, Kleijmeer M, Davoust J, Van Endert P, Amigorena S. ER-phagosome fusion defines an MHC class I cross-presentation compartment in dendritic cells. *Nature.* 2003; **425**: 397-402.
23. Wang C, Li P, Liu L, Pan H, Li H, Cai L, *et al.* Self-adjuvanted nanovaccine for cancer immunotherapy: Role of lysosomal rupture-induced ROS in MHC class I antigen presentation. *Biomaterials.* 2016; **79**:

- 88-100.
24. Segura E, Durand M, Amigorena S. Similar antigen cross-presentation capacity and phagocytic functions in all freshly isolated human lymphoid organ-resident dendritic cells. *J Exp Med.* 2013; **210**: 1035-1047.
 25. Segura E, Amigorena S. Cross-presentation by human dendritic cell subsets. *Immunol Lett.* 2014; **158**: 73-78.
 26. Chatterjee B, Smed-Sorensen A, Cohn L, Chalouni C, Vandlen R, Lee BC, *et al.* Internalization and endosomal degradation of receptor-bound antigens regulate the efficiency of cross presentation by human dendritic cells. *Blood.* 2012; **120**: 2011-2020.
 27. Schuren AB, Costa AI, Wiertz EJ. Recent advances in viral evasion of the MHC Class I processing pathway. *Curr Opin Immunol.* 2016; **40**: 43-50.
 28. Mayerhofer PU, Tampe R. Antigen translocation machineries in adaptive immunity and viral immune evasion. *J Mol Biol.* 2015; **427**: 1102-1118.
 29. Hu Z, Usherwood EJ. Immune escape of gamma-herpesviruses from adaptive immunity. *Rev Med Virol.* 2014; **24**: 365-378.
 30. Alzhanova D, Fruh K. Modulation of the host immune response by cowpox virus. *Microbes Infect.* 2010; **12**: 900-909.
 31. Rowe M, Zuo J. Immune responses to Epstein-Barr virus: molecular interactions in the virus evasion of CD8+ T cell immunity. *Microbes Infect.* 2010; **12**: 173-181.
 32. Hansen TH, Bouvier M. MHC class I antigen presentation: learning from viral evasion strategies. *Nat Rev Immunol.* 2009; **9**: 503-513.
 33. Byun M, Verweij MC, Pickup DJ, Wiertz EJ, Hansen TH, Yokoyama WM. Two mechanistically distinct immune evasion proteins of cowpox virus combine to avoid antiviral CD8 T cells. *Cell Host Microbe.* 2009; **6**: 422-432.
 34. Verweij MC, Horst D, Griffin BD, Luteijn RD, Davison AJ, Rensing ME, *et al.* Viral inhibition of the transporter associated with antigen processing (TAP): a striking example of functional convergent evolution. *PLoS Pathog.* 2015; **11**: e1004743.
 35. Alzhanova D, Edwards DM, Hammarlund E, Scholz IG, Horst D, Wagner MJ, *et al.* Cowpox virus inhibits the transporter associated with antigen processing to evade T cell recognition. *Cell Host Microbe.* 2009; **6**: 433-445.
 36. Luteijn RD, Hoelen H, Kruse E, van Leeuwen WF, Grootens J, Horst D, *et al.* Cowpox virus protein CPXV012 eludes CTLs by blocking ATP binding to TAP. *J Immunol.* 2014; **193**: 1578-1589.
 37. Lin J, Eggensperger S, Hank S, Wycisk AI, Wieneke R, Mayerhofer PU, *et al.* A negative feedback modulator of antigen processing evolved from a frameshift in the cowpox virus genome. *PLoS Pathog.* 2014; **10**: e1004554.
 38. Grotzke JE, Harriff MJ, Siler AC, Nolt D, Delepine J, Lewinsohn DA, *et al.* The Mycobacterium tuberculosis phagosome is a HLA-I processing competent organelle. *PLoS Pathog.* 2009; **5**: e1000374.
 39. van Montfoort N, Camps MG, Khan S, Filippov DV, Weterings JJ, Griffith JM, *et al.* Antigen storage compartments in mature dendritic cells facilitate prolonged cytotoxic T lymphocyte cross-priming capacity. *Proc Natl Acad Sci U S A.* 2009; **106**: 6730-6735.
 40. Spel L, Boelens JJ, Nierkens S, Boes M. Antitumor immune responses mediated by dendritic cells: How signals derived from dying cancer cells drive antigen cross-presentation. *Oncoimmunology.* 2013; **2**: e26403.
 41. Fuchs R, Schmid S, Mellman I. A possible role for Na⁺,K⁺-ATPase in regulating ATP-dependent endosome acidification. *Proc Natl Acad Sci U S A.* 1989; **86**: 539-543.
 42. Gainey MD, Rivenbark JG, Cho H, Yang L, Yokoyama WM. Viral MHC class I inhibition evades CD8+ T-cell effector responses in vivo but not CD8+ T-cell priming. *Proc Natl Acad Sci U S A.* 2012; **109**: E3260-3267.
 43. Firat E, Saveanu L, Aichele P, Staeheli P, Huai J, Gaedicke S, *et al.* The role of endoplasmic reticulum-associated aminopeptidase 1 in immunity to infection and in cross-presentation. *J Immunol.* 2007; **178**: 2241-2248.
 44. Mantegazza AR, Savina A, Vermeulen M, Perez L, Geffner J, Hermine O, *et al.* NADPH oxidase controls phagosomal pH and antigen cross-presentation in human dendritic cells. *Blood.* 2008; **112**: 4712-4722.
 45. Rock KL, Farfan-Arribas DJ, Shen L. Proteases in MHC class I presentation and cross-presentation. *J Immunol.* 2010; **184**: 9-15.
 46. Accapezzato D, Visco V, Francavilla V, Molette C, Donato T, Paroli M, *et al.* Chloroquine enhances

- human CD8+ T cell responses against soluble antigens in vivo. *J Exp Med.* 2005; **202**: 817-828.
47. Verweij MC, Lipinska AD, Koppers-Lalic D, Quinten E, Funke J, van Leeuwen HC, *et al.* Structural and functional analysis of the TAP-inhibiting UL49.5 proteins of varicelloviruses. *Mol Immunol.* 2011; **48**: 2038-2051.
48. Hiemstra HS, Duinkerken G, Benckhuijsen WE, Amons R, de Vries RR, Roep BO, *et al.* The identification of CD4+ T cell epitopes with dedicated synthetic peptide libraries. *Proc Natl Acad Sci U S A.* 1997; **94**: 10313-10318.

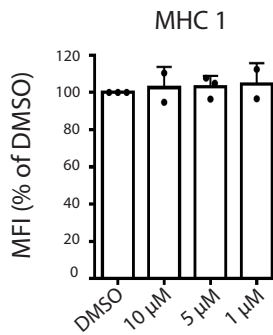

Supplemental information

Figure S1. MHC 1 surface levels in CPXV012-treated moDCs (n=3). Indicated concentrations of soluble CPXV012 were added to human moDCs for 24hrs. Next, DCs were harvested, stained for surface MHC I and measured by flow cytometry.

Chapter 4

Cognate CD4 T-cell licensing of dendritic cells heralds anti-cytomegalovirus CD8 T-cell immunity after human allogeneic umbilical cord blood transplantation.



Authors

Thijs W.H. Flinsenbergh, Lotte Spel, Manon Jansen, Dan Koning, Colin de Haar, Maud Plantinga, Rianne Scholman, Marleen M. van Loenen, Stefan Nierkens, Louis Boon, Debbie van Baarle, Mirjam H.M. Heemskerk, Jaap-Jan Boelens, Marianne Boes

Published in

Journal of Virology 2015

Abstract

Reactivation of human cytomegalovirus (CMV) is hazardous to patients undergoing allogeneic cord blood transplantation (CBT), lowering survival rates by approximately 25%. While antiviral treatment ameliorates viremia, complete viral control requires CD8⁺ T-cell-driven immunity. Mouse studies suggest that cognate antigen-specific CD4⁺ T-cell licensing of dendritic cells (DCs) is required to generate effective CD8⁺ T-cell responses. For humans, this was not fully understood. We here show that CD4⁺ T cells are essential for licensing of human DCs to generate effector and memory CD8⁺ T-cell immunity against CMV in CBT patients. First, we show in CBT recipients that clonal expansion of CMV-pp65-specific CD4⁺ T cells precedes the rise in CMV-pp65-specific CD8⁺ T cells. Second, the elicitation of CMV-pp65-specific CD8⁺ T cells from rare naive precursors in cord blood requires DC licensing by cognate CMV-pp65-specific CD4⁺ T cells. Finally, also CD8⁺ T-cell memory responses require CD4⁺ T-cell-mediated licensing of DCs in our system, by secretion of gamma interferon (IFN- γ) by pp65-specific CD4⁺ T cells. Together, these data show that human DCs require licensing by cognate antigen-specific CD4⁺ T cells to elicit effective CD8⁺ T-cell-mediated immunity and fight off viral reactivation in CBT patients.

Introduction

Cytomegalovirus (CMV)-seropositive patients who are immunocompromised are at increased risk for developing potentially life-threatening CMV reactivation. Especially after allogeneic cord blood (CB) transplantation (CBT), the first weeks of immune reconstitution are hazardous for developing CMV reactivation, which is associated with decreased survival rates (1, 2). Antiviral treatment can reduce CMV viremia, but effective viral control requires induction of CMV-directed immunity by T lymphocytes. In particular, CD8⁺ cytotoxic T lymphocytes (CTLs) fulfill a predominant role in protection against CMV disease (2,–4). Therefore, strategies that increase early CMV-specific adaptive immune responses after transplantation are currently being explored, which could ultimately help to establish full clearance of, and long-term immunological memory against, CMV. In the human setting, cell-based therapy is being explored, geared toward dendritic cell (DC)-mediated activation of CTLs (5, 6). The elicitation of antigen-specific CTL immunity was in mouse models shown to require cognate CD4⁺ T-cell licensing (7,–10). Furthermore, priming of naive CD8⁺ T cells requires both the CD4⁺ T-helper cells and CD8⁺ T cells to recognize antigen on the same antigen-presenting cell (5, 11, 12). Such CD4⁺ T-cell help can involve CD40 ligand (CD40L) binding to CD40 on DCs (9, 13, 14). For humans, a requirement for CD4⁺ T-cell help in DC licensing for formation of effector and memory CTLs has not yet been demonstrated. It is also not yet clear what are the signaling pathways through which CD4⁺ T cells might execute their licensing.

CMV-specific CD4⁺ T-cell clones are present in the healthy population, suggesting a role for antigen-specific CD4⁺ T cells in immunity against CMV, as 50 to 80% of adults experience CMV infection in their lifetime (6, 15). Moreover, effective control of CMV infection was attained in patients when CMV-specific T cells, of which 77% were CD4⁺ T cells, were infused (16). Further, human DCs loaded with both HLA class I and II/peptide complexes were more effective at generating antigen-specific CTL responses than were those loaded with solely major histocompatibility complex (MHC) class I/peptide complexes (17). In a different setting, not only the absence of antigen-specific CTLs but also the absence of specific CD4⁺ T-helper cells resulted in higher CMV loads (18). Thus, CD4⁺ T-helper cells are likely to participate in CMV control.

We set out to clarify the role of human CD4⁺ T-helper cells in DC licensing for CTL-mediated immunity for both CTL priming and memory CTL activation. First, we show in CBT recipients that clonal expansion of CMV-pp65-specific CD4⁺ T-helper cells precedes the expansion of primary CMV-pp65-specific CTLs. We clarified that DC licensing is cognate, as expansion of primary CMV-pp65-specific CTLs from naive CB precursors requires the presence of pp65-specific CD4⁺ T-helper cells, in cocultures. Finally, also DC licensing is required for CTL memory, as DCs licensed by CD4⁺ T cells, which they do through secretion of gamma interferon (IFN- γ), stimulate much more efficient CMV-pp65-specific CTL memory responses. Together, these data imply that in humans CD4⁺ T-helper cells are pivotal in DC licensing to elicit CD8⁺ T-cell immunity during CMV reactivation in CBT patients.

Materials and Methods

Patient inclusion and human samples. Approval for this study was obtained from the ethics committees of the University Medical Centre Utrecht (METC-05-143, METC-11-063, and METC-13-437). Written informed consent was obtained from all participating patients or their legal

representatives prior to CBT. In this consent, it was stated that their medical data may be used for research purposes. According to the hospital's standard operating procedures, regular blood samples were taken for viral load detection by quantitative PCR (qPCR) and T-cell number measurements (see below). All children below the age of 18 who received an allogeneic CBT between 2010 and 2013 at the hematopoietic stem cell transplant (HSCT) unit of the Wilhelmina Children's Hospital were evaluated. All patients received a fludarabine- and busulfan-containing regimen with early-given (day -9) antithymoglobulin (19). Eight patients suffered from CMV reactivation post-CBT. These patients were all CMV positive prior to transplantation. Two were excluded because maximum CMV loads did not reach 1,000 copies/ml. From the 6 other patients, CMV loads and CD4⁺ and CD8⁺ counts were evaluated and plotted over time. We also included 8 control patients who did not have events that are likely to impact the T-cell counts (T-cell-impacting events), such as viral reactivations of >1,000 copies (cp)/ml (human herpesvirus 6 [HHV-6], CMV, Epstein-Barr virus [EBV], or adenovirus), graft-versus-host disease (GvHD) of \geq grade 2, or graft rejection. CD4⁺ T-cell counts within the first 3 months after CBT were evaluated using the area under the curve (AUC) trapezoidal method: $\sum(\text{cell number}_{\text{time } y} + \text{cell number}_{\text{time } x})/2 \times (\text{time } y - \text{time } x)$ (20). Trends in CD4⁺ T-cell count were evaluated using a Pearson correlation coefficient.

Immune phenotyping. Immune phenotyping was performed on whole-blood samples every other week once the leukocyte count was $>0.4 \times 10^9/\text{liter}$. Absolute numbers of T cells (CD3⁺) helper T cells (CD3⁺ CD4⁺), and cytotoxic T cells (CD3⁺ CD8⁺) were determined using Trucount technology (BD Biosciences). A volume of 20 μl of CD3-fluorescein isothiocyanate (FITC), CD45-peridinin chlorophyll protein (PerCP), and CD19-allophycocyanin (APC) or CD3-FITC, CD8-phycoerythrin (PE), CD45-PerCP, and CD4-APC reagent (Multitest; BD Biosciences) was added to a Trucount tube containing a known quantity of beads, followed by 100 μl of EDTA-treated whole blood and incubated for 15 min at room temperature. Erythrocytes (RBCs) were subsequently lysed for 15 min with 450 μl of fluorescence-activated cell sorting (FACS) lysing solution (BD Biosciences). Samples were acquired using a FACSCalibur cytometer and analyzed with Multiset software (BD Biosciences). Qualitative and subset analyses of T-cell compartments were performed as described previously (21).

Cord blood dendritic cell culture. CD34⁺ cells were isolated according to the manufacturer's instructions (Miltenyi Biotec) and expanded using 20 ng/ml interleukin-3 (IL-3) (Invitrogen), 20 ng/ml IL-6 (BD Biosciences), and 50 ng/ml stem cell factor (SCF) and 50 ng/ml FLT3-L (both from Peprotech). For DC culture, 3×10^6 CD34⁺ cells were cultured in a T25 flask (Thermo) in X-Vivo medium (Lonza) containing 2 mM l-glutamine, 100 U/ml penicillin-streptomycin, and 5% human serum in the presence of 20 ng/ml granulocyte-macrophage colony-stimulating factor (GM-CSF) and 20 ng/ml IL-4 (all from Invitrogen), 20 ng/ml SCF, and 100 ng/ml FLT3-L at 37°C and 5% CO₂ for 7 days.

CD8⁺ T-cell priming assay. CB CD34⁺-derived DCs were loaded with 10 $\mu\text{g}/\text{ml}$ pp65 (Miltenyi Biotec; purity, >95%; low endotoxin; <10 endotoxin units [EU]/ml), medium, or 10 $\mu\text{g}/\text{ml}$ bovine serum albumin (BSA) (Roche; 10,000 DCs in 100 μl 5% X-Vivo plus human serum per well, 96-well plate [Thermo]). Then, 50,000 donor-matched naive CD8⁺ T cells were added (separated from

CD34⁻ fraction using Miltenyi Biotec magnetically activated cell sorting [MACS] beads according to the manufacturer's instructions) together with medium, 50,000 CD4⁺ T cells (separated using MACS beads), or 10 µg/ml CD40 agonist clone 7 (Bioceros). All were cocultured for 3 weeks at 37°C and 5% CO₂ for 7 days. On days 8 and 15, CD34⁺-derived DCs were loaded with 1 × 10^{-6.5} M NLV peptide and irradiated with 30 Gy. Ten thousand DCs were plated per well, and the T cells were added for restimulation. Every week at days 2 and 5, IL-7 and IL-15 (Immunotools) were added, both at a final concentration of 5 ng/ml. After 3 weeks, cells were stained with an HLA-A2 pp65⁴⁻⁵⁰³ pentamer (ProImmune) and positive cells were single-cell sorted and stimulated for several weeks as described under "CD8⁺ T-cell cloning." Prior to cryopreservation, a small aliquot of T cells (1 × 10⁵ to 5 × 10⁵) was harvested for T-cell receptor (TCR) sequencing.

TCRβ chain sequencing. TCRβ chains were sequenced as previously described (22). Briefly, a one-sided anchored reverse transcription-PCR (RT-PCR) was performed in order to amplify TCRβ mRNA. Amplified products were purified from the agarose gel and ligated into a pGEM-T Easy vector (Promega), followed by transformation into chemically competent Escherichia coli DH5α bacteria. Thirty-two bacterial colonies were screened for the presence of a TCR construct and subsequently sequenced via capillary electrophoresis. Sequences were analyzed using web-based software (www.imgt.org) (23), and TCRs were identified using the official ImMunoGeneTics nomenclature as previously shown (24).

Cross-presentation assay. Cross-presentation essays with monocyte-derived DCs (MoDCs) and CMV peptide NLVPMVATV (NLV)-specific CD8⁺ T-cell clones were performed as described in reference 25. In addition, stimulation of DCs was performed by coincubation after loading with a range of CD40 antibody (0.1 to 10 µg/ml clone 7; Bioceros), a range of pp65⁵⁻⁵²³-specific CD4⁺ T cells or donor-matched nonspecific T cells (CD4 MACS; Miltenyi Biotec), or a range of recombinant IFN-γ (Immunotools). Blocking of the CD40-CD40L interaction was done by preincubating CD4⁺ T cells with 10 µg/ml CD40L antibody for 30 min at 37°C and 5% CO₂ (Bioceros). Blocking of the CD80/CD86 (B7-1/B7-2)-CD28/CD152 (CTLA-4) interaction was done by preincubating the loaded DCs with 10 µg/ml anti-CD80/CD86 for 30 min at 37°C and 5% CO₂ (10 µg/ml abatacept). Blocking of CD137-CD147L interaction was done by preincubating CD4⁺ T cells with 10 µg/ml CD137 antibody (clone 4b4-1; BioLegend) (26) for 30 min at 37°C and 5% CO₂.

For the supernatant exchange experiment, pp65-loaded HLA-DRB1*01 MoDCs were cocultured with cognate CMV-pp65⁵⁻⁵²³-specific CD4⁺ T cells overnight. Next, we collected the supernatant, added this in the presence of phosphate-buffered saline (PBS) or 10 µg/ml IFN-γ blocking antibody (BD Biosciences) to new pp65-loaded MoDCs, and incubated the cells for another 24 h. After incubation, DCs were washed and human CMV (HCMV) pp65-specific CD8⁺ T cells were cocultured with pp65-loaded DCs for 4 to 6 h in the presence of GolgiStop (1/1,500; BD Bioscience). Cells were subsequently stained for surface markers and the presence of intracellular IFN-γ and tumor necrosis factor (TNF), followed by flow cytometry-based analysis.

CD4⁺ T-cell cloning. HCMV-pp65-specific CD4⁺ T cells were isolated from HLA-DRB1*0101⁺ peripheral blood mononuclear cells (PBMCs) using the IFN-γ secretion assay (Miltenyi Biotec, Bergisch Gladbach, Germany). Briefly, PBMCs were stimulated with 2 µg/ml pp65-KYQEFFWDANDIYRI peptide (HLA-DRB1*0101 binding pp65 peptide), and after 4 h of stimulation,

IFN- γ -secreting CD4⁺ T cells were isolated using FACS. The CMV-pp65-specific CD4⁺ T-cell line was stimulated three times weekly with irradiated (30-Gy) allogeneic PBMCs (1×10^6 cells/ml) and 800 ng/ml phytohemagglutinin (PHA; Murex Biotec Limited, Dartford, United Kingdom).

CD8⁺ T-cell cloning. An HLA-A*0201-restricted, HCMV-pp65-specific CD8⁺ T-cell clone was prepared. In brief, T cells from an HLA-A*0201⁺ donor were stained with HLA-A2/pp65⁴⁻⁵⁰³ tetramers and subsequently single-cell sorted in a 96-well plate (Thermo) containing irradiated B lymphoblastoid cell line (B-LCL) feeder cells (1×10^5 cells/ml, irradiated with 70 Gy) and PBMCs from 3 healthy donors (1×10^6 cells/ml, irradiated with 30 Gy). One microgram/milliliter leucoagglutinin PHA-L (Sigma-Aldrich) and 120 U/ml of recombinant IL-2 (Immunotools) were added. T-cell clones specific to pp65⁴⁻⁵⁰³ were selected using tetramer staining. Positive clones were restimulated and expanded during several stimulation cycles and frozen in aliquots that were freshly thawed before each use in an assay.

Monocyte-derived DC culture. Peripheral blood mononuclear cells (PBMCs) from healthy HLA-A*02.01/HLA-DR*01.01-positive donors were separated from peripheral blood by Ficoll Isopaque density gradient centrifugation (GE Healthcare Bio-Sciences AB) and either were used directly or frozen until further experimentation. For DC induction, PBMCs were incubated at 37°C and 5% CO₂ for 1 h with plastic for the monocytes to adhere, in X-Vivo 15 medium (Lonza) containing 2 mM l-glutamine, 100 U/ml penicillin-streptomycin, and 2% human serum (all obtained from Invitrogen). Cells were washed 3 times with PBS (room temperature) and subsequently cultured for 5 days at 37°C and 5% CO₂ in X-Vivo 15 medium containing 450 U/ml GM-CSF (Immunotools) and 300 U/ml IL-4 (Immunotools). Cytokines were refreshed after 3 days. DCs were collected for experiments on day 5 by incubation in PBS (4°C) for 1 h.

DC maturation assay. Day 4 monocyte-derived DCs (MoDCs) were incubated overnight (O/N) in the presence of medium, pp65 (3 μ g/ml), pp65 and CD40 antibody clone 7 (10 μ g/ml; Bioceros), pp65 and CD40L antibody clone 5c8 (10 μ g/ml; Bioceros), pp65 and 200,000 pp65⁵⁻⁵²³-specific CD4⁺ T cells, or poly(I-C) (30 μ g/ml; Sigma-Aldrich) and lipopolysaccharide (LPS) (100 ng/ml [Sigma-Aldrich]). In mouse DCs, maturation signals elicited via LPS triggering stimulated acquisition of antigen cross-presentation capacity (27). Cells were subsequently harvested and analyzed for costimulatory marker expression using flow cytometry.

Flow cytometry. For staining, cells were first washed twice in PBS containing 2% fetal calf serum (FCS) (Invitrogen) and 0.1% sodium azide (NaN₃; Sigma-Aldrich). Next, antigen nonspecific binding was prevented by prior incubation of cells with 10% mouse serum (Fitzgerald). Cells were next incubated with combinations of Pacific blue, phycoerythrin (PE), fluorescein isothiocyanate (FITC), allophycocyanin (APC), and PE-Cy7-conjugated mouse anti-human antibody (Ab) (CD3, CD4, CD8, CD11c, CD40, CD45, CD69, CD80, CD83, CD86, CD107a, HLA-DR, HLA-ABC, and TRAIL). Where indicated, after surface staining, T cells were washed twice in PBS-2% FCS-0.1% NaN₃) and fixed, permeabilized, and intracellularly stained using monoclonal antibodies (MAbs) to IFN- γ and TNF. Cells were acquired on a FACSCanto II cytometer and analyzed using FACS Diva version 6.13 (BD Bioscience) or FlowJo version 7.6.5 software. Data were analyzed using GraphPad Prism 5.

Detection of cytokines in culture supernatant. Cytokine concentrations were measured by the MultiPlex Core Facility of the Laboratory of Translational Immunology (LTI) using Luminex technology with in-house-developed bead sets and Bio-Plex Manager version 6.1 software (Bio-Rad Laboratories) as previously described (28).

Detection of CMV-specific CD4⁺ and CD8⁺ T cells in patient samples. NLV-specific CD8⁺ T cells were detected using HLA-A2 pp65⁴⁻⁵⁰³ pentamer (ProImmune) or HLA-B7 pp65⁴⁻⁴²⁶ tetramer (produced in-house). Antigen-specific CD4⁺ and CD8⁺ T cells were detected with intracellular IFN- γ staining after stimulation with a pp65 and IE-1 15-mer overlapping peptide mix (JPT Peptide Technologies), as described in reference 29.

Results

CD4⁺ and CD8⁺ T-cell dynamics after cord blood transplantation in patients with and without CMV reactivation. We studied early T-cell reconstitution in pediatric patients undergoing complete immune reconstitution through allogeneic cord blood transplantation (CBT), in relation to CMV reactivation. Six CBT recipients experienced CMV reactivation (>1,000 virus copies/ml), and eight control patients were included (without infectious complications). We analyzed the reconstitution of CD4⁺ and CD8⁺ T cells and CMV loads (Fig. 1). We observed expansion and contraction of the CD8⁺ T-cell population as CMV viral load increased and regressed (Fig. 1A). The control patients instead experienced a consistent and gradual increase in CD8⁺ T-cell numbers during reconstitution (Fig. 1B). The CD4⁺ T-helper cell numbers also fluctuated more in patients with CMV reactivation than in control patients (Fig. 1C). Such an expansion and contraction pattern for CD4⁺ T cells was previously observed in reconstitution under viral pressure (30). Of note, while the total numbers of CD4⁺ T cells were comparable during the first 90 days after CBT (Fig. 1D, measured as area under the curve of CD4⁺ T-cell measurements during the first 90 days post-SCT), in CMV-reactivating patients the percentage of activated, HLA-DR⁺/CD38⁺ CD4⁺ T cells was increased (Fig. 1E and F).

CMV-specific CD4⁺ T-helper cells precede primary CMV-specific CTL expansion after CBT. We hypothesized that CD4⁺ T cells, through DC licensing, may support CMV-specific CTL responses, as was shown in mouse-based research (31,–33). Cognate interaction between CD4⁺ T-helper cells and DCs would thereby enable DCs to stimulate more effective CTL responses. To first investigate expansion of the primary CMV-specific CTL population in relation to CMV viremia, we analyzed PBMCs from 4 available CBT recipients who exhibited CMV reactivation (Fig. 1G, patients 1 to 4). We measured a sample prior to and during CMV reactivation and after CMV control (time points indicated in Fig. 1A). As control samples, we included samples from two patients, 5 and 6, who carried CMV prior to CBT and yet did not reactivate (Fig. 1G). In all CBT patients who cleared CMV reactivation, we observed expansion of the primary CMV-specific CTL population (Fig. 1G, right column, patients 1 to 4; mean, 127 days post-SCT). These cells were of CB origin, as confirmed by chimerism analyses (data not shown). The two control patients, 5 and 6, did not elicit CMV-specific CD8⁺ T cells at 120 and 180 days post-SCT. Early on during CMV reactivation, CMV-specific CTLs did not yet expand, except in patient 4 (Fig. 1G). Considering the CMV-specific CD4⁺ T-helper cell population, we next measured IFN- γ production in CD4⁺ T cells after stimulation with a

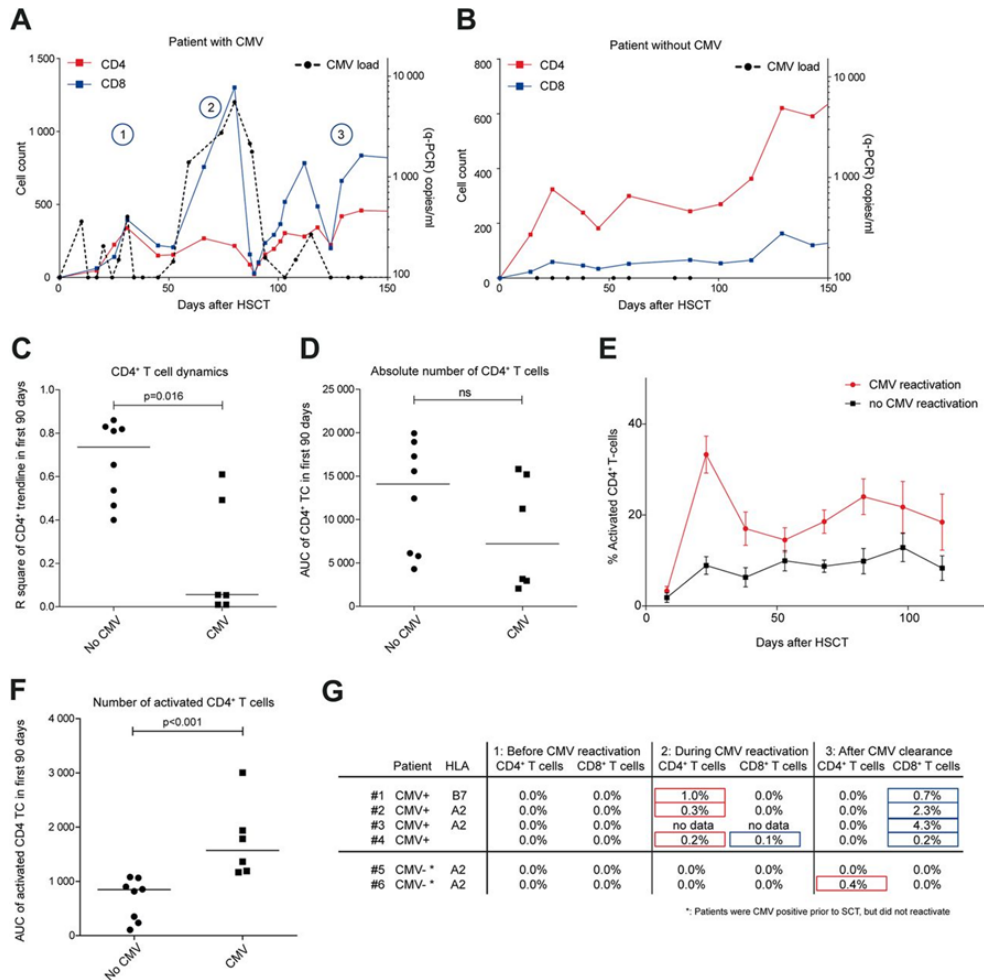


Figure 1. T-cell dynamics in CBT recipients. (A and B) T-cell development over time in CBT recipients with (A) or without (B) CMV reactivation (load of >1,000 copies/ml). Red and blue lines represents CD4⁺ and CD8⁺ T-cell numbers, respectively (absolute counts). The black dashed line represents CMV loads (copies/ml). The numbers 1, 2, and 3 (in blue circles) correspond with referred time points in panel G. (C) CD4⁺ T-cell dynamics (R² of CD4⁺ trendline) and median in the first 90 days after transplantation in CBT recipients without (dots) or with (squares) CMV reactivation. A high R² indicates little fluctuation from the predicted trendline. (D) Total CD4⁺ T-cell numbers (area under the curve [AUC]) and median in the first 90 days after transplantation in CBT recipients without (dots) or with (squares) CMV reactivation. ns, not significant. (E) Mean percentage (+ standard error of the mean [SEM]) of activated CD4⁺ T cells in CBT recipients with (red line) or without (black line) CMV reactivation (average of 15 days per data point). (F) AUCs and medians of activated CD4⁺ T cells in the first 90 days. (G) Percentages of pp65-specific CD4⁺ and CD8⁺ T cells (tetramer and/or IFN- γ release upon pp65-peptide mix stimulation) before CMV reactivation (1), during CMV reactivation (2), and after CMV clearance to below detection limits (3) (see panel A) in 4 CBT recipients with reactivation (1 to 4) and 2 CBT recipients without reactivation (5 and 6). Red boxes, CD4⁺ T cells; blue boxes, CD8⁺ T cells (corresponding to panels A and B). No samples were available during CMV reactivation for patient 3. Significance in panels C, D, and F was determined using a nonparametric Mann-Whitney test.

CMV-pp65-overlapping peptide mix as described previously (3, 18, 34) (also data not shown). We observed expansion of the primary CMV-specific CD4⁺ T-helper cell population in all analyzed samples of reactivating patients, early on during CMV reactivation (Fig. 1G, middle column). Finally, in control patient 6, we detected CMV-specific CD4⁺ T cells at day 180, indicating that CMV-positive patients (IgG positivity prior to SCT) may eventually develop anti-CMV T cells but later than do patients who reactivate.

Taken together, recovery of the CMV-pp65-specific CD4⁺ T-cell population precedes expansion of primary CMV-pp65-specific CTLs, supporting a role of CD4⁺ T cells in CD8⁺ T-cell priming.

CD4⁺ T-cell licensing of DCs is necessary to prime naive CD8⁺ T cells in vitro. To address whether cognate CD4⁺ T cells facilitate DC licensing for CD8⁺ T-cell priming, we performed cocultures of CB-derived naive CD8⁺ T cells with donor-matched CD34⁺-derived DCs, in the presence or absence of polyclonal donor-matched CD4⁺ T cells. DCs had been preloaded with pp65 protein or BSA, and cocultures were allowed to proceed for 3 weeks of duration. Using HLA-A2 pentamers loaded with the CMV-derived peptide NLVPMVATV (NLV/A2 in short), we identified pp65⁴⁻⁵⁰³-specific CTLs (Fig. 2A). Only when CD8⁺ T-cell priming had been performed in the presence of pp65 protein and CD4⁺ T cells did we observe CD8⁺ T cells that bound NLV/A2 pentamers (bright fluorescence, >log₄ intensity) (Fig. 2B). To confirm that NLV/A2 reactivity represents pp65⁴⁻⁵⁰³-specific CD8⁺ T cells, we performed single-cell sorting of events over log₄ intensity and derived clones. As a control, we sorted several cells from the cultures with BSA or pp65 without CD4⁺ T cells (>log_{3.5} intensity, as not much NLV/A2 reactivity was present). We succeeded in derivation of 5 independent CMV-specific CTL clones but only from DC/CTL cultures supplemented with both pp65 and CD4⁺ T cells (Fig. 2C). Of note, we derived one CMV-specific CTL clone from DC/CTL cultures supplemented with both pp65 protein antigen and anti-CD40 antibody but no CD4⁺ T cells. Together, these data show that CD4⁺ T cells can license DCs to expand a primary CTL population and that such DC licensing can involve CD40-CD40L interaction, as previously observed in mice (Fig. 2D, clone 6) (7, 9, 13, 35, 36).

We wished to further strengthen the finding that the T-cell clones grown from rare precursor cells within the polyclonal cord blood T-cell population harbor in fact TCRs specific to CMV-derived epitopes, using DNA sequencing of the recombined CDR3β TCR regions as a second method (Fig. 2C and D). We found that our derived CDR3β sequences are frequently shared in CMV-specific CD8⁺ T cells, supporting CMV specificity (Fig. 2D) (37). CDR3β sequence variants were unique and not yet described (37).

We next investigated the cellular characteristics of CTL clones that were generated from naive CB precursors. All clones had an effector memory phenotype (CD45RO^{high}/CCR7⁻/CD62L^{int}/CD27^{int}, Fig. 2E) (38). CD5, CD25, and CD127 levels were comparable, while CD28 expression varied between different clones (Fig. 2F), and none of the clones expressed PD-1 or CTLA-4 in a resting state (data not shown). Functionally, we could not detect cytokine production, possibly since clonal expansion ensued for nearly 3 months, inducing T-cell exhaustion. Using phorbol myristate acetate (PMA)/ionomycin, we circumvented this state, now yielding high levels of cytokine production (Fig. 2G), indicating that these clones were able to respond appropriately. In conclusion, we used human CB-derived cocultures of antigen-loaded DCs and naive lymphocytes to show that CD4⁺ T-cell licensing of DCs is necessary for antigen-specific CD8⁺ T-cell priming.

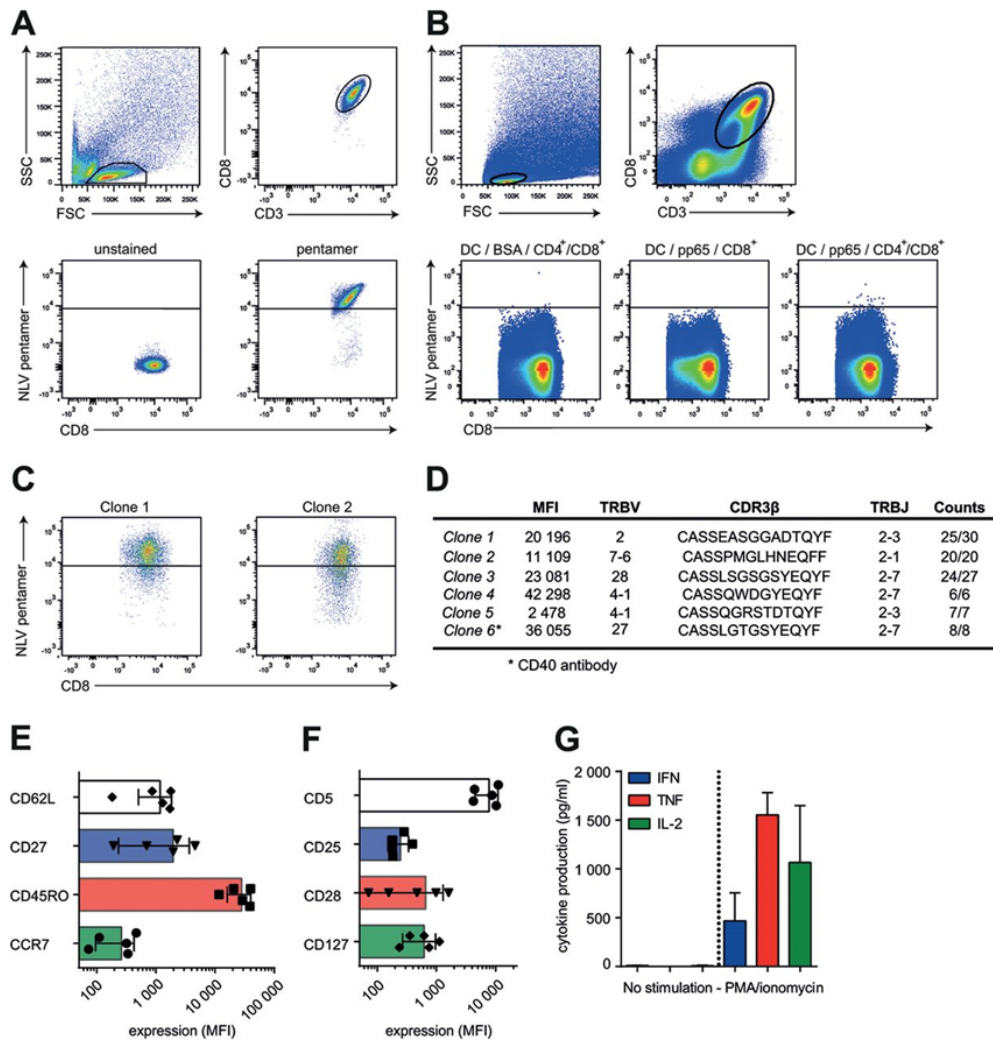


Figure 2. CD4⁺ T-cell licensing of DCs is necessary to prime naive CD8⁺ T cells *in vitro*.

(A) Gating strategy and pentamer staining of CMV-pp65-specific CD8⁺ T cells. SSC, side scatter; FSC, forward scatter. (B) Gating strategy and pentamer staining of primed CB-derived CD8⁺ T cells. DCs were loaded with 10 μ g/ml BSA (left graph) or 10 μ g/ml pp65 (middle and right graph) and cocultured with donor-matched naive CD8⁺ T cells in the absence (middle graph) or presence (left and right graphs) of CD4⁺ T cells. High-level pentamer staining events ($>10^4$ intensity) were single-cell sorted and clonally expanded for 4 to 6 weeks (representative of 6 independent experiments). (C) Representative pentamer staining of two individually derived CD8⁺ T-cell clones. (D) Characteristics of 6 clones from 3 independent experiments. Shown are mean fluorescence intensity (MFI) values of pentamer stainings and TCR sequences. Clone 6 was produced using a CD40 agonist antibody. TRBV, T-cell receptor beta variable gene; TRBJ, T-cell receptor beta joining gene. (E and F) Phenotype analysis of pp65-specific CD8⁺ T-cell clones. (G) Cytokine production (IFN- γ , TNF, and IL-2; pg/ml) of CD8⁺ T cells after PMA/ionomycin stimulation.

Cognate CD4⁺ T cells induce licensing of DCs for enhanced memory CTL responses. DCs are not only instrumental during T-cell priming but also important for restimulation of antigen-specific

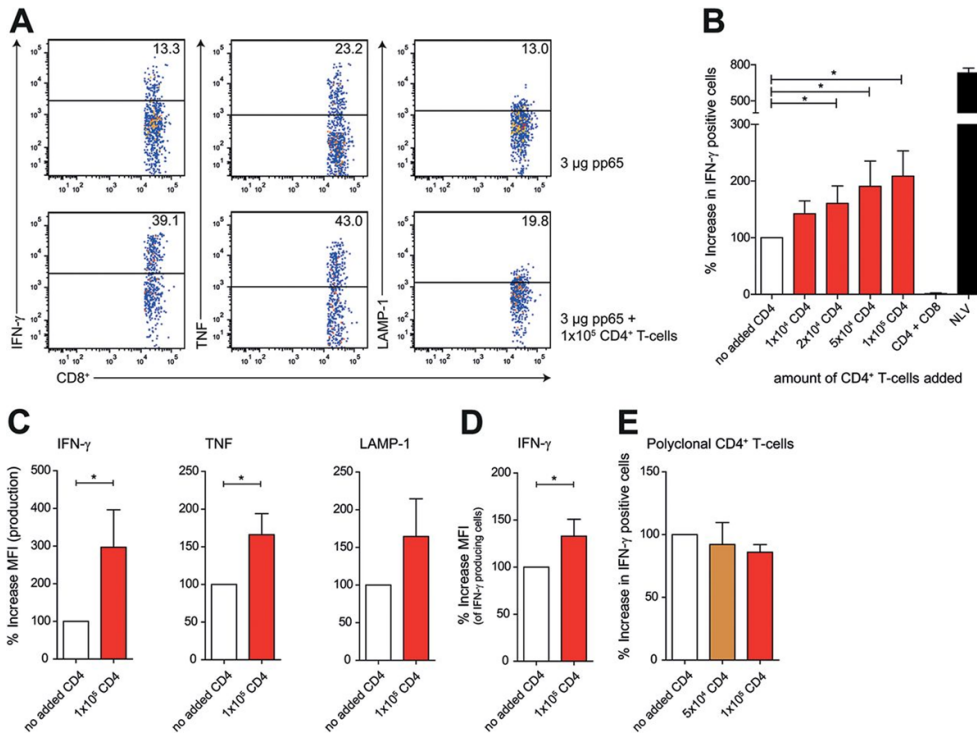


Figure 3. Cognate CD4 $^+$ T cells induce licensing of DCs for enhanced memory CTL responses. (A to D) Summary and representative plots of CD8 $^+$ T-cell activation. (A) MoDCs were loaded with HCMV-derived pp65 and cocultured with 50,000 A2/NLVPMVATV-specific CD8 $^+$ T cells in the absence (upper graphs) or presence (lower graphs) of HLA-DRB1*01/KYQEFFWDANDIYRI-specific CD4 $^+$ T cells. Freshly thawed T cells were gated based on CD3 and CD8 expression and analyzed for activation-induced production of IFN- γ (left) and TNF (middle) and LAMP-1 surface expression (right). (B) Summary (mean + standard error of the mean [SEM]) of HCMV pp65₄₋₅₀₃ cross-presentation. Bars represent production of IFN- γ after coculture with MoDCs loaded with 3 μ g pp65 in the presence of antigen-specific CD4 $^+$ T cells (mean, 120.9%; SEM, 15.8%; n = 6). The black bar shows a maximum response after stimulation with NLV peptide-loaded DCs. (C) Mean fluorescence intensity (MFI) of CD8 $^+$ T-cell cytokine production (IFN- γ and TNF) and LAMP-1 surface expression after coculture with pp65-loaded DCs with (red bars) or without (white bars) 100,000 antigen-specific CD4 $^+$ T cells (mean + SEM, n = 4). (D) MFI of IFN- γ , gated on IFN- γ -producing CD8 $^+$ T cells (mean + SEM, n = 4). (E) MoDCs were loaded with HCMV-derived pp65 and cocultured with 50,000 A2/NLVPMVATV-specific CD8 $^+$ T cells in the presence of donor-matched polyclonal CD4 $^+$ T cells (mean + SEM, n = 4). Significance in all panels was determined using a nonparametric Mann-Whitney test. *, P < 0.05.

T-cell clones. We therefore next asked whether human cognate CD4 $^+$ T cells are necessary to licensing of DCs for CD8 $^+$ T-cell memory (10). To this end, we derived human HLA-A2*01/HLA-DRB1*01 $^+$ monocyte-derived DCs and loaded these with pp65 protein antigen for presentation via HLA-DRB1 and HLA-A2. Next, we induced licensing of the DCs by administration of CMV-pp65⁵⁻⁵²³-specific CD4 $^+$ T cells recognizing HLA-DRB1*01/KYQEFFWDANDIYRI complexes presented by the DCs (50,000 DCs and increasing numbers of CD4 $^+$ T cells) (39). Medium was refreshed to avoid the possibility of CD4 $^+$ T-cell-derived cytokines directly stimulating CTL activation. We added 50,000 memory CMV-pp65⁴⁻⁵⁰³-specific CTLs to the licensed DCs and determined memory CTL activation

by intracellular cytokine staining after 4 hours of coculture of clones (25) in the presence of GolgiStop. NLVPMVATV peptide (1×10^{-6} M) was added to DCs as a positive control for CTL activation (Fig. 3B). We found that upon licensing of DCs, CD8⁺ T-cell activation was enhanced, as determined by percentages of IFN- γ - and TNF-producing cells and surface-expressed LAMP-1 (Fig. 3A and B) or amounts of IFN- γ and TNF produced (Fig. 3C and D and data not shown). Next, is cognate CD4⁺ T-cell licensing required for DC-mediated CTL memory responses? We repeated the DC licensing experiment using polyclonal DRB1*01⁺-restricted CD4⁺ T cells and found that CD4⁺ T cells needed to be antigen specific to induce DC licensing, as no induction of CTL activation was seen after addition of polyclonal CD4⁺ T cells (Fig. 3E). Finally, CD4⁺ T cells enhanced CTL stimulation via DC licensing and not by direct stimulation of the memory CTLs, as coculture of CD4⁺ T cells, pp65, and CD8⁺ T cells in the absence of DCs did not yield cytokine production by the memory CTLs (Fig. 3B).

CD40-CD40L, CD80/86-CD28, and CD137-CD137L are not involved in CD4⁺ T-cell-mediated memory CD8⁺ T-cell activation. We next asked if CD4⁺ T cells facilitate licensing of DCs via CD40L molecules, as was suggested in mouse studies (7, 9, 13, 35, 36). We therefore exchanged cognate CD4⁺ T cells with a stimulating CD40 antibody in our MoDC/CTL cocultures described for Fig. 3. As a negative control, we included an agonist CD40L antibody. We observed only a modest effect on CD8⁺ T-cell activation (Fig. 4A). The CD40L antibody did not influence CD8⁺ T-cell activation. We confirmed these data by performing the CD4⁺ T-cell coincubation experiments in the presence of CD40L-blocking antibodies (Fig. 4B). We similarly tested CD80/CD86 (B7-1/B7-2)-CD28 signaling, considering their importance in DC/T-cell interaction (40) and that CD80/86 blockade using abatacept is used in several autoimmune disorders (41, 42). Abatacept treatment did not inhibit the CD4⁺ T-cell-induced activation of memory CD8⁺ T cells (Fig. 4C). CD137-CD137L (4-1BB-4-1BBL) was also recently implicated in DC-mediated T-cell priming (40, 43). We therefore tested whether blocking of CD137L modulates CD4⁺ T-cell-induced activation of memory CD8⁺ T cells. This was not the case (Fig. 4D). Taken together, we conclude that CD4⁺ T-cell-induced licensing of DCs is not attributable to CD40L-, CD28-, or CD137L-mediated interaction.

Finally, is enhanced stimulation of memory CTLs by licensed DCs a mere consequence of cognate CD4⁺ T-cell-mediated upregulation of DC surface molecules (Fig. 4E and F)? This does not seem to be the case, as incubation of pp65-loaded DCs with antigen-specific CD4⁺ T cells or CD40L did not cause an overt increase of HLA-ABC; costimulatory marker CD40, CD80, or CD86; or HLA-DR (Fig. 4E and F). Instead, cognate CD4⁺ T-cell licensing of DCs may involve the enhanced stimulation of memory CTLs via increased antigen presentation of HLA-A2/NLVPMVATV complexes.

Identification of candidate soluble CD4⁺ T-cell-secreted mediators for licensing of DCs.

Cognate CD4⁺ T cells may exert DC licensing for enhanced CTL memory responses via secretion of soluble mediators. To test this hypothesis, we cocultured pp65-loaded HLA-DRB1*01 MoDCs with cognate CMV-pp65⁵⁻⁵²³-specific CD4⁺ T cells overnight. Next, we collected the supernatant and added this to new pp65-loaded MoDCs. After overnight incubation, CTL activation was assessed (Fig. 5A). We found that the enhanced DC licensing was transferred via the supernatant, indicating that CD4⁺-mediated DC licensing occurs at least partly through soluble factors (Fig. 5B). To identify possible proteins involved, we next analyzed culture supernatants of cocultures of pp65-loaded HLA-DRB1*01 MoDCs with cognate CMV-pp65⁵⁻⁵²³-specific CD4⁺ T cells or polyclonal

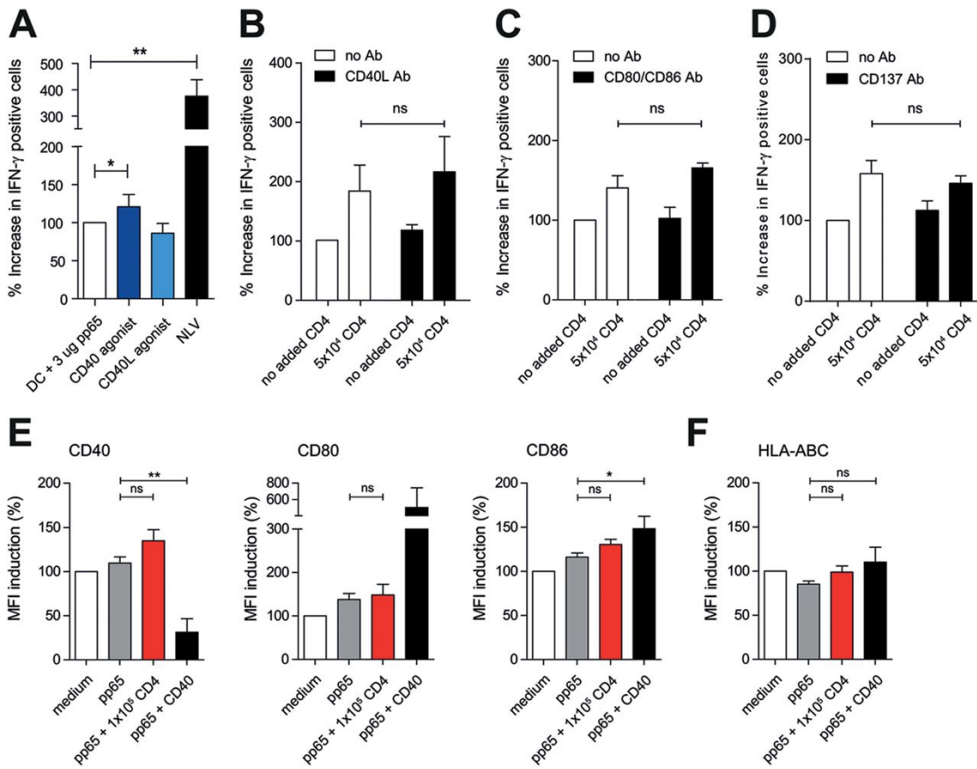


Figure 4. CD40-CD40L, CD80/86-CD28, and CD137-CD137L are not involved in CD4⁺ T-cell-mediated memory CD8⁺ T-cell activation. (A) IFN-γ production of CD8⁺ T cells after coculture with pp65-loaded DCs in the presence of a CD40 (dark blue) or CD40L (light blue) agonist. (B to D) IFN-γ production of CD8⁺ T cells after coculture with pp65-loaded DCs and antigen-specific CD4⁺ T cells in the presence of CD40-CD40L blocking (B), CD80/CD86 blocking (C), or CD137-CD137L blocking Ab (mean + standard error of the mean [SEM], n = 4). Significance in all panels was determined using a nonparametric Mann-Whitney test. (E and F) Expression of DC maturation markers CD40, CD80, and CD86 (E) and HLA-ABC (F) after stimulation with medium (white bars), pp65 (gray bars), pp65- and antigen-specific CD4⁺ T cells (red bars), and pp65 and anti-CD40 (black bars) (mean + SEM, n = 4). *, P < 0.05; **, P < 0.01; ns, not significant.

HLA-DRB1*01-restricted CD4⁺ T cells (37°C, O/N), by cytokine multiplex array. The supernatants of cognate DC/T-cell cocultures but not DC/polyclonal T-cell cocultures contained increased amounts of IFN-γ, TNF, and IL-6 cytokines and CCL3 and CCL4 chemokines (Fig. 5C and D). Intracellular cytokine staining confirmed that both IFN-γ and TNF are produced by cognate CD4⁺ T cells when cocultured with medium, pp65-loaded MoDCs, or PMA/ionomycin (Fig. 6A). While IL-12 was proposed as a cytokine produced by human CD1c⁺ DCs involved in CD8⁺ T-cell priming (44), we did not detect IL-12 (Fig. 5E) or IL-10 or IL-15 (data not shown) in our human DC/T-cell cocultures.

IFN-γ produced by cognate CD4⁺ T cells enhances memory CTL stimulation by licensed DCs. The multiplex array revealed IFN-γ as a candidate cytokine produced by cognate CD4⁺ T cells that enhances DC licensing and consequential memory CTL stimulation, mainly since IFN-γ was the

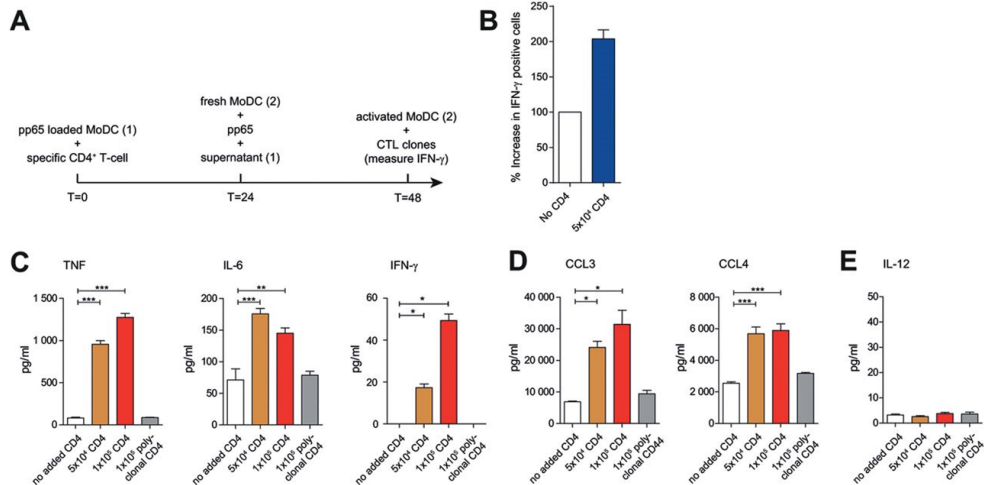


Figure 5. Identification of candidate soluble CD4⁺ T-cell-secreted mediators for licensing of DCs. (A) Schematic outline of supernatant exchange experiments. (B) Summary (mean + standard error of the mean [SEM]) of HCMV pp65₄₋₅₀₃ cross-presentation. Bars represent production of IFN-γ after coculture with loaded MoDCs in the presence of supernatant of pp65-loaded MoDCs (white bar) or pp65-loaded MoDCs cocultured with antigen-specific CD4⁺ T cells (blue bar). (C to E) Cytokine and chemokine production. MoDCs were loaded with pp65 and cocultured for 12 to 16 h without T cells (white bars) or with antigen-specific (orange and red bars) or polyclonal (gray bars) CD4⁺ T cells. Shown are amounts (pg/ml) of TNF (80 to 1,270 pg/ml), IL-6 (71 to 176 pg/ml), IFN-γ (0 to 50 pg/ml), CCL3 (6.9 to 31 ng/ml), CCL4 (2.6 to 5.9 ng/ml), and IL-12 measured with multiplex assay (mean + SEM, n = 4). Significance in all panels was determined using a nonparametric Mann-Whitney test. *, P < 0.05; **, P < 0.01; ***, P < 0.001.

only factor produced exclusively by cognate CD4⁺ T cells and not by DCs (Fig. 5C). We confirmed this by intracellular IFN-γ staining of the stimulated CD4⁺ T cells (Fig. 6A). To address the possibility that IFN-γ contributes to DC licensing, we again performed supernatant exchange experiments as described above, but only now, we preincubated the supernatant with IFN-γ-blocking antibodies (10 μg/ml) or PBS as a control. We found that the increased DC licensing partly depends on IFN-γ, although other factors are likely to contribute (Fig. 6B). Next, we added recombinant IFN-γ (ranging from 0.15 to 150 ng/ml) to 50,000 pp65-loaded HLA-A2*01⁺ MoDCs in the absence of CMV-pp65₄₋₅₀₃-specific CD4⁺ T cells. After 12 to 16 h, we added 50,000 memory CMV-pp65₄₋₅₀₃-specific CTLs and analyzed cells for CTL stimulation by intracellular cytokine staining after 4 hours of coculture in the presence of GolgiStop. NLVPMVATV peptide (1 × 10⁻⁶ M) was included as a positive control for CTL activation (Fig. 6C). We found increased CD8⁺ T-cell stimulation in an IFN-γ dose-dependent manner, as determined by percentages of IFN-γ- and TNF-producing cells and surface-expressed LAMP-1 (Fig. 6C and D) or amounts of IFN-γ and TNF produced. Thus, the coculture of CMV-pp65 antigen-loaded DCs with cognate CD4⁺ T cells provokes IFN-γ production by these CD4⁺ T cells, which consequently facilitates the display of CMV-pp65 peptide/A2 complexes to CD8⁺ T cells. In conclusion, cognate CD4⁺ T cells enhanced DC licensing for memory CD8⁺ immunity, in a manner that requires MHC class II-TCR interaction and subsequent release of IFN-γ by CD4⁺ T cells. Primary antigen-specific CTL expansion also requires cognate CD4⁺ T cells, but here, DC licensing appears to work via the

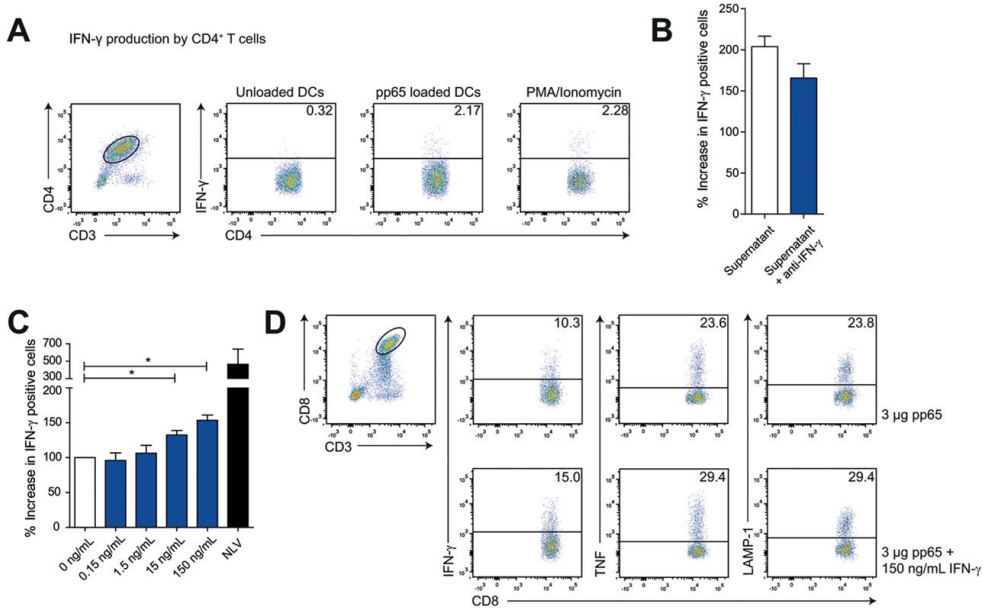


Figure 6. IFN- γ produced by cognate CD4⁺ T cells enhances memory CTL stimulation by licensed DCs. (A) Intracellular staining for IFN- γ gated on CD3- and CD4-positive cells after 12 to 16 h of coculture of antigen-specific CD4⁺ T cells with medium (left graph), pp65-loaded MoDCs (middle graph), or PMA/ionomycin (right graph). (B) CTL activation after coculture with pp65-loaded MoDCs and supernatant of pp65-loaded MoDCs cocultured with antigen-specific CD4⁺ T cells in the presence of PBS (white bar) or IFN- γ -blocking antibodies (blue bar). (C) Summary (mean + standard error of the mean [SEM]) of HCMV pp65₄₋₅₀₃ cross-presentation. Bars represent production of IFN- γ after coculture with MoDCs loaded with 3 μ g pp65 in the presence of recombinant IFN- γ (0.15 to 150 ng/ml, mean + SEM, n = 4). (D) MoDCs were loaded with HCMV-derived pp65 and cocultured with 50,000 A2/NLVP MVATV-specific CD8⁺ T cells in the absence (upper graphs) or presence (lower graphs) of recombinant IFN- γ . Freshly thawed T cells were gated based on CD3 and CD8 expression and analyzed for activation-induced production of IFN- γ (left) and TNF (middle) and LAMP-1 surface expression (right). Significance in all panels was determined using a nonparametric Mann-Whitney test. *, P < 0.05.

CD40-CD40L axis, as in mice (7,-9). Taken together, these data provide mechanistic support for how early reconstitution of CD4⁺ T cells in CBT recipients helps early antigen-driven CD8⁺ T-cell-mediated immune protection against viral reactivation.

Discussion

Infection-related mortality and GvHD are major causes of death after CBT in both adults and pediatric patients (45, 46). Patients are particularly vulnerable to viral reactivation, including reactivation with CMV (1), Epstein-Barr virus (EBV) (47), human herpesvirus 6 (HHV-6) (48), and varicella-zoster virus (VZV) (49). As the immune system is rebuilt from stem cell precursors, immune protective CD8⁺ T cells are formed, which exhibit antigen-specific receptors that recognize epitopes from viruses, including CMV. It had not been fully understood whether and how virus-specific CD4⁺ T cells participate in CD8⁺ T-cell-mediated protection against viral reactivation. From mouse-based research, a role of CD4⁺ T cells in CD8⁺ T-cell priming was

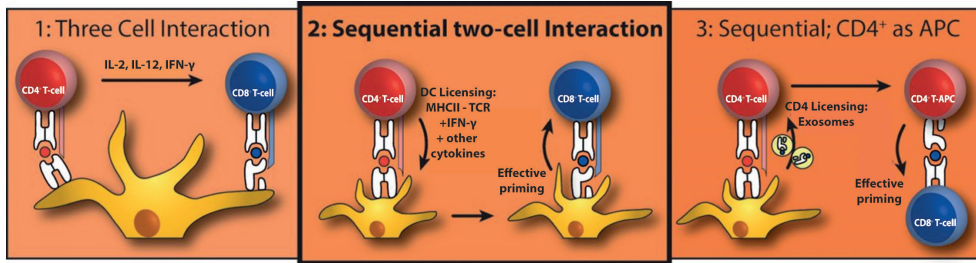


Figure 7. Three suggested mechanisms for CD4⁺ T-cell-mediated CTL priming. (1) Three-cell interaction, where an antigen-specific CD4⁺ T cell and CD8⁺ T cell are in close proximity, interacting through the same DC. The CD4⁺ T cell directly influences CTL priming by cytokine release. (2) Sequential two-cell interaction, where the DC is licensed by an antigen-specific CD4⁺ T cell. This licensing happens by a combination of signals 1, 2, and 3; our data support this model best. (3) Sequential; CD4⁺ as antigen-presenting cell (APC), where the CD4⁺ T cell acquires antigen-presenting cell capacities by receiving peptide-MHC complexes. One proposed mechanism is via exosomes.

deduced. For example, effective CTL induction was seen only when CD4⁺ T cells were present (50,–53). At the same time, from SCT studies, there had been speculation that CD4⁺ T cells may somehow bolster CD8⁺ T-cell-mediated viral immune protection (54). For example, studies show that not only CMV-specific CD8⁺ T cells but also CMV-specific CD4⁺ T-cell numbers can be used to predict the risk for reactivation in patients after allo-SCT (34). Additional support for CD4⁺ T cells in CMV immunity comes from CBT patients, showing that recovery of CD4⁺ CD45RA⁺ T cells is required to clear CMV viremia (55). From mouse-based research, it was learned that the induction of virus antigen-specific CD8⁺ T cells requires the prior licensing of DCs by interaction with cognate, antigen-specific CD4⁺ T cells (7,–12, 56) (summarized in Fig. 7). It was our aim to show the possible applicability of such studies to viral reactivation after SCT in human patients. We here show that antigen-specific CD4⁺ T cells precede the rise of antigen-specific CD8⁺ T cells after CBT, which are necessary to control CMV reactivation. Using a CB-based culture system, we further show that CD4⁺ T cells are required to prime antigen-specific CD8⁺ T cells. These results are in line with conclusions based on mouse work.

The role of CD4⁺ T cells in providing help in elicitation of CTL-mediated viral control may be different when using bone marrow or mobilized peripheral stem cells, although in these settings, CD4⁺ T-cell reconstitution is also correlated with long-term survival (57, 58). When using adult bone marrow or mobilized peripheral stem cells, CMV-specific CD4⁺ and CD8⁺ T cells can be detected independently of CMV viremia, but levels of CMV-specific CD4⁺ (54) or CD8⁺ (3, 59) T cells are protective in these settings. A major difference is the fact that these patients receive antigen-specific CD8⁺ T cells from their donor that can clonally expand, circumventing the required priming in the CB setting. Therefore, expansion of antigen-specific CD8⁺ T cells could be seen as early as 21 days after SCT (59). The mechanism by which CD4⁺ T cells contribute to survival in the bone marrow or mobilized peripheral stem cell transplantation setting is not fully known, although it has been shown that CD4⁺ T-cell help is important to maintain CTL effector function in chronic viral infections in mice. Our data presented here on how cognate antigen-specific CD4⁺ T cells provide DC licensing for effective memory CD8⁺ T-cell responses by secreting IFN-γ provide experimental support for the described observations (60).

As stated in the introduction, CMV reactivation after CBT correlates with decreased survival rates (61,–64). Besides CMV-induced pneumonitis, CMV reactivation is associated with increased risk of GvHD, while GvHD is also a risk factor for viral reactivations (62, 65,–68). CMV is the most frequent reactivation, but other viruses also hamper survival. Reactivation of EBV (47), HHV-6 (48), and VZV (49) plays a major role after CBT. We here describe that CMV control coincides with the presence of CMV-specific CD8⁺ T-cell expansion, which is preceded by the appearance of a CMV-specific CD4⁺ T-cell population. Using CB-based cocultures, we show the requirement for cognate CD4⁺ T cells in DC licensing for the expansion of antigen-specific CD8⁺ T cells. We believe that this is a general mechanism that can be applied broadly to antiviral and possibly even antitumor immune responses. Especially considering the important role of CD8⁺ T cells in relapse control, this work supports the importance of monitoring the CD4⁺ T-cell reconstitution early after CBT and paves the road to CD4⁺ T-cell-based intervention strategies.

Acknowledgements

We thank members of the Boes laboratory for helpful discussions and Esther Quakkelaar for help with the TCR sequencing.

References

1. Boeckh M, Ljungman P. 2009. How we treat cytomegalovirus in hematopoietic cell transplant recipients. *Blood* 113:5711–5719.
2. Flinsenberg TW, Compeer EB, Boelens JJ, Boes M. 2011. Antigen cross-presentation: extending recent laboratory findings to therapeutic intervention. *Clin Exp Immunol* 165:8–18.
3. Tormo N, Solano C, Benet I, Nieto J, de la Cámara R, Lopez J, Garcia Noblejas A, Munoz-Cobo B, Costa E, Clari MA, Hernandez-Boluda JC, Remigia MJ, Navarro D. 2011. Reconstitution of CMV pp65 and IE-1-specific IFN-gamma CD8(+) and CD4(+) T-cell responses affording protection from CMV DNAemia following allogeneic hematopoietic SCT. *Bone Marrow Transplant* 46:1437–1443.
4. Polic B, Hengel H, Krmpotic A, Trgovcich J, Pavic I, Luccaronin P, Jonjic S, Koszinowski UH. 1998. Hierarchical and redundant lymphocyte subset control precludes cytomegalovirus replication during latent infection. *J Exp Med* 188:1047–1054.
5. Andersen BM, Ohlfest JR. 2012. Increasing the efficacy of tumor cell vaccines by enhancing cross priming. *Cancer Lett* 325:155–164.
6. Loeth N, Assing K, Madsen HO, Vindelov L, Buus S, Stryhn A. 2012. Humoral and cellular CMV responses in healthy donors; identification of a frequent population of CMV-specific, CD4+ T cells in seronegative donors. *PLoS One* 7:e31420.
7. Bennett SR, Carbone FR, Karamalis F, Flavell RA, Miller JF, Heath WR. 1998. Help for cytotoxic-T-cell responses is mediated by CD40 signalling. *Nature* 393:478–480.
8. Ridge JP, Di Rosa F, Matzinger P. 1998. A conditioned dendritic cell can be a temporal bridge between a CD4+ T-helper and a T-killer cell. *Nature* 393:474–478.
9. Schoenberger SP, Toes RE, van der Voort EI, Offringa R, Melief CJ. 1998. T-cell help for cytotoxic T lymphocytes is mediated by CD40-CD40L interactions. *Nature* 393:480–483.
10. Smith CM, Wilson NS, Waithman J, Villadangos JA, Carbone FR, Heath WR, Belz GT. 2004. Cognate CD4(+) T cell licensing of dendritic cells in CD8(+) T cell immunity. *Nat Immunol* 5:1143–1148.
11. Bennett SR, Carbone FR, Karamalis F, Miller JF, Heath WR. 1997. Induction of a CD8+ cytotoxic T lymphocyte response by cross-priming requires cognate CD4+ T cell help. *J Exp Med* 186:65–70.
12. Keene JA, Forman J. 1982. Helper activity is required for the in vivo generation of cytotoxic T lymphocytes. *J Exp Med* 155:768–782.
13. Franssen MF, Sluijter M, Morreau H, Arens R, Melief CJ. 2011. Local activation of CD8 T cells and systemic tumor eradication without toxicity via slow release and local delivery of agonistic CD40 antibody. *Clin Cancer Res* 17:2270–2280.
14. Nguyen LT, Elford AR, Murakami K, Garza KM, Schoenberger SP, Odermatt B, Speiser DE, Ohashi PS. 2002. Tumor growth enhances cross-presentation leading to limited T cell activation without tolerance. *J Exp Med* 195:423–435.
15. Staras SA, Dollard SC, Radford KW, Flanders WD, Pass RF, Cannon MJ. 2006. Seroprevalence of cytomegalovirus infection in the United States, 1988–1994. *Clin Infect Dis* 43:1143–1151.
16. Einsele H, Roosnek E, Rufer N, Sinzger C, Riegler S, Loffler J, Grigoleit U, Moris A, Rammensee HG, Kanz L, Kleihauer A, Frank F, Jahn G, Hebart H. 2002. Infusion of cytomegalovirus (CMV)-specific T cells for the treatment of CMV infection not responding to antiviral chemotherapy. *Blood* 99:3916–3922.
17. Aarntzen EH, de Vries I, Lesterhuis WJ, Schuurhuis D, Jacobs JF, Bol K, Schreiber G, Mus R, De Wilt JH, Haanen JB, Schadendorf D, Croockewit A, Blokx WA, Van Rossum MM, Kwok WW, Adema GJ, Punt CJ, Figdor CG. 2013. Targeting CD4(+) T-helper cells improves the induction of antitumor responses in dendritic cell-based vaccination. *Cancer Res* 73:19–29.
18. Clari MA, Aguilar G, Benet I, Belda J, Gimenez E, Bravo D, Carbonell JA, Henae L, Navarro D. 2013. Evaluation of cytomegalovirus (CMV)-specific T-cell immunity for the assessment of the risk of active CMV infection in non-immunosuppressed surgical and trauma intensive care unit patients. *J Med Virol* 85:1802–1810.
19. Lindemans CA, Chiesa R, Amrolia PJ, Rao K, Nikolajeva O, de Wildt A, Gerhardt CE, Gilmour KC, Bierings B, Veys P, Boelens JJ. 2014. Impact of thymoglobulin prior to pediatric unrelated umbilical cord blood transplantation on immune reconstitution and clinical outcome. *Blood* 123:126–132.
20. Bartelink IH, Belitser SV, Knibbe CA, Danhof M, de Pagter AJ, Egberts TC, Boelens JJ. 2013. Immune reconstitution kinetics as an early predictor for mortality using various hematopoietic stem cell sources in children. *Biol Blood Marrow Transplant* 19:305–313.
21. Fujii H, Cuvelier G, She K, Aslanian S, Shimizu H, Kariminia A, Krailo M, Chen Z, McMaster R, Bergman

- A, Goldman F, Grupp SA, Wall DA, Gilman AL, Schultz KR. 2008. Biomarkers in newly diagnosed pediatric-extensive chronic graft-versus-host disease: a report from the Children's Oncology Group. *Blood* 111:3276–3285.
22. Quigley MF, Almeida JR, Price DA, Douek DC. 2011. Unbiased molecular analysis of T cell receptor expression using template-switch anchored RT-PCR. *Curr Protoc Immunol Chapter 10:Unit 10.33*.
 23. Giudicelli V, Brochet X, Lefranc MP. 2011. IMGT/V-QUEST: IMGT standardized analysis of the immunoglobulin (IG) and T cell receptor (TR) nucleotide sequences. *Cold Spring Harb Protoc* 2011:695–715.
 24. Koning D, Costa AI, Hasrat R, Grady BP, Spijkers S, Nanlohy N, Kesmir C, van Baarle D. 2014. In vitro expansion of antigen-specific CD8 T cells distorts the T-cell repertoire. *J Immunol Methods* 405:199–203.
 25. Flinsenberg TW, Compeer EB, Koning D, Klein M, Amelung FJ, van Baarle D, Boelens JJ, Boes M. 2012. Fcγ receptor antigen targeting potentiates cross-presentation by human blood and lymphoid tissue BDCA-3+ dendritic cells. *Blood* 120:5163–5172.
 26. Salih HR, Kosowski SG, Haluska VF, Starling GC, Loo DT, Lee F, Aruffo AA, Trail PA, Kiener PA. 2000. Constitutive expression of functional 4-1BB (CD137) ligand on carcinoma cells. *J Immunol* 165:2903–2910.
 27. Palliser D, Ploegh H, Boes M. 2004. Myeloid differentiation factor 88 is required for cross-priming in vivo. *J Immunol* 172:3415–3421.
 28. de Jager W, Hoppenreijns EP, Wulffraat NM, Wedderburn LR, Kuis W, Prakken BJ. 2007. Blood and synovial fluid cytokine signatures in patients with juvenile idiopathic arthritis: a cross-sectional study. *Ann Rheum Dis* 66:589–598.
 29. Kern F, Faulhaber N, Frommel C, Khatamzas E, Prosch S, Schonemann C, Kretzschmar I, Volkmer-Engert R, Volk HD, Reinke P. 2000. Analysis of CD8 T cell reactivity to cytomegalovirus using protein-spanning pools of overlapping pentadecapeptides. *Eur J Immunol* 30:1676–1682.
 30. de Pagter AP, Boelens JJ, Scherrenburg J, Vroom-de BT, Tesselaar K, Nanlohy N, Sanders EA, Schuurman R, van Baarle D. 2012. First analysis of human herpesvirus 6T-cell responses: specific boosting after HHV6 reactivation in stem cell transplantation recipients. *Clin Immunol* 144:179–189.
 31. Matloubian M, Concepcion RJ, Ahmed R. 1994. CD4+ T cells are required to sustain CD8+ cytotoxic T-cell responses during chronic viral infection. *J Virol* 68:8056–8063.
 32. Nakanishi Y, Lu B, Gerard C, Iwasaki A. 2009. CD8(+) T lymphocyte mobilization to virus-infected tissue requires CD4(+) T-cell help. *Nature* 462:510–513.
 33. Zajac AJ, Blattman JN, Murali-Krishna K, Sourdive DJ, Suresh M, Altman JD, Ahmed R. 1998. Viral immune evasion due to persistence of activated T cells without effector function. *J Exp Med* 188:2205–2213.
 34. Solano C, Benet I, Clari MA, Nieto J, de la Cámara R, Lopez J, Hernandez-Boluda JC, Remigia MJ, Jarque I, Calabuig ML, Garcia-Noblejas A, Alberola J, Tamarit A, Gimeno C, Navarro D. 2008. Enumeration of cytomegalovirus-specific interferon gamma CD8+ and CD4+ T cells early after allogeneic stem cell transplantation may identify patients at risk of active cytomegalovirus infection. *Haematologica* 93:1434–1436.
 35. Schuurhuis DH, Laban S, Toes RE, Ricciardi-Castagnoli P, Kleijmeer MJ, van der Voort EI, Rea D, Offringa R, Geuze HJ, Melief CJ, Ossendorp F. 2000. Immature dendritic cells acquire CD8(+) cytotoxic T lymphocyte priming capacity upon activation by T helper cell-independent or -dependent stimuli. *J Exp Med* 192:145–150.
 36. Toes RE, Schoenberger SP, van der Voort EI, Offringa R, Melief CJ. 1998. CD40-CD40 ligand interactions and their role in cytotoxic T lymphocyte priming and anti-tumor immunity. *Semin Immunol* 10:443–448.
 37. Venturi V, Chin HY, Asher TE, Ladell K, Scheinberg P, Bornstein E, van Bockel D, Kelleher AD, Douek DC, Price DA, Davenport MP. 2008. TCR beta-chain sharing in human CD8+ T cell responses to cytomegalovirus and EBV. *J Immunol* 181:7853–7862.
 38. Sallusto F, Geginat J, Lanzavecchia A. 2004. Central memory and effector memory T cell subsets: function, generation, and maintenance. *Annu Rev Immunol* 22:745–763.
 39. van Loenen MM, Hagedoorn RS, de Boer R, Falkenburg JH, Heemskerk MH. 2013. Extracellular domains of CD8α and CD8β subunits are sufficient for HLA class I restricted helper functions of TCR-engineered CD4(+) T cells. *PLoS One* 8:e65212.
 40. Chen L, Flies DB. 2013. Molecular mechanisms of T cell co-stimulation and co-inhibition. *Nat Rev*

- Immunol 13:227–242.
41. Keating GM. 2013. Abatacept: a review of its use in the management of rheumatoid arthritis. *Drugs* 73:1095–1119.
 42. Rosman Z, Shoenfeld Y, Zandman-Goddard G. 2013. Biologic therapy for autoimmune diseases: an update. *BMC Med* 11:88.
 43. Harfuddin Z, Kwajah S, Chong Nyi Sim A, Macary PA, Schwarz H. 2013. CD137L-stimulated dendritic cells are more potent than conventional dendritic cells at eliciting cytotoxic T-cell responses. *Oncoimmunology* 2:e26859.
 44. Nizzoli G, Krietsch J, Weick A, Steinfelder S, Facciotti F, Gruarin P, Bianco A, Steckel B, Moro M, Crosti M, Romagnani C, Stolzel K, Torretta S, Pignataro L, Scheibenbogen C, Neddermann P, De Francesco R, Abrignani S, Geginat J. 2013. Human CD1c+ dendritic cells secrete high levels of IL-12 and potently prime cytotoxic T-cell responses. *Blood* 122:932–942.
 45. Kurtzberg J, Prasad VK, Carter SL, Wagner JE, Baxter-Lowe LA, Wall D, Kapoor N, Guinan EC, Feig SA, Wagner EL, Kernan NA. 2008. Results of the Cord Blood Transplantation Study (COBLT): clinical outcomes of unrelated donor umbilical cord blood transplantation in pediatric patients with hematologic malignancies. *Blood* 112:4318–4327.
 46. Rocha V, Labopin M, Sanz G, Arcese W, Schwerdtfeger R, Bosi A, Joacbsen N, Ruutu T, de Lima M, Finke J, Frassoni F, Fluckman E. 2004. Transplants of umbilical-cord blood or bone marrow from unrelated donors in adults with acute leukemia. *N Engl J Med* 351:2276–2285.
 47. Rasche L, Kapp M, Einsele H, Mielke S. 2014. EBV-induced post transplant lymphoproliferative disorders: a persisting challenge in allogeneic hematopoietic SCT. *Bone Marrow Transplant* 49:163–167.
 48. de Pagter PJ, Schuurman R, Keukens L, Schutten M, Cornelissen JJ, van Baarle D, Fries E, Sanders EA, Minnema MC, van der Holt BR, Meijer E, Boelens JJ. 2013. Human herpes virus 6 reactivation: important predictor for poor outcome after myeloablative, but not non-myeloablative allo-SCT. *Bone Marrow Transplant* 48:1460–1464.
 49. Vandenbosch K, Ovetchkine P, Champagne MA, Haddad E, Alexandrov L, Duval M. 2008. Varicella-zoster virus disease is more frequent after cord blood than after bone marrow transplantation. *Biol Blood Marrow Transplant* 14:867–871.
 50. Gao FG, Khammanivong V, Liu WJ, Leggatt GR, Frazer IH, Fernando GJ. 2002. Antigen-specific CD4+ T-cell help is required to activate a memory CD8+ T cell to a fully functional tumor killer cell. *Cancer Res* 62:6438–6441.
 51. Ossendorp F, Toes RE, Offringa R, van der Burg SH, Melief CJ. 2000. Importance of CD4(+) T helper cell responses in tumor immunity. *Immunol Lett* 74:75–79.
 52. Sun JC, Bevan MJ. 2003. Defective CD8 T cell memory following acute infection without CD4 T cell help. *Science* 300:339–342.
 53. Sun JC, Williams MA, Bevan MJ. 2004. CD4+ T cells are required for the maintenance, not programming, of memory CD8+ T cells after acute infection. *Nat Immunol* 5:927–933.
 54. Szabolcs P, Niedzwiecki D. 2008. Immune reconstitution in children after unrelated cord blood transplantation. *Biol Blood Marrow Transplant* 14:66–72.
 55. Brown JA, Stevenson K, Kim HT, Cutler C, Ballen K, McDonough S, Reynolds C, Herrera M, Liney D, Ho V, Kao G, Armand P, Koreth J, Alyea E, McAfee S, Attar E, Dey B, Spitzer T, Soiffer R, Ritz J, Antin JH, Boussiotis VA. 2010. Clearance of CMV viremia and survival after double umbilical cord blood transplantation in adults depends on reconstitution of thymopoiesis. *Blood* 115:4111–4119.
 56. Lanzavecchia A. 1998. Immunology. Licence to kill. *Nature* 393:413–414.
 57. Fedele R, Martino M, Garreffa C, Messina G, Console G, Princi D, Dattola A, Moscato T, Massara E, Spiniello E, Irrera G, Iacopino P. 2012. The impact of early CD4+ lymphocyte recovery on the outcome of patients who undergo allogeneic bone marrow or peripheral blood stem cell transplantation. *Blood Transfus* 10:174–180.
 58. Berger M, Figari O, Bruno B, Raiola A, Dominiotto A, Fiorone M, Podesta M, Tedone E, Pozzi S, Fagioli F, Madon E, Bacigalupo A. 2008. Lymphocyte subsets recovery following allogeneic bone marrow transplantation (BMT): CD4+ cell count and transplant-related mortality. *Bone Marrow Transplant* 41:55–62.
 59. Cwynarski K, Ainsworth J, Cobbold M, Wagner S, Mahendra P, Apperley J, Goldman J, Craddock C, Moss PA. 2001. Direct visualization of cytomegalovirus-specific T-cell reconstitution after allogeneic stem cell transplantation. *Blood* 97:1232–1240.
 60. Kalams SA, Walker BD. 1998. The critical need for CD4 help in maintaining effective cytotoxic T

- lymphocyte responses. *J Exp Med* 188:2199–2204.
61. Gandhi MK, Khanna R. 2004. Human cytomegalovirus: clinical aspects, immune regulation, and emerging treatments. *Lancet Infect Dis* 4:725–738.
 62. Ljungman P, Perez-Bercoff L, Jonsson J, Avetisyan G, Sparrelid E, Aschan J, Barkholt L, Larsson K, Winiarski J, Yun Z, Ringden O. 2006. Risk factors for the development of cytomegalovirus disease after allogeneic stem cell transplantation. *Haematologica* 91:78–83
 63. Ljungman P, Hakki M, Boeckh M. 2010. Cytomegalovirus in hematopoietic stem cell transplant recipients. *Infect Dis Clin North Am* 24:319–337.
 64. Mikulska M, Raiola AM, Bruzzi P, Varaldo R, Annunziata S, Lamparelli T, Frassoni F, Tedone E, Galano B, Bacigalupo A, Viscoli C. 2012. CMV infection after transplant from cord blood compared to other alternative donors: the importance of donor-negative CMV serostatus. *Biol Blood Marrow Transplant* 18:92–99.
 65. George B, Pati N, Gilroy N, Ratnamohan M, Huang G, Kerridge I, Hertzberg M, Gottlieb D, Bradstock K. 2010. Pre-transplant cytomegalovirus (CMV) serostatus remains the most important determinant of CMV reactivation after allogeneic hematopoietic stem cell transplantation in the era of surveillance and preemptive therapy. *Transpl Infect Dis* 12:322–329.
 66. Jaskula E, Dlubek D, Sedzimirska M, Duda D, Tarnowska A, Lange A. 2010. Reactivations of cytomegalovirus, human herpes virus 6, and Epstein-Barr virus differ with respect to risk factors and clinical outcome after hematopoietic stem cell transplantation. *Transplant Proc* 42:3273–3276.
 67. Miller W, Flynn P, McCullough J, Balfour HH Jr, Goldman A, Haake R, McGlave P, Ramsay N, Kersey J. 1986. Cytomegalovirus infection after bone marrow transplantation: an association with acute graft-v-host disease. *Blood* 67:1162–1167.
 68. Pichereau C, Desseaux K, Janin A, Scieux C, Peffault de Latour R, Xhaard A, Robin M, Ribaud P, Agbalika F, Chevret S, Socie G. 2012. The complex relationship between human herpesvirus 6 and acute graft-versus-host disease. *Biol Blood Marrow Transplant* 18:141–144.

Chapter 5

Preliminary evaluation of a bunyavirus vector for cancer immunotherapy.

Authors

Nadia Oreshkova, Lotte Spel, Rianka P. M. Vloet, Paul J. Wichgers Schreur, Rob J. M. Moormann, Marianne Boes, Jeroen Kortekaas

Published in

Journal of Virology 2015



Abstract

Replicon particles of Rift Valley fever virus, referred to as nonspreading Rift Valley fever virus (NSR), are intrinsically safe and highly immunogenic. Here, we demonstrate that NSR-infected human dendritic cells can activate CD8⁺ T cells in vitro and that prophylactic and therapeutic vaccinations of mice with NSR encoding a tumor-associated CD8 peptide can control the outgrowth of lymphoma cells in vivo. These results suggest that the NSR system holds promise for cancer immunotherapy.

Results

Dendritic cells (DCs) are the most potent antigen-presenting cells in the body and are instrumental in directing adaptive immune responses against pathogens and tumors. DCs are naturally targeted by many arboviruses. Infection induces DC maturation and presentation of virus-associated antigens, explaining the interest in using these viruses as therapeutic vectors of tumor-associated antigens. Members of the positive-strand RNA virus families *Togaviridae* and *Flaviviridae* have been extensively evaluated for cancer immunotherapy (1,–4), some of which have already entered clinical trials (2). Remarkably, arboviruses with segmented negative-strand RNA genomes have remained largely unexplored in this field. The genome segments of these viruses form double-stranded RNA panhandles that, in some viruses, contain a 5' triphosphate. This structure is an optimal ligand for the cytoplasmic pattern recognition receptor RIG-I and thereby an excellent inducer of adjuvanting innate immune responses (5). We therefore propose that arboviruses with segmented negative-strand RNA genomes that activate RIG-I hold promise for cancer immunotherapy.

Rift Valley fever virus (RVFV), a member of the *Bunyaviridae* family, was recently shown to productively infect immature DCs with high efficiency (6). Whereas wild-type RVFV counteracts innate immune responses via the NSs protein (7), infection of DCs with RVFV variants lacking the NSs protein was shown to result in strong interferon (IFN) responses triggered by RIG-I signaling (8). We recently developed RVFV particles that lack not only the gene for NSs but also the glycoprotein-encoding genome segment (9). The resulting nonspreading RVFV (NSR) particles are unable to produce progeny virions, ensuring their safe application (9). Moreover, the absence of the gene for NSs provides a slot for the expression of a gene of interest. Vaccination with NSR particles was shown to be highly effective in protecting livestock from RVFV (10,–12), and NSR particles expressing the influenza virus hemagglutinin gene protected mice from lethal influenza (13). The remarkable efficacy of NSR-based vaccines in both inbred and outbred animals, particularly its association with Th1-type immune responses (13), prompted the present study on the use of NSR for cancer immunotherapy.

Initially, we investigated whether NSR-infected human monocyte-derived DCs (MoDCs) can activate CD8⁺ T cells *in vitro*. MoDCs were derived from peripheral blood mononuclear cells of healthy donors by Ficoll-Isopaque density gradient centrifugation (GE Healthcare Bio-Sciences AB) and cultured as previously described (14). Infection of DCs was remarkably efficient, resulting in over 90% green fluorescent protein (GFP)-positive cells under optimal conditions (data not shown). To study the T-cell activation capacity of infected DCs, an NSR variant was constructed that encodes the immunodominant NLVPMVATV epitope of human cytomegalovirus pp65 (pp65⁴⁹⁵⁻⁵⁰³) fused to the C terminus of GFP (Fig. 1A). NSR particles encoding this fusion protein (NSR_{NLV}) and particles encoding GFP only (NSR_{GFP}) were used to infect DCs obtained from an HLA A2-positive donor. As a positive control, DCs were incubated with a synthetic NLVPMVATV peptide (1 μM), and culture medium was used as a negative control. After overnight incubation, HLA A*0201-restricted, NLVPMVATV-specific CD8⁺ T cells (14) were added to the DCs and cocultured for 4.5 h. T cells were harvested, stained for CD3, CD8, and CD107a (LAMP-1) surface markers, and subsequently intracellularly stained for IFN-γ and tumor necrosis factor (TNF). The results of this experiment demonstrate that NSR can be successfully used as a vector to deliver specific immunogenic epitopes to human DCs, which trigger an effector function in corresponding CD8⁺

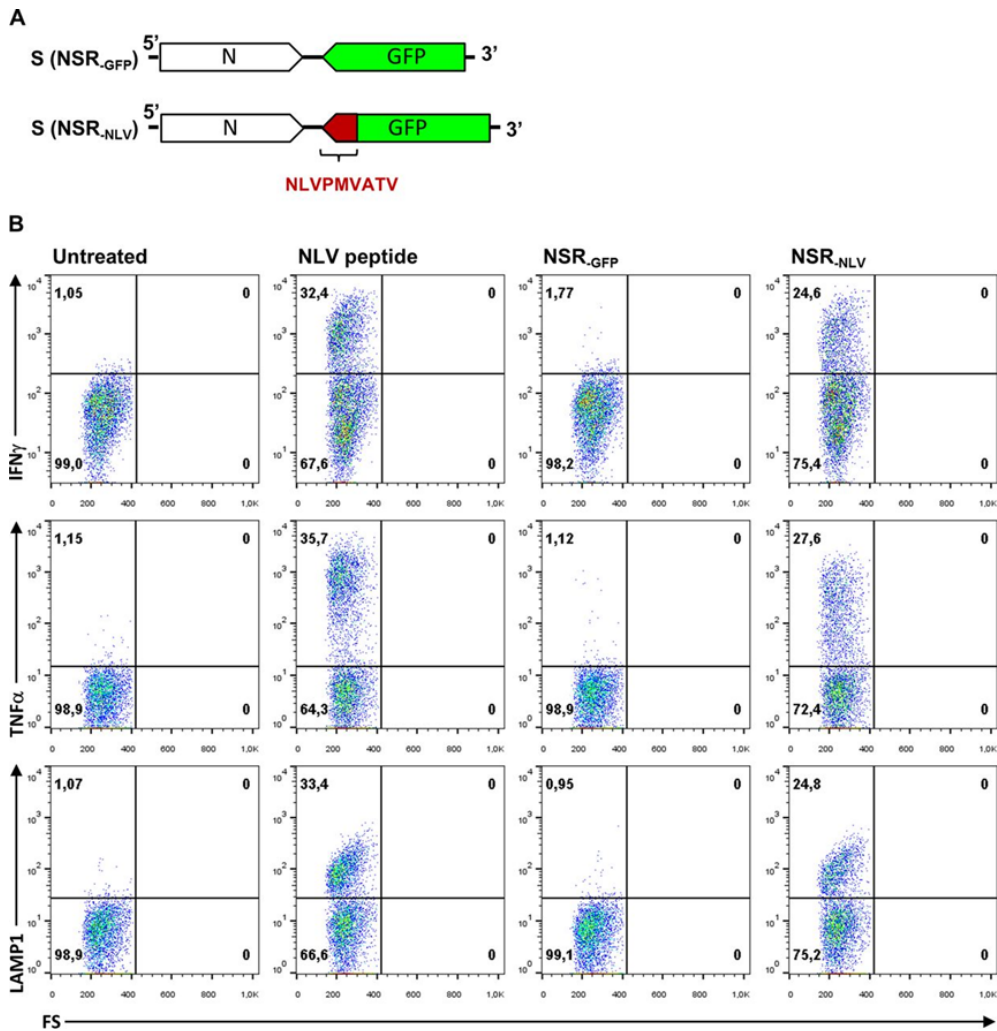


Figure 1. (A) Schematic representation of the NSR S segment encoding GFP (top) or the C-terminally fused pp65₄₉₅₋₅₀₃ epitope (bottom) in an antigenomic orientation. (B) NSR-infected human DCs activate antigen-specific CD8⁺ T cells. HLA A2⁺ DCs were infected with NSR_{GFP} or NSR_{NLV} and cultured overnight. As a negative control, DCs were left untreated; as positive control, DCs were loaded with synthetic peptide pp65₄₉₅₋₅₀₃. An A2-restricted CD8⁺ T cell clone specific for the pp65₄₉₅₋₅₀₃ epitope was added for 4.5 h of incubation in the presence of GolgiStop (Becton Dickinson) and analyzed for activation. The expression of IFN- γ , TNF, and LAMP-1 in the CD8/CD3-positive cell population is depicted. All three parameters are induced specifically in NSR_{NLV}-infected cells and not in NSR_{GFP}-infected cells. FS, forward scatter.

T cells (Fig. 1B).

To investigate the feasibility of using NSR for cancer immunotherapy, we made use of C57BL/6 Kh (B6, H-2b) mice and E.G7-OVA cells, a chicken ovalbumin (OVA) gene-transfected clone of mouse lymphoma EL4 cells obtained from the American Type Culture Collection (Manassas, VA, USA). (The animal experiments described here were conducted in accordance with the Dutch Law on Animal Experiments [Wod, ID no. BWR0003081] and approved by the Animal Ethics Committee

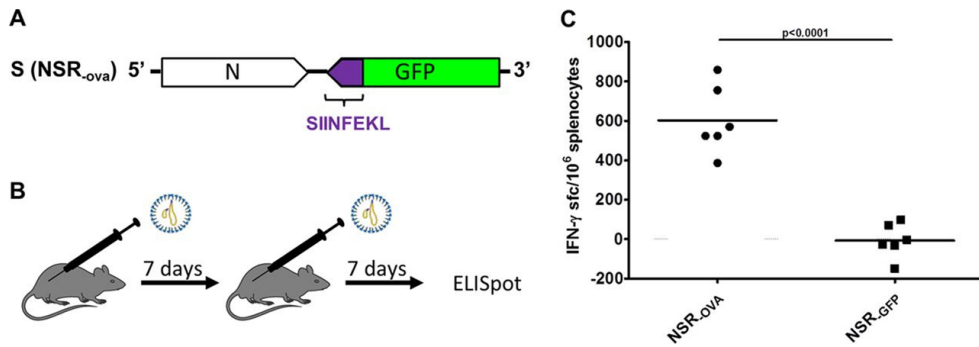


Figure 2. (A) Schematic representation of the NSR S segment encoding the OVA₂₅₇₋₂₆₄ peptide fused to GFP in an antigenomic orientation. (B) Representation of the regimens used for vaccination with NSR_{OVA} or control NSR_{GFP} vaccine. (C) ELISpot assay showing IFN- γ responses of splenocytes collected from mice that were vaccinated with either NSR_{GFP} or NSR_{OVA} (n = 6). Symbols represent individual counts of IFN- γ spot-forming cells (sfc). Statistical significance (Student's t test) is indicated.

of the Central Veterinary Institute [permit no. 2014101.c.] An NSR variant was constructed that encodes the CD8-restricted SIINFEKL epitope of OVA (OVA²⁵⁷⁻²⁶⁴) fused to GFP (NSR_{OVA}) (Fig. 2A). To determine whether NSR_{OVA} vaccination elicits a cellular immune response specific for this epitope, mice were vaccinated twice via the intramuscular route (thigh muscle), at a 1-week interval, with 10⁸ 50% tissue culture infective doses of NSR_{OVA} (Fig. 2B). Control mice were vaccinated with NSR_{GFP}. One week after the second vaccination, spleen cells were collected and evaluated for the ability to produce IFN- γ after stimulation with a synthetic SIINFEKL peptide (10 μ g/ml; Invitrogen) in an enzyme-linked immunospot assay (ELISpot) assay (10). This experiment demonstrated that NSR_{OVA} vaccination elicits a SIINFEKL-specific cellular immune response (Fig. 2C).

We finally asked whether prophylactic or therapeutic vaccination with NSR_{OVA} can reduce the outgrowth of E.G7-OVA tumor cells (Fig. 3A). Mice were subcutaneously inoculated with 10⁶ E.G7-OVA cells and euthanized by cervical dislocation when the tumor size reached 5,000 mm³. Both prophylactic and therapeutic vaccinations via the intramuscular route with NSR_{OVA} resulted in increased survival times compared to those of control mice that had received NSR_{GFP} (Fig. 3B). Therapeutic vaccination resulted in complete tumor clearance in 2/10 mice, whereas prophylactic vaccination resulted in clearance of tumors in 6/10 mice. As expected, recultured tumor cells collected from NSRGFP-vaccinated mice upon necropsy were found to express OVA, as determined by a commercial OVA enzyme-linked immunosorbent assay (ELISA; Agro-Bio). Surprisingly, tumor cells collected from mice vaccinated with NSR_{OVA} did not express detectable levels of OVA (Fig. 3C). This finding suggests that small numbers of the inoculated cells did not express OVA or lost OVA expression in time and that tumor cells expressing OVA were efficiently cleared by either prophylactic or therapeutic vaccination.

The present work demonstrates that NSR particles can successfully deliver an immunogenic peptide to human DCs and that these cells are capable of activating CD8⁺ T cells. In addition, vaccination of mice with NSR expressing a single CD8-restricted epitope resulted in the complete clearance of lymphoma cells expressing the targeted antigen. Future experiments will address the efficacy of NSR vaccination to control outgrowth of tumors expressing self-antigens. Considering

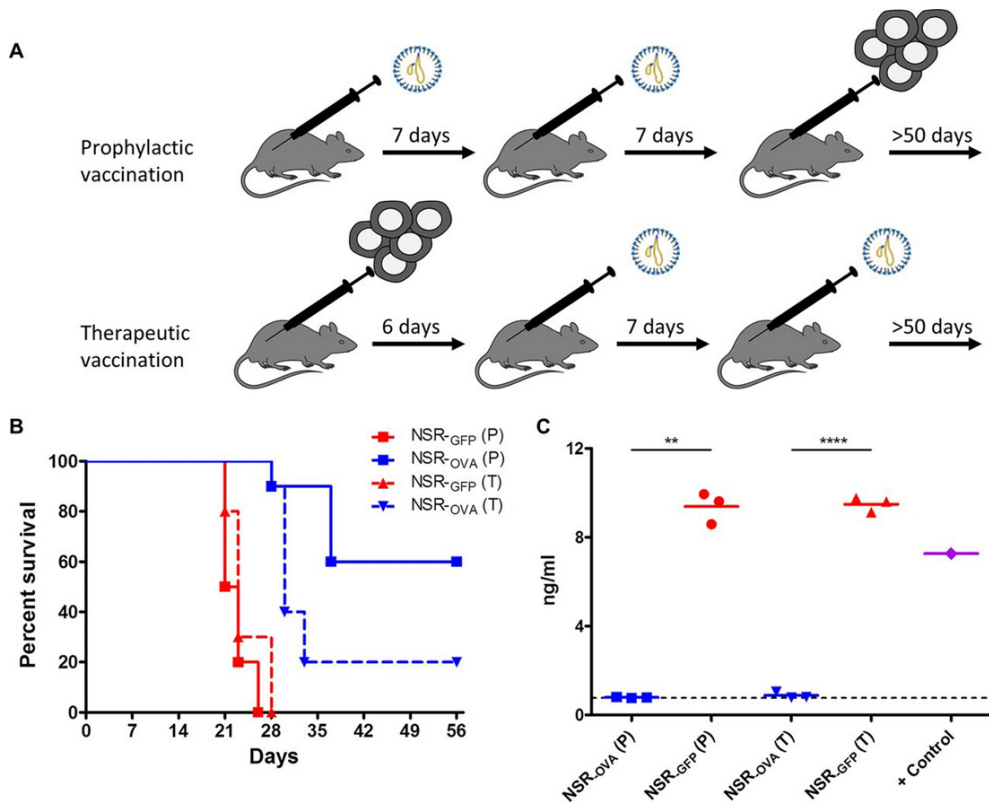


Figure 3. (A) Prophylactic and therapeutic regimens used for vaccination with NSR_{OVA} or control NSR_{GFP} vaccine. The primary therapeutic vaccination was applied when more than 50% of the E.G7-OVA-inoculated mice had palpable tumors. (B) Survival curves of mice prophylactically (P, solid lines) or therapeutically (T, interrupted lines) vaccinated with NSR_{GFP} or NSR_{OVA}. Statistical analyses were performed with GraphPad Prism. Log-rank (Mantel-Cox) tests revealed statistically significant differences ($P < 0.0001$) between NSR_{GFP} and NSR_{OVA} vaccinations with either a prophylactic or a therapeutic regimen. (C) Detection of OVA in supernatants of cultured E.G7-OVA cells by ELISA. Cells were recultured for 7 days after being collected from mice ($n = 3/\text{group}$) that had reached the humane endpoint. Statistical significance (Student's t test with Welch's correction for unequal variances) is shown. E.G7-OVA cells that were used for the inoculation of mice were used to obtain a positive-control (+ Control) sample.

that self-antigens are much less immunogenic, NSR particles will be designed to express not only CD8⁺ peptides but also CD4⁺ and B-cell epitopes.

Acknowledgements

We thank Tuna Mutis and Anton Martens (VU University Medical Center, Department of Hematology) for useful discussions.

References

1. Moran TP, Collier M, McKinnon KP, Davis NL, Johnston RE, Serody JS. 2005. A novel viral system for generating antigen-specific T cells. *J Immunol* 175:3431–3438.
2. Morse MA, Hobeika AC, Osada T, Berglund P, Hubby B, Negri S, Niedzwiecki D, Devi GR, Burnett BK, Clay TM, Smith J, Lysterly HK. 2010. An alphavirus vector overcomes the presence of neutralizing antibodies and elevated numbers of Tregs to induce immune responses in humans with advanced cancer. *J Clin Invest* 120:3234–3241.
3. Anraku I, Harvey TJ, Linedale R, Gardner J, Harrich D, Suhrbier A, Khromykh AA. 2002. Kunjin virus replicon vaccine vectors induce protective CD8+ T-cell immunity. *J Virol* 76:3791–3799.
4. Herd KA, Harvey T, Khromykh AA, Tindle RW. 2004. Recombinant Kunjin virus replicon vaccines induce protective T-cell immunity against human papillomavirus 16 E7-expressing tumour. *Virology* 319:237–248.
5. Schlee M, Roth A, Hornung V, Hagmann CA, Wimmenauer V, Barchet W, Coch C, Janke M, Mihailovic A, Wardle G, Juranek S, Kato H, Kawai T, Poeck H, Fitzgerald KA, Takeuchi O, Akira S, Tuschl T, Latz E, Ludwig J, Hartmann G. 2009. Recognition of 5' triphosphate by RIG-I helicase requires short blunt double-stranded RNA as contained in panhandle of negative-strand virus. *Immunity* 31:25–34.
6. Lozach PY, Kühbacher A, Meier R, Mancini R, Bitto D, Bouloy M, Helenius A. 2011. DC-SIGN as a receptor for phleboviruses. *Cell Host Microbe* 10:75–88.
7. Le May N, Mansuroglu Z, Leger P, Josse T, Blot G, Billecoq A, Flick R, Jacob Y, Bonnefoy E, Bouloy M. 2008. A SAP30 complex inhibits IFN-beta expression in Rift Valley fever virus infected cells. *PLoS Pathog* 4:e13.
8. Ermler ME, Yerukhim E, Schriewer J, Schattgen S, Traylor Z, Wespiser AR, Caffrey DR, Chen ZJ, King CH, Gale M Jr, Colonna M, Fitzgerald KA, Buller RM, Hise AG. 2013. RNA helicase signaling is critical for type I interferon production and protection against Rift Valley fever virus during mucosal challenge. *J Virol* 87:4846–4860.
9. Kortekaas J, Oreshkova N, Cobos-Jimenez V, Vloet RP, Potgieter CA, Moormann RJ. 2011. Creation of a nonspreading Rift Valley fever virus. *J Virol* 85:12622–12630.
10. Oreshkova N, van Keulen L, Kant J, Moormann RJ, Kortekaas J. 2013. A single vaccination with an improved nonspreading Rift Valley fever virus vaccine provides sterile immunity in lambs. *PLoS One* 8:e77461.
11. Kortekaas J, Antonis AF, Kant J, Vloet RP, Vogel A, Oreshkova N, de Boer SM, Bosch BJ, Moormann RJ. 2012. Efficacy of three candidate Rift Valley fever vaccines in sheep. *Vaccine* 30:3423–3429.
12. Kortekaas J, Oreshkova N, van Keulen L, Kant J, Bosch BJ, Bouloy M, Moulin V, Goovaerts D, Moormann RJ. 2014. Comparative efficacy of two next-generation Rift Valley fever vaccines. *Vaccine* 32:4901–4908.
13. Oreshkova N, Cornelissen LA, de Haan CA, Moormann RJ, Kortekaas J. 2014. Evaluation of nonspreading Rift Valley fever virus as a vaccine vector using influenza virus hemagglutinin as a model antigen. *Vaccine* 32:5323–5329.
14. Flinsenberg TW, Compeer EB, Koning D, Klein M, Amelung FJ, van Baarle D, Boelens JJ, Boes M. 2012. Fcγ receptor antigen targeting potentiates cross-presentation by human blood and lymphoid tissue BDCA-3+ dendritic cells. *Blood* 120:5163–5172.

Chapter 6

Natural Killer cells facilitate PRAME-specific T-cell reactivity against neuroblastoma

Authors

Lotte Spel, Jaap-Jan Boelens, Dirk M. van der Steen, Nina J.G. Blokland, Max M. van Noesel, Jan J. Molenaar, Mirjam H.M. Heemskerk, Marianne Boes and Stefan Nierkens

Published in

Oncotarget 2015



Abstract

Neuroblastoma is the most common solid tumor in children with an estimated 5-year progression free survival of 20-40% in stage 4 disease. Neuroblastoma actively avoids recognition by natural killer (NK) cells and cytotoxic T lymphocytes (CTLs). Although immunotherapy has gained traction for neuroblastoma treatment, these immune escape mechanisms restrain clinical results. Therefore, we aimed to improve neuroblastoma immunogenicity to further the development of antigen-specific immunotherapy against neuroblastoma. We found that neuroblastoma cells significantly increase surface expression of MHC I upon exposure to active NK cells and thereby readily sensitize neuroblastoma cells for recognition by CTLs. We show that oncoprotein PRAME serves as an immunodominant neuroblastoma as NK-modulated neuroblastoma cells are recognized by PRAME_{SLLQHLIGL}/A2-specific CTL clones. Furthermore, NK cells induce MHC I upregulation in neuroblastoma through contact-dependent secretion of IFN γ . Our results demonstrate remarkable plasticity in the peptide/MHC I surface expression of neuroblastoma cells, which is reversed when neuroblastoma cells experience innate immune attack by sensitized NK cells. These findings support the exploration of NK cells as adjuvant therapy to enforce neuroblastoma-specific CTL responses.

Introduction

Tumor cells evade immune surveillance most notably through changes in surface expression of membrane receptors, antigen presentation and/or initiation of an inhibitory microenvironment (1). Cancer immunotherapies that target these immune evasion mechanisms have resulted in clinical benefits (2-4), providing experimental support for plasticity in the immunogenicity of the tumor and its microenvironment. Neuroblastoma, which is considered a poorly immunogenic tumor, accounts for 15% of childhood cancer deaths (5). It is the most common solid tumor in infancy that manifests in extracranial neural tissues. Despite intense treatments, stage 4 neuroblastoma patients have merely 20% survival rates due to tumor relapses.

Recently, interest for immunotherapy in neuroblastoma patients has grown. Antibody therapy in neuroblastoma initially yielded promising event-free survival benefits (6), however tumor relapse still occurred in the majority of the patients. The cytotoxic effects of antibody therapy do not involve adaptive immune cells that exert specific immunity against the tumor antigen. To date, the best clinical results for anti-tumor immunotherapy were obtained with strategies that are aimed at generating or improving adaptive immune responses (7-10), such as adoptive T-cell therapy and checkpoint inhibitors. We therefore hypothesize that stimulating antigen-specific immune responses may be imperative for effective immunotherapy in neuroblastoma patients.

Antigen-specific immunotherapy requires the expression of tumor-associated antigen(s) (TAA) by the neuroblastoma cells and sufficient TAA-derived peptide/MHC I complex display on the neuroblastoma cell surface to allow for recognition by antigen-specific T-cells. Neuroblastoma has established several mechanisms for the direct evasion of CTL recognition. Most importantly, neuroblastoma tumors show down-regulated surface expression of major histocompatibility complex I (MHC I) molecules (11-14). In addition, the expression of co-stimulatory and adhesion molecules which assist in CTL activation are also decreased on neuroblastoma surfaces (15-17). Of note, the absence of MHC I on neuroblastoma tumors should trigger the active recognition by cytotoxic immune cells of the non-specific innate immune system: the natural killer (NK) cells. Neuroblastoma, however, adapted its surface display of activating and inhibitory NK cell receptors in order to also avoid NK-mediated killing (16-19).

Neuroblastoma further enforces its non-immunogenicity through the expression of only few TAA (20, 21), which limits the repertoire of antigen-specific CTLs responsive against neuroblastoma. TAA encoded by cancer/germline genes, including PRAME, NY-ESO1, MAGE and GAGE, can be expressed by neuroblastoma tumors (20, 21). Whereas the expression of most cancer/germline antigens in neuroblastoma was shown to be very heterogeneous, PRAME expression was observed in 94% of stage 4 neuroblastoma samples. However, specific CTL activity against PRAME-expressing neuroblastoma cells has not yet been described.

Here we investigated whether neuroblastoma cells can be triggered into peptide/MHC I display, as a possible approach towards antigen-specific immunotherapy. Specifically, we investigated whether neuroblastoma cells that have experienced innate immune pressure by NK cells change their immunogenic potential towards adaptive CTLs. We found that neuroblastoma cells increase their surface levels of MHC I in response to active NK cells. This effect is contact-dependent and identifies interferon-gamma as the major factor inducing MHC I upregulation, which could be recapitulated in patient-derived stage 4 neuroblastoma cell cultures. Furthermore, we show for the first time that PRAME serves as an immunogenic tumor antigen for neuroblastoma as

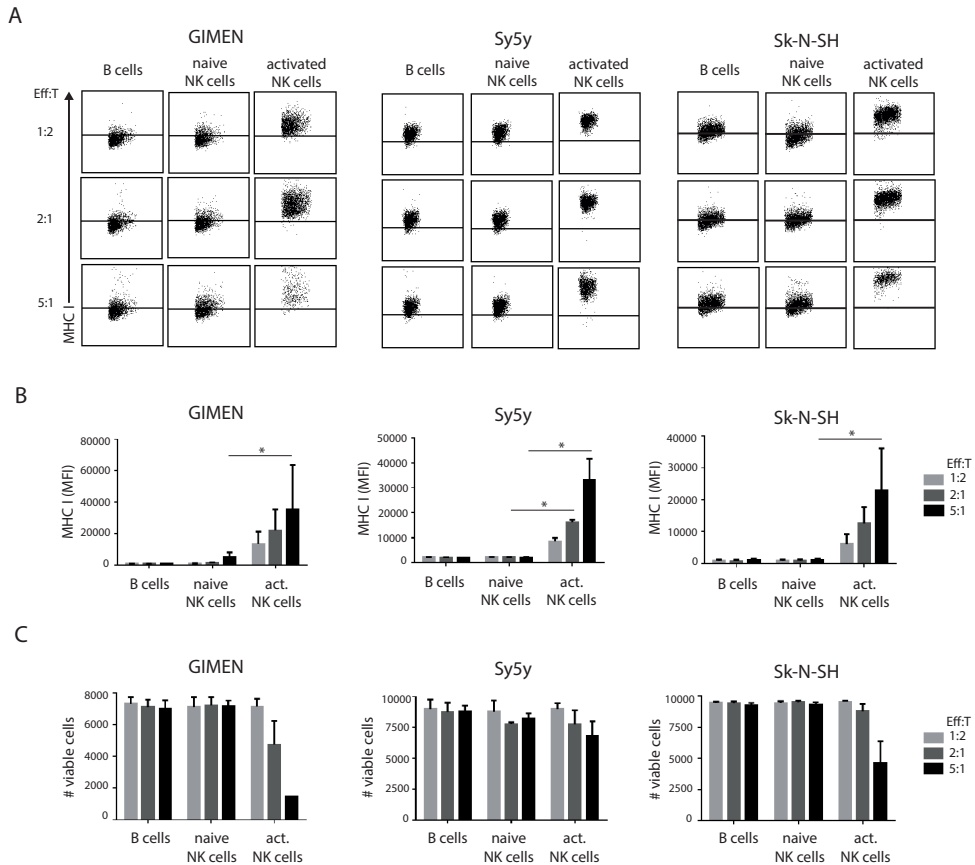


Figure 1. Class I MHC modulation on neuroblastoma cells by NK cell exposure. A. 30,000 GIMEN, Sy5y or Sk-N-SH cells were co-cultured with B cells, naive NK cells or activated NK cells at indicated effector:target ratios for 24 hours. Neuroblastoma cells were harvested and stained for MHC I. MHC I levels were measured by flow cytometry. Representative FACS plots are shown. Data was quantified in B. (n = 3). C. Viable neuroblastoma cells were counted for each condition.

NK-modulated neuroblastoma cells present PRAME-derived peptide/MHC I complexes and are now recognized by PRAME-specific CTLs. Our data reveals that the immunogenic potential of neuroblastoma is amendable to environmental signals, as opposed to being caused by irreversible genetic mutations, a feature that could contribute to the development of antigen-specific immunotherapies for neuroblastoma.

Results

NK cell exposure upregulates surface MHC I on neuroblastoma. By virtue of actively suppressed MHC I membrane expression (11-14), neuroblastoma is a potential target for NK cells (22). We investigated changes in neuroblastoma MHC I expression after NK cell immune pressure, considering that tumor cells often have the ability to escape immune-mediated cytotoxicity. As naive NK cells were shown unable to eradicate neuroblastoma cells, we additionally used NK

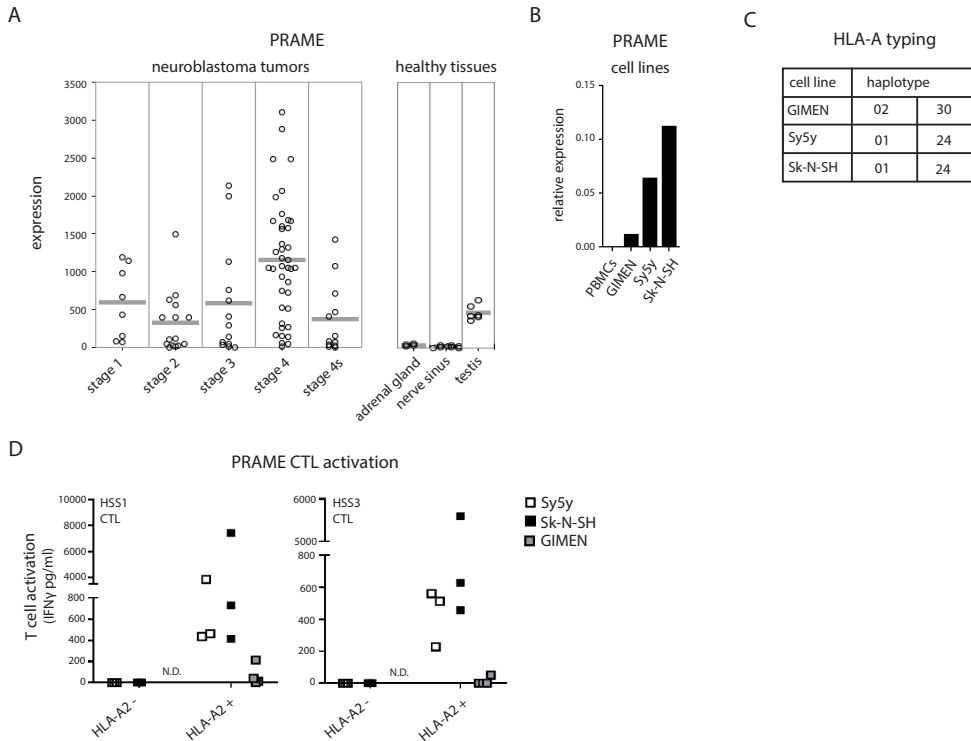


Figure 2. PRAME CTL recognition of neuroblastoma cells. **A.** PRAME gene expression of 88 individual primary neuroblastoma tumors of different disease stages and healthy tissues (NCBI GEO Accession No. GSE 16476; <http://www.ncbi.nlm.nih.gov/geo/>). **B.** PRAME gene expression determined by qPCR of PBMCs (negative control) and neuroblastoma cell lines GIMEN, Sy5y and Sk-N-SH relative to GAPDH. **C.** Overview of HLA-A haplotypes carried by GIMEN, Sy5y and Sk-N-SH cells. **D.** Activation of PRAME^{S₁L₁Q₁H₁L₁G₁L₁}/A2-specific CTLs, clone HSS1 and HSS3, by HLA-A2 negative or HLA-A2 positive neuroblastoma cells.

6

cells that were prior stimulated with IL-2 and IL-15 (Fig. S1), similar to NK cells used in cellular immunotherapy.

NK cells were isolated from healthy donor PBMCs and added these to established neuroblastoma cell cultures, in increasing effector:target ratios (co-cultures of 15,000 or 60,000 or 150,000 NK cells with 30,000 neuroblastoma cells; O/N, 37°C). B cells purified from the same donor PBMCs served as a control population. We observed the significant upregulation of MHC I at the cell surface of GIMEN, Sy5y and Sk-N-SH neuroblastoma lines (Fig. 1AB), specifically when exposed to activated NK cells. With increasing amounts of NK cells, the average increase in MHC I expression was 8, 15 and 26-fold. Stimulation of neuroblastoma cells with the IL2/IL15 cytokine mix alone did not induce MHC I upregulation (Fig. S2). Furthermore, activated NK cells showed lytic capabilities because a notable fraction of the neuroblastoma cells were killed in the co-cultures (Fig. 1C). Interestingly, neuroblastoma cells that were not readily killed by NK cells showed enhanced membrane expression of MHC I. Of note, addition of naive NK cells, or B cells, did not result in cell lysis (Fig. 1C), in accordance with earlier work (16, 19).

These results indicate that peptide/MHC I surface expression on neuroblastoma tumors can be

induced by exposure to activated but not naive NK cells. We therefore next addressed whether elevated MHC I levels might elicit increased immune recognition by CTLs.

PRAME is an immunogenic antigen for neuroblastoma. The activation of CTLs requires triggering of their antigen-restricted T-cell receptor (TCR) by specific peptide/MHC I complexes. We therefore performed an in silico data search for neuroblastoma-specific antigen expression. In an independent dataset of 88 individual neuroblastoma tumors (NCBI GEO Accession No. GSE 16476; <http://www.ncbi.nlm.nih.gov/geo/>), we found PRAME (also known as MAPE) to be significantly expressed in high-risk neuroblastoma tissues (Fig. 2A). Healthy neuronal tissues were negative overall for PRAME expression with the exception of healthy testis, hence its designation as a cancer/testis antigen (23, 24).

We first confirmed PRAME mRNA expression in neuroblastoma cell lines, using quantitative real-time PCR (Fig. 2B). All three neuroblastoma cell lines showed a positive signal for PRAME expression, though with variety between the cell lines, while PRAME was not detected in the negative control PBMCs. In order to address the possibility that increased MHC I surface expression may trigger CTL activation, we employed two different high affinity clones of PRAME-specific CTLs (HSS1 and HSS3). These CTL clones were isolated from patients with a mismatch bone marrow transplantation and previously described to specifically recognize PRAME-derived peptide SLLQHLIGL in combination with HLA-A2 subtype of the MHC I family (25). Gene-profiling of the neuroblastoma cell lines showed GIMEN to carry the HLA-A2 allele whereas Sy5y and Sk-N-SH did not (Fig. 2C). As expected, neither of the HLA-A2-negative cell lines was recognized by PRAMESLLQHLIGL/A2-specific CTLs (Fig. 2D). However, high HLA-A2 expression attained by retroviral introduction of the HLA-A2 gene into Sy5y and Sk-N-SH cells yielded specific recognition by SLLQHLIGL/A2-specific CTLs (Fig. 2D; white and black squares, respectively). HLA-A2+ neuroblastoma cells were not recognized by A2-restricted CTLs with different antigen-specificity (minor antigen HA1, a non-neuroblastoma antigen), indicating that CTL activation was driven by antigen presentation and not a non-specific stimulation caused by lentiviral transduction (unpublished data). This indicates that neuroblastoma cells are intrinsically capable of presenting PRAMESLLQHLIGL/A2 complexes and suggests that the surface display of MHC I complexes that carry immunodominant peptides is actively suppressed. In support, PRAME CTLs were unable to recognize the endogenous HLA-A2-positive GIMEN cells (Fig. 2D; grey squares). Without intervention, endogenous MHC I levels appear to be too low to stimulate PRAMESLLQHLIGL/A2-specific CTLs whereby neuroblastoma escapes CTL-mediated anti-tumor attack.

Activated NK cells transform neuroblastoma cells into CTL targets. We next studied whether the increase in MHC I surface display, as accomplished by prior NK cell exposure, would increase the tumor antigen-specific recognition of neuroblastoma by PRAME-specific T-cells. In a multi-step co-culture setup (Fig. 3A) GIMEN cells or HLA-A2-transduced Sy5y cells (Sy5y+A2) were exposed 1:1 to activated NK cells for 24 hours (see Fig. S1). Then either GIMEN or Sy5y+A2 cultures were washed thoroughly and replated in the presence of PRAMESLLQHLIGL/A2-restricted CTLs for 24 hours (30,000 neuroblastoma cells with 6,000 T-cells). GIMEN neuroblastoma cells that were modulated by activated NK cells, in contrast to naive NK cells, were recognized by PRAMESLLQHLIGL/A2-restricted CTLs (Fig. 3B and Fig. S3). Furthermore, A2-restricted CTLs recognizing a peptide derived from minor antigen HA1 or CMV pp65 protein (negative

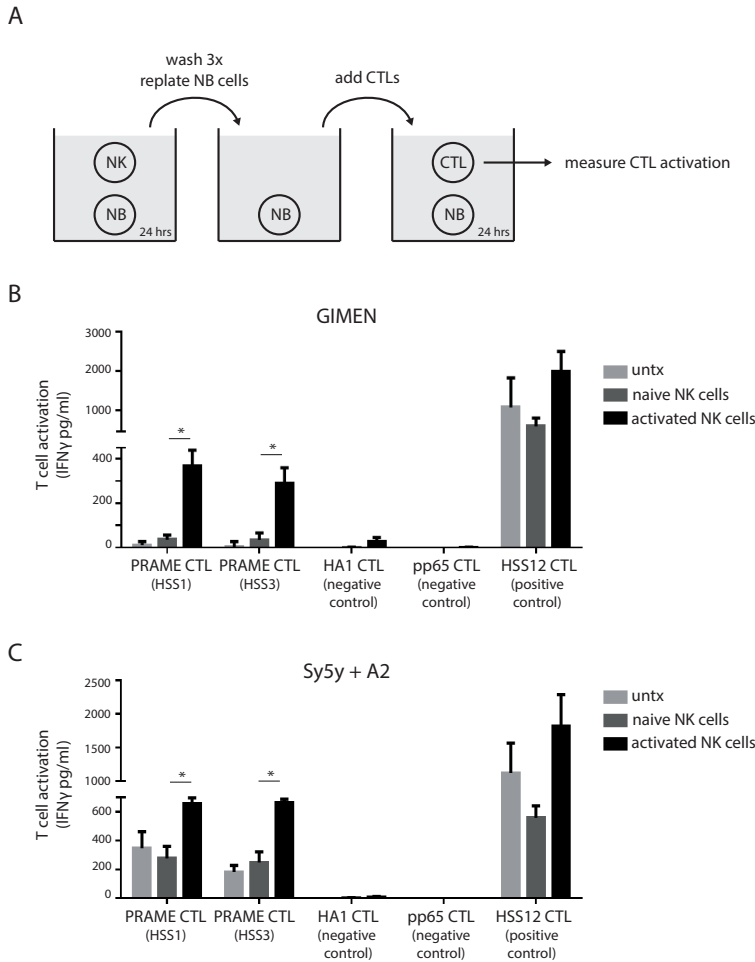


Figure 3. NK cells transform neuroblastoma cells into PRAME CTL targets. **A.** Schematic overview of performed experiment. Neuroblastoma cells are exposed to naive or activated NK cells for 24 hours (ratio 1:1), washed thoroughly and replated in the presence of indicated CTLs. After 24 hours the culture supernatants were collected and IFN γ levels were determined by ELISA as measure of CTL activation. **B** and **C.** Activation of indicated CTLs by GIMEN cells (**B**) or Sy5y+A2 cells (**C**) left untreated or after exposure to naive or activated NK cells (n = 4).

control) could not be activated, supporting that NK cell-modulated neuroblastoma cells do not spontaneously activate CTLs. Also, CTLs were not activated by NK cells only, both before or after incubation with neuroblastoma cells (unpublished data). As positive control A2-restricted CTLs were used that recognize a peptide derived from USP11 (ubiquitin specific peptidase 11), a highly expressed housekeeping protein, which showed T-cell activation in all conditions. The Sy5y+A2 cells, by virtue of their transduced high HLA-A2 expression rate showed enhanced basal recognition, which was however further increased after exposure to activated NK cells but not naive NK cells (Fig. 3C).

Altogether, we show that interactions with activated NK cells transforms neuroblastoma cells

into targets for CD8⁺ T-cells. Moreover, neuroblastoma cells display antigen specificity through MHC I presentation of the PRAME-derived SLLQHLIGL antigenic peptide.

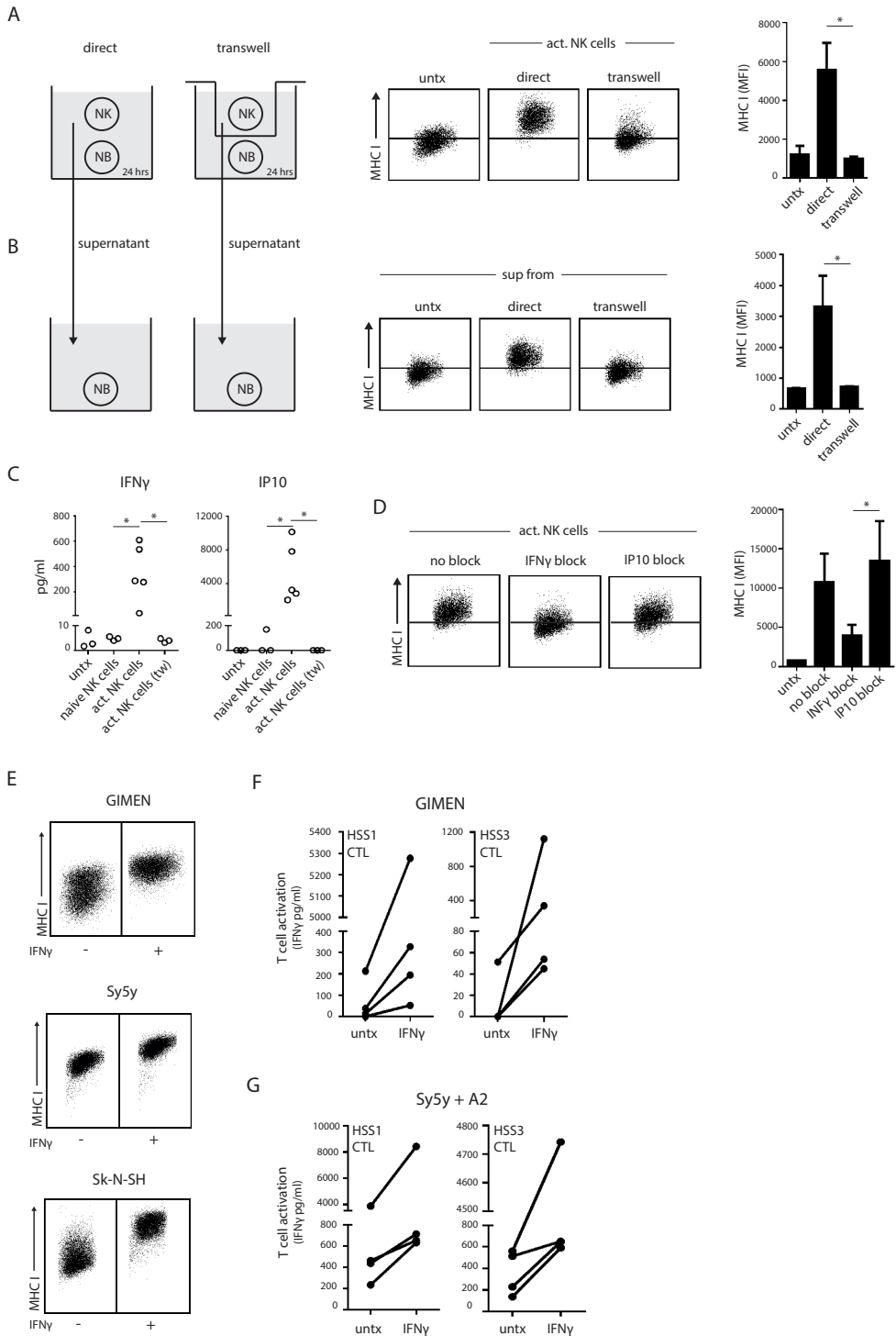
NK cells induce MHC I upregulation in neuroblastoma through contact-dependent IFN γ production.

To gain more insight into the manner by which active NK cells accomplished upregulation of antigenic peptide/MHC complexes on neuroblastoma cells we performed various co-culture experiments. Using a transwell system, we first showed that direct contact between the NK cell and the neuroblastoma cells is necessary for MHC I upregulation, as activated NK cells are unable to do so when cell-cell contact is prevented (Fig. 4A). We collected culture supernatants of these co-cultures, transferred them to untreated neuroblastoma cells and measured MHC I changes. Only supernatants of NK-neuroblastoma co-cultures that had been allowed continuous cell-cell contact could recapitulate MHC I upregulation in fresh neuroblastoma cells (Fig.4B). Thus, NK cells elicit class I MHC upregulation in a strict contact-dependent manner.

We hypothesized that secretion of IFN γ , which can be locally produced by activated immune cells and stimulates antigen presentation in neuroblastoma cells (26), may trigger the enhanced MHC I expression triggered by activated NK cell contact. Indeed, both IFN γ and IP10 (Interferon-induced protein 10) were present in supernatants of activated NK-neuroblastoma cell co-cultures but absent in culture supernatants of neuroblastoma cells co-cultured with B cells or naive NK cells (Fig.4C). Moreover, there was no IFN γ production in a contact-independent co-culture using activated NK cells (Fig 4C). Thus, cell-cell interactions between activated NK cells and neuroblastoma cells elicits the production of IFN γ . To confirm that IFN γ was required for the MHC I upregulation in neuroblastoma cells we used IFN γ blocking antibodies during the co-culture. The IFN γ blocking antibodies were able to inhibit MHC I upregulation by 60% (Fig. 4D and Fig. S4) indicating that IFN γ is the major contributor to MHC I upregulation in this co-culture. In contrast, IP10 does not appear to play a role in MHC I upregulation, as incubation with IP10 blocking antibodies did not inhibit MHC I expression levels on neuroblastoma (Fig. 4D). Additionally, we investigated the direct effect of IFN γ on neuroblastoma MHC I levels. Incubation with recombinant IFN γ could enhance MHC I surface expression on neuroblastoma cells (Fig. 4E) and subsequently increased PRAMESLLQHLIGL/A2-restricted CTL recognition of both GIMEN (Fig. 4F) and Sy5y+A2 cells (Fig. 4G).

In summary, contact-dependent production of IFN γ stimulates the presentation of peptide/MHC I complexes at the cell surface of neuroblastoma cells, for antigen-specific presentation and recognition by PRAMESLLQHLIGL/A2-restricted CTLs.

» Figure 4. Contact-dependent release of IFN γ enhances MHC I on neuroblastoma. **A.** Activated NK cells were co-cultured with neuroblastoma cells in a contact-dependent (direct) or -independent (transwell) system for 24 hrs. MHC I levels on the neuroblastoma cells were measured by flow cytometry. Representative FACS plots are shown and data was quantified in a bar graph. **B.** Supernatant of the co-cultures in A were transferred to untreated neuroblastoma cells and incubated for 24 hrs. Subsequently, MHC I levels on the neuroblastoma cells were measured by flow cytometry as in A. **C.** Concentrations of IFN γ and IP-10 were measured in the supernatant of GIMEN cells left untreated or co-cultured with naive or activated NK cells (direct and transwell). **D.** GIMEN cells were incubated with activated NK cells in the presence of IFN γ - or IP-10-blocking antibodies for 24 hours. MHC I levels were measured by flow cytometry. **E.** Neuroblastoma cells were treated with recombinant IFN γ for 24 hours and MHC I levels were measured by flow cytometry. **F** and **G.** Activation of PRAME_{SLLQHLIGL}/A2-specific CTLs, clone HSS1 and HSS3, by GIMEN (F) or Sy5y+A2 (G) cells that were priorly treated with recombinant IFN γ for 24 hours.



Primary stage 4 neuroblastoma cells increase MHC I upon IFN γ stimulation. Finally, we asked whether primary patient-derived neuroblastoma cells do upregulate MHC I upon IFN γ exposure, as this data would validate our findings in neuroblastoma cell lines. To this end we used tumor initiating cells (TIC) that were recently obtained from primary neuroblastoma tumors or bone marrow infiltrates of stage 4 neuroblastoma patients. TICs were shown to maintain genetic and morphological phenotype of the originating tumor (27). By flow cytometry we confirmed the neuroblastoma phenotype of four TICs as they showed positive membrane expression of CD56, GD2, and CD81 (28-30) (Fig. 5A). Steady-state MHC I levels were low, as expected for neuroblastoma tumor cells (Fig. 5B and C). After stimulation with IFN γ for 24 hours the surface expression of MHC I increased significantly in all four primary tumor cell types. In untreated conditions merely 3.1% (1.1-4.5) of the cells showed positive expression for MHC I which was increased up to approximately 76.9% (55.3-98.2) after IFN γ stimulation (Fig. 5C).

Thus, we confirmed in primary neuroblastoma cells the ability to upregulate MHC I surface levels in response to IFN γ . Altogether, these results indicate that the cells of primary neuroblastoma tumors actively use plasticity in immunogenic surface display of MHC I to avoid immune recognition.

Discussion

High-risk neuroblastoma is currently being treated by radiotherapy, chemotherapy, surgical resection and stem cell transplantation. More recently, these treatment strategies were complemented by antibody-based immunotherapy directed against neuroblastoma membrane marker GD2. The initial promising survival benefits of anti-GD2 therapy (6) encourages the possibility of immunotherapy in neuroblastoma. Unfortunately, the treatment was not sufficient since relapse still occurred in the majority of the patients. This suggests that immunotherapeutic approaches that induce adaptive immunity are additionally needed for complete eradication of relapsing tumor cells.

Cellular immunotherapy is still in its infancy, partly because of immune evasion: how can a cellular immunotherapy be effective if tumor cells are non-immunogenic and tumor-associated antigens are kept hidden? We here described a preclinical study that was aimed at improving TAA peptide presentation in MHC I on neuroblastoma cells. Non-immunogenic neuroblastoma cells, both from the tumor mass and bone marrow metastasis, could be pressured into surface display of immunogenic features, that were recognized by T-cells. The immunogenic potential of neuroblastoma cells exhibits a remarkable plasticity that can be exploited for clinical application. We show that NK cells increase neuroblastoma MHC I levels in a contact-dependent manner. To date, no definitive studies on NK cell infiltration in human neuroblastoma tissue samples were performed. Though, Facchetti et al. succeeded in culturing NK cells from isolated lymphocytes of bulk neuroblastoma tumors (31). While in vitro these NK cells proliferated and were able to produce cytokines upon IL-2 stimulation, in vivo the intratumoral NK cells were presumably inactive evidenced by the absence of MHC I expression in immunohistochemical stainings of neuroblastoma tumor sections (24). In this study we have shed light on the regulation of MHC I surface expression in neuroblastoma and the manner in which NK cells contribute to the modulation thereof.

We found IFN γ to play a major role in MHC I upregulation on neuroblastoma cells. In addition to

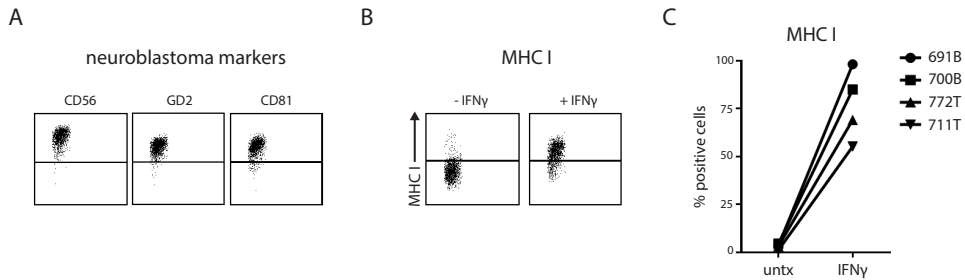


Figure 5. Patient-derived stage 4 neuroblastoma cells show IFN γ -induced MHC I upregulation. Tumor cells were stained for neuroblastoma markers CD56, GD2 and CD81 and analyzed by flow cytometry. Representative plots are shown in **A**. MHC I surface levels were measured on indicated neuroblastoma cells (711T and 772T from tumor mass; 700B and 691B from bone marrow metastasis) which were left untreated or were stimulated with IFN γ for 24 hours. Representative plots are shown in **B**. Summarized data for all four primary neuroblastoma cells in **C**.

upregulation of MHC I, NK cells might also enhance the efficiency of antigen processing as Lorenzi et al. have shown that IFN γ can increase the expression of peptide transporter TAP and ERAP peptidases in neuroblastoma cells (26). One could consider IFN γ treatment of neuroblastoma patients prior to cellular immunotherapy. However, because several studies have shown that interferon treatment has severe toxic effects (32-35) there is reluctance to use IFN γ in cancer patients. As an alternative, IFN γ could be delivered to tumor cells by active immune cells such as ex vivo expanded NK cells.

NK cell therapy has shown to induce therapeutic effects in a stage 4 neuroblastoma mouse model (36). Moreover, in a phase II clinical trial Kloess et al. infused ex vivo expanded allogeneic NK cells into neuroblastoma patients, but tumor cytotoxicity was only observed with high-dose (≥ 107 cells/kg) infusions (17). Growing sufficient numbers remains a challenge for cellular therapies. We were able to show effect with using modest numbers of NK cells suggesting that merely a couple of active NK cells at the tumor site can predispose the tumor for T-cell attack. We hypothesize that dual immune pressure reduces neuroblastoma's resources for immune evasion, leaving them little option for immune escape. We propose that these new findings may be useful for exploration towards multi-attack immunotherapy combining NK cells and T-cells.

We showed for neuroblastoma cells which are modulated by interaction with active NK cells, that the presence of endogenous levels of PRAME is sufficient for productive peptide presentation to T-cells. Morandi et al. used peptide-pulsed T2 cells to mimic PRAME antigen presentation and were able to stimulate patient-derived PRAME-specific CTLs, which indicates not only presence but also functionality of PRAME T-cells in the neuroblastoma patient T-cell pool (37). Altogether, we envision these T-cells to eliminate neuroblastoma tumor cells that were made immunogenic by preceding NK cell therapy.

Thus far, there is limited experimental support for direct cooperation between NK and T-cells regarding MHC I modulation and anti-tumor immunity. In human colorectal carcinoma, infiltration of both NK cells and CD8+ T-cells resulted in prolonged patient survival compared to tumors without NK cells (38). In addition, MHC I analysis of colorectal carcinoma tumors in rats that were injected with IL-2 stimulated NK cells showed enhanced MHC I staining in tumor parts closer

to NK cell infiltrates (39). Similarly, enhanced influx of IL-2 activated NK and CD8+ T-cells into neuroblastoma tumors increased survival in a neuroblastoma mouse model (40). Furthermore, Mocikat et al. showed in a lymphoma tumor model that tumor cells that were previously not recognized by CTLs become CTL targets when injected into mice in a NK cell-dependent manner (41). Synergy between NK cells and CD8+ T-cells concerning tumor eradication is commonly ascribed to increased cytolytic activity within the tumor mass, regardless of the absence of specific receptors such as MHC I. Perhaps underlying such synergy is the modulatory effect of NK cells on tumor immunogenicity that predisposes the tumor for killing by CTLs.

The current study contributes to designing the optimal immunotherapy for neuroblastoma patients. Our findings here support the development of an NK cell-based cellular immunotherapy that may serve as adjuvant therapy together with an antigen-specific immune therapy. The present study contributes to relevant insights for the development of anti-neuroblastoma immunotherapies suggesting that activation of both innate activity and antigen-specific cells may hold promise for treatment of high-risk neuroblastoma patients.

Materials and Methods

Cells and reagents. Neuroblastoma cell lines GIMEN, Sk-N-SH and SH-Sy5y were obtained via the Academic Medical Center of Amsterdam and maintained in DMEM supplemented with 10% FCS (Biowest), 2 mM glutamine (Life Technologies), 50 units/ml penicillin (Life Technologies) and 50 µg/ml streptomycin (Life Technologies). Microarray analysis was performed at AMC on various cell lines (NCBI GEO Accession No. GSE 16476; <http://www.ncbi.nlm.nih.gov/geo/>) confirming neuroblastoma expression profiles, which were confirmed for selected neuroblastoma markers (LIN28B, MYCN, GD2, CD56 and CD81) by qPCR and/or FACS analysis when cells arrived at UMC Utrecht (2012). Cells were frozen in individual aliquots after less than 10 passages and tested regularly for mycoplasma contamination. Tumor initiating cells were cultured as previously described (27). T-cell clones HSS1, HSS3 are high avidity T-cell clones specific for PRAME-derived peptide SLLQHLIGL presented in the context of HLA-A*02:01 (25). These T-cell clones recognize HLA-A*02:01 positive targets only when loaded with the PRAME peptide or when endogenously expressing PRAME (25). T-cell clone HSS12 is specific for peptide FTWEGLYNV derived from USP11 (ubiquitin specific peptidase 11) presented in the context of HLA-A*02:01 (25). The minor histocompatibility antigen specific T-cell clone HA1-CTL, and the cytomegalovirus specific T-cell clone pp65-CTL both also recognize their specific peptide in the context of HLA-A *02:01 and were used as negative controls. T-cell clones were stimulated every 2 weeks with 1 x 10⁶ cells/ml irradiated allogeneic PBMCs (30Gy), 800 ng/ml PHA, and 100 IU/ml IL-2 (Chiron, Amsterdam, The Netherlands). 10-14 days after restimulation the T-cells were used for the different assays.

Flow cytometry. For staining, cells were first detached with trypsin (Life Technologie) and washed twice in PBS containing 2% FCS (Biowest) and 0.1% sodium azide (NaN₃, Sigma-Aldrich). Next, antigen nonspecific binding was prevented by prior incubation of cells with 10% mouse serum (Fitzgerald). Cells were next incubated with combinations of pacific blue, fluorescein isothiocyanate (FITC), and allophycocyanin (APC)–conjugated mouse anti–human antibodies. The following monoclonal antibodies were used: mouse-anti-human CD3 (Clone UCHT1, Biolegend), mouse-anti-human CD19 (Clone HIB19, BD Biosciences), mouse-anti-human CD56 (Clone B159,

BD Biosciences), and mouse-anti-human HLA-ABC (Clone W6/32, Biolegend). Cells were acquired on FACSCanto II and analyzed using FACS Diva Version 6.13 (BD Bioscience) or FlowJo version 7.6.5 software. Data were analyzed using GraphPad Prism 5.

Co-cultures. Peripheral blood mononuclear cells (PBMCs) from healthy donors were separated from peripheral blood by ficoll isopaque density gradient centrifugation (GE Healthcare Bio-Sciences AB) and stained with anti-CD3, anti-CD19 and anti-CD56 antibodies. CD19⁺ B cells and CD3-CD56⁺ NK cells were isolated by FACS sorting and subsequently cultured in RPMI supplemented with 10% human serum (Sigma). For NK cell activation 1000 U/ml interleukin-2 (Proleukin) and 50 ng/ml interleukin-15 (Immunotools) were added for 18 hrs. B cells, naive NK cells or activated NK cells were harvested, washed, counted and added to neuroblastoma cells at indicated effector:target ratios for 24 hrs. For cell-cell contact experiments neuroblastoma cells were added to the lower part of the transwell system (Greiner Bio-one, 1µm pore size) and immune cells were added to the upper part and cultured for 24 hrs. For blocking experiments the NK cells were mixed with anti-IFN γ (BD Biosciences) or anti-IP10 (R&D) neutralizing antibodies (1µg/ml) and subsequently added to the neuroblastoma cells.

Quantative real-time PCR. Total RNA was isolated using tripure (Roche) according to the manufacturer's instructions. cDNA was synthesized from up to 1 µg of total RNA using the iScript cDNA synthesis kit (Biorad). Real-time PCR was performed using IQ SYBR Green PCR Supermix (Biorad) and the CFX96 Touch Real-Time PCR Detection System (Bio-Rad), according to the manufacturer's instructions. PCR assays were done in triplicate. Data were calculated as values relative to GAPDH and further analyzed using Graphpad Prism 5.

HLA typing. One million cells were used for typing of the HLA-A locus of neuroblastoma cells. The LABType SSO HLA A Locus typing kit (OneLambda) was used according to manufacturer's instructions.

Retroviral transduction. Neuroblastoma cells were transduced with a retroviral vector encoding for HLA-A*0201 and the marker gene NGF-R. By MACS separation the NGF-R positive neuroblastoma cells were enriched.

CTL activation. Neuroblastoma cells were pretreated with NK cells (1:1) or 1000 U/ml recombinant IFN γ (eBioscience) as indicated for 24 hrs. Then, neuroblastoma cells were harvested, washed thoroughly and replated in the presence of CTLs (30,000 neuroblastoma cells with 6,000 CTLs). After 24 hrs culture supernatants were collected and CTL activation was measured as production of IFN γ , IL-2 and TNF.

Cytokine detection. Cytokine concentrations were measured by the MultiPlex Core Facility of the LTI using Luminex technology with in house developed bead-sets and Bio-Plex Manager Version 6.1 software (Bio-Rad Laboratories) as previously described (42). IFN γ concentrations were measured using ELISA (eBiosciences).

Statistics. Differences in MHC I surface expression levels, T cell activation levels, and cytokines

(IFN γ and IP10) secretion levels were analyzed with non-parametric Mann-Whitney U test between separate groups. Values of $p < 0.05$ were considered significant. Analyses were performed with GraphPad Prism 5 software.

Acknowledgements

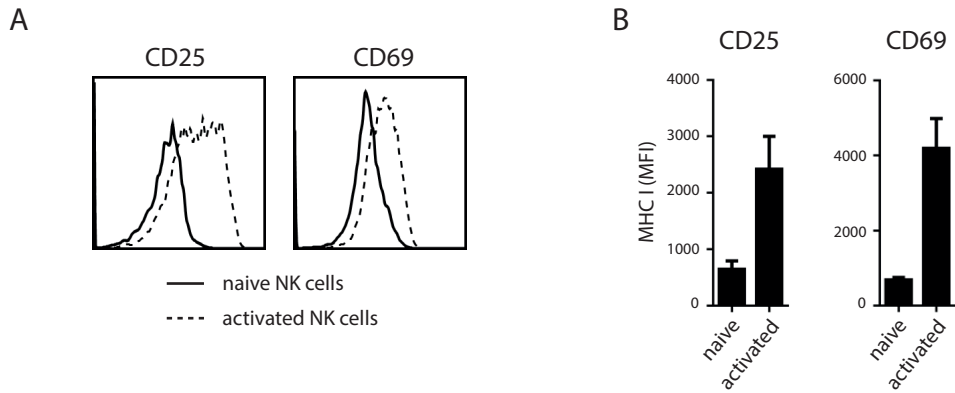
This work was supported by the Villa Joep foundation and Ammodo. We thank the CFF and multiplex core facility of the LTI for technical support.

References

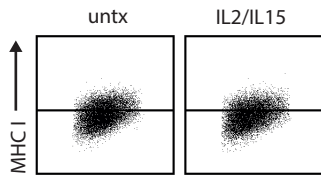
1. Dunn GP, Old LJ, Schreiber RD. The three Es of cancer immunoediting. *Annu Rev Immunol.* 2004;22:329-360.
2. Disis ML. Mechanism of action of immunotherapy. *Semin Oncol.* 2014;41 Suppl 5:S3-13.
3. Mellman I, Coukos G, Dranoff G. Cancer immunotherapy comes of age. *Nature.* 2011;480(7378):480-489.
4. Gattinoni L, Powell DJ, Jr, Rosenberg SA, Restifo NP. Adoptive immunotherapy for cancer: building on success. *Nat Rev Immunol.* 2006;6(5):383-393.
5. Davidoff AM. Neuroblastoma. *Semin Pediatr Surg.* 2012;21(1):2-14.
6. Yu AL, Gilman AL, Ozkaynak MF, London WB, Kreissman SG, Chen HX, Smith M, Anderson B, Villablanca JG, Matthay KK, Shimada H, Grupp SA, Seeger R, et al. Anti-GD2 antibody with GM-CSF, interleukin-2, and isotretinoin for neuroblastoma. *N Engl J Med.* 2010;363(14):1324-1334.
7. Kissick HT, Sanda MG. The role of active vaccination in cancer immunotherapy: lessons from clinical trials. *Curr Opin Immunol.* 2015;35:15-22.
8. Hinrichs CS, Rosenberg SA. Exploiting the curative potential of adoptive T-cell therapy for cancer. *Immunol Rev.* 2014;257(1):56-71.
9. Barrett DM, Singh N, Porter DL, Grupp SA, June CH. Chimeric antigen receptor therapy for cancer. *Annu Rev Med.* 2014;65:333-347.
10. Domogala A, Madrigal JA, Saudemont A. Natural Killer Cell Immunotherapy: From Bench to Bedside. *Front Immunol.* 2015;6:264.
11. Wolfl M, Jungbluth AA, Garrido F, Cabrera T, Meyen-Southard S, Spitz R, Ernestus K, Berthold F. Expression of MHC class I, MHC class II, and cancer germline antigens in neuroblastoma. *Cancer Immunol Immunother.* 2005;54(4):400-406.
12. Bao L, Dunham K, Lucas K. MAGE-A1, MAGE-A3, and NY-ESO-1 can be upregulated on neuroblastoma cells to facilitate cytotoxic T lymphocyte-mediated tumor cell killing. *Cancer Immunol Immunother.* 2011;60(9):1299-1307.
13. Gross N, Beck D, Favre S. In vitro modulation and relationship between N-myc and HLA class I RNA steady-state levels in human neuroblastoma cells. *Cancer Res.* 1990;50(23):7532-7536.
14. Prigione I, Corrias MV, Airoidi I, Raffaghello L, Morandi F, Bocca P, Cocco C, Ferrone S, Pistoia V. Immunogenicity of human neuroblastoma. *Ann N Y Acad Sci.* 2004;1028:69-80.
15. Favrot MC, Combaret V, Goillot E, Tabone E, Bouffet E, Dolbeau D, Bouvier R, Coze C, Michon J, Philip T. Expression of leucocyte adhesion molecules on 66 clinical neuroblastoma specimens. *Int J Cancer.* 1991;48(4):502-510.
16. Raffaghello L, Prigione I, Airoidi I, Camoriano M, Levreri I, Gambini C, Pende D, Steinle A, Ferrone S, Pistoia V. Downregulation and/or release of NKG2D ligands as immune evasion strategy of human neuroblastoma. *Neoplasia.* 2004;6(5):558-568.
17. Kloess S, Huenecke S, Piechulek D, Esser R, Koch J, Brehm C, Soerensen J, Gardlowski T, Brinkmann A, Bader P, Passweg J, Klingebiel T, Schwabe D, et al. IL-2-activated haploidentical NK cells restore NKG2D-mediated NK-cell cytotoxicity in neuroblastoma patients by scavenging of plasma MICA. *Eur J Immunol.* 2010;40(11):3255-3267.
18. Castriconi R, Dondero A, Corrias MV, Lanino E, Pende D, Moretta L, Bottino C, Moretta A. Natural killer cell-mediated killing of freshly isolated neuroblastoma cells: critical role of DNAX accessory molecule-1-poliovirus receptor interaction. *Cancer Res.* 2004;64(24):9180-9184.
19. Castriconi R, Dondero A, Augugliaro R, Cantoni C, Carnemolla B, Sementa AR, Negri F, Conte R, Corrias MV, Moretta L, Moretta A, Bottino C. Identification of 4Ig-B7-H3 as a neuroblastoma-associated molecule that exerts a protective role from an NK cell-mediated lysis. *Proc Natl Acad Sci U S A.* 2004;101(34):12640-12645.
20. Jacobs JF, Coulie PG, Figdor CG, Adema GJ, de Vries IJ, Hoogerbrugge PM. Targets for active immunotherapy against pediatric solid tumors. *Cancer Immunol Immunother.* 2009;58(6):831-841.
21. Oberthuer A, Hero B, Spitz R, Berthold F, Fischer M. The tumor-associated antigen PRAME is universally expressed in high-stage neuroblastoma and associated with poor outcome. *Clin Cancer Res.* 2004;10(13):4307-4313.
22. Groth A, Kloss S, von Strandmann EP, Koehl U, Koch J. Mechanisms of tumor and viral immune escape from natural killer cell-mediated surveillance. *J Innate Immun.* 2011;3(4):344-354.
23. Ikeda H, Lethe B, Lehmann F, van Baren N, Baurain JF, de Smet C, Chambost H, Vitale M, Moretta A, Boon T, Coulie PG. Characterization of an antigen that is recognized on a melanoma showing partial

- HLA loss by CTL expressing an NK inhibitory receptor. *Immunity*. 1997;6(2):199-208.
24. Pellat-Deceunynck C, Mellerin MP, Labarriere N, Jego G, Moreau-Aubry A, Harousseau JL, Jotereau F, Bataille R. The cancer germ-line genes MAGE-1, MAGE-3 and PRAME are commonly expressed by human myeloma cells. *Eur J Immunol*. 2000;30(3):803-809.
 25. Amir AL, van der Steen DM, van Loenen MM, Hagedoorn RS, de Boer R, Kester MD, de Ru AH, Lugthart GJ, van Kooten C, Hiemstra PS, Jedema I, Griffioen M, van Veelen PA, et al. PRAME-specific Allo-HLA-restricted T cells with potent antitumor reactivity useful for therapeutic T-cell receptor gene transfer. *Clin Cancer Res*. 2011;17(17):5615-5625.
 26. Lorenzi S, Forloni M, Cifaldi L, Antonucci C, Citti A, Boldrini R, Pezzullo M, Castellano A, Russo V, van der Bruggen P, Giacomini P, Locatelli F, Fruci D. IRF1 and NF- κ B restore MHC class I-restricted tumor antigen processing and presentation to cytotoxic T cells in aggressive neuroblastoma. *PLoS One*. 2012;7(10):e46928.
 27. Bate-Eya LT, Ebus ME, Koster J, den Hartog IJ, Zwijnenburg DA, Schild L, van der Ploeg I, Dolman ME, Caron HN, Versteeg R, Molenaar JJ. Newly-derived neuroblastoma cell lines propagated in serum-free media recapitulate the genotype and phenotype of primary neuroblastoma tumours. *Eur J Cancer*. 2014;50(3):628-637.
 28. Mechtersheimer G, Staudter M, Moller P. Expression of the natural killer cell-associated antigens CD56 and CD57 in human neural and striated muscle cells and in their tumors. *Cancer Res*. 1991;51(4):1300-1307.
 29. Cheung NK, Von Hoff DD, Strandjord SE, Coccia PF. Detection of neuroblastoma cells in bone marrow using GD2 specific monoclonal antibodies. *J Clin Oncol*. 1986;4(3):363-369.
 30. Nagai J, Ishida Y, Koga N, Tanaka Y, Ohnuma K, Toyoda Y, Katoh A, Hayabuchi Y, Kigasawa H. A new sensitive and specific combination of CD81/CD56/CD45 monoclonal antibodies for detecting circulating neuroblastoma cells in peripheral blood using flow cytometry. *J Pediatr Hematol Oncol*. 2000;22(1):20-26.
 31. Facchetti P, Prigione I, Ghiotto F, Tasso P, Garaventa A, Pistoia V. Functional and molecular characterization of tumour-infiltrating lymphocytes and clones thereof from a major-histocompatibility-complex-negative human tumour: neuroblastoma. *Cancer Immunol Immunother*. 1996;42(3):170-178.
 32. Pellicano R, Smedile A, Peyre S, Astegiano M, Saracco G, Bonardi R, Rizzetto M. Autoimmune manifestations during interferon therapy in patients with chronic hepatitis C: the hepatologist's view. *Minerva Gastroenterol Dietol*. 2005;51(1):55-61.
 33. Raanani P, Ben-Bassat I. Immune-mediated complications during interferon therapy in hematological patients. *Acta Haematol*. 2002;107(3):133-144.
 34. Vial T, Descotes J. Clinical toxicity of the interferons. *Drug Saf*. 1994;10(2):115-150.
 35. Quesada JR, Talpaz M, Rios A, Kurzrock R, Gutterman JU. Clinical toxicity of interferons in cancer patients: a review. *J Clin Oncol*. 1986;4(2):234-243.
 36. Castriconi R, Dondero A, Cilli M, Ognio E, Pezzolo A, De Giovanni B, Gambini C, Pistoia V, Moretta L, Moretta A, Corrias MV. Human NK cell infusions prolong survival of metastatic human neuroblastoma-bearing NOD/scid mice. *Cancer Immunol Immunother*. 2007;56(11):1733-1742.
 37. Morandi F, Chiesa S, Bocca P, Millo E, Salis A, Solari M, Pistoia V, Prigione I. Tumor mRNA-transfected dendritic cells stimulate the generation of CTL that recognize neuroblastoma-associated antigens and kill tumor cells: immunotherapeutic implications. *Neoplasia*. 2006;8(10):833-842.
 38. Sconocchia G, Eppenberger S, Spagnoli GC, Tornillo L, Droseser R, Caratelli S, Ferrelli F, Coppola A, Arriga R, Lauro D, Iezzi G, Terracciano L, Ferrone S. NK cells and T cells cooperate during the clinical course of colorectal cancer. *Oncoimmunology*. 2014;3(8):e952197.
 39. Jonges LE, Giezeman-Smits KM, van Vlierberghe RL, Ensink NG, Hagenaars M, Joly E, Eggermont AM, van de Velde CJ, Fleuren GJ, Kuppen PJ. NK cells modulate MHC class I expression on tumor cells and their susceptibility to lysis. *Immunobiology*. 2000;202(4):326-338.
 40. Yang RK, Kalogiropoulos NA, Rakhmilevich AL, Ranheim EA, Seo S, Kim K, Alderson KL, Gan J, Reisfeld RA, Gillies SD, Hank JA, Sondel PM. Intratumoral treatment of smaller mouse neuroblastoma tumors with a recombinant protein consisting of IL-2 linked to the hu14.18 antibody increases intratumoral CD8+ T and NK cells and improves survival. *Cancer Immunol Immunother*. 2013;62(8):1303-1313.
 41. Mocikat R, Braumuller H, Gumy A, Egeter O, Ziegler H, Reusch U, Bubeck A, Louis J, Mailhammer R, Riethmuller G, Koszinowski U, Rocken M. Natural killer cells activated by MHC class I(low) targets prime dendritic cells to induce protective CD8 T cell responses. *Immunity*. 2003;19(4):561-569.
 42. de Jager W, Hoppenreijns EP, Wulffraat NM, Wedderburn LR, Kuis W, Prakken BJ. Blood and synovial

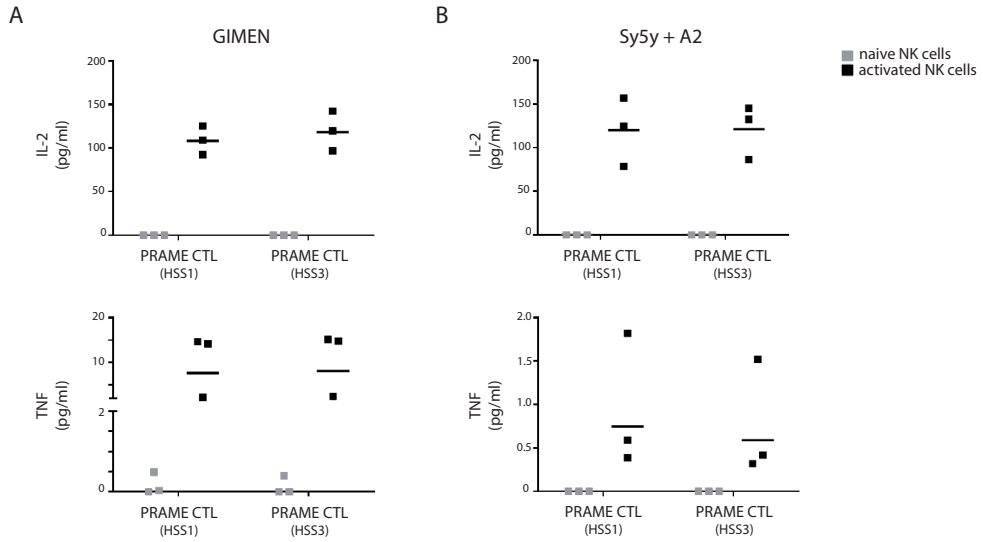
fluid cytokine signatures in patients with juvenile idiopathic arthritis: a cross-sectional study. *Ann Rheum Dis.* 2007;66(5):589-598.

Supplemental information

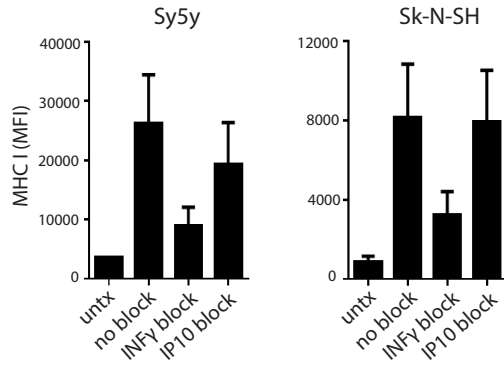
Supplementary Figure 1. NK cell activation. CD3-CD56⁺ NK cells were FACS sorted from healthy donor PBMCs and cultured in absence or presence of IL2 and IL15 for 18 hours. Membrane expression of CD25 and CD69 was determined on the NK cells by flow cytometry as measure of cell activation. Representative FACS plots are shown in A. Data was quantified in B.



Supplementary Figure 2. IL2/IL15 cytokines do not influence neuroblastoma MHC I levels. GIMEN cells were left untreated or stimulated with IL2 and IL15 for 24 hours. MHC I levels were measured by flow cytometry.



Supplementary Figure 3. PRAME-CTL activation by NK cell-modulated neuroblastoma cells. GIMEN A. and Sy5y+A2 B. cells were exposed to naive or activated NK cells, derived from three different donors, for 24 hours (ratio 1:1), washed thoroughly and replated in the presence of PRAME-specific CTLs. After 24 hours the culture supernatants were collected. IL-2 and TNF levels were determined by Luminex as measure of CTL activation.



Supplementary Figure 4. NK cell-induced MHC I upregulation on neuroblastoma is IFN γ -dependent. Sy5y and Sk-N-SH cells were incubated with activated NK cells in the presence of IFN γ - or IP-10-blocking antibodies for 24 hours. MHC I levels on the neuroblastoma cells were measured by flow cytometry.

Chapter 7

A CRISPR/Cas9 knock-out screen reveals NF- κ B suppressors that regulate peptide/MHC-1 display in neuroblastoma tumors

Authors

Lotte Spel*, Joppe Nieuwenhuis*, Rianne Haarsma, Elmer Stickel, Onno Bleijerveld, Jaap-Jan Boelens, Thijn Brummelkamp, Stefan Nierkens[^] and Marianne Boes[^].

* Equal contribution, [^] Shared supervision



Abstract

Neuroblastoma tumors have low MHC-1 expression and express few neo-antigens, supporting their immune escape. Here, we aimed to evoke MHC-1 gene expression to enhance immunogenicity. A genome-wide CRISPR/Cas9 knock-out screen combining MHC-1 surface expression and activity of transcription factor NF- κ B identified TNIP1 and N4BP1 as inhibitory factors of NF- κ B-mediated MHC-1 expression in neuroblastoma. In advanced stage patients, neuroblastoma expression levels of TNIP1 and N4BP1 correlate with worse survival. Depletion of TNIP1 or N4BP1 stimulated the activation of NF- κ B, increased MHC-1 surface display and recognition by antigen-specific CD8⁺ T-cells. We confirmed that TNIP1 targets canonical NF- κ B member RelA by preventing activation of the RelA/p50 NF- κ B dimer. N4BP1 instead binds deubiquitinating enzyme CEZANNE and triggers degradation of NF- κ B-initiating kinase NIK through stabilization of TRAF3, thereby inhibiting the non-canonical pathway. Thus, targeting of N4BP1/CEZANNE or TNIP1 in neuroblastoma tumors might increase peptide/MHC1-mediated tumor reactivity and thereby improve immunotherapy.

Introduction

Neuroblastoma accounts for 15% of pediatric cancer mortality (Davidoff 2012, Maris 2010, Louis et al. 2015). It is the most common solid tumor in children with survival rates of merely 20% in advanced stage (stage 4) disease (Davidoff 2012). Neuroblastoma is an embryonic cancer that originates from neural crest cells. The mutational burden of neuroblastoma tumors is low (Cheung et al. 2013, Schumacher et al. 2015), hence so far no neo-antigens have been reported for neuroblastoma. Instead, expression of cancer/testis antigens have been described in neuroblastoma (Oberthuer et al. 2004, Soling et al. 1999, Wolfi et al. 2005, Jacobs et al. 2007) reflecting the embryonically undifferentiated status of this type of tumor.

Immunotherapy for stage 4 neuroblastoma gains traction. Currently, anti-GD2 antibody therapy is standard protocol succeeding radiotherapy, chemotherapy, surgery and autologous stem cell transplantation. In addition, various immunotherapies are in trial stages (Booker et al. 2009, Croce et al. 2015, Seeger 2011). However, due to its low immunogenicity (Raffaghello et al. 2005, Coughlin et al. 2006, Favrot et al. 1991, Foreman et al. 1993, Castriconi et al. 2004, Raffaghello et al. 2004, Morandi et al. 2012, Shurin et al. 1998, Liu et al. 2012), neuroblastoma tumors are a challenge to be treated with immunotherapies. In particular, low levels of MHC class 1 (MHC-1) prevents recognition and lysis of neuroblastoma cells by cytotoxic T lymphocytes (CTLs).

Activation of NF- κ B in neuroblastoma cell lines induces transient MHC-1 membrane expression (Forloni et al. 2010, Lorenzi et al. 2012, van 't Veer et al. 1993) which facilitates recognition by CTLs in vitro (Lorenzi et al. 2012, Bao et al. 2011, Vertuani et al. 2003, Spel et al. 2015), underscoring that reconstitution of MHC-1 in these tumors might increase their immunogenicity. In this study, we aimed to identify target proteins that control peptide/MHC-1 display in neuroblastoma by performing a genome-wide CRISPR knock-out screen combining NF- κ B activity and cell-surface MHC-1 membrane expression.

Results

Low expression of MHC-1 and NF- κ B in neuroblastoma. MHC-1 expression is low in neuroblastoma tumors and cell lines (Wolfi et al. 2005, Morandi et al. 2013, Lampson et al. 1983). Because neuroblastoma is an embryonic tumor that arises when immunological features are not fully developed yet, we asked whether MHC-1 gene expression in neuroblastoma tumor cells actually differs from healthy developing neural crest cells. Using gene expression datasets, we compared MHC-1 gene expression between neuroblastoma tumors and healthy neural crest cell and found no differences (Fig.1A). When neural crest cells differentiate into neurons, MHC-1 expression is unlocked in mature neuronal cells (Garay et al. 2010, Boulanger 2009, Shatz 2009). Indeed, compared to healthy mature nerve tissue, MHC-1 gene expression in neuroblastoma tumors is low (Fig.1A). Neuroblastoma appears to reflect the underdeveloped state of the neural crest in which MHC-1 expression is still low, but can be evoked.

Transcription factors that stimulate the expression of MHC-1 were not highly expressed in neuroblastoma, compared to healthy neural crest cells (Fig.1B and S1). NLRC5 and IRF1 showed similar expression levels between neuroblastoma tumors and neural crest cells (Fig.S1A). In contrast, gene expression of the NF- κ B family members (RelA, RelB, NFKB1, NFKB2 and Rel) differed between neuroblastoma tumors and neural crest cells. Expression of RelA, RelB and NFKB1 was significantly decreased in neuroblastoma tumors (Fig.1B). Also compared to mature

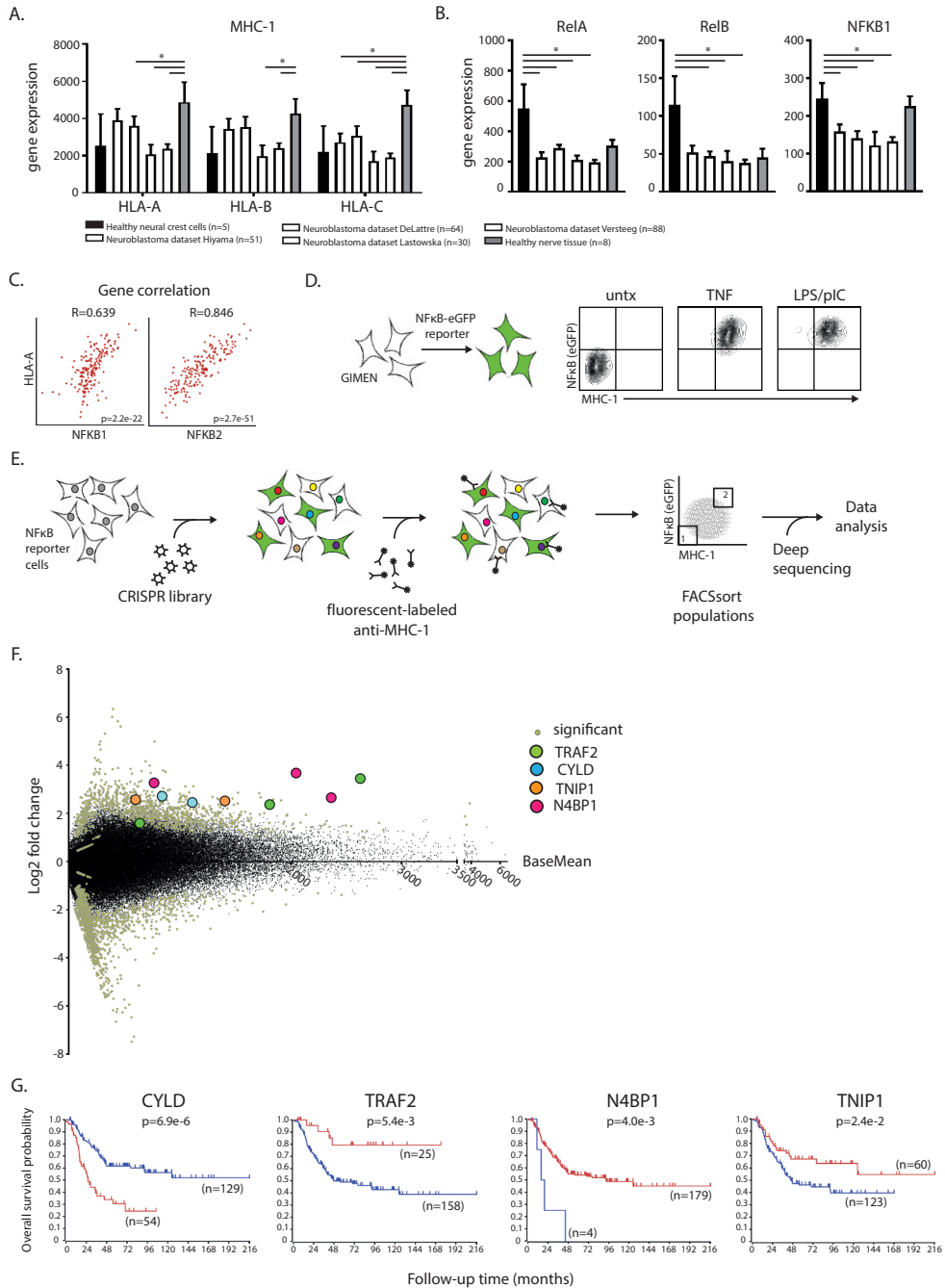


Figure 1. Identification of NF-κB and MHC-1 suppressors in neuroblastoma. A and B. Gene expression datasets of neural crest cells, healthy nerve tissue and neuroblastoma tumors were analyzed for the expression of MHC-1 alleles HLA-A, HLA-B and HLA-C (A); NF-κB alleles RelA, RelB, and NFKB1 (B). Two-way ANOVA test was used, $p < 0.05$ was considered significant. C. Gene expression of HLA-A in neuroblastoma tumor samples (cohort of 183 stage-4 neuroblastoma patients) was correlated with NFKB genes. Significance test for the Pearson correlation coefficient r was conducted, $p < 0.5$ was considered significant. D. Generation of an NF-κB reporter cell line.

«« NF- κ B activation and MHC-1 expression of the reporter cells was measured when untreated or after treatment with TNF or TLR ligands (LPS + polyI:C). E. Schematic overview of the performed screen. In short, neuroblastoma cells containing a NF- κ B-eGFP reporter were subjected to a lentiviral CRISPR/Cas9 library. Cells were stained for MHC-1 using fluorescently labeled antibodies and sorted by FACS. DNA was isolated from the collected populations and prepared for deep-sequencing to reveal the CRISPR content per population. F. CRISPR screen results are shown as log₂ fold change of gRNAs in NF- κ B+MHC+ population vs. NF- κ B-MHC- population. Significant gRNAs are highlighted and significant genes are depicted in circles. G. In a cohort of 183 stage-4 neuroblastoma patients the expression levels of NF- κ B suppressors CYLD, N4BP1, TNIP1 and TRAF2 were correlated with survival data. Log-rank test was used, $p < 0.05$ was considered significant.

nerve cells, RelA and NFKB1 expression was reduced. Furthermore, gene expression of MHC-1 alleles correlated with NFKB gene expression in stage-4 neuroblastoma tumors (Fig.1C and S1C). NF- κ B family member Rel was upregulated in neuroblastoma (Fig.S1B), which is in agreement with its role in anti-apoptotic signaling (Gilmore et al. 2011, Hunter et al. 2016). Thus, the abnormal development from healthy neural crest cell to malignant neuroblastoma coincides with down-regulation of NF- κ B family members. In line with this observation, several studies have shown that transcriptional activity of NF- κ B in neuroblastoma cells is indeed repressed (van 't Veer et al. 1993, Lorenzi et al. 2012, Forloni et al. 2010). These data together support that reversal of repressed NF- κ B might steer neuroblastoma away from tumorigenic development and possibly unlock MHC-1 expression for immunogenic display.

Identification of NF- κ B-dependent MHC-1 suppressors in neuroblastoma. NF- κ B is repressed in neuroblastoma on both gene level (Fig.1B) as well as activation level (Forloni et al. 2010, Lorenzi et al. 2012, van 't Veer et al. 1993). Active NF- κ B can temporarily restore MHC-1 expression in neuroblastoma. In order to establish stable MHC-1 expression in neuroblastoma, we set out to identify the factors that negatively regulate NF- κ B-mediated MHC-1 expression in neuroblastoma. To this end, we generated a clonal cell line bearing a NF- κ B reporter, which upon activation of the NF- κ B pathway expresses eGFP (Fig.1D). Indeed, elevated MHC-1 levels were observed upon stimulation of the NF- κ B pathway using TNF or TLR ligands. These cells were mutagenized by lentiviral transduction using a genome-wide CRISPR/Cas9 knock-out library containing 118,000 individual gRNAs with an average of 6 gRNAs per gene (Sanjana et al. 2014). The mutagenized cells were expanded and stained for cell surface expression of MHC-1. NF- κ B^{neg}MHC^{neg} and NF- κ B^{pos}MHC^{pos} populations were isolated using FACS sorting. Using deep-sequencing we identified the enriched gRNAs for both population (Fig.1E).

GuideRNAs that were traced back in significantly different amounts between NF- κ B^{neg}MHC^{neg} and NF- κ B^{pos}MHC^{pos} populations are highlighted in figure 1F. Combining the data of all gene-specific gRNAs used (average of 6 per gene), a total of 4 genes showed to significantly impact NF- κ B activity and MHC-1 expression upon depletion in neuroblastoma cells (Fig.1F). These included Nedd4 binding protein 1 (N4BP1), TNFAIP3 interacting protein 1 (TNIP1), cylindromatosis (CYLD) and TNF-receptor associated factor 2 (TRAF2). The expression of the identified NF- κ B suppressors N4BP1, TNIP1 and TRAF2 correlated with worse survival in stage-4 neuroblastoma patients (Fig.1G), suggesting an important role for NF- κ B suppression in malicious outcome of neuroblastoma.

CYLD and TRAF2 are well-established regulators of NF- κ B and previously described (Kovalenko

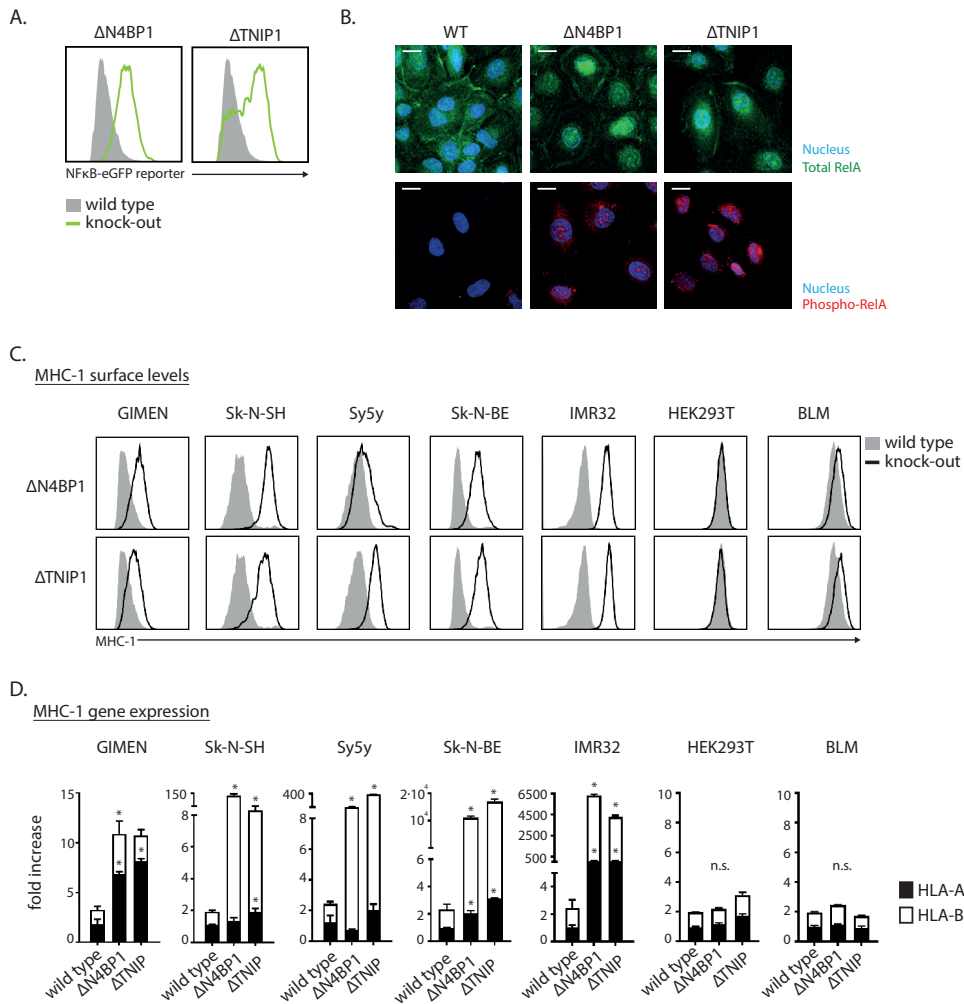


Figure 2. Effect of N4BP1 and TNIP1 depletion on NF- κ B and MHC-1 across cell lines. A. The eGFP fluorescence produced by NF- κ B reporter activity was measured in single cell clones of Δ N4BP1 and Δ TNIP1 neuroblastoma GIMEN cells compared to WT (= empty vector control). B. Confocal images of WT, Δ N4BP1 and Δ TNIP1 neuroblastoma GIMEN cells stained for total RelA protein (green) and phospho-RelA protein (red). Nuclei are depicted in blue. Scale bar represents 10 μ m. C. N4BP1 or TNIP1 was depleted in indicated cell lines and surface expression of MHC-1 was measured by flow cytometry. D. Relative gene expression of MHC-1 alleles HLA-A and HLA-B was measured by qPCR in WT, Δ N4BP1 and Δ TNIP1 cells. Fold increase of HLA-A expression (black) or HLA-B expression (white) in knockout cells compared to WT cells is depicted in the graphs. Mann-Whitney U-tests were used, $p < 0.05$ was considered significant.

et al. 2003, Brummelkamp et al. 2003, Wu et al. 2005). The inhibitory activity of TNIP1 on NF- κ B is concentrated on the canonical pathway (Heyninck et al. 1999, Mauro et al. 2006, Cohen et al. 2009), whereas for N4BP1 the mechanism remains elusive.

These results suggest that upon depletion of N4BP1 or TNIP1, NF- κ B^{neg}MHC^{neg} neuroblastoma cells transform into cells endowed with stable expression of MHC-1 and an active NF- κ B transcription factor.

Depletion of NF- κ B suppressors enhances MHC-1 in neuroblastoma. Using CRISPR/Cas9, we generated N4BP1- and TNIP1-depleted single cell neuroblastoma reporter clones and empty vector-treated wild type (WT) reporter cells for control purposes. NF- κ B activity and MHC-1 expression were measured by flow cytometry. Depletion of N4BP1 or TNIP1 resulted in expression of the NF- κ B reporter, indicating functional NF- κ B activation and transcriptional activity (Fig.2A). Activation of NF- κ B was also shown by confocal microscopy of WT and knock-out neuroblastoma cells (Fig.2B). Total RelA protein localized to the cytosol in WT cells, but spontaneously translocated to the nucleus in Δ N4BP1 and Δ TNIP1 cells. Nuclear translocation requires phosphorylation of RelA protein, thus phospho-RelA was only detected in Δ N4BP1 and Δ TNIP1 cells and not WT neuroblastoma cells. In addition, Δ N4BP1 and Δ TNIP1 cells showed increased surface levels of MHC-1 compared to WT cells (Fig.2C), corroborating the findings of the CRISPR screen.

To investigate whether the inhibitory effects of N4BP1 and TNIP1 on NF- κ B and MHC-1 are specific for neuroblastoma, we generated a panel of N4BP1 and TNIP1 mutants in a range of cell lines (Fig.S2). MHC-1 expression levels were measured in WT and knockout cells using flow cytometry (Fig.2C). Depletion of N4BP1 or TNIP1 generally resulted in increased MHC-1 membrane expression across five neuroblastoma cell lines. Differences in gene expression of either HLA-A or HLA-B genes were measured using qPCR (Fig.2D). Interestingly, in non-neuroblastoma cell lines HEK293T and BLM, MHC-1 upregulation was not clearly different between WT and knockout cells. The high steady-state expression levels of MHC-1 in HEK293T and BLM make them less prone for MHC-1 increase. Western blot analysis of Δ N4BP1 and Δ TNIP1 cells of HEK293T and BLM shows increased levels of phospho-RelA, indicating that NF- κ B is activated (Fig.S3). These results suggest that NF- κ B inhibition by N4BP1 and TNIP1 is conserved across multiple cell types, but its effect on MHC-1 levels is controlled at the cell type level.

Anti-tumor T-cell reactivity against NF- κ B-active neuroblastoma cells. Expression of MHC-1 on neuroblastoma cell surface determines T-cell recognition (Spel et al. 2015, Lorenzi et al. 2012, Vertuani et al. 2003). We next addressed if increased MHC-1 expression in Δ N4BP1 and Δ TNIP1 neuroblastoma cells can result in functional antigen presentation and T-cell reactivity, and therefore performed co-culture experiments using neuroblastoma cells and MHC-matched antigen-specific CTLs. To this end, we generated WT and knockout neuroblastoma cells that stably express the model antigen pp65, and exposed these cells to MHC-1-restricted pp65-specific CTLs. We found that while CTLs were activated upon co-culture with Δ N4BP1 or Δ TNIP1 cells, WT cells failed to do so (Fig.3A). Indicative of T-cell activation and granule release, the CTLs produced IFN γ and showed LAMP1 surface staining, respectively.

Demethylating agent decitabine (DAC) has been shown to increase MHC-1 expression and is currently being scrutinized in several clinical trials for neuroblastoma patients (Adair et al. 2009, Serrano et al. 2001, Krishnadas et al. 2015). Treatment with decitabine indeed increased MHC-1 levels on neuroblastoma cells to a similar extent as Δ N4BP1/TNIP1 depletion (Fig.3B). The combination of DNA demethylation with active NF- κ B transcription shows a 2-fold higher induction of MHC-1 surface expression. Such a synergistic effect is also observed when testing the T-cell reactivity against decitabine-treated knockout cells. T-cell recognition of Δ N4BP1 and Δ TNIP1 cells increased by 7-fold and 5-fold, respectively, when treated with decitabine (Fig.3A).

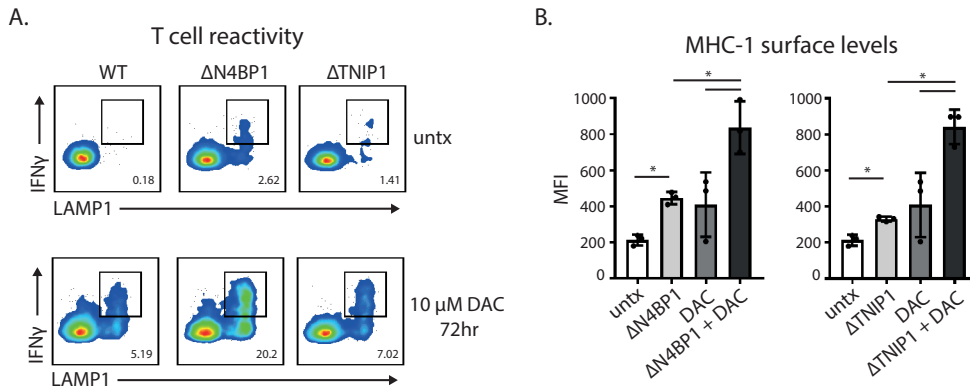


Figure 3. CD8⁺ T-cell recognition of Δ N4BP1 and Δ TNIP1 neuroblastoma cells. WT, Δ N4BP1 and Δ TNIP1 neuroblastoma GIMEN cells stably expressing pp65 model antigen were left untreated or were treated with decitabine for 72 hrs. A. After co-culture with pp65-specific CD8⁺ T-cells in a 1:1 ratio, T-cells were stained for surface LAMP1 expression and intracellular production of IFN γ and analyzed by flow cytometry. B. Membrane MHC-1 expression levels were measured by flow cytometry. Mann-Whitney U-tests were used, $p < 0.05$ was considered significant.

Thus, active NF- κ B makes neuroblastoma cells immunogenic for T-cell reactivity. These results highlight the significance of NF- κ B modulation for anti-neuroblastoma immunotherapies, alone or as adjuvant treatment to currently tested protocols.

Differential NF- κ B activation in Δ N4BP1 and Δ TNIP1 cells. TNIP1 modulates NF- κ B activity by destabilizing the IKK complex (G'Sell et al. 2015) with a consequential sequestering of RelA by I κ B, less nuclear translocation and diminished transcription of target genes including MHC-1. How N4BP1 modulates NF- κ B activity remains unclear. In order to investigate which NF- κ B members play a role in Δ N4BP1 cells, we looked at the expression levels of the five transcriptionally active subunits (phospho-RelA, RelB, p50, p52 and c-Rel) of NF- κ B by Western blot. Compared to WT, Δ N4BP1 cells showed increased levels of phosphorylated RelA, of RelB and p52 (Fig.4A). This is different from Δ TNIP1 cells that only showed increases in p-RelA and RelB, but no effects on the other subunits. Next, we tested whether these subunits also contribute to NF- κ B-mediated gene expression by mutating each subunit in the Δ N4BP1 or Δ TNIP1 neuroblastoma reporter cells. We designed guideRNAs against the NF- κ B genes RelA, RelB, NFKB1 and NFKB2 and cloned them into the Cas9-lentiviral vector. Seven days after transduction, the cells were harvested and NF- κ B reporter activity was measured by flow cytometry. In Δ N4BP1 cells, NF- κ B reporter activity was decreased when RelA or NFKB2 (=p52) was depleted (Fig.4B). In Δ TNIP1 cells, NF- κ B reporter activity was decreased only when RelA was depleted. In contrast, RelB depletion did not affect reporter activity in either Δ N4BP1 or Δ TNIP1 cells, despite increased RelB expression.

Thus, while N4BP1 and TNIP1 both inhibit NF- κ B activity, they appear to do so using different mechanisms. In Δ N4BP1 cells both RelA and p52 contribute to NF- κ B-mediated gene transcription, indicating that N4BP1 inhibitory effect targets two subunits simultaneously. In Δ TNIP1 cells on the other hand, is only RelA the driver of NF- κ B-mediated gene activation.

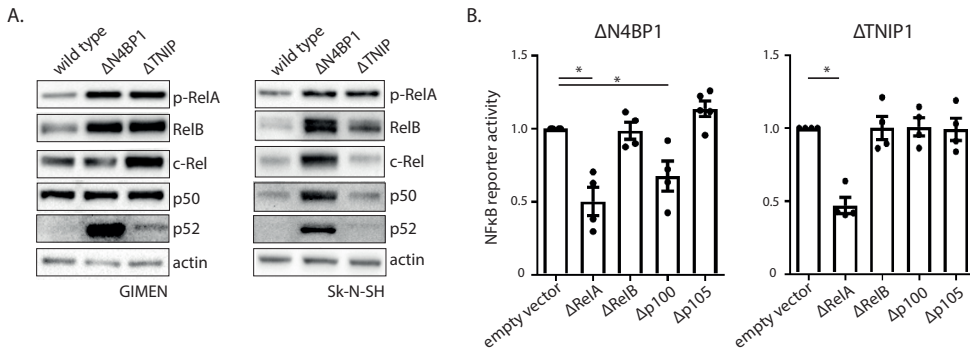


Figure 4. Contribution of NF-κB family members to increased NF-κB activity in ΔN4BP1 and ΔTNIP1 neuroblastoma cells. A. Immunoblot analysis of phospho-RelA, RelB, c-Rel, p50 (cleaved from p105) and p52 (cleaved from p100) in WT, ΔN4BP1 and ΔTNIP1 cells. B. Genes encoding RelA, RelB, p105 (=NFKB1) and p100(=NFKB2) were depleted in ΔN4BP1 and ΔTNIP1 neuroblastoma GIMEN cells using the CRISPR/Cas9 lentiviral construct. An empty vector construct was used as negative control. After a week, cells were collected and NF-κB-eGFP reporter signal was measured by flow cytometry. One-way ANOVA tests were used, $p < 0.05$ was considered significant.

N4BP1 coordinates degradation of NF-κB-initiating kinase NIK. To gain more insight into the mechanism by which N4BP1 inhibits both p-RelA and p52, we decided to elucidate the binding partners of N4BP1. To this end, a protein-protein interaction experiment was performed combining antibody-mediated pulldown with mass spectrometry. WT neuroblastoma cells were transfected with His-tagged N4BP1-expressing constructs and after 48 hours lysed for co-immunoprecipitation experiments using anti-His beads. The pellets were analyzed by mass spectrometry to identify proteins bound to N4BP1-His.

Among all proteins that were found to bind N4BP1, one in particular caught our attention. The deubiquinating enzyme CEZANNE was significantly enriched in N4BP1-His co-immunoprecipitates (Fig.5A). As observed for N4BP1, also CEZANNE expression levels correlated with worse survival in stage-4 neuroblastoma patients (Fig.5B). Mechanistically, CEZANNE stabilizes TRAF3 by removing TRAF3-bound ubiquitin modifications, thereby controlling NF-κB activation (Hu et al. 2013). Stabilized TRAF3 takes part in a protein complex that retains NIK and facilitates ubiquitination and degradation of NIK. Conversely, the degradation of TRAF3 causes NIK to accumulate and phosphorylate down-stream targets thereby initiating p100 cleavage into p52 and activation of non-canonical NF-κB. In addition, TRAF3 degradation was shown to also activate the canonical pathway involving RelA (Bista et al. 2010).

To confirm that N4BP1 is involved in stabilizing TRAF3 and break-down of NIK, the protein levels of TRAF3 and NIK were measured in WT and ΔN4BP1 cells using Western blot (Fig.5C and D). In ΔN4BP1 cells, we detected decreased levels of TRAF3 protein compared to WT cells, suggesting that TRAF3 is degraded when N4BP1 is absent. Additionally, higher levels of NIK kinase are detected in ΔN4BP1 cells compared to WT cells indicating that NIK accumulates in absence of N4BP1. Given that TRAF3 degradation and subsequent NIK accumulation leads to processing of p100 into p52, these results could explain the spontaneous activation of non-canonical NF-κB in ΔN4BP1 neuroblastoma cells.

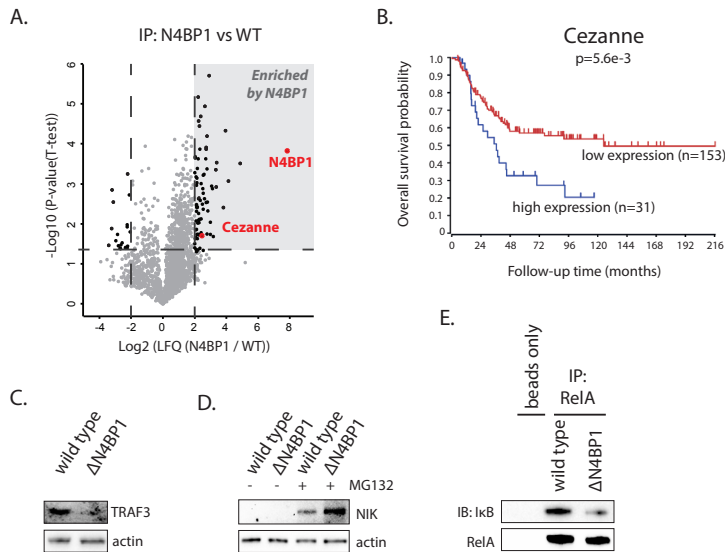


Figure 5. N4BP1 inhibits both canonical and non-canonical NF- κ B through CEZANNE. A. Identification of possible binding partners of N4BP1. WT neuroblastoma cells were transfected with N4BP1-His6 or left untreated. After 48 hours, cells were lysed and proteins were immunoprecipitated using anti-HIS-beads. Immunoprecipitates were analyzed by mass spectrometry. B. Immunoblot analysis of TRAF3 in WT and ΔN4BP1 cells. C. Immunoblot analysis of NIK in WT and ΔN4BP1 cells treated with proteasome inhibitor MG132. D. The amount of sequestered RelA protein in WT and ΔN4BP1 cells. Total RelA protein of WT and ΔN4BP1 cells was immunoprecipitated using beads and analyzed for presence of I κ B protein.

TRAF3 was shown to also control the canonical pathway through attenuating phosphorylation and degradation of the Inhibitor of NF- κ B (I κ B) (Bista et al. 2010), which sequesters RelA protein. To determine the role of I κ B in ΔN4BP1 cells, we measured the levels of I κ B bound to RelA using immunoprecipitation followed by Western blot (Fig.5E). We found that RelA was hardly in complex with I κ B in ΔN4BP1 cells, rendering RelA free for activation, which was not the case in WT cells. In WT cells, I κ B abundantly bound to RelA suggesting sequestering and inhibition of RelA and canonical NF- κ B.

Thus, N4BP1 inhibits both canonical and non-canonical NF- κ B using CEZANNE to stabilize TRAF3, resulting in degradation of NIK and sequestering of RelA by I κ B. Upon depletion of N4BP1, TRAF3 is degraded, NIK levels accumulate and I κ B detaches from RelA.

Discussion

In this study, we investigated the repressed NF- κ B-mediated MHC-1 expression in neuroblastoma. We show that gene expression levels of NF- κ B members are actively repressed during tumorigenic development of neural crest cells towards neuroblastoma tumor cells. Repression of NF- κ B proteins in neuroblastoma has been reported previously (van 't Veer et al. 1993, Forloni et al. 2010, Lorenzi et al. 2012). Van 't Veer et al use neuroblastoma rat cell lines to show decreased expression of p105/p50 protein and regulation thereof by the oncogene NMYC. In contrast, a study in human neuroblastoma cell lines shows low transcriptional availability of NF- κ B in neuroblastoma in an NMYC-independent manner (Forloni et al. 2010). In support of

the latter study, the performed CRISPR/Cas9 knock-out screen we describe here also did not identify NMYC as a negative regulator of NF- κ B; NMYC may not be involved in NF- κ B inhibition in neuroblastoma. Of note, we found no role for p105/p50 in NF- κ B-active neuroblastoma cells indicating that the NMYC-p50 regulation that was found by van 't Veer et al was not apparent in our experimental set-up.

Nevertheless, restoration of canonical NF- κ B can increase MHC-1 expression in neuroblastoma (Forloni et al. 2010, Lorenzi et al. 2012, van 't Veer et al. 1993). Transfection of NMYC-amplified cells with a p50-expressing construct showed MHC-1 expression (van 't Veer et al. 1993). Moreover, transfection of RelA increased MHC-1 membrane levels in neuroblastoma (Lorenzi et al. 2012, Forloni et al. 2010). In Δ N4BP1 and Δ TNIP1 cells we clearly observe activation of canonical NF- κ B as RelA is dissociated from I κ B protein and highly phosphorylated. In addition, in Δ N4BP1 cells we also observe activation of non-canonical NF- κ B involving the RelB and p100/p52 proteins.

In 2009 N4BP1 was implicated in NF- κ B regulation by Fenner et al (Fenner et al. 2009). In a co-immunoprecipitation experiment using poly-ubiquitin, N4BP1 and other proteins were isolated. A number of these ubiquitin-binding proteins were revealed as negative regulators of NF- κ B. Although N4BP1 was not followed-up in this study, its ubiquitin-binding capacity implicated the possibility for regulating NF- κ B. Then, in 2011 a direct role of N4BP1 in controlling NF- κ B activity was first observed (Li et al. 2011). Through overexpression in NF- κ B reporter cells, N4BP1 was found as the biggest negative regulator of NF- κ B. We here extend the knowledge about N4BP1 as an NF- κ B suppressor by showing its interaction with de-ubiquitinating enzyme CEZANNE. CEZANNE regulates TRAF3 levels (Hu et al. 2013), by which it controls both canonical and non-canonical NF- κ B (Bista et al. 2010). As such, N4BP1 prevents NF- κ B activation by orchestrating CEZANNE-mediated de-ubiquitination of TRAF3 thereby stabilizing TRAF3 protein. Intact TRAF3 results in constant degradation of NIK and thus obstruction of non-canonical NF- κ B activation. Also, RelA protein was sequestered by I κ B when TRAF3 was present leading to inhibition of canonical NF- κ B.

The NF- κ B suppressors N4BP1, CEZANNE and TNIP1 independently correlate with worse survival in stage-4 neuroblastoma patients. Despite the clear role shown here of NF- κ B suppressors preventing T-cell recognition, there is yet no evidence for an immunological reason underpinning this difference in survival. Since low expression of NF- κ B suppressors did not prevent neuroblastoma development, a survival difference might be explained by predisposition of the tumor for post-treatment immune responses. One possibility is that after stem cell transplantation of neuroblastoma patients, newly developing immune cells can eliminate residing tumor cells that express low levels of NF- κ B suppressors better than tumor cells that express high levels of NF- κ B suppressors, which would result in better clearance of NF- κ B-active neuroblastomas. Alternatively, low expression of NF- κ B suppressors may render neuroblastoma tumors more sensitive for current treatment. For example, NF- κ B activation is required for certain cytotoxic agents to kill neuroblastoma cells (Bian et al. 2001, Armstrong et al. 2007). Also, efficacy of retinoic acid-induced differentiation of neuroblastoma cells requires an active NF- κ B pathway (Feng et al. 1999, Condello et al. 2008, de Bittencourt Pasquali et al. 2016).

Taken together, we have uncovered that aberrant NF- κ B functioning in neuroblastoma results in decreased MHC-1 expression, escape from T cell immune surveillance and poor survival in stage-4 patients. The strategy chosen here, combining a NF- κ B reporter and MHC-1 cell surface

staining in combination with a genome-wide CRISPR/CAS9 library, has to our knowledge not been performed before. The identification of novel and previously identified members of the NF- κ B signaling pathway illustrates that this strategy has been successful. However, it is important to note that most described NF- κ B and MHC-1 regulators were not identified using this method. A possible explanation for this is the quality of this early generation CRISPR/CAS9 library is not optimal. A library containing more, and better validated, gRNAs targeting each gene could lead to a better separation of mutants. Nevertheless, we have identified NF- κ B suppressors which may serve as drug targets to increase neuroblastoma immunogenicity which is necessary for immunotherapies to translate into clinical benefits for stage-4 neuroblastoma patients.

Methods

Cells and culture conditions. Neuroblastoma cell lines GIMEN, Sk-N-SH, SH-Sy5y Sk-N-BE and IMR32 were obtained via the Academic Medical Center of Amsterdam. Melanoma cell line BLM was obtained via the Radboud University Medical Center of Nijmegen. All cells were maintained in DMEM GlutaMAX supplemented with 10% FCS (Biowest), 50 units/ml penicillin (Life Technologies) and 50 μ g/ml streptomycin (Life Technologies) and cultured at 37°C at 5% CO₂.

Reagents and antibodies. Human recombinant TNF was purchased from Miltenyi. Decitabine, LPS and poly(I:C) were purchased from Sigma Aldrich. Hoechst was purchased from Thermo Fisher Scientific. Antibodies used: anti-CD3 (Clone UCHT1, Sony Biotechnology); anti-CD8 (Clone RPA-T8, BD Biosciences); anti-LAMP1 (Clone H4A3, BD Biosciences); anti-TNF (Clone MAB11, Sony Biotechnology); anti-IFN γ (Clone 4S.B3, BD Biosciences); mouse-anti-human HLA-ABC (Clone W6/32, Biolegend); anti-actin (polyclonal, Santa Cruz); anti-RelA (Clone D14E12, Cell Signaling Techniques); anti-phospho-RelA (Clone 93H1, Cell Signaling Techniques); anti-RelB (Clone C1E4, Cell Signaling Techniques); anti-Rel (Clone D3B8S, Cell Signaling Techniques); anti-p100/p52 (Clone 18D10, Cell Signaling Techniques); anti-p105/p50 (Clone D7H5M, Cell Signaling Techniques); anti-I κ B α (Clone 112B2, Cell Signaling Techniques); anti-TRAF3 (polyclonal, Cell Signaling Techniques); anti-NIK (polyclonal, Cell Signaling Techniques).

Constructs and plasmids. For generating NF- κ B reporter cells, a pTRH1 plasmid was used containing a NF- κ B transcriptional response element (TRE) and a minimum CMV (mCMV) promoter followed by eGFP gene and upstream of the blasticidin S resistance gene (BSR) from *Bacillus cereus* (Lee et al. 2013). N4BP1- and TNIP1-knockout cells were generated using pXPR_001 (Addgene) and gRNAs sequences 5' -(g)CTCCAAAGACCATCCGGGC- 3' for N4BP1 and 5' - (g)ACTGGTGTGGCTTGACT-3' for TNIP1. Where (g) represents a non-annealing nucleotide that was added to the actual gRNA to initiate gRNA transcription. Empty pxpr_001 vector was used as negative control. Mutations in Δ N4BP1 and Δ TNIP1 cell lines were validated by PCR using primers: Fw_N4BP1: 5' -GTTGTTTTGCCTTAGTATGGGTCTTGC- 3' ; Rv_N4BP1: 5' -ACCTACCAACCAGACTACAATATCTGC- 3' ; Fw_TNIP1: 5' -AGGCCATTTTCTCAGACTACCTGG- 3' ; Rv_TNIP1: 5' -CGATGGACTTGCCCAATATCACC- 3'. Clonal cell lines GIMEN Δ N4BP1 and Δ TNIP1, used in all follow-up experiments, were analyzed by TA-cloning (Strataclone PCR cloning kit, agilent #240205). At least 20 colonies were picked and subjected to sequencing to ensure no allele would be unannotated. For non-clonal cell lines (as shown in fig.S2B),

PCR product was subjected to sanger sequencing to obtain mutation profiles based on TIDE assay (Brinkman et al. 2014). Using nested sanger sequencing primers Fw_N4BP1_seq: 5' – CTACAGCTCTCCAAGTGAACATTTGAG-3' and Fw_TNIP1_seq: 5' –CATTCTCCCACACTCGAGTGG- 3'. RelA-, RelB-, p100- and p105-knockout cells were generated using pL-CRISPR.SFFV.tRFP (Addgene) and gRNA sequences 5' –GCTTCCGCTACAAGTGCAG-3' and 5'-(g)AGCGCCCTCGCACTTGAG-3' for RelA; 5' –GCCACGCCTGGTGTCTCGCG- 3' and 5' –(g)TGGGGACACTAGTCGGCCCA- 3' for RelB; 5' –(g)CCATCCCATGGTGGACTACC- 3' and 5' –GGCACCAGGTAGTCCACCAT- 3' for NFKB1; 5' – (g) AGAGGCTCCGATTTGATA- 3' and 5' – (g)CTTCACAGCCATATCGAAAT- 3' for NFKB2. N4BP1-His6) was purchased from Source Bioscience.

Gene expression analysis. Gene datasets were selected from the Gene Expression Omnibus: neural crest cells (GSE14340), neuroblastoma Hiyama cohort (GSE16237), neuroblastoma DeLattre cohort (GSE12460), neuroblastoma Lastowska cohort (GSE13136), neuroblastoma Versteeg cohort (GSE16476) and healthy nerve tissue (GSE7307). Gene expression data (U133 P2 microarray chip, MAS5.0 normalization) was accessed through the Genomics Analysis and Visualization Platform (r2.amc.nl).

Flow cytometry. Cells were detached with trypsin (Life Technologie) and washed twice in PBS containing 2% FCS (Biowest) and 0.1% sodium azide (NaN₃, Sigma-Aldrich). Next, antigen nonspecific binding was prevented by prior incubation of cells with 10% mouse serum (Fitzgerald). Cells were incubated with indicated anti-human antibodies for 30 minutes on ice and washed twice. In case of intracellular stainings, cells were fixed and permeabilized (Fix/Perm kit BD Biosciences) after surface staining and subsequently stained with indicated antibodies for 30 minutes on ice and washed twice. Cells were taken up in PBS (2% FCS/0,1% NaN₃) to be used for measurement using either FACSCanto II or Fortessa with FACS Diva Version 6.13 (BD Bioscience). Analysis was done using FlowJo Version 10 software.

CRISPR screen sequence analysis. Raw sequence reads were extracted from the FASTQ files using AWK and subsequently, using regular expression in SED, sequences of 19-21b flanked by ACCG and GTT were distilled. Bowtie 1 (Langmead et al. 2009) was used to align the reads to the lentivirus library in two consecutive rounds. In the first round, a single mismatch was allowed while demanding alignment to only a single guide. In the second round, the reads that aligned to multiple guides in the first round where re-aligned with a more stringent setting of zero mismatches to see if they could be aligned unambiguously.

Scoring sgRNA using differential expression analysis. Readcount files were generated from Bowtie output using a shell script and differential expression analysis was carried out using the R package DESeq2 (Love et al. 2014). The NF-κBlowMHClow population from both screens were used as replicates for the low population and the NF-κBhighMHChigh populations as replicates for the high population. Guides that had 20 or less reads in the total of 4 samples were removed. Differences in guide abundance between the low and high populations were tested using a Walt test with default size factor normalization of DESeq2. Shrinkage of Log2FoldChanges was applied.

Scoring genes. Guides with an FDR-corrected (Benjamini-Hochberg) p-value that met the threshold of 0.05 were scored significant. Using a custom Python script, the number of guides per gene with a p-value below or equal to the threshold was determined. Genes having at least three significant guides with identical directionality were scored significant. To include the non-targeting control guides in this analysis, 167 imaginary genes were randomly assigned 6 non-targeting control guides.

Immunofluorescence microscopy. Cells were cultured in LabTek 8 well chambers in culture medium. Cells were subsequently washed and fixed for 10 min at RT using PBS supplemented with 4% formaldehyde. Cells were permeabilized and blocked for 60 min with PBS supplemented with 5% BSA and 0.3% Triton-X100. Next, slides were incubated with primary antibodies diluted in PBS supplemented with 1% BSA and 0.3% Triton-X100 for 16 hours. Cells were washed with PBS and incubated with secondary antibodies for 1 hour. After washing, slides mounted on a microscope slide using Mowiol 4-88 (Carl Roth, Germany). Samples were imaged using a Zeiss LSM710 confocal microscope equipped with a Plan-Apochromat 63×1.40 oil differential interference contrast M27 objective (Zeiss). Fluorescent signals were detected with PMTs set at the appropriate bandwidth using 633 nm helium neon laser for Alexa647. Images were processed using the Zeiss Enhanced Navigation (ZEN) 2009 software.

Quantitative real-time PCR. Total RNA was isolated using RNA isolation columns (Qiagen) according to the manufacturer's instructions. cDNA was synthesized from 1 µg of total RNA using the iScript cDNA synthesis kit (Biorad). Real-time PCR was performed using IQ SYBR Green PCR Supermix (Biorad) and the CFX96 Touch Real-Time PCR Detection System (Bio-Rad), according to the manufacturer's instructions. PCR assays were done in triplicate. Data were calculated as values relative to GAPDH and further analyzed using Graphpad Prism 7.02.

T-cell activation assay. A HCMV pp65-specific CD8+ T-cell clone was prepared previously. In brief, T-cells from an HLA-A*0201+ donor were stained with HLA-A2/pp65495-503 tetramers, and subsequently single-cell sorted in a 96-well plate (Thermo) containing irradiated B-LCL feeder cells (1x10⁵ cells/mL, irradiated with 70 Gy) and PBMCs from 3 healthy donors (1 x 10⁶ cells/mL, irradiated with 30 Gy). One µg/mL leucoagglutinin PHA-L (Sigma-Aldrich) and 120 U/mL of recombinant IL-2 (Immunotools) were added. T-cell clones specific to pp65495-503 were selected using tetramer staining. Positive clones were restimulated and expanded during several stimulation cycles and frozen in aliquots that were freshly thawed before each use in an assay. Neuroblastoma cells were co-cultured with HCMV pp65-specific CD8+T-cells 4,5 hours in the presence of Golgistop (1/1500; BD Bioscience). Cells were subsequently stained for surface markers and presence of intracellular IFN γ and TNF, followed by flow cytometry-based analysis.

Immunoblotting. Cells were lysed in sample buffer, separated by SDS-PAGE and transferred onto polyvinylidene fluoride (PVDF) membranes (Millipore) by wet western blotting. Membranes were blocked with 4% non-fat milk powder (Campina) in PBS 0.1% Tween-20 (Bio-Rad) for 1 hour and subsequently incubated with a primary antibody for 16 hours at 4°C. After washing, membranes were incubated with HRP-coupled secondary antibody for 1 hour followed by analysis on chemidoc imaging system (Bio-Rad).

Immunoprecipitation assay. Cells were lysed in PBS(1% CHAPS, 30 mM Tris-HCL pH 8.0, 150 mM NaCl) for 30 minutes on ice and spun down at 13,000g for 15 minutes. Supernatants were incubated with uncoupled or antibody-coupled beads (Protein A-agarose beads, Roche) for 16 hours under constant agitation. Beads were separated from lysates by centrifugation, washed twice and resuspended in sample buffer. Protein interactions were analyzed using immunoblotting (see above).

Mass spectrometry. Immunoprecipitation beads were heated in sample loading buffer for 5 min. at 95°C, eluates were run into the stacking of a 4-12% Bis-Tris gel and coomassie-stained bands were excised. Proteins were reduced with 6.5mM DTT, alkylated with 54 mM iodoacetamide and digested in-gel with trypsin (Gold, mass spectrometry grade, Promega, 3 ng/μL) overnight at 37°C. Extracted peptides were vacuum dried, reconstituted in 10% formic acid and analyzed by nanoLC-MS/MS on an Orbitrap Fusion Tribrid mass spectrometer equipped with a Proxeon nLC1000 system (Thermo Scientific). Peptides were loaded directly on the analytical column (Agilent Poroshell EC-C18 120 2.7 μm, 50 μm×500 mm, packed in-house) and separated in a 140-min gradient containing a 124-min linear increase from 6-30% solvent B (0.1% formic acid/80% acetonitrile), with 0.1% formic acid/water as Solvent A. Further settings were as described previously (Ameziane et al. 2015).

Proteomic analysis. Raw data was analyzed by MaxQuant (version 1.5.8.3) (Cox et al. 2014) employing the label-free quantitation (LFQ) algorithm and the 'match between runs' tool, with default settings. MS/MS data were searched against the human Swissprot database (20,197 entries, release 2016_09) complemented with a list of common contaminants and concatenated with the reversed version of all sequences. Trypsin/P was chosen as cleavage specificity allowing two missed cleavages. Carbamidomethylation (C) and oxidation (M) were set as fixed and variable modification, respectively. LFQ intensities were log₂-transformed in Perseus (version 1.5.5.3) (Tyanova et al. 2016) after which proteins were filtered for at least two valid values (out of 3 total). Missing values were replaced by imputation based on a normal distribution using a width of 0.3 and a downshift of 1.8. p-values of all quantified proteins were calculated in a Student's t-test and plotted against the log₂ (bait/control) LFQ abundance difference in a Volcano plot. Proteins were considered enriched by immunoprecipitation when they met the criteria $p < 0.05$ and $\log_2 \text{LFQ}[\text{bait/control}] \geq 2$.

Survival analysis. RNA seq dataset (GSE62564) was selected from the Gene Expression Omnibus and analyzed through the Genomics Analysis and Visualization Platform. Kaplan-Meier estimates of overall survival were determined using expression cut-offs based on statistical significant differences using log-rank test.

Statistics. All statistical analyses were performed using Graphpad Prism 7.02.

Acknowledgements

We thank J.E. Carette for kindly providing us with the NF- κ B reporter plasmid. This work was supported by the Villa Joep Foundation, and the Netherlands Organization for Scientific Research (NWO), as part of the National Roadmap Large-scale Research Facilities of the Netherlands, Proteins@Work (project number 184.032.201).

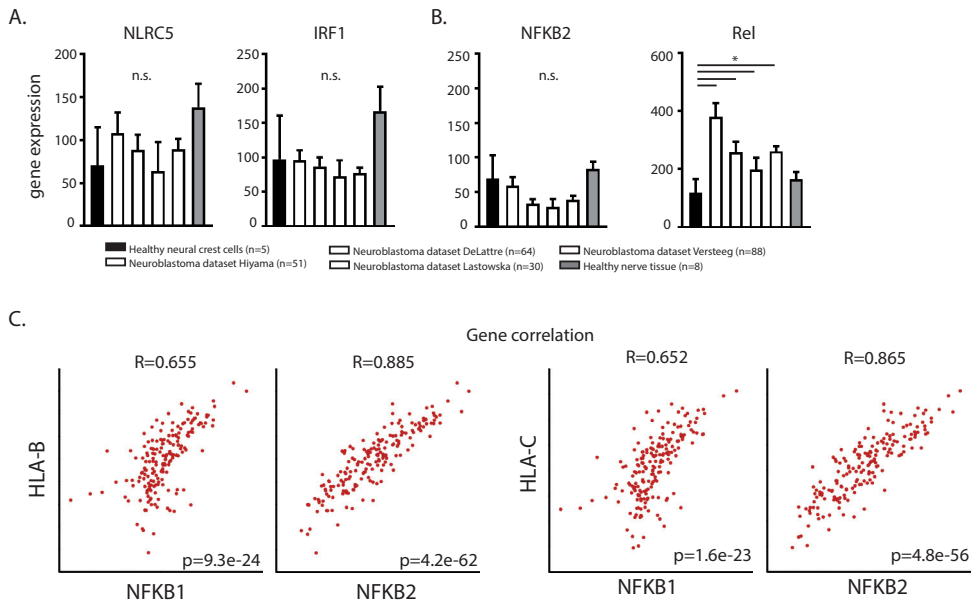
References

- ADAIR, S. J. & HOGAN, K. T. 2009. Treatment of ovarian cancer cell lines with 5-aza-2'-deoxycytidine upregulates the expression of cancer-testis antigens and class I major histocompatibility complex-encoded molecules. *Cancer Immunol Immunother*, 58, 589-601.
- AMEZIANE, N., MAY, P., HAITJEMA, A., VAN DE VRUGT, H. J., VAN ROSSUM-FIKKERT, S. E., RISTIC, D., WILLIAMS, G. J., BALK, J., ROCKX, D., LI, H., et al. 2015. A novel Fanconi anaemia subtype associated with a dominant-negative mutation in RAD51. *Nat Commun*, 6, 8829.
- ARMSTRONG, J. L., VEAL, G. J., REDFERN, C. P. & LOVAT, P. E. 2007. Role of Noxa in p53-independent fenretinide-induced apoptosis of neuroectodermal tumours. *Apoptosis*, 12, 613-22.
- BAO, L., DUNHAM, K. & LUCAS, K. 2011. MAGE-A1, MAGE-A3, and NY-ESO-1 can be upregulated on neuroblastoma cells to facilitate cytotoxic T lymphocyte-mediated tumor cell killing. *Cancer Immunol Immunother*, 60, 1299-307.
- BIAN, X., MCALLISTER-LUCAS, L. M., SHAO, F., SCHUMACHER, K. R., FENG, Z., PORTER, A. G., CASTLE, V. P. & OPIPARI, A. W., JR. 2001. NF-kappa B activation mediates doxorubicin-induced cell death in N-type neuroblastoma cells. *J Biol Chem*, 276, 48921-9.
- BISTA, P., ZENG, W., RYAN, S., BAILLY, V., BROWNING, J. L. & LUKASHEV, M. E. 2010. TRAF3 controls activation of the canonical and alternative NFkappaB by the lymphotoxin beta receptor. *J Biol Chem*, 285, 12971-8.
- BOOKER, L. Y., ISHOLA, T. A., BOWEN, K. A. & CHUNG, D. H. 2009. Research Advances in Neuroblastoma Immunotherapy. *Curr Pediatr Rev*, 5, 112-117.
- BOULANGER, L. M. 2009. Immune proteins in brain development and synaptic plasticity. *Neuron*, 64, 93-109.
- BRINKMAN, E. K., CHEN, T., AMENDOLA, M. & VAN STEENSEL, B. 2014. Easy quantitative assessment of genome editing by sequence trace decomposition. *Nucleic Acids Res*, 42, e168.
- BRUMMELKAMP, T. R., NIJMAN, S. M., DIRAC, A. M. & BERNARDS, R. 2003. Loss of the cylindromatosis tumour suppressor inhibits apoptosis by activating NF-kappaB. *Nature*, 424, 797-801.
- CASTRICONI, R., DONDERO, A., AUGUGLIARO, R., CANTONI, C., CARNEMOLLA, B., SEMENTA, A. R., NEGRI, F., CONTE, R., CORRIAS, M. V., MORETTA, L., et al. 2004. Identification of 4Ig-B7-H3 as a neuroblastoma-associated molecule that exerts a protective role from an NK cell-mediated lysis. *Proc Natl Acad Sci U S A*, 101, 12640-5.
- CHEUNG, N. K. & DYER, M. A. 2013. Neuroblastoma: developmental biology, cancer genomics and immunotherapy. *Nat Rev Cancer*, 13, 397-411.
- COHEN, S., CIECHANOVER, A., KRAVTSOVA-IVANTSIV, Y., LAPID, D. & LAHAV-BARATZ, S. 2009. ABIN-1 negatively regulates NF-kappaB by inhibiting processing of the p105 precursor. *Biochem Biophys Res Commun*, 389, 205-10.
- CONDELLO, S., CACCAMO, D., CURRO, M., FERLAZZO, N., PARISI, G. & IENTILE, R. 2008. Transglutaminase 2 and NF-kappaB interplay during NGF-induced differentiation of neuroblastoma cells. *Brain Res*, 1207, 1-8.
- COUGHLIN, C. M., FLEMING, M. D., CARROLL, R. G., PAWEL, B. R., HOGARTY, M. D., SHAN, X., VANCE, B. A., COHEN, J. N., JAIRAJ, S., LORD, E. M., et al. 2006. Immunosurveillance and survivin-specific T-cell immunity in children with high-risk neuroblastoma. *J Clin Oncol*, 24, 5725-34.
- COX, J., HEIN, M. Y., LUBER, C. A., PARON, I., NAGARAJ, N. & MANN, M. 2014. Accurate proteome-wide label-free quantification by delayed normalization and maximal peptide ratio extraction, termed MaxLFQ. *Mol Cell Proteomics*, 13, 2513-26.
- CROCE, M., CORRIAS, M. V., RIGO, V. & FERRINI, S. 2015. New immunotherapeutic strategies for the treatment of neuroblastoma. *Immunotherapy*, 7, 285-300.
- DAVIDOFF, A. M. 2012. Neuroblastoma. *Semin Pediatr Surg*, 21, 2-14.
- DE BITTENCOURT PASQUALI, M. A., DE RAMOS, V. M., ALBANUS, R. D. O., KUNZLER, A., DE SOUZA, L. H. T., DALMOLIN, R. J. S., GELAIN, D. P., RIBEIRO, L., CARRO, L. & MOREIRA, J. C. F. 2016. Gene Expression Profile of NF-kappaB, Nrf2, Glycolytic, and p53 Pathways During the SH-SY5Y Neuronal Differentiation Mediated by Retinoic Acid. *Mol Neurobiol*, 53, 423-435.
- FAVROT, M. C., COMBARET, V., GOILLOT, E., TABONE, E., BOUFFET, E., DOLBEAU, D., BOUVIER, R., COZE, C., MICHON, J. & PHILIP, T. 1991. Expression of leucocyte adhesion molecules on 66 clinical neuroblastoma specimens. *Int J Cancer*, 48, 502-10.
- FENG, Z. & PORTER, A. G. 1999. NF-kappaB/Rel proteins are required for neuronal differentiation of SH-SY5Y neuroblastoma cells. *J Biol Chem*, 274, 30341-4.
- FENNER, B. J., SCANNELL, M. & PREHN, J. H. 2009. Identification of polyubiquitin binding proteins involved in

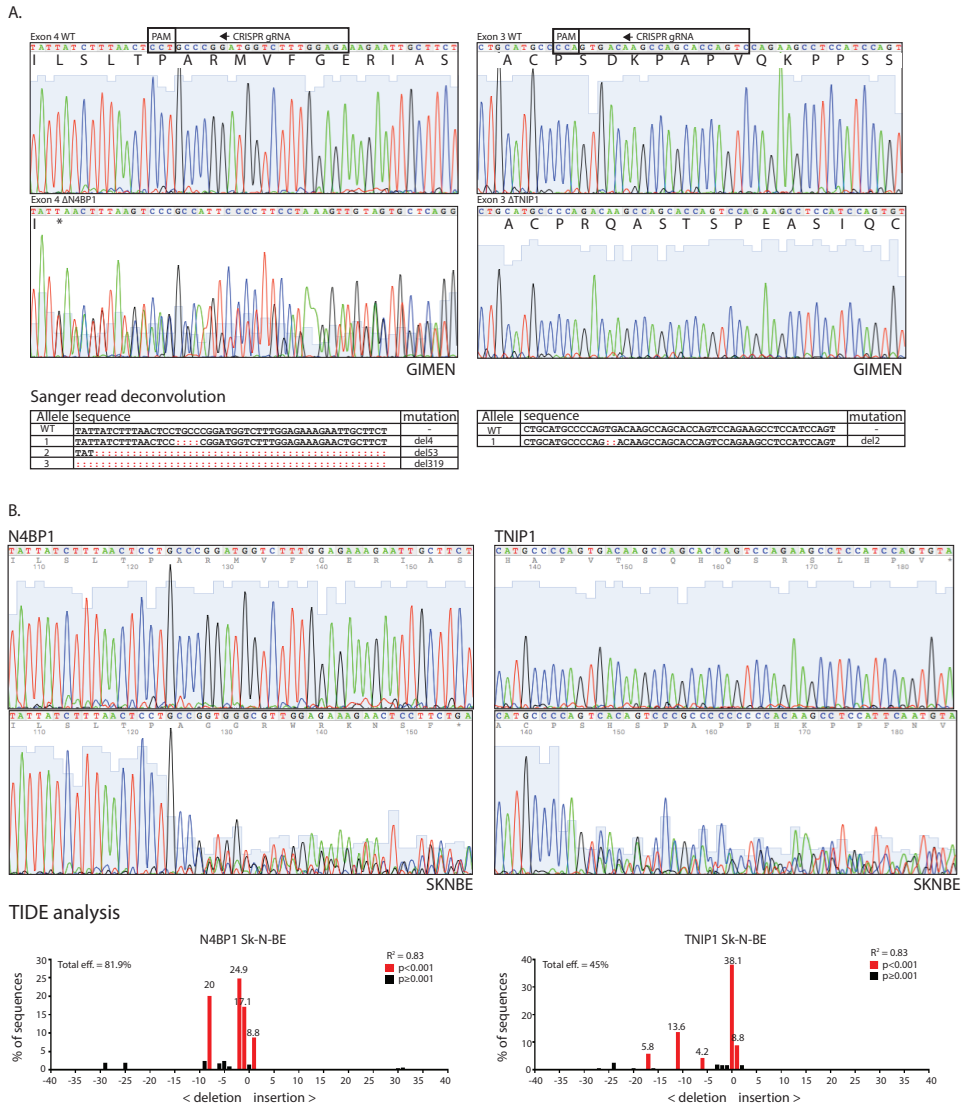
- NF-kappaB signaling using protein arrays. *Biochim Biophys Acta*, 1794, 1010-6.
- FOREMAN, N. K., RILL, D. R., COUSTAN-SMITH, E., DOUGLASS, E. C. & BRENNER, M. K. 1993. Mechanisms of selective killing of neuroblastoma cells by natural killer cells and lymphokine activated killer cells. Potential for residual disease eradication. *Br J Cancer*, 67, 933-8.
- FORLONI, M., ALBINI, S., LIMONGI, M. Z., CIFALDI, L., BOLDRINI, R., NICOTRA, M. R., GIANNINI, G., NATALI, P. G., GIACOMINI, P. & FRUCI, D. 2010. NF-kappaB, and not MYCN, regulates MHC class I and endoplasmic reticulum aminopeptidases in human neuroblastoma cells. *Cancer Res*, 70, 916-24.
- G'SELL, R. T., GAFFNEY, P. M. & POWELL, D. W. 2015. A20-Binding Inhibitor of NF-kappaB Activation 1 is a Physiologic Inhibitor of NF-kappaB: A Molecular Switch for Inflammation and Autoimmunity. *Arthritis Rheumatol*, 67, 2292-302.
- GARAY, P. A. & MCALLISTER, A. K. 2010. Novel roles for immune molecules in neural development: implications for neurodevelopmental disorders. *Front Synaptic Neurosci*, 2, 136.
- GILMORE, T. D. & GERONDAKIS, S. 2011. The c-Rel Transcription Factor in Development and Disease. *Genes Cancer*, 2, 695-711.
- HEYNINCK, K., DE VALCK, D., VANDEN BERGHE, W., VAN CRIEKINGE, W., CONTRERAS, R., FIERIS, W., HAEGEMAN, G. & BEYAERT, R. 1999. The zinc finger protein A20 inhibits TNF-induced NF-kappaB-dependent gene expression by interfering with an RIP- or TRAF2-mediated transactivation signal and directly binds to a novel NF-kappaB-inhibiting protein ABIN. *J Cell Biol*, 145, 1471-82.
- HU, H., BRITTAIN, G. C., CHANG, J. H., PUEBLA-OSORIO, N., JIN, J., ZAL, A., XIAO, Y., CHENG, X., CHANG, M., FU, Y. X., et al. 2013. OTUD7B controls non-canonical NF-kappaB activation through deubiquitination of TRAF3. *Nature*, 494, 371-4.
- HUNTER, J. E., LESLIE, J. & PERKINS, N. D. 2016. c-Rel and its many roles in cancer: an old story with new twists. *Br J Cancer*, 114, 1-6.
- JACOBS, J. F., BRASSEUR, F., HULSBERGEN-VAN DE KAA, C. A., VAN DE RAKT, M. W., FIGDOR, C. G., ADEMA, G. J., HOOGERBRUGGE, P. M., COULIE, P. G. & DE VRIES, I. J. 2007. Cancer-germline gene expression in pediatric solid tumors using quantitative real-time PCR. *Int J Cancer*, 120, 67-74.
- KOVALENKO, A., CHABLE-BESSIA, C., CANTARELLA, G., ISRAEL, A., WALLACH, D. & COURTOIS, G. 2003. The tumour suppressor CYLD negatively regulates NF-kappaB signalling by deubiquitination. *Nature*, 424, 801-5.
- KRISHNADAS, D. K., SHUSTERMAN, S., BAI, F., DILLER, L., SULLIVAN, J. E., CHEERVA, A. C., GEORGE, R. E. & LUCAS, K. G. 2015. A phase I trial combining decitabine/dendritic cell vaccine targeting MAGE-A1, MAGE-A3 and NY-ESO-1 for children with relapsed or therapy-refractory neuroblastoma and sarcoma. *Cancer Immunol Immunother*, 64, 1251-60.
- LAMPSON, L. A., FISHER, C. A. & WHELAN, J. P. 1983. Striking paucity of HLA-A, B, C and beta 2-microglobulin on human neuroblastoma cell lines. *J Immunol*, 130, 2471-8.
- LANGMEAD, B., TRAPNELL, C., POP, M. & SALZBERG, S. L. 2009. Ultrafast and memory-efficient alignment of short DNA sequences to the human genome. *Genome Biol*, 10, R25.
- LEE, C. C., CARETTE, J. E., BRUMMELKAMP, T. R. & PLOEGH, H. L. 2013. A reporter screen in a human haploid cell line identifies CYLD as a constitutive inhibitor of NF-kappaB. *PLoS One*, 8, e70339.
- LI, S., WANG, L., BERMAN, M., KONG, Y. Y. & DORF, M. E. 2011. Mapping a dynamic innate immunity protein interaction network regulating type I interferon production. *Immunity*, 35, 426-40.
- LIU, D., SONG, L., WEI, J., COURTNEY, A. N., GAO, X., MARINOVA, E., GUO, L., HECZEY, A., ASGHARZADEH, S., KIM, E., et al. 2012. IL-15 protects NKT cells from inhibition by tumor-associated macrophages and enhances antimetastatic activity. *J Clin Invest*, 122, 2221-33.
- LORENZI, S., FORLONI, M., CIFALDI, L., ANTONUCCI, C., CITTI, A., BOLDRINI, R., PEZZULLO, M., CASTELLANO, A., RUSSO, V., VAN DER BRUGGEN, P., et al. 2012. IRF1 and NF-kB restore MHC class I-restricted tumor antigen processing and presentation to cytotoxic T cells in aggressive neuroblastoma. *PLoS One*, 7, e46928.
- LOUIS, C. U. & SHOHET, J. M. 2015. Neuroblastoma: molecular pathogenesis and therapy. *Annu Rev Med*, 66, 49-63.
- LOVE, M. I., HUBER, W. & ANDERS, S. 2014. Moderated estimation of fold change and dispersion for RNA-seq data with DESeq2. *Genome Biol*, 15, 550.
- MARIS, J. M. 2010. Recent advances in neuroblastoma. *N Engl J Med*, 362, 2202-11.
- MAURO, C., PACIFICO, F., LAVORGNA, A., MELLONE, S., IANNETTI, A., ACQUAVIVA, R., FORMISANO, S., VITO, P. & LEONARDI, A. 2006. ABIN-1 binds to NEMO/IKKgamma and co-operates with A20 in inhibiting NF-kappaB. *J Biol Chem*, 281, 18482-8.
- MORANDI, F., CANGEMI, G., BARCO, S., AMOROSO, L., GIULIANO, M., GIGLIOTTI, A. R., PISTOIA, V. & CORRIAS,

- M. V. 2013. Plasma levels of soluble HLA-E and HLA-F at diagnosis may predict overall survival of neuroblastoma patients. *Biomed Res Int*, 2013, 956878.
- MORANDI, F., SCARUFFI, P., GALLO, F., STIGLIANI, S., MORETTI, S., BONASSI, S., GAMBINI, C., MAZZOCCO, K., FARDIN, P., HAAPT, R., et al. 2012. Bone marrow-infiltrating human neuroblastoma cells express high levels of calprotectin and HLA-G proteins. *PLoS One*, 7, e29922.
- OBERTHUER, A., HERO, B., SPITZ, R., BERTHOLD, F. & FISCHER, M. 2004. The tumor-associated antigen PRAME is universally expressed in high-stage neuroblastoma and associated with poor outcome. *Clin Cancer Res*, 10, 4307-13.
- RAFFAGHELLO, L., PRIGIONE, I., AIROLDI, I., CAMORIANO, M., LEVRERI, I., GAMBINI, C., PENDE, D., STEINLE, A., FERRONE, S. & PISTOIA, V. 2004. Downregulation and/or release of NKG2D ligands as immune evasion strategy of human neuroblastoma. *Neoplasia*, 6, 558-68.
- RAFFAGHELLO, L., PRIGIONE, I., BOCCA, P., MORANDI, F., CAMORIANO, M., GAMBINI, C., WANG, X., FERRONE, S. & PISTOIA, V. 2005. Multiple defects of the antigen-processing machinery components in human neuroblastoma: immunotherapeutic implications. *Oncogene*, 24, 4634-44.
- SANJANA, N. E., SHALEM, O. & ZHANG, F. 2014. Improved vectors and genome-wide libraries for CRISPR screening. *Nat Methods*, 11, 783-784.
- SCHUMACHER, T. N. & SCHREIBER, R. D. 2015. Neoantigens in cancer immunotherapy. *Science*, 348, 69-74.
- SEEGER, R. C. 2011. Immunology and immunotherapy of neuroblastoma. *Semin Cancer Biol*, 21, 229-37.
- SERRANO, A., TANZARELLA, S., LIONELLO, I., MENDEZ, R., TRAVERSARI, C., RUIZ-CABELLO, F. & GARRIDO, F. 2001. Repression of HLA class I antigens and restoration of antigen-specific CTL response in melanoma cells following 5-aza-2'-deoxycytidine treatment. *Int J Cancer*, 94, 243-51.
- SHATZ, C. J. 2009. MHC class I: an unexpected role in neuronal plasticity. *Neuron*, 64, 40-5.
- SHURIN, G. V., GEREIN, V., LOTZE, M. T. & BARKSDALE, E. M., JR. 1998. Apoptosis induced in T cells by human neuroblastoma cells: role of Fas ligand. *Nat Immun*, 16, 263-74.
- SOLING, A., SCHURR, P. & BERTHOLD, F. 1999. Expression and clinical relevance of NY-ESO-1, MAGE-1 and MAGE-3 in neuroblastoma. *Anticancer Res*, 19, 2205-9.
- SPEL, L., BOELEN, J. J., VAN DER STEEN, D. M., BLOKLAND, N. J., VAN NOESEL, M. M., MOLENAAR, J. J., HEEMSKERK, M. H., BOES, M. & NIERKENS, S. 2015. Natural killer cells facilitate PRAME-specific T-cell reactivity against neuroblastoma. *Oncotarget*, 6, 35770-81.
- TYANOVA, S., TEMU, T., SINITSYN, P., CARLSON, A., HEIN, M. Y., GEIGER, T., MANN, M. & COX, J. 2016. The Perseus computational platform for comprehensive analysis of (prote)omics data. *Nat Methods*, 13, 731-40.
- VAN 'T VEER, L. J., BEIJERSBERGEN, R. L. & BERNARDS, R. 1993. N-myc suppresses major histocompatibility complex class I gene expression through down-regulation of the p50 subunit of NF-kappa B. *EMBO J*, 12, 195-200.
- VERTUANI, S., DE GEER, A., LEVITSKY, V., KOGNER, P., KIESSLING, R. & LEVITSKAYA, J. 2003. Retinoids act as multistep modulators of the major histocompatibility class I presentation pathway and sensitize neuroblastomas to cytotoxic lymphocytes. *Cancer Res*, 63, 8006-13.
- WOLFL, M., JUNGBLUTH, A. A., GARRIDO, F., CABRERA, T., MEYEN-SOUTHARD, S., SPITZ, R., ERNESTUS, K. & BERTHOLD, F. 2005. Expression of MHC class I, MHC class II, and cancer germline antigens in neuroblastoma. *Cancer Immunol Immunother*, 54, 400-6.
- WU, C. J., CONZE, D. B., LI, X., YING, S. X., HANOVER, J. A. & ASHWELL, J. D. 2005. TNF-alpha induced c-IAP1/ TRAF2 complex translocation to a Ubc6-containing compartment and TRAF2 ubiquitination. *EMBO J*, 24, 1886-98.

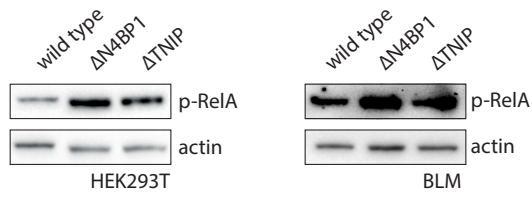
Supplemental information



Supplemental figure 1. Gene expression of transcription factors regulating MHC-1 in neuroblastoma. Gene expression datasets of neural crest cells, healthy nerve tissue and neuroblastoma tumors were analyzed for the expression of NLRC5, IRF1 (A) and NF- κ B alleles NFKB2 and REL (B). Two-way ANOVA test was used, $p < 0.05$ was considered significant. C. Gene expression of MHC-1 alleles HLA-B and HLA-C in neuroblastoma tumor samples (cohort of 183 stage-4 neuroblastoma patients) was correlated with NFKB genes. Significance test for the Pearson correlation coefficient r was conducted, $p < 0.5$ was considered significant.



Supplemental figure 2. Generation of cells deficient for N4BP1 and TNIP1 using CRISPR/CAS9. To obtain Δ N4BP1 and Δ TNIP1 cell lines, CRISPR/CAS9 targeting the 4th exon of N4BP1 or the 3rd exon of TNIP1 were used to mutate the respective genes. gRNAs were cloned in pxpr_001 vector, encoding for both gRNA, CAS9 and puromycin resistance. Virus was obtained using standard protocols and cells were transduced. After 48 hours, cells were selected using 0.75 μ g ml⁻¹ puromycin for 48 hours or until non-transduced control populations died. A. GIMEN clonal Δ N4BP1 and Δ TNIP1 cell lines were generated by limiting dilutions to ensure clonality. Allele annotations of the clonal cell lines are shown. N4BP1 is found mutated differently on 3 independent alleles while the same -2 mutation is found in all alleles in TNIP1 mutated cells. B. TIDE analysis for polyclonal Δ N4BP1 and Δ TNIP1 cell line, Sk-N-BE is shown as example.



Supplemental figure 3. Activation of NF- κ B in non-neuroblastoma cell lines. Immunoblot analysis of phospho-RelA in WT, Δ N4BP1 and Δ TNIP1 mutants in HEK293T or BLM.

Chapter 8

**Reviewing discussion:
Immunogenicity during neuroblastoma development; insights
for immunotherapy**

Authors

Lotte Spel, Ariën Schiepers, Marianne Boes



Introduction

Fifteen percent of all pediatric cancer deaths are caused by neuroblastoma tumors (1-3). Neuroblastoma is the most common solid tumor in infancy, with merely 20% survival within the high-risk disease group. Patients are generally diagnosed between ages 0-18 months. Low-risk and intermediate-risk neuroblastoma is well treatable by surgical resection, chemotherapy and/or radiotherapy, resulting in >93% cures (2, 4). Treatment options for high-risk neuroblastoma patients are hematopoietic stem cell transplantation, in addition to chemotherapy, radiotherapy and surgical resection. Yet, survival rates remain detrimental due to tumor relapses.

Neuroblastoma classifies as an embryonic tumor, rising from incompletely committed peripheral nerve precursor cells of the neural crest that have become cancerous during development and differentiation (5). Long-term survival is primarily related to the degree of differentiation, with high-risk patients exhibiting more primitive crest-like tumors compared to low-risk patients with more differentiated tumors who have a more favorable outcome (6). Therefore, standard treatment for high-risk neuroblastoma includes administration of neuronal differentiating agents after chemotherapy (7).

Since 2005, high-risk neuroblastoma patients can receive immunotherapy consisting of anti-GD2 antibodies and IL-2 (8). Unfortunately, while initial results seemed promising, the majority of the patients undergoing anti-GD2/IL2 treatment eventually relapses. Still, immunotherapy has given remarkable results in the cancer field overall, during the last decades (9-11). Embryonal tumors like neuroblastoma may be less immunogenic than adult tumors, providing fewer targets for immune intervention. My goal here, was to clarify immunogenic features of neuroblastoma tumors, to provide new cues for immunotherapy to apply towards effectively targeting these type of tumor cells.

Immunogenicity during embryonic development

The immunogenicity of any cell describes its ability to be seen by the immune system as well as its ability to provoke an immune response. MHC 1 antigen presentation is one immunogenic feature that is pivotal for T cell recognition of cells and thus underpins a cell's immunogenicity towards CD8⁺ T cells. During embryogenesis the fetal immune system is in development, as is the immunogenicity of all somatic cells to prepare for immune-mediated defense against pathogens. Embryonic stem cells (ESC) are considered immune-privileged as they display very low levels of MHC class 1 molecules on their cell surface (12, 13, 14). Hence, ES cells are not immunogenic yet. With each consecutive differentiation step, MHC 1 expression will increase until the cell reaches final differentiation (15, 16). As a result, ESC-derived cells appeared to be less well rejected than adult cells when transplanted into immune-competent mice (13, 17). The major component responsible for immune rejection of the adult cells was shown to be CD8⁺ T cells. Moreover, upon induction of MHC 1 expression in ESC-derived cells they could be killed by CD8⁺ T cells as well, indicating the importance of MHC 1 expression for immunogenicity. I will give additional support for the importance of MHC 1 expression to cellular immunogenicity below.

While the brain has long been thought to lack MHC 1 expression, it is now clear that neuronal cells do express MHC 1 in the steady-state (18, 19, 20, 21), albeit at low levels. Indeed, peripheral nerve cells were shown to express MHC 1 to similar extent as other fully differentiated neural crest derivatives such as melanocytes and smooth muscle cells (22, 23, 24, 25, 26, 27, 28, 29,

30). Peptide/MHC 1 expression appears to be sufficient for antigen presentation, as healthy melanocytes could be recognized by an antigen-specific CD8⁺ T cell clone (31). Furthermore, T cell immunity against melanocyte-expressed antigen has also been shown in patients suffering from vitiligo (32).

Studies investigating herpes infection provide evidence for MHC 1-mediated T cell immunity against peripheral nerves. Herpes simplex virus (HSV) causes skin infections associated with sores, vesicles or ulcers. Typically, HSV persists in peripheral nerves as a latent infection that can reactivate at any moment. Latency of HSV is controlled by CD8⁺ T cells (33, 34, 35). CD8⁺ T cells isolated from HSV-infected neural ganglia at latency state can block viral reactivation in vitro, whereas CD4⁺ T cells can't (33). In further support, in vivo mouse experiments showed that depletion of CD8⁺ T cells triggers significantly higher viral copies during the latency phase of HSV-infected mice compared to control mice (34). Furthermore, perforin^{-/-} or granzymeB (grB)^{-/-} mice were unable to control HSV latency. Indeed, in co-cultures of infected neurons with perforin^{-/-} or grB^{-/-} HSV-specific CTLs reactivations were observed. In contrast, wild type CTLs were able to establish latency (34). Control of HSV latency by CD8⁺ T cells is dependent on MHC 1 expression. Given that in HSV-infected neurons, down-regulation of MHC 1 resulted in abrogated latency and viral reactivation (36). These studies indicate that endogenous MHC 1 antigen presentation in peripheral nerves is sufficient for recognition by CD8⁺ T cells.

Neuroblastoma tumors typically present with extremely low levels of MHC 1, especially in high-risk patients (37). Neuroblastomas with low classical (HLA-A, -B, and -C) MHC 1 expression were shown to have higher non-classical HLA expression (HLA-E, -F, and -G), whose plasma levels correlated with worse survival (38). Aberrant NFκB activity causes both low MHC 1 and decreased expression of the antigen processing machinery required for functional antigen presentation by the MHC 1 molecule. In some cases, these proteins can be re-expressed by exposure to IFNγ (39, 40, 41), then allowing for CD8⁺ T cell recognition of the neuroblastoma cells (39, 41).

Development of neuroblastoma tumors

Neuroblastoma arises in cells of the peripheral nervous system, most commonly the sympathetic nerves of the adrenal gland or the paraspinal ganglia. As neuroblastoma is found in children as young as 3 months old, the cause of the tumor is thought to lie in aberrant development and differentiation during embryogenesis rather than exogenous mutagenic factors.

Initiation of neural tissue development begins with the formation of the neural tube around day 26-30 after conception. In this process called neurulation, the dorsal positioned neural plate folds inwards to form not only the neural tube but also the aligning neural crest cells (Figure 1A-C). Neural stem cells will develop in the linings of the neural tube and give rise to all tissues of the central nervous system, including the brain and spinal cord. Concurrently, the neural crest cells give rise to diverse cell lineages that will migrate throughout the embryo and develop into various tissues, including the skull, smooth muscle cells of the heart, melanocytes, peripheral nerves and more.

The neural crest tissue can be divided into four functional regions along the anterior-to-posterior axis: the cranial neural crest, the trunk neural crest, the vagal/sacral neural crest and the cardiac neural crest. Of these, the trunk neural crest cells contain the precursors for the sympathetic nerves and dorsal root ganglia. Additionally, some trunk neural crest cells migrate towards the

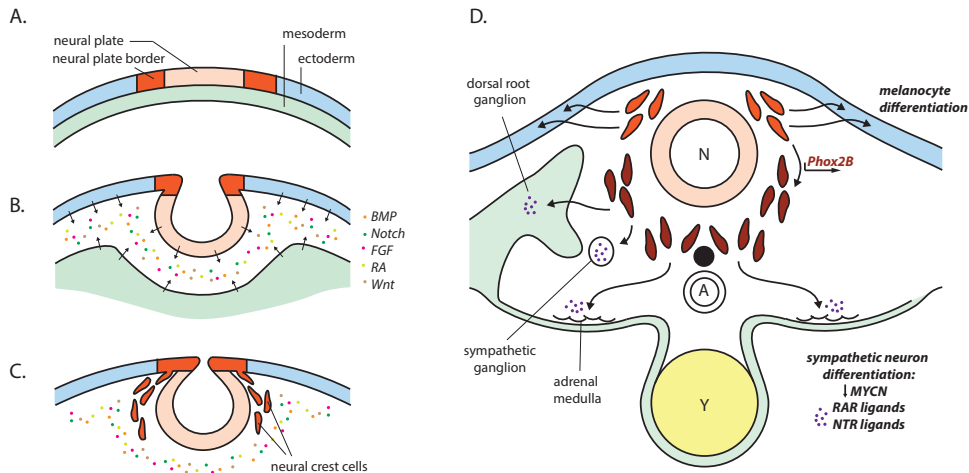


Figure 1. Neural crest cell induction and differentiation. A. Central in the ectodermal layer resides the neurectoderm, consisting of the neural plate and the neural plate border. On the ventral side of the ectoderm is the mesoderm layer positioned. B. The neural plate, the ectoderm and the mesoderm start the production of neural crest-inducing signals while the neural plate is growing inwards. C. Neural crest cells start migrating out of the ectodermal layer alongside the neural tube. D. Neural crest cells can migrate back into the ectodermal layer for differentiation into melanocytes. Other neural crest cells will upregulate the expression of Phox2B which marks their commitment to sympathetic neuron differentiation. Phox2B-expressing cells of the trunk neural crest migrate towards areas of the dorsal root ganglia, sympathetic ganglia and adrenal medulla where final neuron differentiation occurs through down-regulation of MYCN and signaling through RA receptors (RAR) and neurotrophin receptors (NTR). N = neural tube, A = aorta, Y = yolk sac.

skin layer to become melanocytes (Figure 1D).

An elaborate interplay of signals determines the formation, migration and differentiation of neural crest cells and its destined lineages (3, 42-44). Induction of the neural crest requires the surrounding ectoderm, neurepithelium and mesoderm to produce signals consisting of bone morphogenetic protein (BMP), Wnt, fibroblast growth factor (FGF), retinoic acid (RA) and Notch (43, 45-47) (Figure 1B). These cascading signaling gradients allow for the neural crest cells to separate from the neurepithelium and ectoderm and trigger their migration (Figure 1C). Migration of neural crest cells is controlled by the permissiveness of the extracellular matrix (48-50), and a range of guidance signals (51). Part of the migrating neural crest cell precursors will activate the transcription factor Phox2B, which drives differentiation toward sympathetic neurons (52) (Figure 1D). When arrived at their destined location, post-migratory sympathetic precursors differentiate into their mature status, which is accompanied by down-regulation of MYCN and subsequent signaling through neurotrophin receptors and retinoic acid receptors (45, 53, 54) (Figure 1D).

Errors that may occur during the development of neural crest cells and the differentiation of its diverse lineages contribute to the formation of neuroblastoma tumors. In spite the fact that no single mutation or genomic alteration accounts for all neuroblastoma cases (55), certain genetic changes are more common than others. In 40% of high-risk neuroblastomas the MYCN gene is amplified (56), directly antagonizing the process of neuronal differentiation. Anaplastic

lymphoma kinase (ALK), a transcriptional target of MYCN, regulates survival of migratory neural crest cells and stimulates self-renewal (57, 58). In 5% of the high-risk neuroblastoma cases ALK was shown to have gain-of-function mutations (59).

In 23% of high-risk neuroblastomas that lack MYCN amplifications, rearrangements of the telomerase reverse transcriptase gene could be found (60). TERT rearrangements result in overexpression of TERT, which lengthens the telomeres and thereby prolongs the lifespan of neuroblastoma cells. Telomere length is also regulated by the ATRX gene, an epigenetic factor of the SWI/SNF family of chromatin modifiers that play a critical role in neural crest maturation (61). In 11% of high-risk neuroblastomas ATRX is inactivated resulting in preservation of telomere length.

The transcription factor Phox2B carries loss-of-function mutations in 4% of high-risk neuroblastoma. Since Phox2B plays a critical role in sympathetic neuron differentiation, neuroblastoma cells expressing mutated Phox2B were shown to resist RA-induced neuroblastoma differentiation (62).

Although many different genetic defects are found in neuroblastoma tumor, the majority appears involved in differentiation processes of neuronal development. In line with this observation, part of high-risk neuroblastoma treatment regimen is focused on differentiating the immature cancerous cells using retinoic acid. Indeed, results of a randomized phase III trial of high-dose 13-cis-RA after chemotherapy showed increased 3-year event-free survival (EFS) of 14% in high-risk neuroblastoma patients (63). Also following autologous bone marrow transplantation, 13-cis-RA treatment resulted in 14% higher 3-year EFS (63).

Nuclear factor *kappa* B during neuronal development

In cancer, nuclear factor kappa B (NFκB) signaling is often affected. In most tumors NFκB is constitutively active, including in prostate cancer, small and non-small lung cancer, breast cancer and head and neck cancer (64). In contrast, in neuroblastoma, abnormally low levels of NFκB have been reported on both protein and gene level (39, 65, 66, This thesis: chapter 7). The NFκB family of transcription factors consists of five members: RelA (p65), RelB, c-Rel, NFκB1 (p50) and NFκB2 (p52) (Figure 2A). Unlike the RelA, RelB and C-Rel, p50 and p52 are proteolytically cleaved from precursors p105 and p100 (67). All five NFκB subunits can form homo- and heterodimers. Different combinations of NFκB dimers can have different target DNA preferences and different effects on gene activity. RelA, RelB and c-Rel harbor transactivation domains at the C-terminus, which are absent in p105 and p100 (68). NFκB can be activated through the canonical or non-canonical pathway (Figure 2B), primarily activating p50/p65 or p52/RelB homodimers, respectively.

NFκB plays a pivotal role in embryonic development and neurogenesis (69-72). In mice, NFκB is shown to be active in zones of neurogenesis (69, 70). RelA knockout mice die at E15 due to liver degeneration (73, 74). IKKα/β double knockout mice die at E12 due to apoptosis of neural epithelial cells and impaired neurogenesis (75). Specifically neural crest derivatives are effected when mutations occur in regulating kinases within the non-canonical pathway, TGFβ-activating kinase 1 (TAK1) or TAK1-binding protein 2 (TAB2). Patients carrying TAK1 mutations present with skeletal dysplasia of the skull (76, 77). A TAB2 deficiency was discovered in patients suffering from congenital heart defects (78) (Figure 2B).

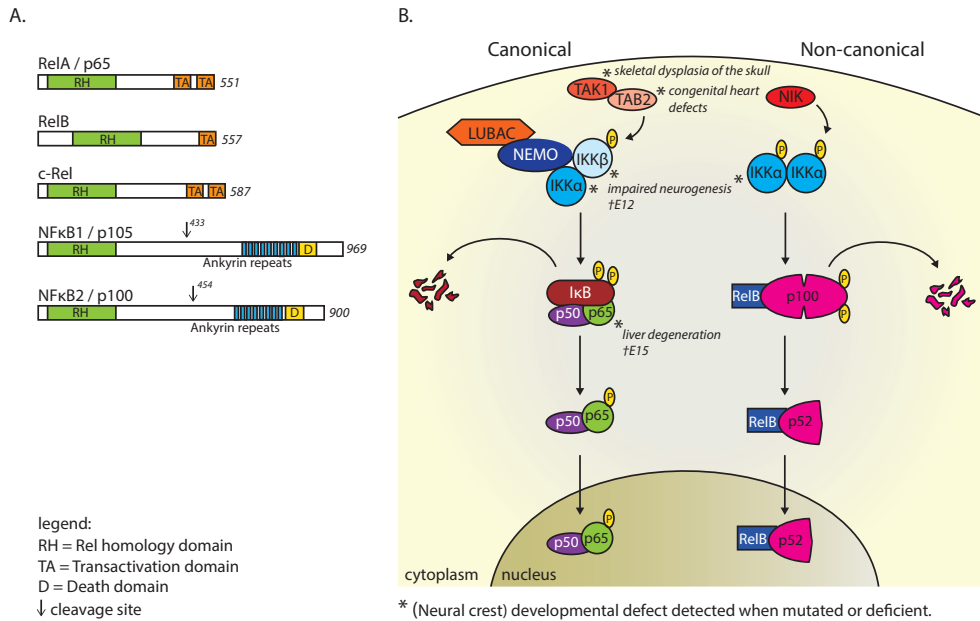


Figure 2. NFκB aberrations in neuronal development. A. Representation of the five NFκB family members. The NFκB transcription factor can consist of any two members of the NFκB family. Which combination determines its transcriptional targets and activity. B. Regulation of the canonical and non-canonical activation pathways of NFκB. Among other kinases, the TAK1/TAB2 complex regulate the canonical pathway by phosphorylating IKK. In turn, the IKKα/β-complex phosphorylates IκB which is then targeted to the proteasome for degradation, freeing the p50/p65 NFκB dimer. After phosphorylation of p65, this NFκB dimer translocates to the nucleus to initiate gene transcription. The non-canonical pathway is activated when NIK phosphorylates IKKα. The IKKα/α-complex phosphorylates p100, which is then partially degraded by the proteasome producing the RelB/p52 NFκB dimer. RelB/p52 can directly translocate to the nucleus to start gene transcription. Proteins highlighted with an asterisk were found to have an important role in neuronal development; the effect observed when they are deficient or mutated is depicted.

During embryonic development, the NFκB levels change. Human embryonic stem cells display low levels of NFκB (79). Upon differentiation, the NFκB levels increase (80, 81). In fact, forced expression of RelA in ES cells drives differentiation and results in loss of pluripotency (82). In particular, epithelial-to-mesenchymal transition (EMT) was shown to depend on active NFκB levels (82, 83), a crucial step that underlies the formation of neural crest cells as they delaminate from the neurepithelium into the mesenchyme.

Besides playing a role in early development of neural crest cells, NFκB is also involved in the differentiation and maturation into neurons. In the healthy developing hippocampus, neuronal differentiation was established through PKC-dependent NFκB activation (70). With regard to neuroblastoma, Körner and colleagues showed that retinoic acid (RA) induced phenotypical differentiation of neuroblastoma cells, measured by dendrite outgrowth (84). However, NFκB was not activated in their experiments. Nonetheless, NFκB was implicated in RA-mediated differentiation by using neuroblastoma cells with dominant negative IκB activity. RA was unable to differentiate these NFκB-null cells (85). In support of these data, RA-mediated NFκB activation was observed in multiple studies (86-89), suggesting that NFκB is pivotal for neuroblastoma

differentiation. Moreover, differentiation of neuroblastoma cells using neural growth factor NGF also resulted in NF κ B activation (88).

NF κ B & MHC 1 in neuroblastoma

Different from tumors in adult patients that usually harbor numerous mutations acquired during their life time driving tumorigenesis, neuroblastoma tumors derive from erroneous underdeveloped cells, accompanied by decreased MHC 1 levels and suppressed NF κ B activity. Since the expression of MHC 1 is under transcriptional control of NF κ B (90), NF κ B may not only be involved in differentiation of neuroblastoma but also regulate immunogenicity of neuroblastoma tumors.

NF κ B directly transactivates the gene transcription of MHC 1 heavy chains, as well as the β 2-microglobulin (β 2m) light chain. In induced pluripotent stem cells, NF κ B signaling was demonstrated to be required for MHC 1 expression (91). Not only MHC 1 itself, but also the expression of genes encoding the antigen presentation machinery, including TAP1 and TAP2, ERAP1 and ERAP2 and tapasin, is regulated by NF κ B transcription factors (39, 90). Therefore, it stands to reason that MHC 1 downregulation in neuroblastoma tumors is influenced by aberrant NF κ B signaling. Indeed, reports have shown that in neuroblastoma tumor cells expressing very low MHC 1 levels, NF κ B signaling was impaired (39, 40, This thesis: chapter 7). Indeed, MHC 1 gene transcription was diminished when NF κ B binding sites were deleted from the promoter region in neuroblastoma cells (92). Furthermore, upon inhibition of NF κ B, MHC 1 levels decreased in both steady-state and TNF-treated conditions (40). Moreover, by reconstituting NF κ B expression, MHC 1 surface expression was restored (39, 40, This thesis: chapter 7).

Research into the mechanistic insights showed that n-Myc suppresses NF κ B activity in neuroblastoma, thereby down-regulating MHC 1 expression (66). This data was contradicted by Forloni and colleagues in 2010, who showed that n-Myc does not regulate MHC 1 in neuroblastoma although MHC 1 expression did depend on NF κ B (40). Indeed, n-Myc levels did not influence NF κ B activation upon RA-treatment either (86). Instead, n-Myc may play a role in preventing neuroblastoma differentiation as n-Myc was shown to disrupt protein kinase C-mediated signaling (65), which is activated by differentiating agent NGF (88), and n-Myc correlated with resistance to differentiation (86).

We and others have shown that neuroblastoma cells can be recognized by CTLs when MHC 1 expression is restored (39, 41, 93, This thesis: chapter 6 and 7). Using CTL clone BK289 which is specific for an EBV nuclear antigen 4-derived peptide, recognition of peptide-pulsed neuroblastoma cells could be observed (93). Different from peptide-pulsing, Lorenzi and colleagues used effector cells recognizing neuroblastoma endogenous antigen MAGE-A3 and showed T cell reactivity when neuroblastoma cells were transfected with NF κ B subunit RelA (39). We were able to show T cell recognition of neuroblastoma cells when 1) transfected with HLA-A2 gene construct, 2) treated with IFN γ or 3) pre-exposed to activated natural killer cells (41, This thesis: chapter 6). All three conditions resulted in enhanced MHC 1 surface expression and subsequent presentation of endogenous tumor antigen PRAME. Furthermore, we were able to identify two genes that regulate NF κ B activity in neuroblastoma (This thesis: chapter 7). Through deletion of these genes, TNIP1 and N4BP1, we generated NF κ B-active neuroblastoma cells which show enhanced MHC 1 antigen presentation capacity and can now be recognized by CTLs.

Different from tumors in adults that usually have actively mutated to avoid T cell reactivity, neuroblastoma tumors seem to lack their full immunogenic potential as a consequence of arrested development. Thus, neuroblastoma cells can remain unseen by T cells due to the fact that they are stuck in development.

T cell-based immunotherapy against neuroblastoma

Lots of strategies exist in the immunotherapy field that focus on T cell-mediated killing of tumor cells. With regard to neuroblastoma, I will now discuss immune checkpoint inhibitors, adoptive cell transfers and dendritic-cell vaccination.

Immune-checkpoint inhibitors

Immune-checkpoint inhibitors are used to give tumor-infiltrated T cells more power to overcome the inhibitory micro-environment of the tumor. Most important immune checkpoints inhibitors include anti-CTLA-4, anti-PDL1 and anti-PD1 antibodies. CTLA-4 and PD1 receptors are expressed on CD8⁺ T cells and function as switch-off receptors that gradually inhibit T cell reactivity and ultimately shut down the immune reaction. PDL1, the ligand to the PD1 receptor, is expressed on antigen-presenting cells and target cells, and is often upregulated in the cancer micro-environment.

Immunohistochemical analysis of neuroblastoma tumor sections revealed the presence of tumor-infiltrated CD8⁺ T cells (94, 95). Although an immunosuppressive micro-environment of neuroblastoma tumors has been reported (96-99), these CD8⁺ T cells displayed an effector memory phenotype, expressed IL-2 receptor CD25 and showed intra-tumoral proliferative capacity (95). In corroboration, pediatric tumors including neuroblastoma were shown to have low expression of PDL1 (100) indicating that T cells are not actively silenced by neuroblastoma tumors. Indeed, PD1 blockade showed no beneficial effects in a murine tumor model of neuroblastoma (101) (Figure 3).

Adoptive T cell transfer

In adoptive T cell therapy, patient-derived T cells are isolated, selected and expanded *ex vivo* followed by re-infusion into the patient. This strategy is focused on increasing the number of tumor-specific T cells in the patient's body. Prerequisite to this approach is knowledge about the antigen specificity of the immunodominant T cells. The mutational burden of neuroblastoma tumors is usually low, which makes the use of potential neo-antigens unfeasible. Instead, antigens that are expressed in neuroblastoma include the cancer/testis antigens, such as NY-ESO1, MAGE and PRAME (37, 102-104). The recognition of neuroblastoma cells by antigen-specific T cell clones has been observed, however only in conditions of MHC 1 upregulation (39, 41, 105, This thesis: chapter 6). Patient-derived lymphocytes transgenically engineered to express $\alpha\beta$ TCRs directed against neuroblastoma antigens may indeed offer a powerful treatment option for high-risk neuroblastoma patients, if at least antigen specificity is known (Figure 3).

Infusion of NY-ESO1 transgenic T cells significantly delayed tumor progression in neuroblastoma-bearing mice but did not eliminate all tumor cells (105). The efficacy of T cell therapies in high-risk neuroblastoma could possibly benefit from a combination with strategies to increase MHC 1 expression on the tumor cells, thereby increasing their immunogenicity as a whole.

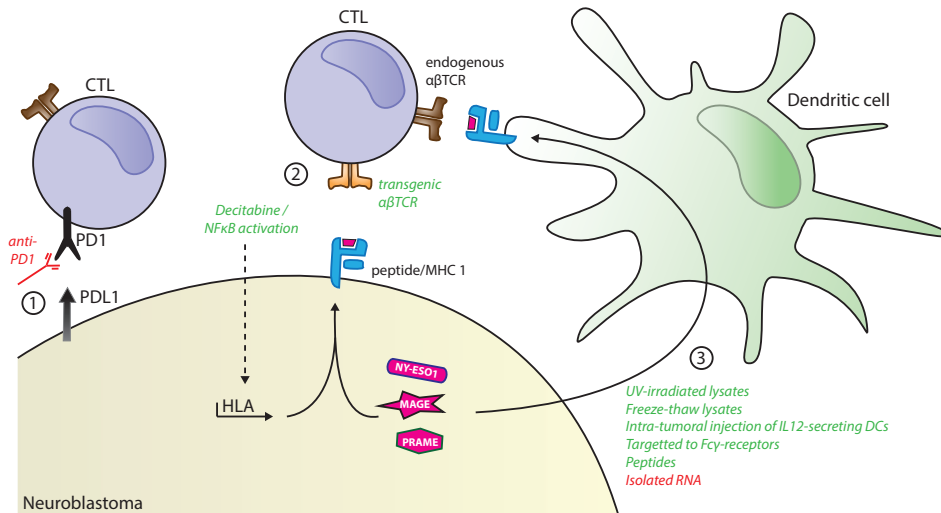


Figure 3. T cell-based immunotherapies in neuroblastoma. Anti-PD1 antibodies block the inhibitory receptor PD1 on the T cell membrane (1). Isolated T cells are transgenically engineered to express the $\alpha\beta$ TCR recognizing neuroblastoma-specific tumor antigens, such as NY-ESO1, MAGE or PRAME, presented in MHC 1 molecules (2). Isolated dendritic cells are loaded with neuroblastoma material as to present its antigens towards T cells as peptide/MHC 1 complexes. Then, the activated T cells recognize and eliminate the neuroblastoma cells (3). Dicitabine treatment or NF κ B activation will increase MHC 1 expression and antigen presentation by neuroblastoma cells. Indicated therapies were tested in either patients or mouse models. Therapies with (partial) beneficial results are depicted in green, therapies with no beneficial results or depicted in red.

Vaccination strategies

A third option is the activation of tumor-specific T cells in vivo. This strategy will elicit endogenous T cell reactivity against specific tumor antigen(s) and induce memory T cells that can re-activate in case of tumor relapses. There are several options when it comes to vaccination. Particulate vaccines can consist of whole tumor cells, DNA, RNA, peptide or protein; possibly targeted towards a specific receptor. Cellular vaccines often include a type of antigen-presenting cell, pre-treated ex vivo to specifically stimulate tumor-directed T cells in vivo.

In a phase 1 trial of subcutaneous vaccination with patient-derived neuroblastoma cells that were genetically modified to secrete IL2 and XCL1 chemokine, in vivo anti-tumor T cell activation was measured (106). In this setting, T cell reactivity was however insufficient as all patients progressed and were unable to overcome the recurrent neuroblastoma. As opposed to a direct injection, whole tumor cells or lysates thereof can be fed to patient-derived dendritic cells (DCs) ex vivo for vaccination with antigen-presenting DCs, an approach that may work better. Geiger and colleagues prepared monocyte-derived dendritic cells (moDC) from patient-isolated monocytes and pulsed them with syngeneic tumor freeze-thaw lysates prior to administration of the moDC vaccine (107). Here, tumor-specific T cell activation after vaccination was detected in 1 of 3 neuroblastoma patients. Similar to this study, induction of cytolytic T cells was monitored using moDCs pulsed with UVB-irradiated tumor lysates (108). Here, amongst the isolated lymphocytes from 7 out of 9 patients tumor-specific CTLs could be activated which subsequently were able to

kill the tumor target cells in vitro.

Instead of feeding whole tumor lysates to DCs, some studies opt for extracting RNA out of tumor cells to feed to DCs. Unfortunately, no objective tumor responses were observed in 11 high-risk neuroblastoma patients vaccinated with tumor RNA-pulsed moDCs (109). In vitro, RNA-loaded DCs were able to generate CTLs recognizing neuroblastoma antigens (110). Of note, the tumor RNA in this study was transfected into rather than phagocytosed by moDCs.

Evidence of in vivo anti-neuroblastoma immunity induced by dendritic cell vaccines comes from two studies using murine models of neuroblastoma. Intra-tumoral injection of IL12-secreting DCs resulted in effective anti-tumor CTL responses and neuroblastoma clearance within 3 weeks (111). Also, targeting antigen to activating Fc-gamma receptors on DCs increased the induction of anti-tumor immunity and protected against neuroblastoma tumor challenge after vaccination (112). In human patients, however, the efficacy of DC vaccination against cancer has been limited. In a recent peptide-pulsed DC vaccination trial with relapsed neuroblastoma patients, T cell responses were measured in 3 out of 8 patients (113). Of these 3 patients, 1 relapsed 10 months after therapy, 1 remained disease-free 2 years after therapy and 1 is in complete remission already 3,5 years after therapy. Patients who failed to mount an immune response after vaccination also underwent disease progression (Figure 3). It is noteworthy to mention that the DC vaccination was combined with administration of decitabine, an epigenetic drug shown to increase MHC 1 expression in tumor cells (114, 115). Though the results of this trial are modest, they illustrate the potential of T cell-mediated therapy against neuroblastoma whether or not induced by a DC vaccine or via adoptive transfer of T cells and combined with MHC 1-increasing agents.

Concluding remarks

The embryonic status of neuroblastoma tumors helps us understand how immunogenicity of this type of cancer is regulated. Given that an embryonic status associates with underdevelopment, lack of differentiation and absence of immunogenic features, it stands to reason that the immunogenic potential of neuroblastoma tumor cells is a direct results of its embryonic origin. Correlating with neural precursor cells going awry is the suppression of the NFκB transcription factor, which also regulates MHC 1 expression. Active NFκB not only sensitizes neuroblastoma for differentiation, but also makes neuroblastoma receptive for T cell-mediated anti-tumor immunity. Insights into neuroblastoma immunogenic regulations will further the development of immunotherapy against neuroblastoma.

References

1. Maris JM. Recent advances in neuroblastoma. *N Engl J Med*. 2010; **362**: 2202-2211.
2. Davidoff AM. Neuroblastoma. *Semin Pediatr Surg*. 2012; **21**: 2-14.
3. Louis CU, Shohet JM. Neuroblastoma: molecular pathogenesis and therapy. *Annu Rev Med*. 2015; **66**: 49-63.
4. Baker DL, Schmidt ML, Cohn SL, Maris JM, London WB, Buxton A, *et al*. Outcome after reduced chemotherapy for intermediate-risk neuroblastoma. *N Engl J Med*. 2010; **363**: 1313-1323.
5. Hoehner JC, Gestblom C, Hedborg F, Sandstedt B, Olsen L, Pahlman S. A developmental model of neuroblastoma: differentiating stroma-poor tumors' progress along an extra-adrenal chromaffin lineage. *Lab Invest*. 1996; **75**: 659-675.
6. Fredlund E, Ringner M, Maris JM, Pahlman S. High Myc pathway activity and low stage of neuronal differentiation associate with poor outcome in neuroblastoma. *Proc Natl Acad Sci U S A*. 2008; **105**: 14094-14099.
7. Hammerle B, Yanez Y, Palanca S, Canete A, Burks DJ, Castel V, *et al*. Targeting neuroblastoma stem cells with retinoic acid and proteasome inhibitor. *PLoS One*. 2013; **8**: e76761.
8. Yu AL, Gilman AL, Ozkaynak MF, London WB, Kreissman SG, Chen HX, *et al*. Anti-GD2 antibody with GM-CSF, interleukin-2, and isotretinoin for neuroblastoma. *N Engl J Med*. 2010; **363**: 1324-1334.
9. Galluzzi L, Vacchelli E, Bravo-San Pedro JM, Buque A, Senovilla L, Baracco EE, *et al*. Classification of current anticancer immunotherapies. *Oncotarget*. 2014; **5**: 12472-12508.
10. Yang Y. Cancer immunotherapy: harnessing the immune system to battle cancer. *J Clin Invest*. 2015; **125**: 3335-3337.
11. Kamta J, Chaar M, Ande A, Altomare DA, Ait-Oudhia S. Advancing Cancer Therapy with Present and Emerging Immuno-Oncology Approaches. *Front Oncol*. 2017; **7**: 64.
12. Drukker M, Katz G, Urbach A, Schuldiner M, Markel G, Itskovitz-Eldor J, *et al*. Characterization of the expression of MHC proteins in human embryonic stem cells. *Proc Natl Acad Sci U S A*. 2002; **99**: 9864-9869.
13. Li L, Baroja ML, Majumdar A, Chadwick K, Rouleau A, Gallacher L, *et al*. Human embryonic stem cells possess immune-privileged properties. *Stem Cells*. 2004; **22**: 448-456.
14. International Stem Cell I, Adewumi O, Aflatoonian B, Ahrlund-Richter L, Amit M, Andrews PW, *et al*. Characterization of human embryonic stem cell lines by the International Stem Cell Initiative. *Nat Biotechnol*. 2007; **25**: 803-816.
15. Okamura RM, Lebkowski J, Au M, Priest CA, Denham J, Majumdar AS. Immunological properties of human embryonic stem cell-derived oligodendrocyte progenitor cells. *J Neuroimmunol*. 2007; **192**: 134-144.
16. Drukker M, Benvenisty N. The immunogenicity of human embryonic stem-derived cells. *Trends Biotechnol*. 2004; **22**: 136-141.
17. Drukker M, Katchman H, Katz G, Even-Tov Friedman S, Shezen E, Hornstein E, *et al*. Human embryonic stem cells and their differentiated derivatives are less susceptible to immune rejection than adult cells. *Stem Cells*. 2006; **24**: 221-229.
18. Garay PA, McAllister AK. Novel roles for immune molecules in neural development: implications for neurodevelopmental disorders. *Front Synaptic Neurosci*. 2010; **2**: 136.
19. Boulanger LM. Immune proteins in brain development and synaptic plasticity. *Neuron*. 2009; **64**: 93-109.
20. Shatz CJ. MHC class I: an unexpected role in neuronal plasticity. *Neuron*. 2009; **64**: 40-45.
21. Stephan AH, Barres BA, Stevens B. The complement system: an unexpected role in synaptic pruning during development and disease. *Annu Rev Neurosci*. 2012; **35**: 369-389.
22. Smit N, Le Poole I, van den Wijngaard R, Tigges A, Westerhof W, Das P. Expression of different immunological markers by cultured human melanocytes. *Arch Dermatol Res*. 1993; **285**: 356-365.
23. Marincola FM, Shamamian P, Alexander RB, Gnarr JR, Turetskaya RL, Nedospasov SA, *et al*. Loss of HLA haplotype and B locus down-regulation in melanoma cell lines. *J Immunol*. 1994; **153**: 1225-1237.
24. Krasagakis K, Garbe C, Eberle J, Orfanos CE. Tumour necrosis factors and several interleukins inhibit the growth and modulate the antigen expression of normal human melanocytes in vitro. *Arch Dermatol Res*. 1995; **287**: 259-265.
25. Hedley SJ, Metcalfe R, Gawkrödger DJ, Weetman AP, Mac Neil S. Vitiligo melanocytes in long-term culture show normal constitutive and cytokine-induced expression of intercellular adhesion

- molecule-1 and major histocompatibility complex class I and class II molecules. *Br J Dermatol.* 1998; **139**: 965-973.
26. Ito T, Ito N, Bettermann A, Tokura Y, Takigawa M, Paus R. Collapse and restoration of MHC class-I-dependent immune privilege: exploiting the human hair follicle as a model. *Am J Pathol.* 2004; **164**: 623-634.
 27. Thams S, Brodin P, Plantman S, Saxelin R, Karre K, Cullheim S. Classical major histocompatibility complex class I molecules in motoneurons: new actors at the neuromuscular junction. *J Neurosci.* 2009; **29**: 13503-13515.
 28. Stemme S, Fager G, Hansson GK. MHC class II antigen expression in human vascular smooth muscle cells is induced by interferon-gamma and modulated by tumour necrosis factor and lymphotoxin. *Immunology.* 1990; **69**: 243-249.
 29. Theobald VA, Lauer JD, Kaplan FA, Baker KB, Rosenberg M. "Neutral allografts"--lack of allogeneic stimulation by cultured human cells expressing MHC class I and class II antigens. *Transplantation.* 1993; **55**: 128-133.
 30. Hosenpud JD, Chou SW, Wagner CR. Cytomegalovirus-induced regulation of major histocompatibility complex class I antigen expression in human aortic smooth muscle cells. *Transplantation.* 1991; **52**: 896-903.
 31. Chang GY, Kohrt HE, Stuge TB, Schwartz EJ, Weber JS, Lee PP. Cytotoxic T lymphocyte responses against melanocytes and melanoma. *J Transl Med.* 2011; **9**: 122.
 32. van den Boorn JG, Konijnenberg D, Dellemijn TA, van der Veen JP, Bos JD, Melief CJ, *et al.* Autoimmune destruction of skin melanocytes by perilesional T cells from vitiligo patients. *J Invest Dermatol.* 2009; **129**: 2220-2232.
 33. Liu T, Khanna KM, Chen X, Fink DJ, Hendricks RL. CD8(+) T cells can block herpes simplex virus type 1 (HSV-1) reactivation from latency in sensory neurons. *J Exp Med.* 2000; **191**: 1459-1466.
 34. Knickelbein JE, Khanna KM, Yee MB, Baty CJ, Kinchington PR, Hendricks RL. Noncytotoxic lytic granule-mediated CD8+ T cell inhibition of HSV-1 reactivation from neuronal latency. *Science.* 2008; **322**: 268-271.
 35. Egan KP, Wu S, Wigdahl B, Jennings SR. Immunological control of herpes simplex virus infections. *J Neurovirol.* 2013; **19**: 328-345.
 36. Orr MT, Mathis MA, Lagunoff M, Sacks JA, Wilson CB. CD8 T cell control of HSV reactivation from latency is abrogated by viral inhibition of MHC class I. *Cell Host Microbe.* 2007; **2**: 172-180.
 37. Wolf M, Jungbluth AA, Garrido F, Cabrera T, Meyen-Southard S, Spitz R, *et al.* Expression of MHC class I, MHC class II, and cancer germline antigens in neuroblastoma. *Cancer Immunol Immunother.* 2005; **54**: 400-406.
 38. Morandi F, Cangemi G, Barco S, Amoroso L, Giuliano M, Gigliotti AR, *et al.* Plasma levels of soluble HLA-E and HLA-F at diagnosis may predict overall survival of neuroblastoma patients. *Biomed Res Int.* 2013; **2013**: 956878.
 39. Lorenzi S, Forloni M, Cifaldi L, Antonucci C, Citti A, Boldrini R, *et al.* IRF1 and NF- κ B restore MHC class I-restricted tumor antigen processing and presentation to cytotoxic T cells in aggressive neuroblastoma. *PLoS One.* 2012; **7**: e46928.
 40. Forloni M, Albini S, Limongi MZ, Cifaldi L, Boldrini R, Nicotra MR, *et al.* NF- κ B, and not MYCN, regulates MHC class I and endoplasmic reticulum aminopeptidases in human neuroblastoma cells. *Cancer Res.* 2010; **70**: 916-924.
 41. Spel L, Boelens JJ, van der Steen DM, Blokland NJ, van Noesel MM, Molenaar JJ, *et al.* Natural killer cells facilitate PRAME-specific T-cell reactivity against neuroblastoma. *Oncotarget.* 2015; **6**: 35770-35781.
 42. Takahashi Y, Sipp D, Enomoto H. Tissue interactions in neural crest cell development and disease. *Science.* 2013; **341**: 860-863.
 43. Newbern JM. Molecular control of the neural crest and peripheral nervous system development. *Curr Top Dev Biol.* 2015; **111**: 201-231.
 44. Mayor R, Theveneau E. The neural crest. *Development.* 2013; **140**: 2247-2251.
 45. Maden M. Retinoic acid in the development, regeneration and maintenance of the nervous system. *Nat Rev Neurosci.* 2007; **8**: 755-765.
 46. Milet C, Monsoro-Burq AH. Neural crest induction at the neural plate border in vertebrates. *Dev Biol.* 2012; **366**: 22-33.
 47. Shyamala K, Yanduri S, Girish HC, Murgod S. Neural crest: The fourth germ layer. *J Oral Maxillofac Pathol.* 2015; **19**: 221-229.

48. Perris R, Perissinotto D. Role of the extracellular matrix during neural crest cell migration. *Mech Dev.* 2000; **95**: 3-21.
49. Dutt S, Matasci M, Sommer L, Zimmermann DR. Guidance of neural crest cell migration: the inhibitory function of the chondroitin sulfate proteoglycan, versican. *ScientificWorldJournal.* 2006; **6**: 1114-1117.
50. Rorth P. Collective cell migration. *Annu Rev Cell Dev Biol.* 2009; **25**: 407-429.
51. Shellard A, Mayor R. Chemotaxis during neural crest migration. *Semin Cell Dev Biol.* 2016; **55**: 111-118.
52. Pei D, Luther W, Wang W, Paw BH, Stewart RA, George RE. Distinct neuroblastoma-associated alterations of PHOX2B impair sympathetic neuronal differentiation in zebrafish models. *PLoS Genet.* 2013; **9**: e1003533.
53. Zimmerman EA. From neurosecretion to neural communication and beyond. The 26th annual Robert Wartenberg lecture. *Neurology.* 1986; **36**: 809-814.
54. Marshall GM, Carter DR, Cheung BB, Liu T, Mateos MK, Meyerowitz JG, *et al.* The prenatal origins of cancer. *Nat Rev Cancer.* 2014; **14**: 277-289.
55. Pugh TJ, Morozova O, Attiyeh EF, Asgharzadeh S, Wei JS, Auclair D, *et al.* The genetic landscape of high-risk neuroblastoma. *Nat Genet.* 2013; **45**: 279-284.
56. Brodeur GM, Seeger RC, Schwab M, Varmus HE, Bishop JM. Amplification of N-myc in untreated human neuroblastomas correlates with advanced disease stage. *Science.* 1984; **224**: 1121-1124.
57. Reiff T, Huber L, Kramer M, Delattre O, Janoueix-Lerosey I, Rohrer H. Midkine and Alk signaling in sympathetic neuron proliferation and neuroblastoma predisposition. *Development.* 2011; **138**: 4699-4708.
58. Wang M, Zhou C, Sun Q, Cai R, Li Y, Wang D, *et al.* ALK amplification and protein expression predict inferior prognosis in neuroblastomas. *Exp Mol Pathol.* 2013; **95**: 124-130.
59. Mosse YP, Laudenslager M, Longo L, Cole KA, Wood A, Attiyeh EF, *et al.* Identification of ALK as a major familial neuroblastoma predisposition gene. *Nature.* 2008; **455**: 930-935.
60. Valentijn LJ, Koster J, Zwijnenburg DA, Hasselt NE, van Sluis P, Volckmann R, *et al.* TERT rearrangements are frequent in neuroblastoma and identify aggressive tumors. *Nat Genet.* 2015; **47**: 1411-1414.
61. Eroglu B, Wang G, Tu N, Sun X, Mivechi NF. Critical role of Brg1 member of the SWI/SNF chromatin remodeling complex during neurogenesis and neural crest induction in zebrafish. *Dev Dyn.* 2006; **235**: 2722-2735.
62. Wang W, Zhong Q, Teng L, Bhatnagar N, Sharma B, Zhang X, *et al.* Mutations that disrupt PHOXB interaction with the neuronal calcium sensor HPCAL1 impede cellular differentiation in neuroblastoma. *Oncogene.* 2014; **33**: 3316-3324.
63. Matthay KK, Villablanca JG, Seeger RC, Stram DO, Harris RE, Ramsay NK, *et al.* Treatment of high-risk neuroblastoma with intensive chemotherapy, radiotherapy, autologous bone marrow transplantation, and 13-cis-retinoic acid. Children's Cancer Group. *N Engl J Med.* 1999; **341**: 1165-1173.
64. Chaturvedi MM, Sung B, Yadav VR, Kannappan R, Aggarwal BB. NF-kappaB addiction and its role in cancer: 'one size does not fit all'. *Oncogene.* 2011; **30**: 1615-1630.
65. Bernards R. N-myc disrupts protein kinase C-mediated signal transduction in neuroblastoma. *EMBO J.* 1991; **10**: 1119-1125.
66. van 't Veer LJ, Beijersbergen RL, Bernards R. N-myc suppresses major histocompatibility complex class I gene expression through down-regulation of the p50 subunit of NF-kappa B. *EMBO J.* 1993; **12**: 195-200.
67. Vallabhapurapu S, Karin M. Regulation and function of NF-kappaB transcription factors in the immune system. *Annu Rev Immunol.* 2009; **27**: 693-733.
68. Hoesel B, Schmid JA. The complexity of NF-kappaB signaling in inflammation and cancer. *Mol Cancer.* 2013; **12**: 86.
69. Denis-Donini S, Caprini A, Frassoni C, Grilli M. Members of the NF-kappaB family expressed in zones of active neurogenesis in the postnatal and adult mouse brain. *Brain Res Dev Brain Res.* 2005; **154**: 81-89.
70. Rolls A, Shechter R, London A, Ziv Y, Ronen A, Levy R, *et al.* Toll-like receptors modulate adult hippocampal neurogenesis. *Nat Cell Biol.* 2007; **9**: 1081-1088.
71. Zhang Y, Hu W. NFkappaB signaling regulates embryonic and adult neurogenesis. *Front Biol (Beijing).* 2012; **7**.

72. Aloor R, Zhang C, Bandyopadhyay M, Dasgupta S. Impact of nuclear factor-kappaB on restoration of neuron growth and differentiation in hippocampus of degenerative brain. *J Neurosci Res.* 2015; **93**: 1471-1475.
73. Beg AA, Sha WC, Bronson RT, Ghosh S, Baltimore D. Embryonic lethality and liver degeneration in mice lacking the RelA component of NF-kappa B. *Nature.* 1995; **376**: 167-170.
74. Gerondakis S, Grossmann M, Nakamura Y, Pohl T, Grumont R. Genetic approaches in mice to understand Rel/NF-kappaB and IkappaB function: transgenics and knockouts. *Oncogene.* 1999; **18**: 6888-6895.
75. Li Q, Estepa G, Memet S, Israel A, Verma IM. Complete lack of NF-kappaB activity in IKK1 and IKK2 double-deficient mice: additional defect in neurulation. *Genes Dev.* 2000; **14**: 1729-1733.
76. Basart H, van de Kar A, Ades L, Cho TJ, Carter E, Maas SM, et al. Frontometaphyseal dysplasia and keloid formation without FLNA mutations. *Am J Med Genet A.* 2015; **167**: 1215-1222.
77. Wade EM, Daniel PB, Jenkins ZA, McInerney-Leo A, Leo P, Morgan T, et al. Mutations in MAP3K7 that Alter the Activity of the TAK1 Signaling Complex Cause Frontometaphyseal Dysplasia. *Am J Hum Genet.* 2016; **99**: 392-406.
78. Weiss K, Applegate C, Wang T, Batista DA. Familial TAB2 microdeletion and congenital heart defects including unusual valve dysplasia and tetralogy of fallot. *Am J Med Genet A.* 2015; **167A**: 2702-2706.
79. Torres J, Watt FM. Nanog maintains pluripotency of mouse embryonic stem cells by inhibiting NFkappaB and cooperating with Stat3. *Nat Cell Biol.* 2008; **10**: 194-201.
80. Kang HB, Kim YE, Kwon HJ, Sok DE, Lee Y. Enhancement of NF-kappaB expression and activity upon differentiation of human embryonic stem cell line SNUhES3. *Stem Cells Dev.* 2007; **16**: 615-623.
81. Kim YE, Kang HB, Park JA, Nam KH, Kwon HJ, Lee Y. Upregulation of NF-kappaB upon differentiation of mouse embryonic stem cells. *BMB Rep.* 2008; **41**: 705-709.
82. Luningschror P, Stocker B, Kaltschmidt B, Kaltschmidt C. miR-290 cluster modulates pluripotency by repressing canonical NF-kappaB signaling. *Stem Cells.* 2012; **30**: 655-664.
83. Luningschror P, Kaltschmidt B, Kaltschmidt C. Knockdown of IKK1/2 promotes differentiation of mouse embryonic stem cells into neuroectoderm at the expense of mesoderm. *Stem Cell Rev.* 2012; **8**: 1098-1108.
84. Korner M, Tarantino N, Pleskoff O, Lee LM, Debre P. Activation of nuclear factor kappa B in human neuroblastoma cell lines. *J Neurochem.* 1994; **62**: 1716-1726.
85. Feng Z, Porter AG. NF-kappaB/Rel proteins are required for neuronal differentiation of SH-SY5Y neuroblastoma cells. *J Biol Chem.* 1999; **274**: 30341-30344.
86. Farina AR, Masciulli MP, Tacconelli A, Cappabianca L, De Santis G, Gulino A, et al. All-trans-retinoic acid induces nuclear factor kappaB activation and matrix metalloproteinase-9 expression and enhances basement membrane invasivity of differentiation-resistant human SK-N-BE 9N neuroblastoma Cells. *Cell Growth Differ.* 2002; **13**: 343-354.
87. Kiningham KK, Cardozo ZA, Cook C, Cole MP, Stewart JC, Tassone M, et al. All-trans-retinoic acid induces manganese superoxide dismutase in human neuroblastoma through NF-kappaB. *Free Radic Biol Med.* 2008; **44**: 1610-1616.
88. Condello S, Caccamo D, Curro M, Ferlazzo N, Parisi G, Ientile R. Transglutaminase 2 and NF-kappaB interplay during NGF-induced differentiation of neuroblastoma cells. *Brain Res.* 2008; **1207**: 1-8.
89. de Bittencourt Pasquali MA, de Ramos VM, Albanus RDO, Kunzler A, de Souza LHT, Dalmolin RJS, et al. Gene Expression Profile of NF-kappaB, Nrf2, Glycolytic, and p53 Pathways During the SH-SY5Y Neuronal Differentiation Mediated by Retinoic Acid. *Mol Neurobiol.* 2016; **53**: 423-435.
90. van den Elsen PJ. Expression regulation of major histocompatibility complex class I and class II encoding genes. *Front Immunol.* 2011; **2**: 48.
91. Pick M, Ronen D, Yanuka O, Benvenisty N. Reprogramming of the MHC-I and its regulation by NFkappaB in human-induced pluripotent stem cells. *Stem Cells.* 2012; **30**: 2700-2708.
92. Lv D, Shen Y, Peng Y, Liu J, Miao F, Zhang J. Neuronal MHC Class I Expression Is Regulated by Activity Driven Calcium Signaling. *PLoS One.* 2015; **10**: e0135223.
93. Vertuani S, De Geer A, Levitsky V, Kogner P, Kiessling R, Levitskaya J. Retinoids act as multistep modulators of the major histocompatibility class I presentation pathway and sensitize neuroblastomas to cytotoxic lymphocytes. *Cancer Res.* 2003; **63**: 8006-8013.
94. Apps JR, Hasan F, Campus O, Behjati S, Jacques TS, N JS, et al. The immune environment of paediatric solid malignancies: evidence from an immunohistochemical study of clinical cases. *Fetal Pediatr Pathol.* 2013; **32**: 298-307.
95. Carlson LM, De Geer A, Sveinbjornsson B, Orrego A, Martinsson T, Kogner P, et al. The

- microenvironment of human neuroblastoma supports the activation of tumor-associated T lymphocytes. *Oncoimmunology*. 2013; **2**: e23618.
96. Yan X, Orentas RJ, Johnson BD. Tumor-derived macrophage migration inhibitory factor (MIF) inhibits T lymphocyte activation. *Cytokine*. 2006; **33**: 188-198.
 97. Mussai F, Egan S, Hunter S, Webber H, Fisher J, Wheat R, *et al*. Neuroblastoma Arginase Activity Creates an Immunosuppressive Microenvironment That Impairs Autologous and Engineered Immunity. *Cancer Res*. 2015; **75**: 3043-3053.
 98. Santilli G, Piotrowska I, Cantilena S, Chayka O, D'Alicarnasso M, Morgenstern DA, *et al*. Polyphenon [corrected] E enhances the antitumor immune response in neuroblastoma by inactivating myeloid suppressor cells. *Clin Cancer Res*. 2013; **19**: 1116-1125.
 99. Hashimoto O, Yoshida M, Koma Y, Yanai T, Hasegawa D, Kosaka Y, *et al*. Collaboration of cancer-associated fibroblasts and tumour-associated macrophages for neuroblastoma development. *J Pathol*. 2016; **240**: 211-223.
 100. Pinto N, Park JR, Murphy E, Yearley J, McClanahan T, Annamalai L, *et al*. Patterns of PD-1, PD-L1, and PD-L2 expression in pediatric solid tumors. *Pediatr Blood Cancer*. 2017.
 101. Eissler N, Mao Y, Brodin D, Reutersward P, Andersson Svahn H, Johnsen JL, *et al*. Regulation of myeloid cells by activated T cells determines the efficacy of PD-1 blockade. *Oncoimmunology*. 2016; **5**: e1232222.
 102. Bao L, Dunham K, Lucas K. MAGE-A1, MAGE-A3, and NY-ESO-1 can be upregulated on neuroblastoma cells to facilitate cytotoxic T lymphocyte-mediated tumor cell killing. *Cancer Immunol Immunother*. 2011; **60**: 1299-1307.
 103. Jacobs JF, Brasseur F, Hulsbergen-van de Kaa CA, van de Rakt MW, Figdor CG, Adema GJ, *et al*. Cancer-germline gene expression in pediatric solid tumors using quantitative real-time PCR. *Int J Cancer*. 2007; **120**: 67-74.
 104. Oberthuer A, Hero B, Spitz R, Berthold F, Fischer M. The tumor-associated antigen PRAME is universally expressed in high-stage neuroblastoma and associated with poor outcome. *Clin Cancer Res*. 2004; **10**: 4307-4313.
 105. Singh N, Kulikovskaya I, Barrett DM, Binder-Scholl G, Jakobsen B, Martinez D, *et al*. T cells targeting NY-ESO-1 demonstrate efficacy against disseminated neuroblastoma. *Oncoimmunology*. 2016; **5**: e1040216.
 106. Russell HV, Strother D, Mei Z, Rill D, Popek E, Biagi E, *et al*. Phase I trial of vaccination with autologous neuroblastoma tumor cells genetically modified to secrete IL-2 and lymphotactin. *J Immunother*. 2007; **30**: 227-233.
 107. Geiger JD, Hutchinson RJ, Hohenkirk LF, McKenna EA, Yanik GA, Levine JE, *et al*. Vaccination of pediatric solid tumor patients with tumor lysate-pulsed dendritic cells can expand specific T cells and mediate tumor regression. *Cancer Res*. 2001; **61**: 8513-8519.
 108. Shilyansky J, Jacobs P, Doffek K, Sugg SL. Induction of cytolytic T lymphocytes against pediatric solid tumors in vitro using autologous dendritic cells pulsed with necrotic primary tumor. *J Pediatr Surg*. 2007; **42**: 54-61; discussion 61.
 109. Caruso DA, Orme LM, Amor GM, Neale AM, Radcliff FJ, Downie P, *et al*. Results of a Phase I study utilizing monocyte-derived dendritic cells pulsed with tumor RNA in children with Stage 4 neuroblastoma. *Cancer*. 2005; **103**: 1280-1291.
 110. Morandi F, Chiesa S, Bocca P, Millo E, Salis A, Solari M, *et al*. Tumor mRNA-transfected dendritic cells stimulate the generation of CTL that recognize neuroblastoma-associated antigens and kill tumor cells: immunotherapeutic implications. *Neoplasia*. 2006; **8**: 833-842.
 111. Shimizu T, Berhanu A, Redlinger RE, Jr, Watkins S, Lotze MT, Barksdale EM, Jr. Interleukin-12 transduced dendritic cells induce regression of established murine neuroblastoma. *J Pediatr Surg*. 2001; **36**: 1285-1292.
 112. Gil M, Bieniasz M, Wierzbicki A, Bambach BJ, Rokita H, Kozbor D. Targeting a mimotope vaccine to activating Fcγ receptors empowers dendritic cells to prime specific CD8+ T cell responses in tumor-bearing mice. *J Immunol*. 2009; **183**: 6808-6818.
 113. Krishnadas DK, Shusterman S, Bai F, Diller L, Sullivan JE, Cheerva AC, *et al*. A phase I trial combining decitabine/dendritic cell vaccine targeting MAGE-A1, MAGE-A3 and NY-ESO-1 for children with relapsed or therapy-refractory neuroblastoma and sarcoma. *Cancer Immunol Immunother*. 2015; **64**: 1251-1260.
 114. Adair SJ, Hogan KT. Treatment of ovarian cancer cell lines with 5-aza-2'-deoxycytidine upregulates the expression of cancer-testis antigens and class I major histocompatibility complex-encoded

- molecules. *Cancer Immunol Immunother.* 2009; **58**: 589-601.
115. Serrano A, Tanzarella S, Lionello I, Mendez R, Traversari C, Ruiz-Cabello F, *et al.* Rexpression of HLA class I antigens and restoration of antigen-specific CTL response in melanoma cells following 5-aza-2'-deoxycytidine treatment. *Int J Cancer.* 2001; **94**: 243-251.

Chapter 9

Summary



In this thesis I have explored the process of MHC-1-mediated antigen presentation in two distinctive cell types. In the first chapters I describe mechanisms in dendritic cells that affect antigen (cross)-presentation and its application for vaccination. In the later chapters I focus on neuroblastoma tumor cells and possible ways to increase their antigen presentation levels towards cytotoxic T-cells.

Dendritic cells are pivotal players that bridge innate and adaptive immunity. As sessile sentinels in barrier tissues, they scan their local environment using the receptors on their cell surface. When sensing inflammatory or danger signals, DCs engulf the receptor-bound material and process it for antigen presentation to T-cells. This process of antigen presentation has great therapeutic potential in the cancer field, driving the development of innovative immunotherapies.

DCs are able to engulf tumor-derived material and cross-present tumor-derived antigen fragments to CD8⁺ T-cells. In Chapter 2, I give an overview of recent literature about cross-presenting tumor cell material by dendritic cells. Especially necrotic or apoptotic tumor cells are recognized by dendritic cells and processed for antigen cross-presentation. Signals on or secreted by the dying cells are important for the intracellular routing of antigens towards the cross-presentation pathway. Within this pathway, a balanced play between antigen degradation and antigen preservation serves to maximize cross-presentation of the phagocytosed cargo and thereby the elicitation of an anti-tumor T-cell response.

Tipping the scale towards antigen preservation causes a complete stop of antigenic peptide production and subsequent loss of antigen cross-presentation, as described in Chapter 3. Here, cowpox virus-derived protein CPXV012 inhibits direct MHC-1 antigen presentation in infected cells. In this chapter CPXV012 is delivered into the endosomal pathway of dendritic cells as a soluble protein. In this endosomal environment, soluble CPXV012 colocalizes with endocytosed antigen. By blocking endosomal acidification, it prevents the degradation of antigen, a process that is required to liberate antigenic peptide to be cross-presented by MHC-1.

Peptides that are produced by endosomal processing of antigen do not only reach MHC-1 for presentation, but also MHC 2. MHC 2 presents antigen to helper CD4⁺ T-cells that aid in the priming of CD8⁺ T-cells. The benefit of reaching both CD4⁺ and CD8⁺ T-cells when initiating an immune response is investigated in Chapter 4. Antigen-specific CD4⁺ T-cells stimulate DC-mediated priming of antigen-specific CD8⁺ T-cells recognizing an epitope of the same antigen. This is accomplished by the production of IFN γ upon binding peptide/MHC 2-complexes on the DC cell surface. These findings are relevant, as after stem cell transplantation, when a newly infused immune system is in development, patients may suffer from viral reactivations such as CMV. In these patients, the presence of CMV-specific CD4⁺ T-cells precedes the induction of CMV-specific CD8⁺ T-cells. After viral clearance, only the CMV-specific CD8⁺ T-cells are still detected.

Given the pivotal role of dendritic cells in eliciting cellular immunity, they may be useful for therapeutic purposes. In Chapter 5, I explore this option using a viral vector that targets dendritic cells *in vitro* and *in vivo*. This viral vector is a derivative from the bunyavirus Rift Valley Fever virus and genetically engineered to express either pp65 (human) or OVA (mouse) antigen. Using the RVFV vector we detected antigen-specific CD8⁺ T-cell activation, both using *in vitro* cultures and using *in vivo* mouse models. Furthermore, in prophylactic and therapeutic settings of vaccination this viral vector was able to confer protection against a lymphoma tumor challenge.

Neuroblastoma is the most deadly pediatric solid tumor and currently lacks a cellular immunotherapeutic treatment strategy. Tumor-specific CD8⁺ T-cells may be effective to destroy neuroblastoma tumor cells. However, neuroblastoma tumors were shown not to be immunogenic due to low MHC-1 expression levels and lack of broadly- expressed antigens. How to increase neuroblastoma immunogenicity is discussed in Chapter 6. Cells with no/low MHC-1 levels can become targets for natural killer (NK) cells. Indeed, part of the neuroblastoma cells could be killed by NK cells in vitro. Those cells surviving the NK cell attack showed upregulation of MHC-1 and could therefore become targets for CD8⁺ T-cells. This hypothesis required the identification of a neuroblastoma-expressed antigen. I show that the preferred antigen in melanoma (PRAME) is expressed in >90% of high-risk neuroblastoma tumors and PRAME-specific T-cells are able to recognize neuroblastoma cells, but only when MHC-1 levels are upregulated e.g. by previous NK cell attack.

The regulation of MHC-1 expression in neuroblastoma is further investigated in Chapter 7. MHC-1 expression, and thus T-cell recognition of neuroblastoma, appears to depend on the activation of the transcription factor NFκB. Through systematic gene deletions, I have identified factors that suppress NFκB activity in neuroblastoma cells. TNIP1 limits NFκB activity in neuroblastoma by destabilizing the canonical IKK-complex. N4BP1 on the other hand shows an inhibitory effect on NFκB that is independent of the canonical IKK-complex. N4BP1 aids OTUD7B to de-ubiquitinate TRAF3, thereby stabilizing TRAF3 protein and ensuring blockage of both canonical and non-canonical NFκB pathways. Depletion of N4BP1 results in degradation of TRAF3 and subsequent accumulation of NIK, which initiates activation of non-canonical NFκB. Both TNIP1 and N4BP1 tumor expression levels are correlated with worse survival of neuroblastoma patients, suggesting they could be relevant targets for the development of future (immuno)therapies against neuroblastoma.

Finally, the role of NFκB suppression in neuroblastoma development, immunogenicity and immunotherapy is reviewed and discussed in Chapter 8.

&

Nederlandse samenvatting

Dankwoord

Curriculum Vitae

Publicatielijst



Nederlandse samenvatting

In dit proefschrift heb ik het proces van antigeen presentatie onderzocht in twee verschillende type cellen, namelijk dendritische cellen en neuroblastoom tumorcellen.

Het eerste hoofdstuk geeft een introductie over antigeen presentatie en beschrijft de focus van dit proefschrift. Een antigeen is een stukje eiwit dat wordt herkend als lichaamsvreemd, zoals bijvoorbeeld afkomstig van een virus of bacterie. Tegen een antigeen kan een immunoreactie worden gestart. Deze immunoreactie kan bestaan uit het maken van antilichamen die het antigeen, en daarmee het virus of de bacterie, vangen of uit het uitgroeien van “killer” immuuncellen die geïnfecteerde lichaamscellen kunnen vernietigen.

Antigenen worden in het lichaam door dendritische cellen (DC) opgespoord; zij patrouilleren door de weefsels en komen in actie wanneer ze gevaar tegen komen. In een dergelijke situatie slokt de DC het antigeen op en gaat vervolgens op weg naar de dichtstbijzijnde lymfeklier om het aan het immuunsysteem te presenteren. Het opgeslokte antigeen wordt binnenin de DC afgebroken tot kleine stukjes, ofwel peptiden. In de cel is ook het presentatiemolecuul MHC-1 aanwezig. MHC-1 is in staat om zich te verbinden met dergelijke peptiden. Het peptide/MHC-1-complex baant vervolgens zijn weg naar het celoppervlak waar het zich presenteert aan “killer” immuuncellen. Het proces waarin een antigeen wordt opgeslokt en afgebroken om te worden gepresenteerd in MHC-1, is uitermate belangrijk voor de activatie van de juiste immunoreactie. In hoofdstukken 2,3,4 en 5 heb ik onderzocht hoe dit proces geremd kan worden, hoe het bijdraagt in het groeiende immuunsysteem na stamceltransplantatie en hoe we het kunnen benutten voor een DC vaccin (tegen kanker).

Niet alleen DCs, maar iedere kernhoudende cel van het lichaam brengt MHC-1 tot expressie waarmee het peptiden presenteert afkomstig uit eigen cel. Het presenteren via de MHC-1 receptor, is voor al deze lichaamscellen de manier om aan het immuunsysteem te laten zien wat er zich afspeelt binnenin de cel. Presentatie van lichaamseigen peptiden zal er geen immunoreactie opwekken. Echter, geïnfecteerde cellen of tumorcellen zullen afwijkende peptiden presenteren en zijn dus in staat het immuunsysteem te alarmeren.

Het type immuuncellen dat peptide/MHC-1-complexen op het celoppervlak van cellen kan lezen zijn de zogeheten T-cellen (hiervoor “killer” cellen genoemd). Iedere T-cel draagt één unieke T-cel receptor (TCR) en kan daarmee één peptide/MHC-1-combinatie herkennen. Zo is er voor ieder antigeen wel een reagerende T-cel te vinden. Het gebruik van T-cellen die specifiek tumor antigenen kunnen herkennen, is een groeiend veld binnen de kankertherapie en heeft ook al enige successen behaald. Voor neuroblastoomkanker is er tot op heden nog geen gestandaardiseerde immunotherapie ontwikkeld die gebaseerd is op T-celherkenning. Neuroblastoom is een type kinderkanker dat zich uit in de sympathische zenuwcellen, vaak in de bijnier of langs de wervelkolom. Neuroblastoom tumorcellen weten het immuunsysteem te ontwijken door geen MHC-1 tot expressie te brengen. Zonder MHC-1 is er geen antigeen presentatie en dus geen herkenning door T-cellen. In hoofdstukken 6, 7 en 8 onderzoek ik de regulatie van zowel

MHC-1 expressie als MHC-1 presentatie in neuroblastoom. Dit is van belang om een effectieve T-celgemedieerde immuuntherapie tegen neuroblastoom te kunnen ontwikkelen.



&

Dankwoord

Een PhD-titel behaal je niet alleen, daarom veel dank aan iedereen die een rol speelde in mijn promotietraject:

Berent, dank voor je steun en luisterend oor.

Marianne, dank dat je altijd voor me klaar staat en voor je onvoorwaardelijke begeleiding.

Stefan en Jaap-Jan, dank dat ik onder jullie hoede mijn eigen weg heb mogen vinden in de wereld van de neuroblastoom.

Aan alle samenwerkingen en studenten: Mirjam, Dirk, Jeroen, Nadia, Emmanuel, Rutger, Thijn, Joppe, Elmer, Rianne, Lianne en Ariën, dank voor het gezamenlijk sparren en experimenteren!

Willemijn, dank dat je non-stop mijn persoonlijke cheerleader bent. Ook voor je prachtige tekeningen op mijn bureau en de zekerheid dat altijd alles goed komt als er maar koffie is.

Arie, Robert, Thijs & Ewoud, dank voor het nespresso-apparaat! En de daarbij horende discussies tijdens de vele koffiemomenten.

Sandra, thanks for being the sweetest and most gezellig neighbour I could wish for. Sometimes, just one sentence is enough to speak our minds...

Lieneke, Tessa, Francesca en Friederike, onze onderzoeksprojecten lopen dan misschien uiteen maar daarom juist te meer dank voor jullie ideeën en overpeinzingen over mijn onderzoek en (wellicht nog belangrijker) over niet-wetenschap gerelateerde onderwerpen! Marthe, Emmerik & Sarah, dank voor jullie kritisch oog tijdens de lab meetings en de gezelligheid tijdens de jaarlijkse Boes barbecue.

Maud, dank voor je positiviteit en relativeringsvermogen.

Colin, Nina, Ester, Rick, Coco, Niek, Celina & Jurgen, dank voor het aanhoren van en meedenken over mijn onderzoek.

Rianne, Marlot, Kerstin, Elena & Anne, thanks for all the bridge nights at the WKZ. I'm so glad I could convince you to learn bridge. Remember, always stick to the plan!

Caroline, Kerstin en Willemijn, dank voor de gezellige etentjes samen! Een traditie om voort te zetten.

Gerdien, dank dat je altijd recht in mijn zicht zat te werken zodat ik je (meestal) kon overhalen voor een kop koffie. Even sparren, praten over de toekomst of kletsen over niks, fijn dat dat kon met jou!

Juud, dank voor het altijd hebben van voedsel na 6u 's avonds. Never underestimate the power of the back-up boterham!

Arjan, dank voor die ene keer bier-van-de-maand! En de dansvloer moves tijdens promotiefestjes en congressen.

Theo, dank voor je gezelligheid! Gelukkig ben je niet weg te slaan bij onze afdeling ;)

Sytze, dank voor de koffie tijdens onze we-doen-niet-mee-met-de-cake-om-de-week-side-parties. En natuurlijk de vrimibo's!

Sylvia, dank voor je goede adviezen en niet te vergeten je pubquiz kennis.

Pien en Jeroen, dank dat jullie me hebben leren sorten! En voor jullie belangstelling en gezelligheid 😊

Rianne en Marlot, naast bridgen delen we nog meer interesses. Dank voor vele onvergetelijke festivalbezoekjes en concertavonden! En wellicht een hike weekend in het verschiet? Met het al bestaande hike-team: Juud, Fran en Lianne, dank voor deze welkome afleiding!

Luuk, Nadia, Sjanna, Eveline, Chiara, Pien, Alsya, Noortje, Mattheus, Pawel, Yvonne, Jenny, Nienke, Lotte, Janneke, Lucas, Sandra, Michiel, Sjors, Selma, Ruben, Kuldeep & Maarten, thanks for all the talks and for the drinks, whether it was coffee, beer or gin-tonic!

Dank aan mijn vriendjes en vriendinnetjes voor samen met mij genieten van sushi-dates, bierfestivals, Lowlands, weekendje Dublin, oud&nieuw in Berlijn, kerstdiners, Where the Wild things are, AIVD kerstpuzzels, vakantie in Révfulöp, weekendje Rome, massages, Best Kept Secret, bridgeclubavonden, paasdinners, NS-wandelingen, vakantie in Toscane, wijnproeverijen, Into the great wide open, glitterbingo, zomerse barbecues, Le Guess Who, weekendje Porto, stappen in Delft/Groningen/Rotterdam/Breda, lomo uit Madrid, hiken in Duitsland, Down the rabbit hole (of toch niet?), bioscoopbezoekjes, boeren bridge, Grasnapolsky, smulpaap avonden, vele concerten, fancy wine, strakke loempia's en niet te vergeten de jaarlijkse terugkeer naar Luxemburg blues festival. Ellen, Fab, Marina, Eric, Marleen, Joost, Dieke, Loes, Eva, Jer, Chamon, Sara, Lennart, Kim, Roos, Lars, Brenda, Mathieu, Celine, Mark, Leonie, Ruud en Johan, jullie zijn top!

Papa en mama, dank voor altijd een warm welkom in Oldenzaal, voor jullie interesse in mijn onderzoek en voor positieve afleiding. Zoals tijdens een middagje helpen met de aanleg van jullie nieuwe tuin of de luxe lunchsessies in Utrecht.

Lien en Guus, dank dat er altijd een plekje voor mij is aan jullie eettafel! Ook dank voor het maken van Nina 😊 en voor de ontspanning tijdens een wijntje of (eigen gebrouwen!) biertje.

Joppe, dank voor alles en nog veel meer.



&

Curriculum Vitae

Lotte was born in Oldenzaal on June 9th 1988. In Oldenzaal she graduated from Twents Carmel College (de Thij) at VWO level. She moved to Utrecht to start her bachelor studies in Biomedical Sciences at Utrecht University, which she finished in 2009. In the following year, Lotte decided to take a break from studying and travel to Australia. A plan that was financially supported by taking on several teaching jobs preceding and following her travels.

In September 2010, she started her master studies in Infection and Immunity at Utrecht University. For 9 months, Lotte joined the Virology division headed by Peter Rottier at UU. There, she investigated the characteristics of bunyaviral glycoproteins in pH-dependent viral entry.

Subsequently, Lotte went to Boston to join the lab of Shannon Turley within the department for Cancer Immunology & AIDS at Dana Farber Cancer Institute. She investigated the role of cancer-associated fibroblasts in a mouse model of triple-negative breast cancer. After 8 months, Lotte returned to Utrecht and started her PhD under joint supervision of Marianne Boes, Stefan Nierkens and Jaap-Jan Boelens studying antigen (cross-)presentation in antigen-presenting cells and cancer cells.

Lotte currently works as junior PhD coordinator of the Immunity & Infection program of the graduate school of Life Sciences at Utrecht University.

List of publications

Spel L, Luteijn RD, Drijfhout JW, Nierkens S, Boes M, Wiertz EJH. Endocytosed soluble cowpox virus protein CPXV012 inhibits antigen cross-presentation in human monocyte-derived dendritic cells. *Immunol Cell Biol.* 2017 Oct 19 [Epub ahead of print].

Silva-Cardoso SC, Affandi AJ, **Spel L**, Cossu M, van Roon JAG, Boes M, Radstake TRDJ. CXCL4 Exposure Potentiates TLR-Driven Polarization of Human Monocyte-Derived Dendritic Cells and Increases Stimulation of T Cells. *J Immunol.* 2017 Jul 1;199(1):253-262.

Oreshkova N, Wichgers Schreur PJ, **Spel L**, Vloet RP, Moormann RJ, Boes M, Kortekaas J. Nonspreading Rift Valley Fever Virus Infection of Human Dendritic Cells Results in Downregulation of CD83 and Full Maturation of Bystander Cells. *PLoS One.* 2015 Nov 17;10(11):e0142670.

Spel L, Boelens JJ, van der Steen DM, Blokland NJ, van Noesel MM, Molenaar JJ, Heemskerk MH, Boes M, Nierkens S. Natural killer cells facilitate PRAME-specific T-cell reactivity against neuroblastoma. *Oncotarget.* 2015 Nov 3;6(34):35770-81.

Oreshkova N, **Spel L**, Vloet RP, Wichgers Schreur PJ, Moormann RJ, Boes M, Kortekaas J. Preliminary Evaluation of a Bunyavirus Vector for Cancer Immunotherapy. *J Virol.* 2015 Sep;89(17):9124-7.

de Haar C, Plantinga M, Blokland NJ, van Til NP, Flinsenberg TW, Van Tendeloo VF, Smits EL, Boon L, **Spel L**, Boes M, Boelens JJ, Nierkens S. Generation of a cord blood-derived Wilms Tumor 1 dendritic cell vaccine for AML patients treated with allogeneic cord blood transplantation. *Oncoimmunology.* 2015 May 27;4(11):e1023973.

Flinsenberg TW, **Spel L**, Jansen M, Koning D, de Haar C, Plantinga M, Scholman R, van Loenen MM, Nierkens S, Boon L, van Baarle D, Heemskerk MH, Boelens JJ, Boes M. Cognate CD4 T-cell licensing of dendritic cells heralds anti-cytomegalovirus CD8 T-cell immunity after human allogeneic umbilical cord blood transplantation. *J Virol.* 2015 Jan 15;89(2):1058-69.

Spel L, Boelens JJ, Nierkens S, Boes M. Antitumor immune responses mediated by dendritic cells: How signals derived from dying cancer cells drive antigen cross-presentation. *Oncoimmunology.* 2013 Nov 1;2(11):e26403.

de Boer SM, Kortekaas J, **Spel L**, Rottier PJ, Moormann RJ, Bosch BJ. Acid-activated structural reorganization of the Rift Valley fever virus Gc fusion protein. *J Virol.* 2012 Dec;86(24):13642-52.



